UNIVERSIDAD DE JAÉN

ESCUELA POLITÉCNICA SUPERIOR DE JAÉN
DEPARTAMENTO DE INGENIERÍA ELECTRÓNICA AUTOMÁTICA

TESIS DOCTORAL

EVALUACIÓN Y DESARROLLO DE TÉCNICAS PARA LA CARACTERIZACIÓN DE SISTEMAS FOTOVOLTAICOS A SOL REAL

PRESENTADA POR:
JESÚS MONTES ROMERO

DIRIGIDA POR:
DR. D. JUAN DE LA CASA HIGUERAS
DR. D. EDUARDO FERNÁNDEZ FERNÁNDEZ

JAÉN, 19 DE MAYO DE 2020

ISBN 978-84-9159-381-2

UNIVERSIDAD DE JAÉN

HIGH POLYTECHNIC SCHOOL OF JAEN
ELECTRONIC AND AUTOMATION ENGINEERING DPT.

PhD THESIS

•

EVALUATION AND DEVELOPMENT OF TECHNIQUES FOR THE CHARACTERIZATION OF PHOTOVOLTAIC SYSTEM UNDER REAL OPERATION CONDITIONS

AUTHOR:

JESÚS MONTES ROMERO

SUPERVISORS:

DR. JUAN DE LA CASA HIGUERAS

DR. EDUARDO FERNÁNDEZ FERNÁNDEZ

JAÉN, FEBRUARY 2020

Universidad de Jaén

TESIS DOCTORAL

EVALUACIÓN Y DESARROLLO DE TÉCNICAS PARA LA CARACTERIZACIÓN DE SISTEMAS FOTOVOLTAICOS A SOL REAL

AUTOR

JESÚS MONTES ROMERO

DIRECTORES

DR. JUAN DE LA CASA HIGUERAS

DR. EDUARDO FERNÁNDEZ FERNÁNDEZ

DEPARTAMENTO DE INGENIERÍA ELECTRÓNICA Y AUTOMÁTICA

ESCUELA POLITÉCNICA SUPERIOR DE JAÉN

JAÉN, FEBRERO DE 2020

UNIVERSIDAD DE JAÉN
ESCUELA POLITÉCNICA SUPERIOR DE JAÉN

TESIS DOCTORAL

La memoria titulada: "Contribución al desarrollo de sistemas fotovoltaicos de alta concentración. análisis de nuevas configuraciones de módulos", presentada por Jesús Montes Romero, aspirante al título de Doctor en "Energías Renovables" ha sido realizada dentro del Departamento de Ingeniería Electrónica y Automática de la Universidad de Jaén, bajo la dirección del Dr. Juan de la Casa Higueras y el Dr. Eduardo Fernández Fernández.

Jaén, febrero 2020

El doctorando

Fdo. Jesús Montes Romero

Los directores de la Tesis

Fdo. Dr. Juan de la Casa Higueras

Fdo. Dr. Eduardo Fernández Fernández

Universidad de Jaén

TESIS DOCTORAL

EVALUACIÓN Y DESARROLLO DE TÉCNICAS PARA LA CARACTERIZACIÓN DE SISTEMAS FOTOVOLTAICOS A SOL REAL

TRIBUNAL EVALUADOR

Presidente:

Secretario:

Vocal:

Suplente:

Suplente:

Jaén, febrero de 2020

AGRADECIMIENTOS

En primer lugar, debo agradecer a Juan de la Casa por ofrecerme continuar trabajando en la Universidad de Jaén tras terminar mi trabajo Fin de Máster y por darme la oportunidad de realizar esta Tesis Doctoral, además de todo el apoyo que me ha dado desde el primer minuto.

También agradezco a Eduardo Fernández todo el esfuerzo, apoyo y trabajo que me ha ofrecido durante todos estos años y que, sin duda, seguirá ofreciendo en los años venideros, además de darme la posibilidad de realizar la estancia en Chipre.

Agradezco también todo el apoyo recibido por los compañeros del departamento de Ingeniería Electrónica, tanto a los que siguen aquí como a los que ya no se encuentran con nosotros.

También agradezco toda la ayuda y el trabajo que han prestado los compañeros de la Universidad del Nordeste en Argentina, como a los de las distintas Universidades del Perú que han colaborado con nosotros. Además de a los miembros del CIEMAT que han contribuido en los trabajos desarrollados.

Finalmente agradezco a los compañeros de la Universidad de Chipre por el excelente trato que han tenido conmigo durante los tres meses de estancia.

RESUMEN

Actualmente, las políticas energéticas mundiales fomentan el uso de fuentes renovables en su matriz energética. Este hecho, junto con la drástica bajada de precios de la tecnología fotovoltaica en la última década, ha supuesto un crecimiento exponencial de la misma. En un mercado tan competitivo como es el de producción de energía eléctrica, los grandes capitales invierten con el propósito de obtener un beneficio económico. Los altos niveles de inversión que se han realizado en esta tecnología durante el último lustro permiten afirmar que, hoy por hoy, la tecnología FV es madura, competitiva y ha entrado de lleno en el mercado de producción energética.

Aunque la gran mayoría de los módulos que se instalan en el mercado se fabrican utilizando tecnología clásica basada en silicio cristalino, se siguen realizando por parte de los fabricantes e investigadores nuevos productos o conceptos que persiguen aumentar la eficiencia y/o disminuir los costos, y, por tanto, mejorar la competitividad de la tecnología. Debido a esta continua evolución, se hace necesario realizar investigaciones detalladas acerca del comportamiento eléctrico que presenta el elemento fotovoltaico en condiciones de operación. En este sentido, el trazado de la curva característica I-V es el experimento esencial que permite obtener una mayor información sobre su comportamiento. Además, aplicando diferentes procedimientos, a partir de la curva I-V se pueden obtener otros parámetros de interés que permiten realizar modelos eléctricos equivalentes del funcionamiento de la célula, módulo o generador FV.

La presente Tesis Doctoral, desarrollada en el seno del grupo de Investigación en Energía Solar de la Universidad de Jaén, trata de dar solución a las principales limitaciones de los actuales sistemas de caracterización FV. Este grupo ha estado trabajado durante más de dos décadas en el desarrollo de equipamiento de laboratorio relacionado con los sistemas de caracterización de elementos fotovoltaicos a sol real. Además, otra de las líneas de investigación más destacadas del grupo durante estos últimos años ha sido la contribución al desarrollo y la interpretación del funcionamiento de las diferentes tecnologías FV, aunque con una mayor presencia en el estudio de tecnologías basadas en concentración con células tándem. Estas dos líneas de trabajo están íntimamente relacionadas, por lo que una unión de ambas en los desarrollos expuestos en la presente Tesis Doctoral está claramente justificada y tiene un gran interés científico.

Como principales resultados, se han propuesto dos sistemas de caracterización de dispositivos fotovoltaicos basados en dos premisas distintas. En primer lugar, se desarrolla un sistema modular y flexible a partir de instrumentación de laboratorio de propósito general y de plataformas de hardware libre. El segundo sistema desarrollado en el marco de la Tesis, se basa exclusivamente en plataformas de hardware libre y diseños electrónicos fácilmente replicables, que ha presentado una alta precisión a un coste muy reducido. Además, varios centros de investigación de alto prestigio en el sector, han corroborado una baja incertidumbre en las medidas de este prototipo.

Atendiendo a la segunda línea de trabajo, se han estudiado varios métodos sencillos de extracción de parámetros para analizar su grado de validez para caracterizar sistemas fotovoltaicos de tercera generación basados en células tándem. Además, se ha llevado a cabo un estudio más extenso del comportamiento de cada uno de estos parámetros en comparación entre tecnologías FV de silicio monocristalino y células tándem.

ABSTRACT

Today, global energy policies encourage the use of renewable sources in their energy matrix. This has led to an almost exponential growth in photovoltaic technology. In a market as competitive as the electricity production sector, large-scale capital is investing with the aim of making an economic profit. With such high levels of investment in this technology, it can be said that today PV technology is mature, competitive and has entered into the energy production market.

Although the majority of the modules installed on the market are manufactured using classic technology based on crystalline silicon, new concepts are still being proposed to increase efficiency and/or reduce costs, and therefore improve the competitiveness of the technology. Due to this continuous evolution, it is necessary to carry out detailed research on the electrical behaviour of the photovoltaic elements. In this sense, the plotting of the I-V characteristic curve is the essential experiment that gives most information about its behaviour. Furthermore, applying different procedures, other parameters of interest can be obtained from the I-V curve in order to obtain equivalent electrical models of the operation of the PV cell, module or generator.

The present PhD Thesis, developed within the Solar Energy Research Group of the University of Jaén, aims to provide a solution to the main limitations of the current PV characterization systems. This group has been working for more than two decades in the development of laboratory equipment related to the characterization systems of photovoltaic elements under real sun conditions. In addition, one of the most remarkable research lines of the group during the last years has been the contribution to the development and interpretation of the operation of the different PV technologies. Although this line of research has been more active in the study of technologies based on concentration with tandem cells, these two lines of work are closely related, so the combination of both in the advances described in this PhD Thesis is clearly justified and has a high scientific interest.

As main results, two systems for characterizing photovoltaic devices have been proposed. In first place, a modular and flexible system is developed from general purpose laboratory instrumentation and free hardware platforms. The second system, developed within the framework of the Thesis, is based exclusively on free hardware platforms and easily replicable electronic designs. This device has presented high accuracy at a very low cost. Moreover, several research centres of high prestige in the sector have corroborated a low uncertainty in the measurements provided by this prototype.

According to the second line of work, several simple parameter extraction methods have been studied to analyse their level of accuracy in characterising third generation photovoltaic systems based on tandem cells. In addition, a more extensive study has been carried out on the behaviour of each parameter in comparison between monocrystalline silicon PV technologies and tandem cells.

ÍNDICE GENERAL

ÍNDICE DE FIGURAS

ÍNDICE DE TABLAS

LISTA DE ACRÓNIMOS

CEM: CONDICIONES ESTÁNDAR DE MEDIDA.

FV: FOTOVOLTAICO.

IEC: *INTERNATIONAL ELECTROTECHNICAL COMMISSION*.

CSR: CONDICIONES A SOL REAL.

CRO: CONDICIONES REALES DE OPERACIÓN.

SFCR: SISTEMA FOTOVOLTAICO CONECTADO A RED.

CPV: CONCENTRACIÓN FOTOVOLTAICA (DEL INGLÉS, *CONCENTRATION PHOTOVOLTAIC*).

IDEA: INVESTIGACIÓN Y DESARROLLO EN ENERGÍA SOLAR.

SAD: SISTEMA DE ADQUISICIÓN DE DATOS.

OSHW: *OPEN-SOURCE HARDWARE ASSOCIATION*.

m-SI: SILICIO MONOCRISTALINO.

p-SI: SILICIO POLICRISTALINO.

HIT: *HETEROJUNCTION INTRINSIC THIN LAYER*..

SEM: MODELO EXPONENCIAL SIMPLE (DEL INGLÉS, *SINGLE EXPONENTIAL MODEL*).

CIEMAT: CENTRO DE INVESTIGACIONES ENERGÉTICAS MEDIOAMBIENTALES Y TECNOLÓGICAS

PVLABDER: LABORATORIO DE COMPONENTES Y SISTEMAS FOTOVOLTAICOS.

LABSOL: LABORATORIO DE ENERGÍA SOLAR.

UFRGS: UNIVERSIDADE FEDERAL DO RIO GRANDE DO SUL.

EMP: E*MERGING PATTERN MINING*

EVAEP: *EVOLUTIONARY ALGORITHM FOR EXTRACTING EMERGING PATTERNS.*

PERC: *PASSIVATED EMITTER REAR CELL.*

CER: CENTRO DE ENERGÍAS RENOVABLES.

PUCP: UNIVERSIDAD CATÓLICA DEL PERÚ.

UNI: UNIVERSIDAD NACIONAL DE INGENIERÍA.

JCR: *JOURNAL CITATION REPORT.*

SJR: *SCIMAGO JOURNAL & COUNTRY RANK.*

DOI: *DIGITAL OBJECT IDENTIFIER.*

LIA: LABORATORIO INDEPENDIENTE ACREDITADO.

GER: GRUPO DE ENERGÍAS RENOVABLES.

UNNE: UNIVERSIDAD NACIONAL DEL NORDESTE.

A/D: ANALÓGICO/DIGITAL.

CEAEMA: CENTRO DE ESTUDIOS AVANZADOS EN ENERGÍA Y MEDIO AMBIENTE.

SOG: *SILICONE-ON-GLASS*.

LISTA DE SÍMBOLOS

APE: ENERGÍA MEDIA DEL FOTÓN (DEL INGLÉS, AVERAGE PHOTON ENERGY) [eV].

TPR: TRUE PERCENTAGE RATIO [-].

FPR: FALSE PERCENTAGE RATIO [-].

SMR: SPECTRAL MATCHING RATIO [-].

I_{SC}: CORRIENTE DE CORTO CIRCUITO [A].

V_{OC}: TENSIÓN DE CIRCUITO ABIERTO [V].

P_M: POTENCIA MÁXIMA [W].

V_M: TENSIÓN EN EL PUNTO DE MÁXIMA POTENCIA [V].

I_M: CORRIENTE EN EL PUNTO DE MÁXIMA POTENCIA [V].

GR: RATIO DE CRECIMIENTO (DEL INGLÉS, GROWTH RATE) [-].

FF: FACTOR DE FORMA [-].

I_{ph}: CORRIENTE FOTOGENERADA [A].

I_0: CORRIENTE DE SATURACIÓN DEL DIODO [A].

R_s: RESISTENCIA SERIE [Ω].

R_{sh}: RESISTENCIA PARALELA [Ω].

m: FACTOR DE IDEALIDAD [-].

V: TENSIÓN [V].

I: CORRIENTE [A].

RMSE : RAÍZ CUADRADA DEL ERROR CUADRÁTICO MEDIO (DEL INGLÉS, ROOT MEAN SQUARE ERROR) [%].

NRMSE : RAÍZ CUADRADA DEL ERROR CUADRÁTICO MEDIO NORMALIZADO (DEL INGLÉS, NOMALISED ROOT MEAN SQUARE ERROR) [%].

MBE : ERROR DE SESGO MEDIO (DEL INGLÉS, MEAN BIAS ERROR) [%].

E_V: ERROR RELATIVO DE TENSIÓN [%].

E_I: ERROR RELATIVO DE CORRIENTE [%].

DNI : IRRADIANCIA NORMAL DIRECTA (DEL INGLÉS, DIRECT NORMAL IRRADIANCE) [W/m^2].

GNI : IRRADIANCIA GLOBAL EN EL PLANO DEL GENERADOR (DEL INGLÉS, GLOBALNORMAL IRRADIANCE) [W/m^2].

T_C: TEMPERATURA DE CÉLULA [˚C].

E_{IV}: ERROR RELATIVO DE LA CURVA I-V [%].

RE: ERROR RELATIVO (DEL INGLÉS, RELATIVE ERROR) [%].

AM: MASA DE AIRE (DEL INGLÉS, AIR MASS) [-].

1

INTRODUCCIÓN

En la actualidad, son muchos los gobiernos estatales que promueven políticas energéticas que fomentan el uso de fuentes renovables en su matriz energética (International Energy Agency, 2017). Se prevé que las técnicas de generación renovable cubran el 50% de la demanda de energía en Europa para el año 2030 y, al menos, el 80% para 2050 (Schneider Electric, 2018). Entre todas las fuentes renovables disponibles, destaca la energía solar fotovoltaica, ya que es la presenta una tasa de crecimiento más alta (Frankfurt School and UNEP, 2016) (SolarPower Europe, 2019). Ya no se pone en duda que la tecnología fotovoltaica se ha convertido en una opción que ofrece soluciones de carácter mundial a los graves problemas derivados del cambio climático o a la previsible escasez de recursos que se producirá por el agotamiento de los combustibles fósiles (BP, 2018) que, en la actualidad, cubren el mayor porcentaje de generación de energía eléctrica a nivel mundial (International Energy Agency, 2017). Los estudios más optimistas (Pam et al., 2017) estiman un escenario de generación eléctrica 100% renovable para el año 2050, con una tasa de origen fotovoltaica cercana al 70%.

Tal y como se puede apreciar en la Figura 1, el crecimiento de la tecnología fotovoltaica a nivel mundial en el siglo XXI ha sido casi exponencial. En 2018 se alcanzó un total de 509,3GW de potencia instalada en todo el mundo. Durante ese año, se instalaron 104,1GW, y las previsiones para el año 2019 son incluso mejores ya que se pronostica que se instalen 129GW (Publicover, 2019). Con carácter general, las inversiones que sustentan este crecimiento son de origen privado.

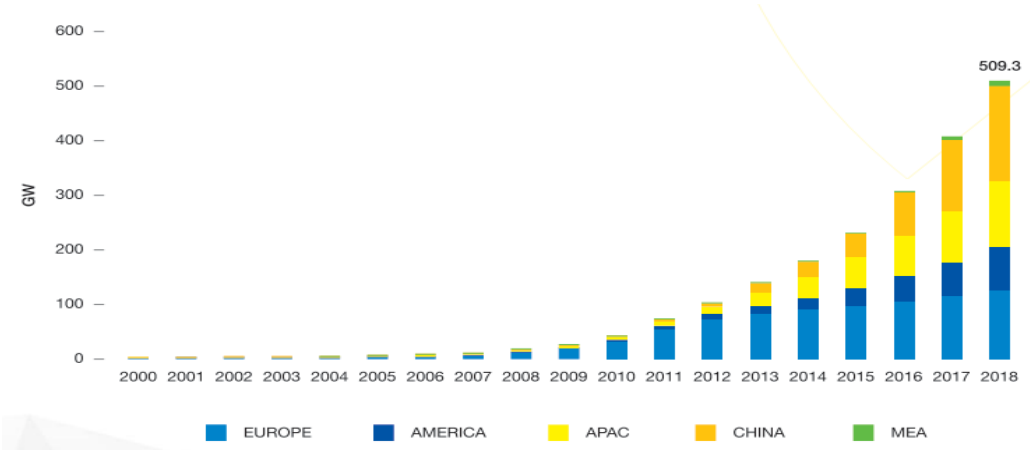

FIGURA 1. Evolución de la capacidad solar FV global total instalada en el periodo 2000-2018 (SolarPower Europe, 2019).

En un mercado tan competitivo como es el de producción de energía eléctrica, los grandes capitales invierten con el propósito de obtener un beneficio económico. Estas inversiones se han producido, aunque el precio final del kWh propuesto en las subastas de energía que se ha ofertado para grandes proyectos, pasó de 8 c$/kWh en el 2013 a menos de 2 c$/kWh en el año 2019. En la Figura 2, de elaboración propia, se muestra claramente esta tendencia. Según el portal Electrek, el precio mínimo para este periodo se alcanzó en 2017, con una oferta final de 1,77 c$/kWh, para una planta FV que operará en México. En febrero de 2018, se ofertó un precio de 2,34 c$/kWh en una planta FV de 300 MW en Arabia Saudita (SolarPower Europe, 2019). Datos recientes, julio de 2019, apuntan una oferta de 1,75 c$/kWh en Brasil (WILLUHN, 2019).

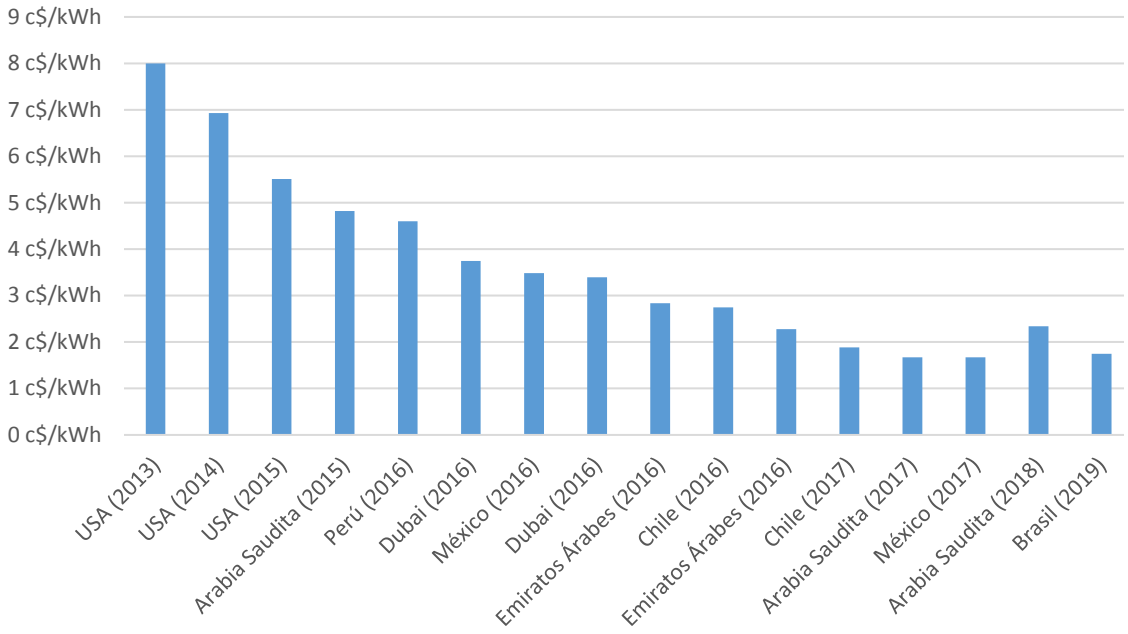

FIGURA 2. Evolución de las ofertas mínimas en subastas de energía solar fotovoltaica para grandes plantas (SolarPower Europe, 2019; WILLUHN, 2019).

Con estos niveles de inversión de capital, se puede afirmar que hoy por hoy, la tecnología FV es madura, competitiva y ha entrado de lleno en el mercado de producción energética a nivel de mayorista. Según un estudio de la asesora financiera Lazard (Lazard, 2018), a escala de decenas de MW, el precio del kWh que se produce utilizando tecnología FV en lugares de nuestro planeta adecuados para ello, es ya más barato que el generado utilizando como origen fuentes nucleares o de carbón, ver Figura 3. Incluso en aplicaciones de centenas de kW orientadas al autoconsumo (aplicaciones comerciales o en pequeñas y medianas industria), en función de las condiciones de recurso y económico-financieras de la inversión, se alcanzarían precios más bajos que las fuentes convencionales antes referidas. Aun así, sin duda, la tecnología FV no ha alcanzado su techo tecnológico, tanto desde el punto de vista de la investigación básica o aplicada, como desde el punto de vista de los productos comerciales que podrían llegar a ofertar las empresas del sector.

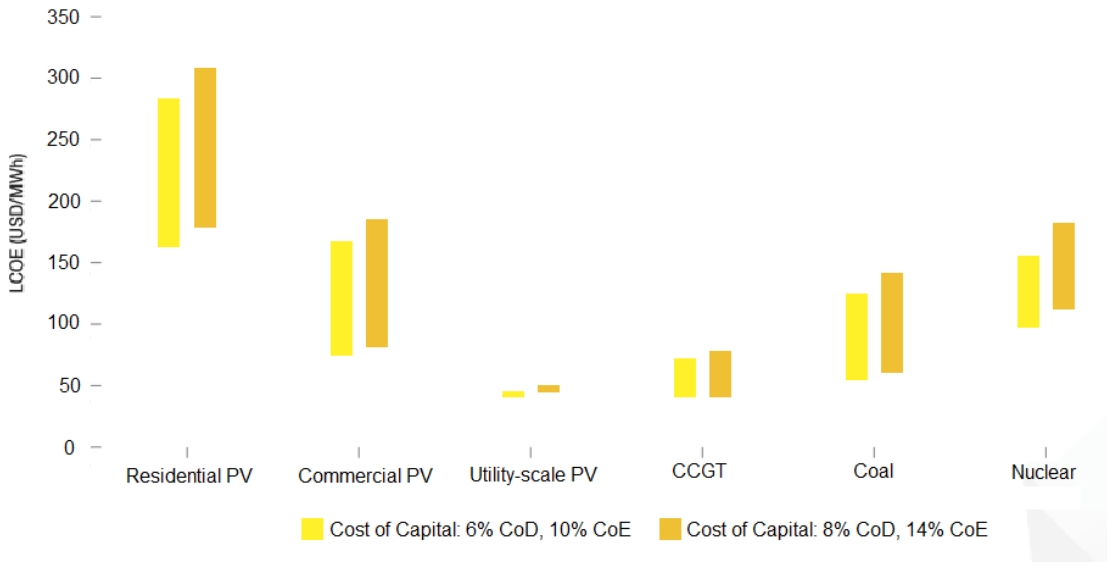

FIGURA 3. Coste de generación de energía solar fotovoltaica en comparación con otras fuentes de energía convencionales (Lazard, 2018).

Aunque actualmente, el 95% de los módulos que se instalan en el mercado se fabrican utilizando tecnología clásica basada en silicio cristalino (Fraunhofer Institute for Solar Energy Systems (ISE), 2018), un enorme número de grupos y centros de investigación están proponiendo nuevas conceptos que permitan aumentar su eficiencia y/o disminuir los costos, y por tanto, mejorar su competitividad. También las empresas del sector continúan invirtiendo en I+D+i para aumentar la calidad final de sus productos comerciales. Por ejemplo, cada vez son más las "seudo-nuevas" tecnologías (PERC, HIT o módulos construidos a partir de células bifaciales, etc.) basadas en silicio cristalino y herederas, en su proceso de fabricación, de los módulos de primera generación (Alaaeddin et al., 2019). Además, los fabricantes clásicos intentan aumentar la cuota de mercado de productos de 2ª generación (tecnología de capa fina o *Thin-film*) aumentando la eficiencia de éstos. Finalmente, no se puede obviar la investigación básica y aplicada que propone conceptos totalmente rompedores en tecnologías de tercera generación como la concentración FV basadas en células multiunión (Fernandez et al., 2018). En cualquier caso, sean cuales sean las tecnologías que dominen el mercado los próximos años, todas las previsiones indican que la energía solar fotovoltaica va a aumentar su contribución, y no de una manera marginal, al sistema energético mundial.

Desde el punto de vista de la investigación, son muchas las universidades, centros y grupos de todas partes del mundo que, desde hace pocos años, han incluido este tópico en sus intereses de trabajo y se han unido a los que ya investigaban desde hace tiempo en esta tecnología, con el objetivo de contribuir al desarrollo de la misma. En el ámbito educativo, la tecnología FV se ha convertido en una parte del conocimiento impartido en cualquier estudio universitario que aborde aspectos relacionados con la producción de energía eléctrica (Casa et al., 2012; Martin et al., 2016). Además, tal y como se aprecia en la Figura 4, este interés se ve reflejado en el crecimiento del número de publicaciones en la última década que abordan la temática.

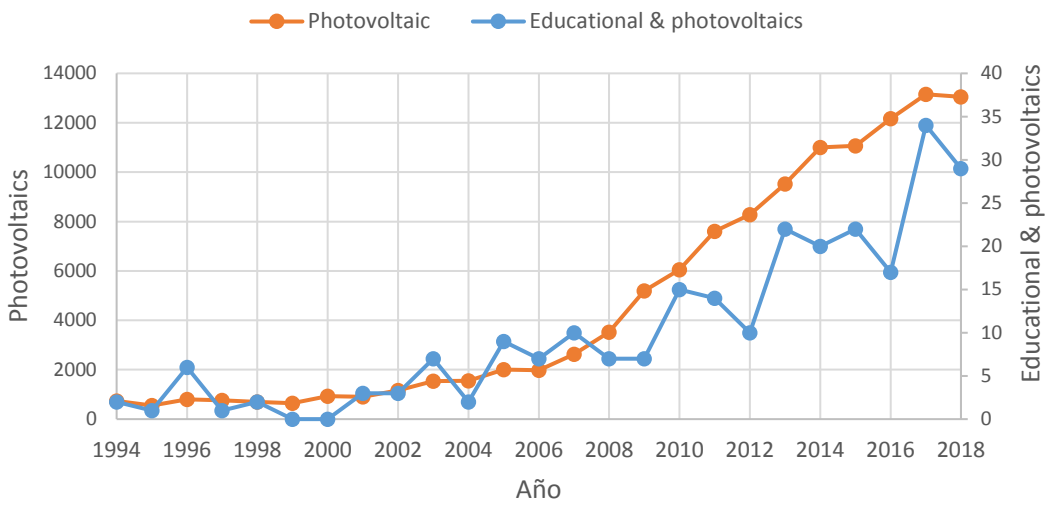

FIGURA 4. Evolución del número de documentos relacionados con educación y fotovoltaico según la base de datos Scopus.

En este escenario, tanto desde el punto de vista científico, como educativo o productivo, la caracterización del comportamiento eléctrico de las tecnologías fotovoltaicas actuales, y de las que están en desarrollo, es una cuestión de vital importancia; ya que, cada tecnología FV, va a tener un comportamiento distinto y variable en función de las condiciones medioambientales del lugar donde sea utilizada.

El elemento clave de cualquier sistema fotovoltaico, independientemente de su topología o aplicación, es el generador FV. Desde el punto de vista comercial, la unidad mínima es el módulo FV y desde el punto de vista científico es la célula FV. Dada la modularidad intrínseca de la tecnología, existirá la necesidad de caracterizar pequeños dispositivos de centenares de mW hasta grandes generadores de cientos de kW. Una correcta caracterización de su comportamiento eléctrico es imprescindible cuando se pretende realizar una estimación adecuada de la energía que podría llegar a generar este elemento (Tossa et al., 2014).

El trazado de la curva característica I-V de cualquier dispositivo fotovoltaico es el experimento esencial que permite obtener información fidedigna sobre su comportamiento (International Electrotechnical Commission, 2006). La curva I-V está formada por los infinitos pares de puntos tensión corriente en los que puede trabajar el dispositivo fotovoltaico para unas condiciones de operación dadas. Este conjunto de datos se obtiene variando en extremos del dispositivo de FV la impedancia de carga desde cero hasta infinito. Si se cuenta con un mínimo conjunto de puntos representativo es posible obtener todos los parámetros eléctricos característicos de interés, pero sin olvidar que su valor variará según las condiciones de operación a las que haya sido expuesto durante el trazado de la curva. En la Figura 5 se muestra un ejemplo de curva I-V típica de un dispositivo fotovoltaico. Los puntos de mayor interés de esta curva característica son: corriente de cortocircuito (I_{SC}), la tensión de circuito abierto (V_{OC}) y el punto de potencia máxima (P_M), que se encuentra definido por la tensión (V_M) y la corriente (I_M) de máxima potencia.

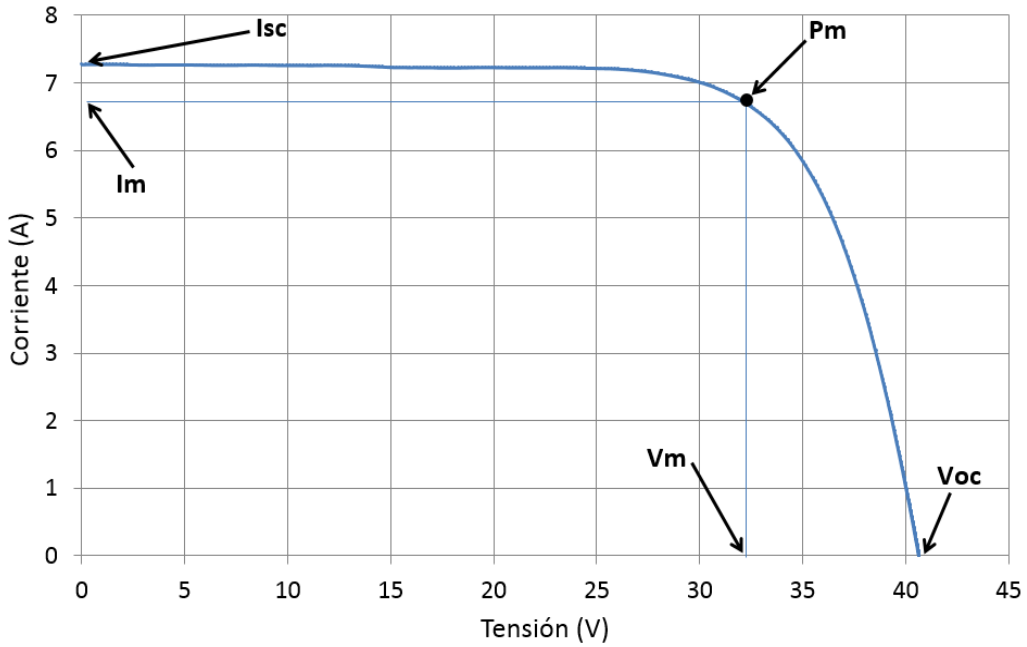

FIGURA 5. Curva característica I-V de un módulo fotovoltaico de tecnología de m-Si y la localización sus parámetros eléctricos básicos. La curva fue obtenida con 963 W/m2 de irradiancia y 46 ℃ de temperatura de célula.

En el caso de productos comerciales, los fabricantes de módulos FV proporcionan el valor de esos parámetros bajo unas condiciones medioambientales específicas, conocidas como Condiciones Estándar de Medida (CEM), que son definidas en la norma IEC 60891 (International Electrotechnical Commission, 2007a). Estas condiciones son 1000 W/m2 de irradiancia, 25˚C de temperatura de célula, espectro solar global AM1.5, definido en la IEC 60904-3, y con una incidencia de la radiación normal al módulo.

Además de aportar los parámetros eléctricos característicos, el conjunto de datos que conforma la curva I-V proporciona información que permite la detección de posibles anomalías en un módulo o generador FV. Por ejemplo, es posible encontrar defectos como sombreado parcial (García et al., 2008), degradación (Smith et al., 2012), *mismatch* (Picault et al., 2010) o incluso de suciedad (Piliougine et al., 2013). Un defecto en la curva puede provocar fallos en el seguimiento del punto de máxima potencia (Munoz et al., 2011; Sanchis et al., 2007), cuando, por ejemplo, se encuentre formando parte de un sistema de conexión a red, ocasionando, por tanto, una operación inadecuada.

Utilizando diferentes procedimientos (Humada et al., 2016) a partir de la información suministrada por la curva I-V, se pueden obtener otros parámetros de interés que permiten realizar modelos eléctricos equivalentes del funcionamiento de la célula, módulo o generador FV. Se pueden distinguir varios tipos de modelos eléctricos equivalentes, generalmente de diodo simple o diodo doble. Su diferencia reside en el número de diodos que dan lugar a una o dos corrientes de saturación. En la Figura 6 se muestra el circuito del modelo equivalente del diodo simple, que es el más usado hoy en día para el estudio del comportamiento de módulos en condiciones externas.

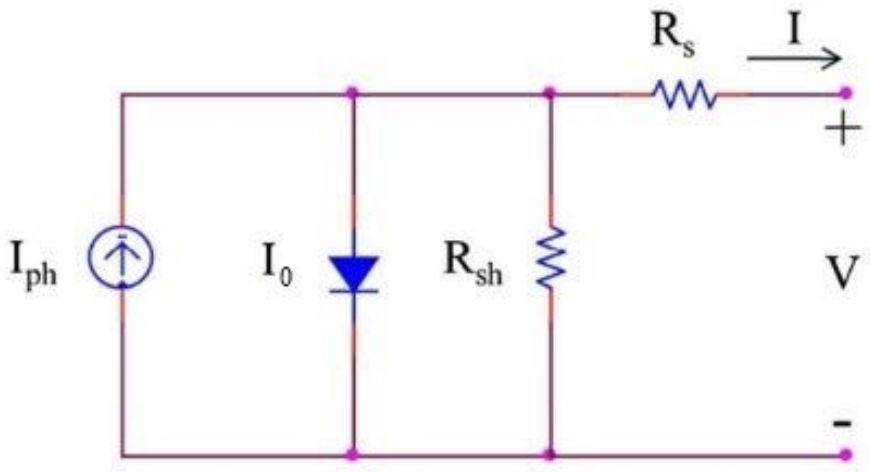

FIGURA 6. Circuito equivalente del modelo del diodo simple de un sistema fotovoltaico. I_{ph}: corriente fotogenerada, I_0: corriente de saturación del diodo, R_s: resistencia serie, R_{sh}: resistencia paralela, V: tensión de la célula, I: corriente de la célula.

Además del tipo de modelo utilizado, los métodos de extracción de parámetros pueden clasificarse en función del número de parámetros que el método extrae. Por ejemplo, para el caso del diodo simple, se pueden encontrar métodos que extraen desde uno hasta cinco parámetros distintos, que son: la corriente fotogenerada (I_{ph}), la corriente de saturación del diodo (I_0), el factor de idealidad del diodo (m), la resistencia serie (R_s) y la resistencia paralela (R_{sh}). Se debe tener en cuenta que, usando modelos de diodo doble, los parámetros I_0 y m son independientes para cada diodo, por lo que es posible obtener hasta siete parámetros en total.

Otra distinción que se puede hacer a estos métodos es según su forma de resolución, ya sea por métodos analíticos, numéricos o heurísticos. Los métodos numéricos requieren valores iniciales adecuados para converger y, por lo tanto, pueden resultar en una menor eficiencia cuando las condiciones iniciales están lejos de las condiciones óptimas (Yu et al., 2017). Por otro lado, los algoritmos heurísticos como el genético, la optimización por enjambres de partículas, las redes neuronales, etc., han demostrado ser una alternativa a los métodos numéricos, ya que no imponen ninguna restricción en la formulación del problema. Sin embargo, los métodos analíticos suelen ser preferibles debido a que son más fáciles de usar y pueden proporcionar resultados comparables en las condiciones de operación típicas de los dispositivos fotovoltaicos (Chan et al., 1986; Ghani et al., 2017).

Lo comentado en los anteriores párrafos resalta la importancia de obtener la curva I-V para obtener certezas acerca de la operación y rendimiento de la tecnología FV. Centrándose exclusivamente en el caso de células y módulos FV, existen dos posibles opciones tecnológicas para obtener la curva característica: medidas en interior utilizando simuladores solares (International Electrotechnical Commission, 2007b) y medidas en el exterior, que denominaremos como Condiciones Reales de Operación (CRO). En la Figura 7 se muestra un ejemplo de estos sistemas, ambos instalados en la Universidad de Jaén.

(a) (b)

FIGURA 7. Ejemplos de las opciones tecnológicas para obtener la curva característica: (a) medida en interior mediante un simulador solar y (b) medidas en exterior.

Un simulador solar es un sistema de laboratorio que tiene la capacidad de recrear la luz solar natural durante un periodo de tiempo. Su finalidad es proporcionar unas condiciones controladas y estables con las que se puedan realizar distintas pruebas en el módulo FV. Para esto, el simulador solar usa normalmente una o varias lámparas de alta potencia y precisión capaz de producir una determinada irradiancia y espectro. Además, los simuladores se clasifican en varias categorías, en concreto: A, B o C en función del contenido espectral, la uniformidad espacial y la estabilidad temporal (ASTM International, 2019; International Electrotechnical Commission, 2007b). La principal ventaja de estos sistemas es que permiten obtener la curva I-V en condiciones controladas de laboratorio, normalmente bajo las CEM comentadas anteriormente. Esto permite, entre otras cosas, reproducir con relativa facilidad las mismas condiciones de operación con las que los fabricantes caracterizan sus productos. Sin embargo, los simuladores solares presentan diversas limitaciones para la evaluación de módulos o sistemas FV. Una de ellas sería que están principalmente destinados a obtener los parámetros bajo las CEM, pero no pueden en ningún caso simular el amplio rango de operación al que se ve sometido un sistema a sol real. Además, este procedimiento no es aplicable para sistemas fotovoltaicos que presenten una superficie mayor que la del propio simulador y en ningún caso para realizar pruebas en generadores ya instalados. Otro inconveniente a tener en cuenta es su elevado coste, ya que normalmente necesitan lámparas de alta potencia que recrean el espectro solar, sensores de radiación usados como referencia, equipos de instrumentación de altas prestaciones y, en muchos casos, elementos ópticos de gran tamaño y precisión para lograr recrear de con forma precisa las características de la radiación en un área de iluminación determinado.

Por otro lado, la caracterización en CRO se realiza en el exterior mediante la exposición del módulo FV a la radiación solar. Esto permite el estudio de los módulos en un rango amplio de operación. Además, tiene la ventaja respecto a los simuladores solares de ser mucho menos costoso. Sin embargo, también cabe señalar que es extremadamente complicado que se produzcan unas condiciones ambientales similares a las CEM. De esta forma, surge la necesidad de utilizar métodos o modelos matemáticos de translación (International Electrotechnical Commission, 2007a) que permitan obtener características eléctricas en CEM a partir de las medidas tomadas de forma experimental en CRO. La bondad de cada uno de estos métodos aplicados a las diferentes tecnologías existentes en el mercado o las que están bajo desarrollo o investigación es un tema de frecuente estudio por parte de la comunidad científica (Fernández et al., 2016)(Appelbaum and Peled, 2014)(Or and Appelbaum, 2013).

Aun así, tanto con medidas en simulador, como con medidas en condiciones a sol real, es necesario disponer de un conjunto de bloques funcionales, que a partir de ahora denominaremos como sistema de trazado de curvas o de caracterización de elementos FV. Este conjunto se presenta una combinación de sistemas electrónicos, más o menos complejos, capaces de emular una variación de impedancia entre cero e infinito para, de este modo, realizar un barrido en todo el rango de funcionamiento de elemento FV. Además, cuenta con un equipamiento electrónico que se encarga de la medida, adquisición, control, almacenamiento y procesamiento de la información adquirida.

El esquema global que presentan este tipo de sistemas se muestra en la Figura 8. En general, el bloque variador de impedancia se encarga de realizar el barrido completo de la curva I-V del módulo FV variando su punto de operación. Para llevar a cabo esta tarea, se pueden distinguir distintos métodos que vienen resumidos en (Duran et al., 2008; Fernández et al., 2018), y entre los que destacan los bloques basados en carga electrónica, en carga capacitiva, en fuentes de alimentación de cuatro cuadrantes o en conversores DC-DC. El bloque de medida tiene la función de adquirir-acondicionar de manera simultánea los valores de tensión y corriente que conforman la curva característica, así como de los parámetros ambientales relevantes a los que se ha realizado el experimento. Todo el proceso, tanto de variación de impedancia como de medida, es gobernado por un bloque de control. Este bloque lo puede formar una gran variedad de componentes, que deberán ser elegidos en función del tipo de variador de impedancia seleccionado ya que, en función del proceso de barrido, se requieran unas características de control distintas. Este bloque también incluye todo el procesamiento de los datos obtenidos y la inteligencia para controlar todos los procesos que componen el sistema.

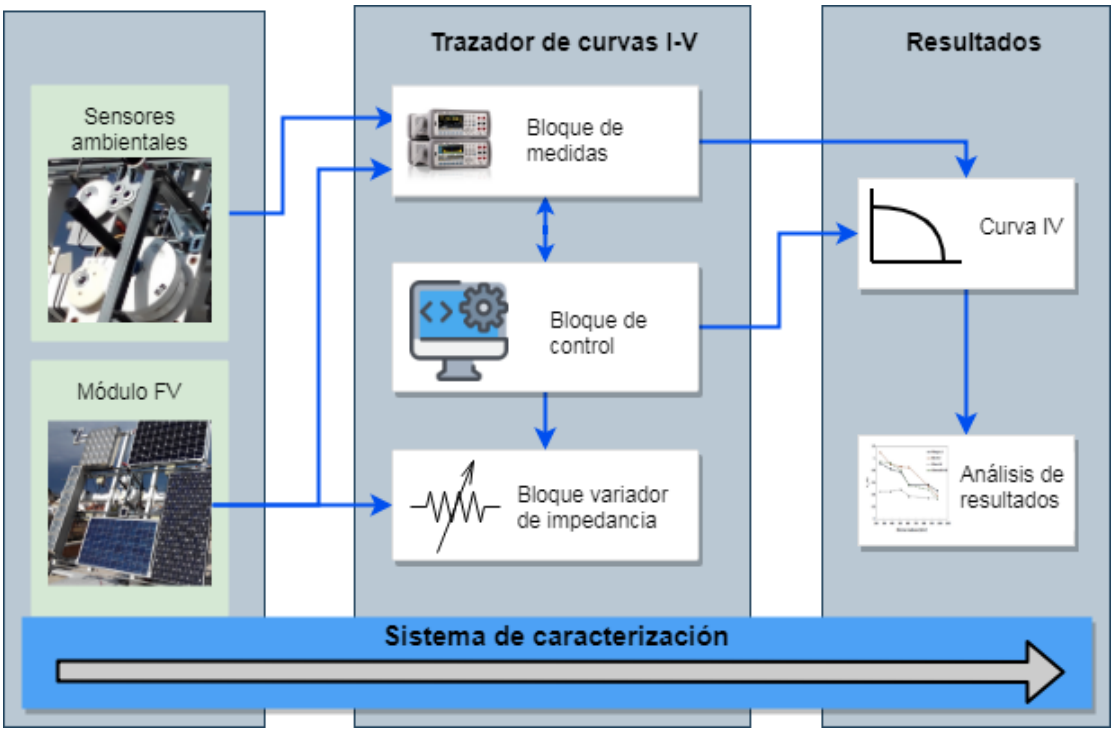

FIGURA 8. Diagrama de bloques básico de un sistema de caracterización de dispositivos FV.

Desde hace aproximadamente una década, y gracias al desarrollo comercial de la tecnología FV, los fabricantes de instrumentación ofrecen equipos comerciales que realizan el trazado de la curva I-V (Neuenstein J., 2009), existiendo actualmente en el mercado equipos tales como: PV-

Engineering, EKO, TRITEC, etc. (EKO Instruments, 2017; PV-Engineering GmbH, 2016; TRITEC Group, 2008). En general, los fabricantes ofrecen varias opciones destinadas a cubrir unas situaciones de medida muy concretas, especialmente aquellas que se orientan a realizar labores de mantenimiento de instalaciones. La mayoría de ellos están pensados para el trazado de la curva I-V a *strings* de módulos FV en grandes instalaciones por lo que se prioriza la portabilidad del equipo. Otros están diseñados para la medida de módulos en laboratorio. Por otro lado, también existen algunos cuyo margen de medida solo permite la caracterización de células FV, etc. En definitiva, de forma comercial es posible encontrar este tipo de equipos, pero cada uno de ellos ofrece un rango de medida específico, dando respuesta a unas condiciones muy concretas para que las medidas del sistema sean realmente fiables. Además, estos equipos son sistemas cerrados que cuentan con un software propietario que limita en número y variedad de sensores ambientales utilizables, no se ofrece ninguna, o muy poca, información sobre sus métodos de extrapolación, son difícilmente configurables para una campaña experimental continuada, etc. En definitiva, se puede concluir de forma general que estos son sistemas con un alto coste y baja flexibilidad.

Además de equipos comerciales, también es posible encontrar en la literatura un gran número de prototipos de trazadores de curvas I-V propuestos por diferentes grupos o equipos de investigación que trabajan en el desarrollo de la tecnología fotovoltaica (Erkaya et al., 2016, 2014; García-Valverde et al., 2016; Hemza et al., 2015; Leite et al., 2012; Piliougine et al., 2011; Rivai and Rahim, 2014). Todos ellos siguen sin dar una respuesta distinta a la que pueden dar los equipos comerciales mencionados anteriormente. De igual forma, son equipos que ofrecen soluciones muy concretas, presentan una limitada flexibilidad y tienen una potencialidad baja para el procesamiento de los datos experimentales obtenidos.

Por su directa relación con los temas abordados en esta Tesis Doctoral indicar que, en los últimos años, se ha producido una creciente tendencia del mercado de la electrónica en el que se oferta una gran cantidad de plataformas de hardware libre, aumentando paralelamente la oferta de componentes electrónicos que pueden ser usados de forma sencilla, ya que muchos de éstos están preparados para su uso directo, aunque los conocimientos de diseño electrónico del usuario final sean mínimos.

La Open-Source Hardware Association (OSHW) define el hardware libre como "hardware cuyo diseño es hecho públicamente disponible para que cualquiera pueda estudiar, modificar, distribuir, crear y vender el diseño o el hardware basado en ese diseño". Estas plataformas se caracterizan por tener unos precios muy competitivos y permitir el diseño de hardware para un propósito específico con unas altas prestaciones en relación a su coste y de una forma muy sencilla. Debido a estas características, se ha incrementado de manera muy importante el número de científicos de múltiples áreas del conocimiento que utilizan este tipo de propuestas para llevar a cabo sus trabajos de investigación, ver Figura 9.

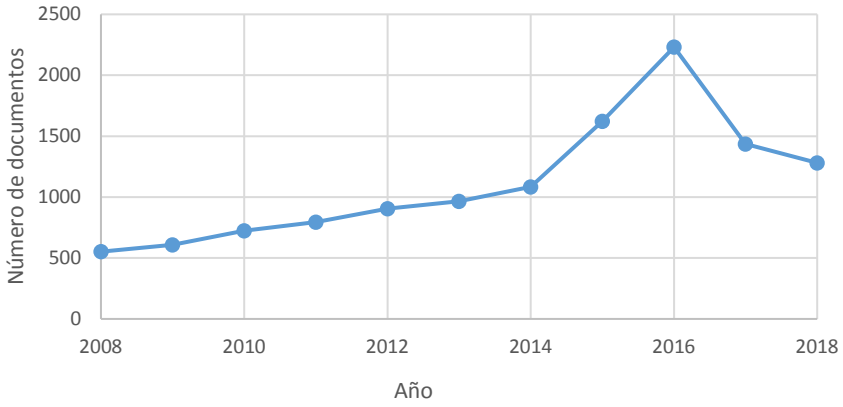

FIGURA 9. Evolución del número de documentos relacionados con "open hardware" según las bases de datos de Scopus.

Esta tesis doctoral trata de dar solución a las principales limitaciones de los actuales sistemas de caracterización FV comentadas anteriormente. Además, por los motivos previamente detallados, se ha estimado que las plataformas de hardware libre son adecuadas para la construcción, parcial o completa, de los equipos que forman los sistemas caracterización de elementos FV. LabVIEW ha sido ampliamente adoptado en el ámbito de las pruebas automatizadas, convirtiéndose en el estándar en ese espacio de aplicación, y ganando terreno en el ámbito de la supervisión y el control. Su uso no se limita exclusivamente al ámbito industrial, también ha conseguido una gran popularidad en investigación y docencia (Azaklar and Korkmaz, 2010; Hammoumi et al., 2018). Una de sus características principales es la facilidad en la conexión y control de todo tipo de instrumentos comerciales y de hardware libre ya que incluye una interfaz gráfica interactiva con la que el usuario puede operar el sistema, modificar variables, mostrar resultados, etc. Todas estas características la convierten en una plataforma ideal para el desarrollo de los sistemas de caracterización abordados en esta Tesis.

2

ANTECEDENTES, JUSTIFICACIÓN, HIPÓTESIS Y OBJETIVOS

Por todos los argumentos expuestos durante la introducción, el Grupo de Investigación y Desarrollo en Energía Solar (IDEA) de la Universidad de Jaén ha identificado un problema real relacionado con la caracterización de elementos fotovoltaicos a sol real mediante su curva I-V. El diseño de instrumentos de medida complejos que permitan abordar este problema, su aplicación a proyectos de investigación y, la transferencia del conocimiento adquirido durante este proceso a distintos grupos o universidades, ha sido uno de los tópicos de investigación abordados por el grupo IDEA desde su creación a finales del pasado siglo.

El problema identificado se resume en: los equipos comerciales son poco flexibles, tienen un coste alto y, en la mayoría de las, ocasiones no ofrecen funciones imprescindibles para la investigación o éstas no se ajustan a lo deseado por los usuarios. Las opciones comerciales no están preparadas para realizar una campaña automática de medida, ni incorporan la posibilidad de realizar medidas sincronizadas y centralizadas de múltiples parámetros medioambientales de manera simultánea al trazado de la curva I-V. Asimismo, no cuentan con la capacidad de extraer otros parámetros de interés del espécimen a estudio ni procesar los datos de una campaña experimental profunda. Por último, y más importante, no son "sistemas abiertos", por lo tanto, difícilmente el usuario final los podrá reconfigurar según sus intereses o necesidades de investigación.

Si se repasa los antecedentes de la presente Tesis Doctoral, se destaca que, aunque existen algunas versiones previas (Garrido, 2000; Guzmán Martínez, 2000), ya en 2002, el grupo IDEA transfirió a la Universidad del Valle (Guatemala) un prototipo de sistema para el trazado de curvas I-V a módulos FV que fue publicado en (Bello et al., 2009; Nofuentes et al., 2003). Este sistema, basado en carga capacitiva, tenía un control manual, usaba un osciloscopio de dos canales independientes para obtener la medida de la curva I-V y era una versión mejorada de la versión propuesta por Blaesser en los Guidelines (Blaesser and Munro, 1995a, 1995b) pero adaptada al ensayo de pequeñas potencias. Nuevas versiones de un instrumento similar al anteriormente citado, pero orientadas a la caracterización de generadores FV fueron presentadas en (Muñoz et al., 2011). En este trabajo, heredero del publicado por el Instituto de Energía Solar en (Muñoz and Lorenzo, 2006), el grupo IDEA presenta por primera vez un desarrollo propio de trazador de curvas, que incluye una versión automatizada de todo el proceso de medida, gracias a la inclusión en el bloque de control de un microcontrolador de bajo coste. Paralelamente, el grupo exploró soluciones automatizadas en la que se utilizan convertidores DC-DC como bloque de variación

de impedancia (Bertolín et al., 2012), obteniéndose resultados previos muy interesantes, que todavía no han sido lo suficientemente explotados científicamente. En el apartado de futuras líneas de investigación de la presente Tesis se plantearán algunos posibles temas de investigación directamente relacionados con esta última idea.

Los desarrollos citados anteriormente, no dejaban de ser una versión propia de lo que comúnmente se conoce como trazador de curvas I-V. Al ser diseñados e implementados en el seno del Grupo, podían ser construidos adaptándose a una aplicación concreta, pero distaban mucho de lo que se podría denominar un "Entorno automático de caracterización de módulos FV". Este concepto comenzó a desarrollarse tras la concesión de varios proyectos del Plan Nacional de I+D a principios de la presente década (ENE 2008-05098; ENE2009-08302; eIPT-2011-1468-920000; TEP2009-5045M), que tenían como uno de sus objetivos principales la caracterización del comportamiento a sol real de diferentes tecnologías FV emergentes, fundamentalmente módulos FV comerciales de 2ª y 3ª generación, y su comparación con las tecnologías clásicas basadas en silicio cristalino. Como un antecedente fundamental de la presente Tesis Doctoral, se procederá a continuación a describir los diseños desarrollados en esa época, que más que como entornos automáticos de "caracterización", podrían definirse como "*sistemas automáticos de trazado de curvas I-V con registro de las condiciones de operación*".

El primero de ellos (Figura 10) fue desarrollado con el objeto de ofrecer el soporte experimental a un proyecto cuyo objetivo principal era la evaluación de la influencia de la distribución espectral en el comportamiento energético de diferentes módulos comerciales de lámina delgada. Se puso en marcha a principios del año 2010, dando lugar a una Tesis Doctoral (Torres-Ramírez, 2015), y a más de 10 publicaciones de impacto. El sistema, todavía en operación (Nofuentes et al., 2017; Silvestre et al., 2016), permite la medida secuencial automatizada de la curva I-V de cuatro módulos FV. De manera simultánea, se obtiene la temperatura de operación de los mismos, la irradiancia incidente en el plano, su distribución espectral, la temperatura ambiente y la corriente de cortocircuito de otros cuatro módulos de igual modelo y fabricante.

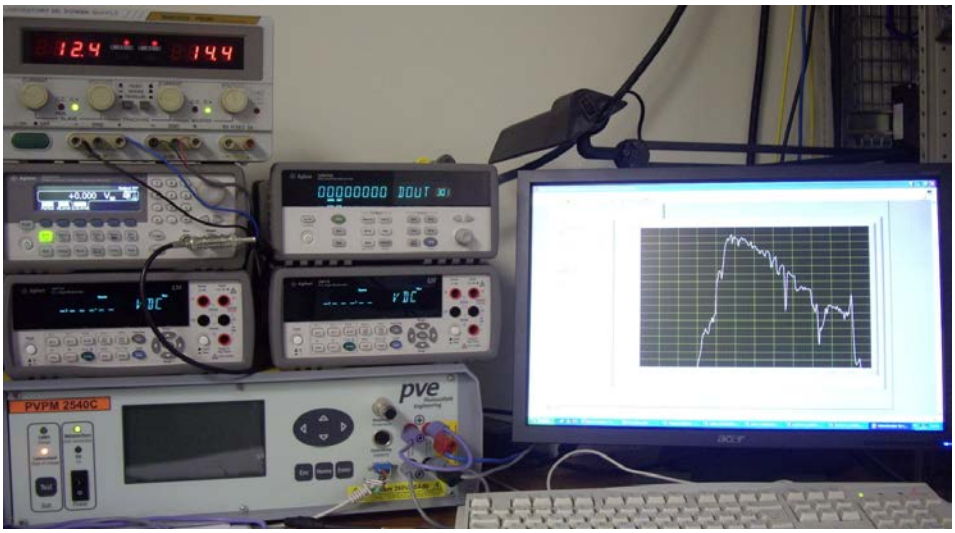

FIGURA 10. Primer sistema automático de trazado de curvas I-V con registro de condiciones de operación desarrollado por el grupo IDEA en el año 2010.

Como breve resumen técnico, este sistema lo constituye un trazador de curvas I-V comercial PVPM 1000C40 del fabricante pve Photovoltaic Engineering, que es usado exclusivamente como

carga capacitiva. La medida de los pares I-V se realiza con dos multímetros Agilent 34411A, uno para la medida de tensión y otro para la medida de corriente, siendo ésta realizada de forma indirecta mediante una resistencia shunt. Para asegurar la completa sincronización de ambos instrumentos de medida, se usa un generador de funciones Agilent 33220A conectado a la señal de disparo de los multímetros. Para la medida de los parámetros ambientales que marcan las condiciones de operación se utiliza un sistema de adquisición de datos HP 34970A. Se completa el sistema con varios diseños electrónicos propios, basados en relés de estado sólido y electromecánicos, que permiten la medida secuencial de hasta cuatro módulos FV. Todos los instrumentos comerciales que componen el sistema están conectados a un PC mediante puertos GPIB para poder ser controlados con una aplicación desarrollada en LabVIEW. El software desarrollado permite la automatización del trazado de la curva I-V, la obtención de parámetros ambientales y el almacenamiento ordenado de todos los datos adquiridos. Como es lógico, en las primeras fases de desarrollo de cualquier sistema de medida complejo, se persigue como característica principal del diseño, su robustez y fiabilidad. En esta búsqueda, el uso de una amplia cantidad de instrumentos comerciales de altas prestaciones está justificado, aunque su coste final total se acercara a los 15.000€.

En cualquier caso, una vez confirmado el correcto funcionamiento del sistema y su utilidad, era necesario la propuesta de posibles mejoras. Un primer análisis de la solución adoptado reveló que, uno de sus mayores inconvenientes era la gran cantidad de instrumentos comerciales implicados en su diseño que, sin mejorar las prestaciones del sistema, sí aumentan significativamente su coste total.

Otra de las líneas de investigación más destacadas del grupo durante estos últimos años ha sido contribución al desarrollo y la interpretación del funcionamiento de la tecnología FV de concentración a sol real. Prueba de ello son las cinco tesis doctorales leídas en este tema en el seno del grupo (Fernández, 2012; Ferrer-Rodríguez, 2018; García-Domingo, 2014; Moya, 2017; Rodrigo Cruz, 2013) y las más de 60 publicaciones de impacto directamente relacionadas con esta temática. Para la obtención de estos resultados científicos ha sido imprescindible desarrollar los entornos de medida adecuados.

Con relación a esta última línea de investigación, a finales de 2010 se puso en marcha un sistema para el trazado automático de curvas I-V de módulos de tecnología FV de concentración en el laboratorio A3-451 de la Escuela Politécnica Superior de Jaén, expuesto en mayor amplitud en (Muñoz et al., 2014), y del que se puede observar un esquemático básico en la Figura 11. La filosofía utilizada durante su diseño fue muy similar a la que se utilizó en el anterior sistema, aunque incorporaba algunas modificaciones que reducían el número de equipos comerciales utilizados para implementar el sistema de trazado de la curva I-V y, al estar orientado a la caracterización de módulos de concentración, se incluyó un seguidor solar a dos ejes donde se fijaron tanto los módulos FV como la instrumentación necesaria para su evaluación. Las modificaciones más destacadas de este sistema fueron la eliminación del generador de funciones, ya que su función pudo ser realizada mediante unas señales de control generadas por el sistema de adquisición de datos presente en el sistema. También se sustituyó el trazador de curvas I-V comercial por una carga capacitiva diseñada por los investigadores del grupo IDEA.

Ambos puestos de laboratorio presentan una gran robustez y fiabilidad. Esto ha quedado demostrado con su funcionamiento ininterrumpido durante años, y aunque éste último es más económico, con un coste total aproximado de 7.500€ (considerando únicamente el sistema destinado a trazar la curva I-V y la adquisición y procesado de datos), se estima que puede ser

mejorable en múltiples aspectos. Cabe destacar que las prestaciones de este sistema son idénticas a las del sistema anterior, a excepción, por supuesto, del seguidor solar en el que se sitúan los módulos FV de este sistema de medida. Una vez finalizados los proyectos de investigación que dieron origen a su puesta en marcha, este sistema se utiliza actualmente para el desarrollo de diferentes experimentos y pruebas entre los que se puede destacar la comparativa entre distintos métodos de trazado de la curva I-V, como pueden ser la carga capacitiva, fuentes de cuatro cuadrantes, etc.

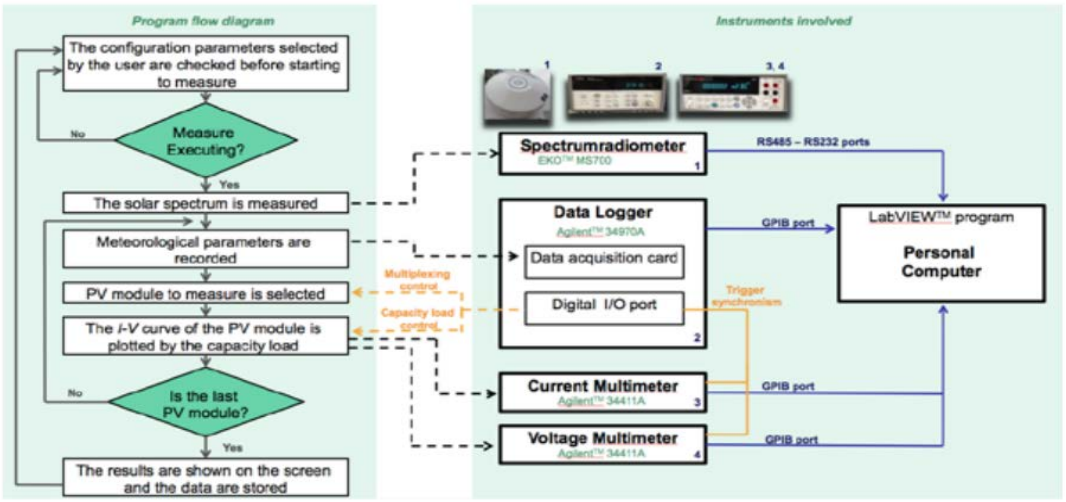

FIGURA 11. Esquemático de los elementos que componen el sistema de medida junto con el flujograma de control.

Finalmente, cabe señalar la experiencia del grupo de investigación en proyectos de cooperación científica con universidades Latinoamérica. Entre estas colaboraciones, destacan la puesta en marcha de un sistema automático de trazado de curvas I-V con registro ambiental equivalente al desarrollado por el grupo IDEA, instalado en el Centro de Energías Renovables (CER) en Lima, ver Figura 12. Paralelamente, también se han desarrollado sistemas de monitorización de parámetros eléctricos de un sistema FV conectado a red mediante hardware comercial de Carlo Gavazzi. y de parámetros ambientales mediante una estación EKO WS-500, sincronizados junto con los parámetros eléctricos. Además, se ha añadido el uso de un SAD GL220 junto a la estación meteorológica para recoger un mayor número de parámetros ambientales mediante sensores externos como son piranómetros, sensores de temperatura, etc.

FIGURA 12. Réplica de la segunda versión del sistema automático de trazado de curvas I-V con registro de condiciones de operación desarrollado por el grupo IDEA e instalado en la UNI de Lima, Perú.

Sin olvidar que el propósito de los sistemas de caracterización es el estudio del comportamiento de las tecnologías FV, también cabe destacar la experiencia previa del grupo en el estudio y desarrollo de métodos de extracción de parámetros de la curva I-V. El estudio de estas variables en función de los parámetros ambientales, ha sido una de las formas empleadas por el grupo de investigación para estudiar el comportamiento de algunas tecnologías FV (Almonacid et al., 2016; Fernández et al., 2017; Rodrigo et al., 2013).

Cabe destacar que el autor de la presente Tesis Doctoral ha estado involucrado de una u otra manera en los trabajos que ha realizado el Grupo en esta línea desde junio de 2014, cuando realizó su Trabajo Fin de Máster (Montes Romero, 2014). En ese trabajo previo, se comenzó el desarrollo de una versión mejorada del sistema de trazado I-V comentado anteriormente mediante la sustitución del sistema de adquisición de datos por elementos de hardware libre.

En **resumen**, el grupo IDEA ha estado trabajado durante más de dos décadas en el desarrollo de equipamiento de laboratorio relacionado con los sistemas de caracterización de elementos fotovoltaicos. Además, una de las líneas prioritarias del grupo ha sido la caracterización y modelado a sol real de nuevas tecnologías FV. Estas dos líneas de trabajo están íntimamente relacionadas, por lo que una unión de ambas en los trabajos desarrollados en la presente Tesis Doctoral está claramente justificada, y bajo nuestro criterio, tienen un gran interés científico. Se han detectado una serie de debilidades en el equipamiento que en la actualidad oferta el mercado o en los sistemas Ad-Hoc diseñados y publicados hasta la fecha por nuestro grupo de investigación u otros que trabajan en la temática (Hemza et al., 2015; Leite et al., 2012; Leite and Chenlo, 2010; Piliougine et al., 2011; Yandt et al., 2015). Esta debilidad abre un amplio abanico de oportunidades para realizar un trabajo de investigación en esta línea, más aún, si se tienen en cuenta las fortalezas, intereses y relaciones internacionales del grupo de investigación descritos en este apartado.

En concreto, los problemas de investigación a los que el presente trabajo pretende dar respuesta pueden resumirse en los siguientes puntos:

1.- Los sistemas comerciales disponibles para el trazado de la curva característica de dispositivos FV se caracterizan por ser entornos muy cerrados, poco flexibles y no estar orientados a la investigación.

2.-Las soluciones presentadas hasta la fecha tienen unos altos costes y no cuentan con capacidad de procesamiento en tiempo real de las campañas experimentales que realizan.

3.- Las tecnologías FV en fase de desarrollo, tales como la concentración FV, necesitan entornos de caracterización que permitan realizar de forma automática campañas experimentales completas y, en los que además, se pueda configurar todos los elementos que conforman el sistema de medida. Campañas experimentales automatizadas y diseñadas a medida permitirán mejorar su interpretación y, a la postre, su rendimiento.

Los trabajos que se exponen en la presente Tesis Doctoral han partido de la siguiente **hipótesis**:

- Las plataformas comerciales de hardware libre de bajo coste disponibles actualmente en el mercado son válidas para diseñar nuevos entornos o sistemas de caracterización de sistemas fotovoltaicos a un coste mucho más reducido, más flexibles en cuanto a sus rangos de medida, y con mayores prestaciones y capacidad de proceso en tiempo real de los datos obtenidos durante cualquier campaña experimental.

Que la comunidad científica disponga de diseños en abierto de sistemas con este potencial, fomentará el desarrollo de la tecnología FV y la interpretación del funcionamiento de nuevas tecnologías emergentes como es el caso de la fotovoltaica de concentración. Por tanto, **el objetivo principal** de la Tesis Doctoral ha sido la **búsqueda, evaluación y propuesta de posibles soluciones que contribuyan al equipamiento de laboratorio orientado a la caracterización de elementos fotovoltaicos**. Además de la posterior **aplicación** de los resultados obtenidos a la mejor interpretación de **tecnologías FV emergentes**. Para alcanzar este objetivo general se han planteado los siguientes objetivos específicos:

1. Identificarlos problemas y soluciones actuales de los sistemas de caracterización de elementos FV y proponer nuevas arquitecturas para su mejora, incluyendo la construcción y validación experimental de las alternativas hardware-software seleccionadas.

2. Diseñar y ejecutar una campaña experimental de caracterización de diferentes tecnologías FV, con especial hincapié en los módulos de concentración basados en células de 3ª generación.

En el siguiente capítulo se describirán las tareas realizadas con el fin de alcanzar cada uno de los objetivos específicos, así como el objetivo principal de esta Tesis. Cabe señalar que se han alcanzado de forma satisfactoria todos los retos planteado mediante aportaciones a los equipos de caracterización, así como de la propia caracterización de elementos FV, centrándose este último mayormente en la tecnología de concentración.

3

RESULTADOS

En esta sección se expondrá un resumen de los principales resultados obtenidos durante la realización de la presente Tesis Doctoral, y de cómo los mismos, han permitido la consecución de los objetivos propuestos en el plan de investigación original.

A fecha de depósito del presente documento, la mayor parte de estos resultados han sido ya difundidos entre la comunidad científica que investiga en el sector gracias a su publicación en revistas indexadas que ocupan puestos en el primer y segundo cuartil de las listas de la categoría de *Energy & Fuels* del *Journal Citation Report* (JCR). Otros resultados obtenidos han sido presentados en congresos internacionales y publicados de manera íntegra en sus actas que, en todos los casos, se encuentran indexadas en las listas *Scimago Journal & Country Rank* (SJR).

Se destaca también como resultado relevante de los trabajos realizados que las investigaciones han permitido concluir con el diseño, implementación y validación experimental, en dos laboratorios independientes acreditados de prestigio internacional, de un prototipo de sistema de caracterización para módulos fotovoltaicos construido utilizando exclusivamente elementos de hardware libre. Toda la documentación relativa a su construcción y puesta en marcha se encuentra a libre disposición de la comunidad académico-científica internacional.

3.1. CONEXIÓN ENTRE LAS PUBLICACIONES Y LOS OBJETIVOS ESPECÍFICOS DE LA TESIS

Los dos objetivos específicos propuestos en esta Tesis Doctoral tienen una clara relación, están subordinados parcialmente, y han sido logrados de manera secuencial. En primer lugar, se pretendió el desarrollo y validación de sistemas de caracterización que cubrieran el vacío de instrumental específico detectado y expuesto en los apartados anteriores. Estos sistemas deberían de ser lo suficientemente versátiles para adaptarse a las múltiples circunstancias o necesidades que se pueden presentar en una campaña experimental cuyo propósito sea un análisis exhaustivo en tiempo real. A partir de estos sistemas, se han diseñado experimentos específicos de caracterización con el fin de realizar estudios del comportamiento de distintas tecnologías FV. De especial importancia son los logros alcanzados en el análisis del comportamiento de módulos de tecnología CPV, ya que éstos se caracterizan por una mayor complejidad en su funcionamiento.

3.2. PUBLICACIONES RELACIONADAS CON EL OBJETIVO ESPECÍFICO 1

El primer objetivo específico se define como "*Análisis de las soluciones actuales para la caracterización de elementos FV. Identificación de las carencias que presentan y propuesta de nuevas arquitecturas para su mejora, incluyendo la construcción y validación experimental de las alternativas hardware-software seleccionadas*" y es abordado en las siguientes publicaciones:

Publicación 1

Título	**"Photovoltaic Device Performance Evaluation Using an Open-Hardware System and Standard Calibrated Laboratory Instruments"**
Autores	Montes-Romero, Jesús; Piliougine, Michel; Muñoz, José Vicente; F. Fernández, Eduardo; de la Casa, Juan
Revista	Energies
Volumen, número, año	10, 1869, 2017
Categoría y posición	ENERGY AND FUELS (48/97)
Factor de impacto	2,676 (2017)
DOI	10.3390/en10111869

En esta publicación, y tras una extensa revisión bibliográfica, se exponen algunos de los principales problemas y carencias encontrados en los equipos de caracterización disponibles actualmente en el mercado o en las propuestas de sistemas ad-hoc realizadas por otros investigadores.

Entre los principales problemas encontrados en los primeros se destaca que, cada equipo comercial, se centra en cubrir una situación de medida concreta, situación que fue puesta de manifiesto en el capítulo anterior del presente documento.

En este artículo, también se analizaron las propuestas presentadas por la comunidad científica que pretenden dar respuesta al problema y se han detectado inconvenientes similares a los presentados por los equipos comerciales. Se destacan las soluciones previas presentadas por el grupo IDEA (Muñoz et al., 2011), (Muñoz et al., 2014), que solventan parte de los problemas enumerados anteriormente como por ejemplo, problemas de sincronización en las medidas con fuentes de cuatro cuadrantes (Piliougine et al., 2011). En cualquier caso, estas soluciones tienen el inconveniente de su alto coste debido al equipamiento comercial requerido.

En esta aportación se presenta con detalle el desarrollo y evaluación de un sistema de caracterización basado en instrumentación de propósito general, en este caso dos multímetros comerciales de alta gama, y sistemas de hardware libre. Una de las características que se perseguían, durante la fase de diseño de este prototipo, fue que el diseño presentara una estructura modular, y de este modo, el equipo pueda ser configurable realizando cambios menores en el hardware del sistema. Además, mediante el uso de instrumentación de propósito general, se aseguran unos márgenes de precisión en la medida de los parámetros eléctricos previamente certificados por el fabricante del instrumento. Además, los multímetros son equipos de fácil uso, comúnmente presentes en cualquier laboratorio de investigación o de docencia en la rama de electricidad-electrónica, por lo que, con un coste muy bajo, cualquier institución podría replicar el sistema propuesto.

El esquema general de la solución propuesta se muestra en la Figura 13.

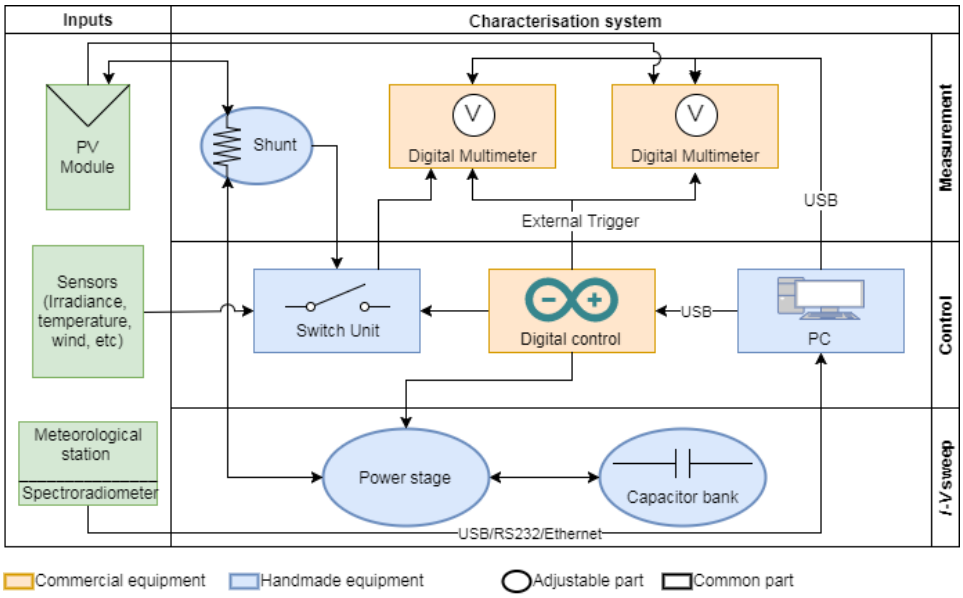

FIGURA 13. Esquema general del sistema de caracterización.

El prototipo experimental propuesto ha sido implementado usando dos multímetros Keysight 34465-A, que realizan de manera simultánea las medidas de tensión y corriente del módulo FV, así como, de los parámetros meteorológicos medidos por los distintos sensores analógicos conectados al sistema. Al disponer exclusivamente de dos canales independientes para la medida, se implementó una placa multiplexora de diseño propio que permite registrar múltiples señales. De este modo, el multímetro A se encargará de medir exclusivamente la tensión del módulo FV. El multímetro B, gracias al bloque multiplexor, medirá tanto la corriente del módulo FV – de manera indirecta gracias a una resistencia shunt calibrada- como los distintos sensores meteorológicos instalados –irradiancia, temperatura, etc. La decisión de incluir un bloque multiplexor ofrece ventajas, entre las que destaca la posibilidad de ampliar, solo por software, el número de canales implementados durante su fase de diseño, en función del número de parámetros ambientales que sea necesario registrar.

Por otra parte, para realizar el barrido de la curva I-V, se ha usado una carga capacitiva. Este bloque funcional estará gobernado por interruptores que controlan la conexión entre el elemento FV y el condensador. Aunque hay una amplia variedad de dispositivos válidos para realizar la conexión entre ambos elementos, en la configuración experimental publicada, se eligió un tiristor para conectar el módulo FV a la carga capacitiva y relés electromecánicos y de estado sólido para controlar la precarga y descarga del mismo.

Como elemento de control se usa una plataforma de hardware libre Arduino UNO que a su vez es controlada mediante un PC. La placa Arduino genera las señales de control necesarias para el proceso de medida que, en el sistema descrito, se usan para las fases de precarga, carga y descarga del condensador, generar el pulso de sincronismo de los multímetros para el proceso de medida y, por último, para controlar la conexión de los sensores meteorológicos y la resistencia *shunt* por medio del bloque multiplexor. El PC es el elemento que indica a la placa Arduino cuándo realizar cada uno de los procesos.

Un esquema más detallado de la etapa de potencia para realizar el barrido de la curva I-V, y de la tarjeta de relés para habilitar la medida de sensores, junto con las conexiones a Arduino, PC y uno de los multímetros, se muestra en la Figura 14.

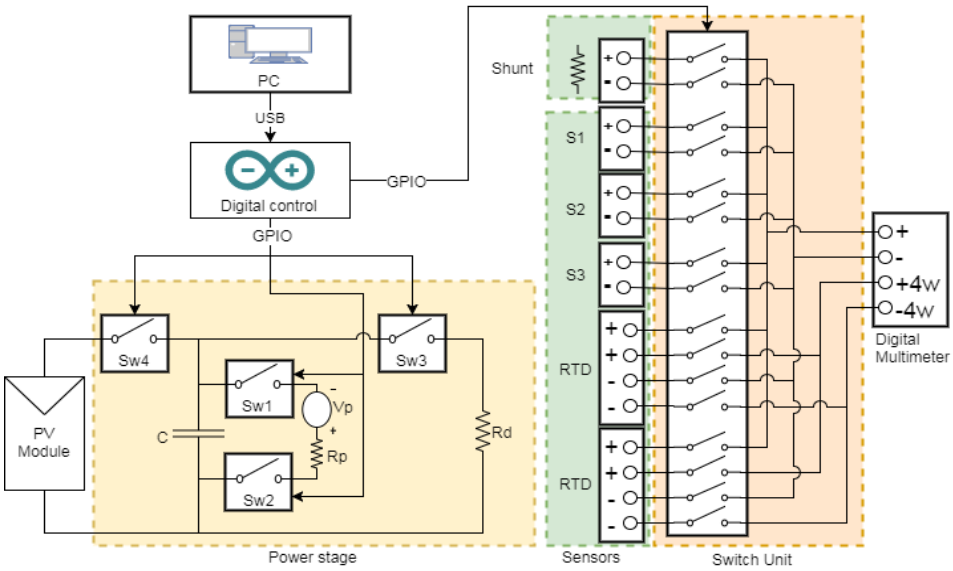

FIGURA 14. Esquema general de la etapa de potencia y placa de relés junto con sus conexiones a Arduino, PC y multímetro.

El software de control global y procesamiento fue desarrollado con la plataforma LabVIEW. Se muestra una captura de pantalla de la ventana principal del programa en la Figura 15. Como características principales se destacan: **(a)** cuenta con una amplia configuración para todos los elementos del sistema, ya que, al ser diseñado de forma modular, los elementos que conforman el sistema pueden variar según el experimento a realizar, **(b)** ha sido diseñado para realizar campañas completas y automáticas de medida en las que se obtienen todos los parámetros periódicamente, y se almacenan los datos de forma ordenada, **(c)** de forma automática, el sistema utiliza, para obtener resultados acerca del comportamiento del elemento FV a estudio, varios métodos de extracción de parámetros (De Blas et al., 2002; Khan et al., 2013; Phang et al., 1984), y varios métodos de extrapolación a CEM (Araujo and Sánchez, 1982; Firman et al., 2011; Osterwald, 1986).

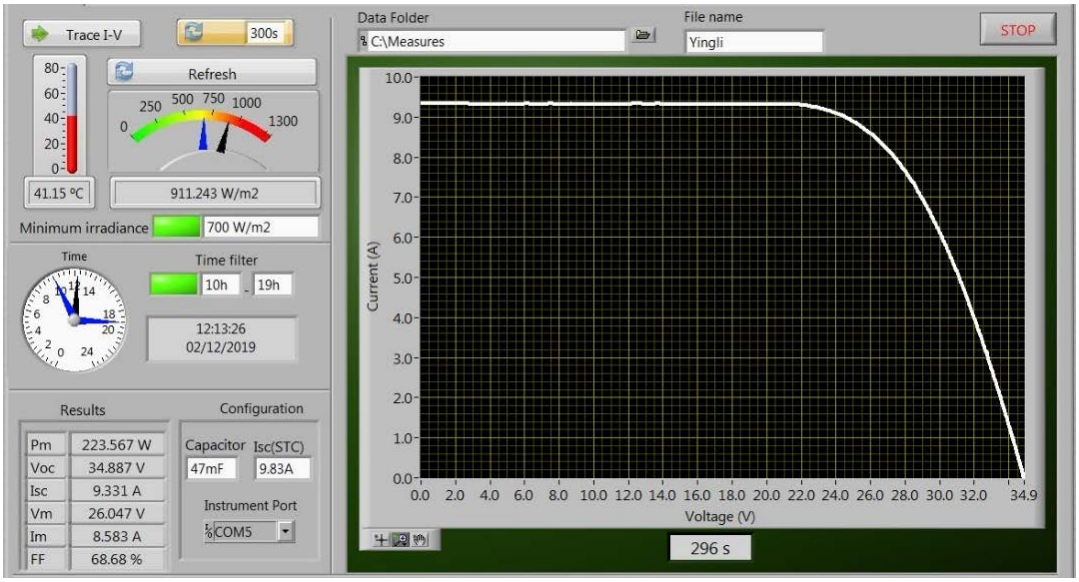

FIGURA 15. Ventana principal del software desarrollado donde se muestra la curva I-V, los principales condiciones meteorológicas y los parámetros eléctricos obtenidos.

Una vez implementados tanto el hardware como el software, se realizó una campaña experimental de medida con el fin de validar el equipo. Durante esta campaña se midieron módulos de tres tecnologías distintas: silicio monocristalino, silicio policristalino y HIT, cuyas características, tanto aportadas por el fabricante como por un Laboratorio Independiente Acreditado (LIA) , se encuentran en la Tabla I.

TABLA I. Características de los módulos FV usados en los experimentos y campañas de medida para validar el prototipo expuesto.

	Módulo 1		**Módulo 2**		**Módulo 3**	
Tecnología	m-Si		p-Si		HIT	
Fabricante	Sharp		Suntech		Sanyo	
Modelo	NU245J5		STP-160		HIT-240HDE4	
Número de células	60		72		60	
Coeficiente α	+0,053%/°C		+0,06%/°C		+2,21 mA/°C	
Coeficiente β	−130 mV/°C		−155 mV/°C		−109 mV/°C	
Coeficiente γ	−0,485%/°C		−0,47%/°C		−0,30%/°C	
Parámetros eléctricos principales en CEM						
	Fabricante	**LIA**	**Fabricante**	**LIA**	**Fabricante**	**LIA**
I_{SC} (A)	8,73	8,68	5,12	5,03	7,37	7,45
V_{OC} (V)	37,5	37,4	42,4	43,6	43,6	42,8
P_m (W)	245	241	160	165	240	242
I_m (A)	8,04	7,92	4,78	4,75	6,77	7,07
V_m (V)	30,5	30,4	33,5	34,8	35,5	34,2

A partir de los datos obtenidos por la campaña experimental, se aplicaron dos procesos distintos de validación. En primer lugar, se estimó teóricamente la incertidumbre de medida de los multímetros comerciales y demás elementos usados en la configuración experimental del sistema propuesto. Destacar que en este artículo se detalla el procedimiento de cálculo de incertidumbre para que sea posible aplicar el mismo a otras posibles configuraciones experimentales que utilicen diferente instrumentación. Con este fin, se incluye un ejemplo de aplicación en la que se estima la incertidumbre de medida de seis parámetros fundamentales para el estudio de las tecnologías FV: irradiancia, temperatura, corriente de cortocircuito, tensión de circuito abierto, potencia máxima y factor de forma.

En una segunda fase se estudió la precisión del sistema mediante el uso de los tres módulos FV comentados anteriormente, que fueron calibrados por un laboratorio certificado y que, por lo tanto, se conocían sus características eléctricas con gran precisión. Para cuantificar el valor del error cometido en la medida, se compararon las medidas realizadas en la campaña con los resultados aportados por el LIA. Como la curva *I-V* varía en función de las variables meteorológicas, para poder realizar una comparación directa, fue necesario el uso de métodos de extrapolación a CEM. En este artículo se usaron los métodos propuestos por Firman (Firman et al., 2011), Araujo (Araujo and Sánchez, 1982) y Osterwald (Osterwald, 1986). Para cuantificar el error de la comparación comentada entre las medidas tomadas en la campaña con los datos del IAL, se han usado dos índices estadísticos: raíz del error cuadrático medio (RMSE por sus siglas en inglés) y Error Relativo (RE por sus siglas en inglés). Como resultado, se obtuvo un error relativo inferior al 5% en I_{SC}, inferior al 4% en P_m, e inferior al 0,5% en V_{OC}.

Publicación 2

Título	**"Software tool for the extrapolation to Standard Test Conditions (STC) from experimental curves of photovoltaic modules"**
Autores	Montes-Romero, J.; de la Casa, J.; Torres-Ramírez, M.; Firmán A.; Cáceres M.
Congreso	Technologies Applied to Electronics Teaching (TAEE)
Año	2016
DOI	10.1109/TAEE.2016.7528252

Uno de las tareas de mayor relevancia realizadas durante la ejecución de la presente Tesis Doctoral está directamente relacionada con el desarrollo de software, tanto de control como de procesamiento de datos experimentales. Los módulos que componen el paquete software global pueden ser compilados por bloques de manera independiente, permitiendo de este modo, generar herramientas específicas. El principal objetivo del trabajo fue la presentación de una herramienta software de libre distribución, enfocada principalmente a tareas docentes o de investigación básica, que permite la aplicación de métodos sencillos de extrapolación a CEM de datos experimentales de curvas características de módulos, *strings* o generadores FV. Esto ha sido presentado en un congreso nacional cuyas actas tienen visibilidad SCOPUS y están albergados en los servicios web de *IEEE Xplore Digital Library*.

En el artículo se comenta someramente las características principales de la curva I-V, los distintos parámetros ofrecidos por los fabricantes y los dos procedimientos posibles con los que es posible obtener la citada curva de un módulo FV: **(a)** medidas en simulador solar, en las que es posible controlar las condiciones de operación a las que se expone el módulo FV a estudio, y **(b)** medidas a sol real, en las que se expone el módulo FV a la radiación solar, con lo que las condiciones ambientales de operación son variables y no se pueden controlar. Debido al interés y la sencillez de las medidas a sol real, se justifica la necesidad de uso de los métodos de extrapolación a CEM.

Los métodos de extrapolación a CEM se pueden agrupar en dos grandes bloques: procedimientos algebraicos y numéricos. La herramienta presentada implementa tres métodos algebraicos (Araujo and Sánchez, 1982; Lorenzo, 2006; Osterwald, 1986) y uno numérico (Firman et al., 2011). Además, en este artículo se presenta otra parte de la herramienta software en la que es posible graficar los parámetros eléctricos medidos a través de la curva I-V y los extrapolados a CEM. A través de estas gráficas, se facilita la explicación y la comprensión a estudiantes o profanos en la tecnología de la relación de algunos parámetros ambientales con las variables eléctricas del módulo FV.

Publicación 3

Título	**"Contributions to the design and construction of characteristic curve tracers for photovoltaic devices"**
Autores	Fernández, E.F.; Firman, A.; Montes-Romero, J.; Cáceres, M.; Vera, L.H.; de la Casa, J.
Congreso	Technologies Applied to Electronics Teaching (TAEE)
Año	2018
DOI	10.1109/TAEE.2018.8476093

Este artículo tiene como principal objetivo servir de guía a cualquier científico o académico que pretenda construir su propio sistema de trazado de curvas características de elementos FV.

Para ello, se revisan las posibles alternativas de diseño, características básicas requeridas y aspectos técnicos a tener en cuenta en el desarrollo de este tipo de equipamiento. En el mismo, se hace especial hincapié en las experiencias desarrolladas por el grupo IDEA de la Universidad de Jaén y el Grupo de Energías Renovables de la Universidad Nacional del Nordeste de Argentina (GER-UNNE).

Al igual que cualquier sistema electrónico que pretenda cumplir esta función, el trabajo se estructura en tres bloques principales: (a) análisis del bloque variador de impedancia, (b) del bloque de medida y (c) del bloque de control. Para cada uno de ellos, se comentan las posibles alternativas tecnológicas que podrían utilizarse, su relación con el resto de los bloques funcionales, así como algunas consideraciones técnicas de interés. Las posibilidades que han sido probadas por ambos grupos se muestra en la Figura 16.

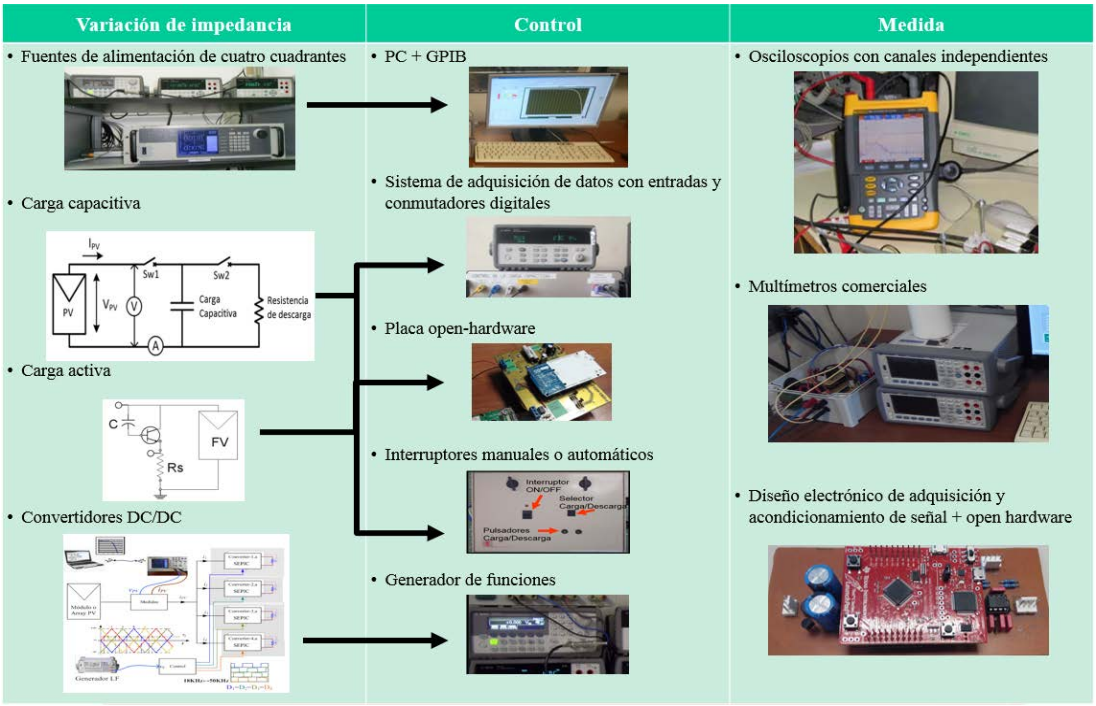

FIGURA 16. Bloques funcionales de un trazador de curvas I-V y alternativas tecnológicas que pueden conformar cada uno de éstos.

Para el bloque variador de impedancia, se enumeran los diferentes métodos que permiten realizar este proceso: resistencias variables, fuentes de alimentación de cuatro cuadrantes, conversores DC/DC, cargas activas y cargas capacitivas. Para cada tipo se comentan algunas ventajas e inconvenientes de su uso. En el bloque de medida, se comenta el esquema general que permite realizar una medida correcta. Para ello, se recomienda la medida directa de la tensión y de la corriente mediante resistencia *shunt*. Además, se comentan los distintos tipos de instrumentos con los que realizar las medidas: osciloscopios, multímetros y etapas electrónicas de medida. Al igual que en el bloque anterior, se comentaron las ventajas e inconvenientes principales de cada una de las posibilidades expuestas. Finalmente, para el bloque de control, se indica cómo es posible realizar el control en función de la etapa de variación de impedancia seleccionada y qué elementos son necesarios para un correcto diseño del bloque funcional.

Indicar por último que, al igual que el anterior artículo, este trabajo ha sido presentado en un congreso internacional cuyas actas tienen visibilidad SCOPUS y están albergadas en los servicios web de *IEEE Xplore Digital Library*.

Publicación 4

Título	**"Low cost I-V curve tracer for PV modules under real operation conditions"**
Autores	Caceres, M.; Firman, A.; Montes-Romero, J.; González Mayans, A.R.; Vera, L.; Fernández, E.F.; de la Casa, J.
Revista	En fase de revisión en IEEE Transactions on Instrumentation and Measurement
Categoría y posición	INSTRUMENTS & INSTRUMENTATION (14/58) ENGINEERING, ELECTRICAL & ELECTRONIC (88/266)
Factor de impacto	3,067 (2018)

Este artículo, en proceso de revisión por pares a fecha de depósito del presente documento, se presenta un diseño propio de prototipo de sistema de caracterización para módulos fotovoltaicos construido utilizando exclusivamente elementos de hardware libre. El sistema propuesto solventa, en gran medida, uno de los principales problemas de los sistemas de caracterización: su coste final. Para ello, se han eliminado todos los elementos comerciales de instrumentación, y se ha reducido el coste final del sistema en un 95% con respecto a la solución presentada en (Montes-Romero et al., 2017).

En primer lugar, y durante la fase de diseño, se realizó una búsqueda de las posibles opciones de sistemas de hardware libre disponibles en el mercado que, además, ofrecieran unas características apropiadas para su construcción. Por sus capacidades óptimas para la adquisición de señales analógicas, su potencial para procesamiento digital de señales y su bajo costo, se escogió el sistema embebido TivaC Series LaunchPad (Texas Instruments, 2019), y basado en un procesador ARM Cortex-M4 de 32 bits que posee dos conversores analógico-digital (A/D) independientes con 12 bits de resolución. Esta facilidad permite realizar la medida simultánea de tensión y corriente, siendo éste uno de los requisitos principales del diseño de la etapa de medida de un sistema de caracterización. Este sistema de hardware-libre también se encarga de realizar la medida de las condiciones de operación del dispositivo FV. Para este primer prototipo, y como prueba de concepto, solo se incluye la medida de la irradiancia incidente y temperatura de operación de módulo. No obstante, la versatilidad del sistema permite añadir un mayor número de sensores en función de las necesidades de forma sencilla, siguiendo el mismo procedimiento que en la publicación 1.

El bloque de medida se completa con un amplio desarrollo electrónico que realiza las funciones de muestreo y acondicionamiento de las diferentes señales eléctricas implicadas en el proceso de medida (tensión en extremos del módulo FV, tensión en extremos de la resistencia shunt para la medida de la corriente, sensor de irradiancia y el sensor de temperatura) en función de las características del conversor A/D del sistema embebido. Con el objeto de maximizar la resolución de la medida se desarrollaron etapas de amplificación para los canales de corriente, irradiancia y temperatura, y una etapa de atenuación para el canal de tensión del módulo FV. Todas las resistencias que componen la etapa de acondicionamiento de señal, tienen una tolerancia de 0,1%, por lo que se minimiza el error que podría cometerse por la tolerancia de los componentes en esta etapa, aunque se recomienda un proceso de calibración en laboratorio de cada uno de los bloques tras su montaje. Los circuitos fueron diseñados en base a un amplificador de instrumentación AD620BNZ (Analog Devices, 2011). Además, para facilitar el procesamiento

digital de señales, y maximizar la relación señal/ruido, se limita el ancho de banda de las entradas diferenciales mediante filtros paso bajo a una frecuencia de corte de 1 kHz.

Por su simplicidad y versatilidad, la etapa de variación de impedancia es tipo capacitiva y se han utilizado transistores IRF540 de tecnología MOSFET para implementar etapa de potencia del sistema. El bloque de control está compuesto, además de por la TivaC, por un PC que se conectan vía USB. La TivaC, trabajando en modo modem nulo, se encarga de generar las señales de control que activan los interruptores necesarios durante el proceso de barrido I-V. El PC da soporte a la aplicación software desarrollada en LabVIEW. El funcionamiento del software es similar al presentado anteriormente en la publicación 1. Al ser un sistema más limitado en cuanto a entradas de sensores, parte de esta configuración no es necesaria en este sistema y la aplicación software solo permitirá seleccionar la constante de calibración del sensor de irradiancia y la constante de calibración de la resistencia shunt usada para la medida de corriente. El resto de funciones, tratamiento de datos (extrapolación a STC, extracción de parámetros, etc) y las ventajas de software que se ofrecían (filtros de medida, sistema de archivos ordenado, automatización de campañas de medida, etc.), siguen estando activas para la presente versión del sistema.

Indicar que este trabajo ha sido financiado por el Centro de Estudios Avanzados en Energía y Medio Ambiente (CEAEMA) de la Universidad de Jaén a través de su línea de proyectos de investigación (CEAEMA-Ujaen, 2014) y ha sido realizado de manera conjunta por investigadores del grupo IDEA-UJA (España) y del GER-UNNE (Argentina). En la Figura 17 se muestran los prototipos de los sistemas montados en la Universidad de Jaén y en la Universidad Nacional del Nordeste.

Finalmente, se destaca que todos los resultados de este trabajo, tanto en su parte hardware como software, se encuentran en abierto con el objeto de que puedan ser replicados fácilmente por cualquier investigador. La documentación se puede descargar en las siguientes direcciones URL:

http://ger-unne.com.ar/IVtracer/IVtracer.zip

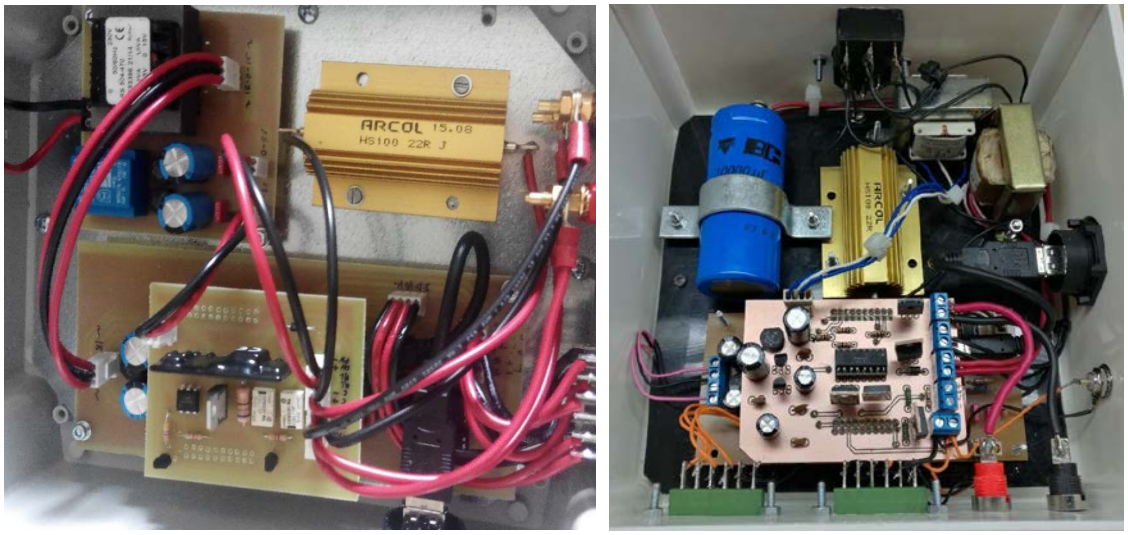

(a) (b)

FIGURA 17. Imagen del sistema de caracterización propuesto en la publicación 4: (a) réplica del sistema en la Universidad de Jaén (España); (b) réplica del sistema en la Universidad Nacional del Nordeste (Argentina).

Con respecto a la bondad en la medida del sistema se destaca que, cada grupo de investigación, de manera independiente, ha realizado similares procesos de validación. En primer lugar, se compararon en paralelo las medidas realizadas por el prototipo y un sistema de referencia basado en instrumentación comercial. Este experimento se realizó tanto en España como en Argentina, utilizando especímenes diferentes desarrollados a partir del mismo diseño. En segundo lugar, se procedió a validar el diseño final en laboratorios certificados.

Respecto al primer caso, se realizó la validación frente al sistema expuesto en la publicación 1, que usa multímetros comerciales y del que sus incertidumbres de medida son conocidas. Para cuantificar el error, se usaron tres variables distintas: error relativo de la curva I-V (E_{IV}), el error relativo del canal de tensión (E_V) y el error relativo del canal de corriente (E_I). Los errores relativos obtenidos por ambos laboratorios para las tecnologías FV consideradas se muestran en la Tabla II.

Tabla II. Resumen de errores obtenidos en dos laboratorios.

Tecnología FV	Laboratorio	$E_V(\%)$	$E_I(\%)$	$E_{IV}(\%)$
Thin-Film (120 W)	IDEA	0,55	0,32	0,87
Poly-Si (160 W)	IDEA	0,45	0,92	1,37
Mono-Si (245 W)	IDEA	0,45	1,23	1,58
Poly-Si (50 W)	GER	0,11	0,26	0,37
Poly-Si (140 W)	GER	0,1	0,8	0,9

El segundo proceso de validación se realizó en laboratorios independientes acreditados. Concretamente, en el Laboratorio de Componentes y Sistemas Fotovoltaicos del Centro de Investigaciones Energéticas, Medioambientales y Tecnológicas de España (PVLabDER – CIEMAT, España), y en el Laboratorio de Energía Solar de la Universidade Federal do Rio Grande do Sul (LABSOL-UFRGS, Brasil). Para la validación en el CIEMAT, se usó como sistema de contraste un vatímetro Yokogawa WT3000, y en LABSOL-UFRGS un sistema basado en una fuente de cuatro cuadrantes KEPCO BOP 100-10 MG y multímetros Agilent 3458A. Estos laboratorios han ofrecido la desviación y/o incertidumbre de los parámetros eléctricos característicos del sistema de medida. En la Tabla III se incluyen los resultados obtenidos de desviación e incertidumbre en la calibración llevada a cabo en CIEMAT, y en la Tabla IV se dan los valores de desviación en la calibración realizada en el LABSOL. Los certificados de calibración del instrumento emitidos por ambas entidades se adjuntan como Anexos I y II del presente documento.

TABLA III. Resultados de desviación e incertidumbre para la calibración en CIEMAT.

Parámetro	Rango	Desviación	Incertidumbre
I_{SC}	1 a 10 A	- 0,10 %	± 0,02 A
V_{OC}	20 a 80 V	- 0,40 %	± 0,2 V
P_M	20 a 250 W	+ 0,35 %	± 2 W

TABLA IV. Resultados de desviación para la calibración en LABSOL.

Parámetro	Desviación
I_{SC}	0,58 %
V_{OC}	0,23 %
P_M	0,05 %

Los resultados obtenidos tanto en las validaciones realizadas por GER e IDEA, como en las realizadas por los laboratorios independientes CIEMAT y LABSOL, demuestran que el equipo presenta una alta calidad de medida en relación a su coste final, ofreciendo características equiparables a las de un equipo comercial. Estos prometedores resultados permiten proponer nuevas líneas de investigación encuadradas en este campo.

3.3. PUBLICACIONES RELACIONADAS CON EL OBJETIVO ESPECÍFICO 2

El segundo objetivo específico se define como *"Diseño y ejecución de campañas experimentales de caracterización de diferentes tecnologías FV, con especial hincapié en los módulos FV de 3ª generación."* y es abordado en las siguientes publicaciones:

Publicación 5

Título	**"Comparative study of methods for the extraction of concentrator photovoltaic module parameters"**
Autores	F. Fernández, E.; Montes-Romero, J.; de la Casa, J.; Rodrigo, P.; Almonacid, F.
Revista	Solar Energy
Volumen, páginas, año	137, 413-423, 2016
Categoría y posición	ENERGY AND FUELS (21/92)
Factor de impacto	4.018 (2016)
DOI	10.1016/j.solener.2016.08.046

En esta publicación, directamente relacionada con el objetivo 2, se plantea la hipótesis de que los métodos de extracción de parámetros existentes pueden ser válidos en su aplicación a módulos de tecnología CPV basados en células multiunión. Por ello, se estudian algunos de éstos con el fin de encontrar cuáles se ajustan bien a esta tecnología para que puedan ser utilizados para estudios más detallados. Esto es fundamental para aumentar nuestra compresión de esta prometedora tecnología. Por ejemplo, la validación de estos métodos daría paso de forma indirecta a la utilización de técnicas ampliamente usadas en FV. Esto permitiría estudiar fenómenos fundamentales no abordados de forma profunda en la CPV, tales como su degradación, evolución temporal y en general facilitaría y simplificaría su modelado eléctrico. Además, la validación los métodos de extracción basados en una solo unión PN no solo tiene interés en el campo de la CPV. Actualmente, el estudio y desarrollo de módulos tándem basados en varias bandas de absorción, tales como Perovskite/Silicon (Hossain et al., 2019) o III-V/Silicon (Cariou et al., 2018), ha cobrado una gran fuerza y se espera que el futuro de la tecnología vaya en esa línea. En este sentido, los resultados de este estudio abrirían una prometedora línea de investigación futura en el ámbito de las tecnologías de 3ª generación.

El principal objetivo de este artículo es la evaluación de cuatro métodos de extracción de parámetros en su aplicación a módulos FV de tecnología CPV. Se aplican los métodos de Phang

(Phang et al., 1984), Khan (Khan et al., 2013), Blas (De Blas et al., 2002), y Almonacid (Almonacid et al., 2016), que nunca han sido probados en dicha tecnología FV. Estos métodos se basan en el modelo exponencial simple (SEM) de cinco parámetros para predecir las características I-V de los módulos FV. La ecuación de este modelo se expone a continuación:

$$I = I_{ph} - I_0\left(exp\left(\frac{V + IR_s}{mV_T}\right) - 1\right) - \frac{V + IR_s}{R_{sh}} \quad (1)$$

Donde I_{ph} es la corriente fotogenerada, I_0 es la corriente de saturación del diodo, m el factor de idealidad del diodo, R_s la resistencia serie y R_{sh} la resistencia paralela. La configuración experimental del sistema empleado para obtener las curvas I-V está basado en un sistema de medida comercial PVPV1000C40. La obtención de los parámetros ambientales se realiza mediante una estación MTD3000 de Geonica. Los parámetros relevantes que fueron obtenidos para este experimento fueron la radiación directa (DNI) y la temperatura de célula (T_c). El módulo CPV utilizado consiste en 20 células de triple unión *lattice-matched* GaInP/GaInAs/Ge. La óptica primaria está formada por lentes Fresnel de tipo SoG (*silicone-on-glass)*, mientras que la óptica secundaria se forma con pirámides truncadas refractivas. La eficiencia óptica de esta configuración es del 80%, consiguiendo una concentración geométrica total de 700. El módulo usa disipadores con aletas de aluminio de convección natural, logrando una temperatura normal de trabajo entre 50-80°C. En la Figura 18 se muestra un esquema detallado de los distintos elementos que componen el receptor solar. Este módulo fue también previamente medido en el simulador solar, y, por lo tanto, se conocen sus características eléctricas con precisión.

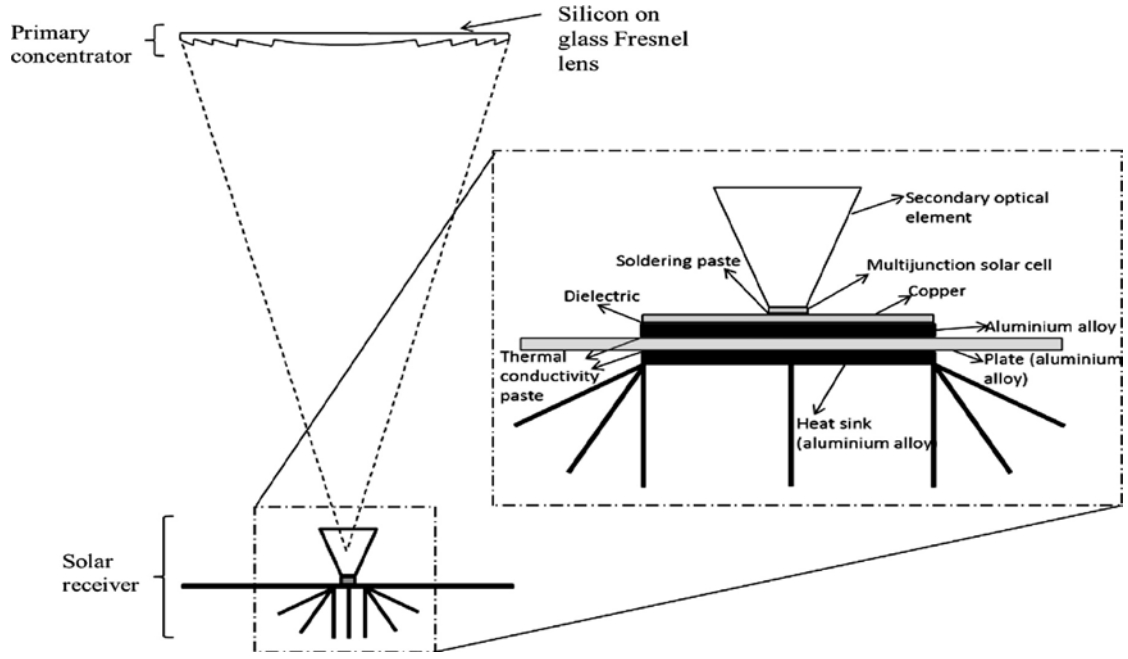

FIGURA 18. Esquema detallado del receptor integrado con las ópticas primaria y secundaria del módulo CPV estudiado.

En la campaña experimental llevada a cabo en este estudio, se usaron las curvas I-V tomadas durante un año natural, aunque para realizar la validación de los métodos, se seleccionaron seis curvas I-V con diferentes características ambientales siguiendo el siguiente patrón: temperatura

alta y baja para radiaciones bajas, temperatura alta y baja para radiaciones típicas, y temperatura alta y baja para radiaciones altas. De este modo, se cubre todo el rango característico de los dos parámetros más influyentes en el comportamiento de la tecnología. La distribución normalizada de irradiancia efectiva, corregida espectralmente, y temperatura de todos los datos disponibles se muestra en la Figura 19.

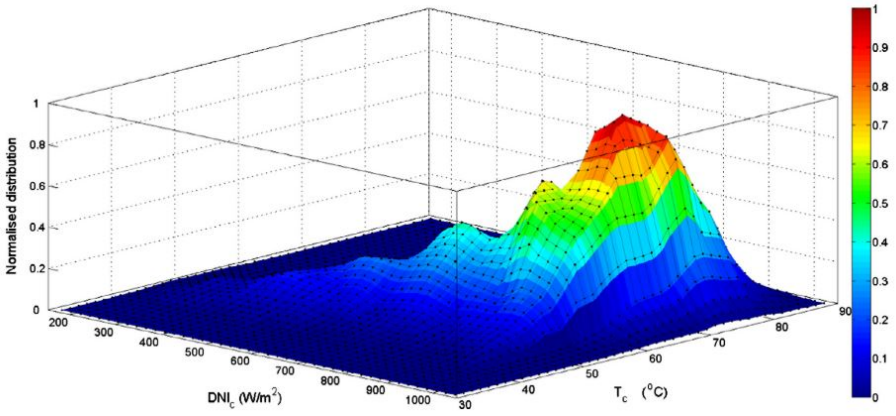

FIGURA 19. Distribución normalizada en función de la temperatura de célula y de la irradiancia efectiva.

Una vez seleccionadas las curvas representativas, se aplicaron los métodos de extracción de parámetros comentados y se obtuvieron los cinco parámetros de cada una de las curvas, a partir de los cuales, usando la ecuación (1), se reconstruyeron las curvas I-V. Un ejemplo se expone en la Figura 20. Se puede apreciar una diferencia notable entre la curva I-V obtenida por el método de Khan y el resto de curvas I-V.

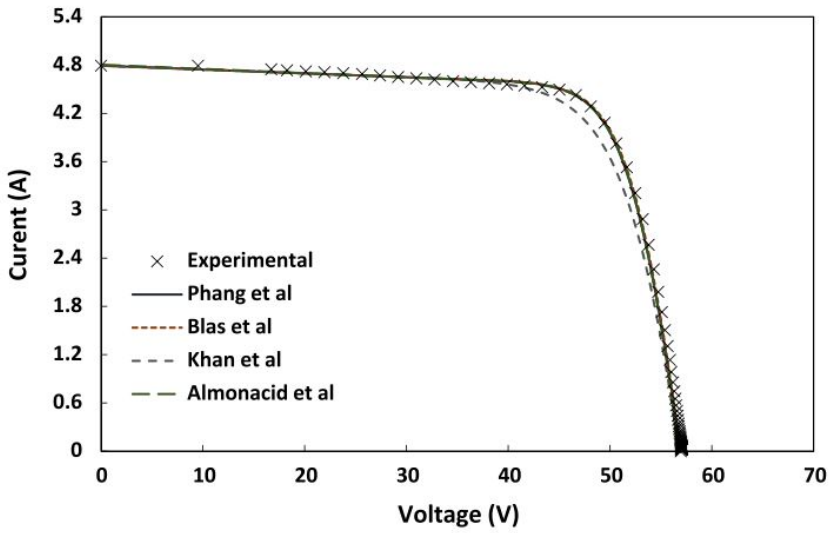

FIGURA 20. Curvas IV medida experimentalmente y modeladas para valores de irradiancia y temperatura altos.

Para estimar bondad de los métodos de extracción de parámetros a estudio se compara la diferencia entre la curva medida experimentalmente y la reconstruida por los métodos. Esta diferencia ha sido cuantificada usando los índices RMSE y el error de sesgo medio (MBE por sus siglas en inglés). Los resultados obtenidos se exponen en la Figura 21. Se puede observar que los

métodos de Phang y Almonacid arrojan los mejores resultados con un RMSE medio de 1,22% y 1,35% y un MBE medio de -0,46% y -0,40% respectivamente. El método de Blas obtiene de media un 1,71% de RMSE y -0,66% de MBE. Por último, el método de Khan da los peores resultados de media con un 3,53% de RMSE y -1,81% de MBE, tal y como se pudo intuir en las curvas I-V obtenidas.

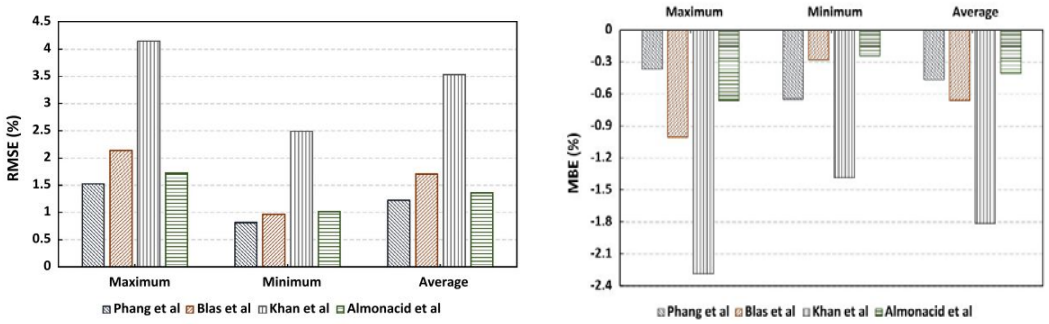

(a) (b)

FIGURA 21. Errores obtenidos entre las curvas IV medidas experimentalmente y las reconstruidas por los métodos de extracción de parámetros.

Además, en este artículo se estudia la linealidad en la estimación de la corriente a partir del coeficiente de correlación (R^2) entre las corrientes experimentales y las modeladas. De igual forma, los métodos de Phang, Almonacid y Blas obtuvieron los mejores resultados con un valor medio de 0,99, mientras que el método de Khan dio los peores resultados con un 0,97. Cabe destacar que todos los métodos tienden a subestimar los valores de corriente y a incrementar su error para valores de bajos de corriente bajos cercanos de V_{oc}.

Finalmente, se estudia muy brevemente la influencia de cada uno de los parámetros con la irradiancia incidente. Todos los métodos muestran la misma tendencia. La corriente fotogenerada, la corriente de saturación del diodo y el factor de idealidad tienden a incrementar su valor con la irradiancia, mientras que la resistencia serie y paralelo muestran una tendencia decreciente.

Publicación 6

Título	**"Comparative analysis of parameter extraction techniques for the electrical characterization of multi-junction CPV and m-Si technologies"**
Autores	Montes-Romero, Jesús; Almonacid, Florencia; Theristis, Marios; de la Casa, Juan; E. Georghiou, George; F. Fernández, Eduardo
Revista	Solar Energy
Volumen, páginas, año	160, 275-288, 2018
Categoría y posición	ENERGY AND FUELS (23/97)
Factor de impacto	4,374 (2017)
DOI	10.1016/j.solener.2017.12.011

Esta segunda publicación tiene una estrecha relación con la hipótesis planteada y los resultados obtenidos en el trabajo anterior. Se comenzó validando los métodos de extracción de parámetros en la primera publicación, para dar lugar a un análisis más profundo del comportamiento de la tecnología CPV y su comparación con la clásica de silicio cristalino. El objetivo principal de este artículo fue la aplicación de varios métodos de extracción de parámetros,

Phang, Khan y Blas en este caso, a módulos FV de distintas tecnologías (m-Si y CPV), y la comparación de los parámetros obtenidos entre ambos para analizar las diferencias existentes entre las dos tecnologías FV.

En primer lugar, se realizó una campaña experimental de medida durante el año 2016 en la que se midieron, simultáneamente, dos módulos FV de tecnologías distintas: CPV y m-Si. Para adquirir los datos necesarios se usó el sistema expuesto en (Muñoz et al., 2014), con el que se trazó la curva I-V de los módulos FV junto con parámetros ambientales como la irradiancia directa (DNI), irradiancia global normal (GNI), etc., así como la temperatura de módulo. La distribución de las condiciones ambientales más influyentes (irradiancia y temperatura) se muestra en la Figura 22. En la tecnología CPV, hay una mayor dispersión en las condiciones de operación, mientras que en m-Si, la mayoría de los datos se agrupan en un rango mucho más ajustado.

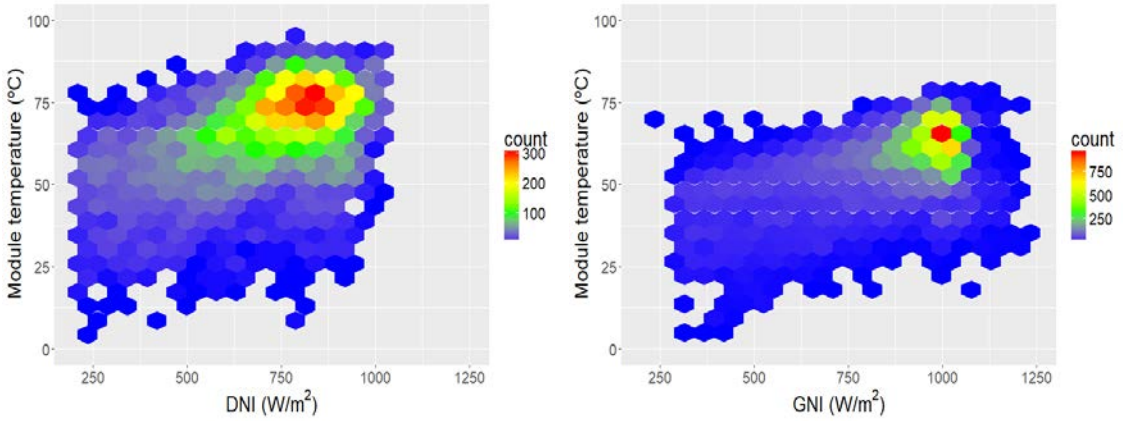

FIGURA 22. Distribución de la temperatura en función de la irradiancia efectiva para: (a) Módulo de tecnología CPV; (b) Módulo de tecnología m-Si.

En este artículo también se presenta el error obtenido entre las curvas I-V, obtenidas experimentalmente y a través de los métodos de extracción de parámetros, mediante los valores del error cuadrático medio normalizado (NRMSE por sus siglas en inglés) y MBE. En concordancia con la publicación anterior, el método de Phang consigue los mejores resultados para el módulo de CPV, seguido por el método de Blas y, obteniendo el peor resultado, el método de Khan. En el módulo de m-Si se consiguen resultados similares entre los tres métodos, consiguiendo el error más bajo mediante el método de Blas, seguido por Phang y, de nuevo, con el peor resultado, el método de Khan. Estos errores se exponen en Figura 23.

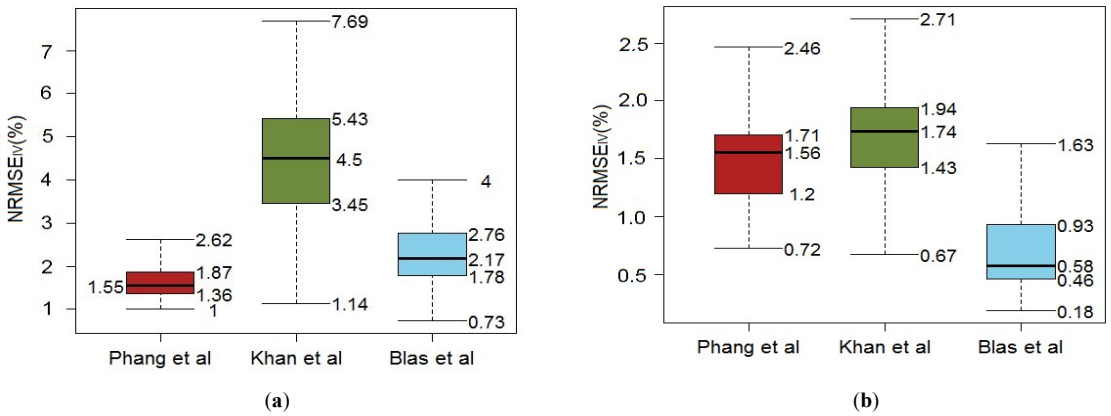

FIGURA 23. Dispersión de NRMSE en función de los tres métodos estudiados para: (a) Módulo CPV; (b) Módulo m-Si.

También se ha analizado el error en función de la irradiancia, temperatura de módulo y el espectro, caracterizado mediante la masa del aire (AM por sus siglas en inglés). De este estudio, se ha llega a la conclusión de que el método de Phang es el más estable para ambas tecnologías FV, manteniendo su error relativamente constante en función de estos parámetros. Para los otros dos métodos se aprecian algunas diferencias en la evolución del índice NRMSE, siendo dicha diferencia mucho más notoria en el método de Khan, lo que es lógico teniendo en cuenta la amplia dispersión de errores obtenida en dicho método.

Otro de los puntos de interés presentado en esta publicación es la evolución de los cinco parámetros obtenidos por cada uno de los métodos en función de la irradiancia incidente. Para R_{sh} e I_{ph}, para todos los métodos y tecnologías estudiadas, no se encontraron diferencias. El parámetro I_{ph} presenta un comportamiento claramente lineal creciente con respecto a la irradiancia, mientras que R_{sh} sigue una tendencia exponencial decreciente. El parámetro R_s sigue una tendencia similar para dichos métodos y tecnologías. En concreto, ésta tiende a decrecer de forma logarítmica con la irradiancia. No obstante, esta dependencia presenta ligeras diferencias en su valor, siendo más significativa en el módulo de CPV. Los parámetros m e I_0 siguen una tendencia similar en los métodos de Phang y Khan, aunque el método de Blas difiere ligeramente en dicha tendencia. De forma general, la m tiende a aumentar muy ligeramente con la irradiancia para los dos primeros métodos, aunque con una significativa diferencia en su valor, mientras que, con el método de Blas, el valor de este parámetro decrece muy levemente. El comportamiento de I_0 tiene un comportamiento similar al de m, aumentando su valor para los métodos de Phang y Khan, y disminuyendo en el método de Blas.

Finalmente, en esta publicación se presentó un análisis en el que se buscó un modelo matemático que relacione cada uno de los cinco parámetros con la irradiancia. Para ello se usó el método de Phang, ya que fue el más estable para ambos módulos FV. Para el parámetro R_s se encuentran dos posibles modelados, uno de función exponencial y otro de función logarítmica. Se obtuvo una mayor relación con el ajuste logarítmico que con el ajuste exponencial. También se encontró una clara relación exponencial para el parámetro R_{sh}. La última relación encontrada fue para el parámetro I_{ph} con una tendencia claramente lineal. Los parámetros m e I_0 se ajustaron de forma lineal con la irradiancia, sin embargo, el índice R^2 indicó que no existe ninguna relación clara con dicho parámetro. Estas tendencias se repiten tanto para el módulo de CPV como para el módulo de m-Si.

Los resultados en la predicción de los parámetros usando el modelo matemático presentado se exponen en la Tabla V y la Tabla VI.

TABLA V. NRMSE, MBE y R^2 para cada parámetro a nivel de célula en el módulo CPV.

Parámetro	NRMSE	MBE	R^2
$R_{s,c}$ (logarítmico)	4,23%	0,007%	0,743
$R_{s,c}$ (potencial)	8,54%	-0,25%	0,695
$R_{sh,c}$	3,79%	0,40%	0,714
m_c	11,73%	-0,35%	0,009
$I_{0,c}$	10,12%	-0,002%	0,076
$I_{ph,c}$	0,12%	1,06%	0,950

TABLA VI. NRMSE, MBE y R^2 para cada parámetro a nivel de célula en el módulo m-Si.

Parámetro	NRMSE	MBE	R^2
$R_{s,c}$ (logarítmico)	5,93%	-0,05%	0,175
$R_{s,c}$ (potencial)	5,96%	-0,54%	0,149
$R_{sh,c}$	7,46%	-0,62%	0,590
m_c	11,53%	0,55%	0,013
$I_{0,c}$	8,09%	0,007%	0,072
$I_{ph,c}$	2,65%	-0,37%	0,9767

Publicación 7

Título	**"Analysing Concentrating Photovoltaics Technology Through the Use of Emerging Pattern Mining"**
Autores	García-Vico, A.M; Montes-Romero, J.; Aguilera, J; Carmona, J.; del Jesus, M.J.
Revista	Advances in Intelligent Systems and Computing
Congreso	International Joint Conference SOCO'16-CISIS'16-ICEUTE'16
Páginas, año	334-344, 2016
CiteScore Rank:	Computer Science: General Computer Science (156/195)
Categoría y posición	Engineering: Control and Systems Engineering (186/224)
Factor de impacto SJR	0.174
DOI	10.1007/978-3-319-47364-2_32

Finalmente, cabe destacar una última publicación en el ámbito de este objetivo de tesis. El objetivo principal de este artículo fue la aplicación de técnicas "E*merging Pattern Mining*" (EPM) a tecnología CPV. Estas técnicas buscan relaciones entre parámetros, y en su aplicación, se buscaron relaciones entre la potencia del módulo CPV y varios parámetros ambientales. En concreto, se usó un algoritmo "*Evolutionary Algorithm for Extracting Emerging Patterns*" (EvAEP). Como parámetros ambientales de interés, se han usado la radiación directa, temperatura ambiente, velocidad de viento, radiación global incidente, energía media del fotón (APE por sus siglas en inglés) y el ratio de equivalencia espectral (SMR por sus siglas en inglés). La característica eléctrica de interés del módulo CPV utilizada en el artículo fue la potencia máxima, extraída de las curvas I-V tomadas durante el experimento. Aplicando esta técnica, se buscaron relaciones entre la potencia máxima del módulo y los parámetros ambientales citados. Para aplicar el método, se usan tres intervalos definidos del parámetro P_M, tal como se muestra en la Tabla VII y diez reglas que incluyen los parámetros ambientales descritos anteriormente. Estas reglas, junto con los resultados obtenidos, se muestran en la Tabla VIII. El ratio de crecimiento (GR, por sus siglas en inglés) indica el ratio entre los patrones positivos y negativos, por lo que un valor alto, indicará un mayor cumplimiento de la regla. El ratio de verdad positivo (TPr, por sus siglas en inglés) indica el porcentaje de ejemplos correctamente clasificados en la regla. El ratio de verdad negativo (FPr, por sus siglas en inglés) indica el porcentaje de ejemplos incorrectamente clasificados por la regla. Como resultado principal de la aplicación del método, se obtiene, de forma general, una relación directa entre la DNI y la potencia del módulo CPV. También se observa una relación baja entre el APE y la potencia, lo que puede explicarse teniendo en cuenta la gran dependencia espectral de esta tecnología.

TABLA VII. Intervalos definidos para el parámetro P_M.

Intervalo	Rango P_M	Rango % P_M	% casos
2	64,5W – 93W	43% - 62%	20%
3	93W – 121,5W	62% - 81%	68%
4	121,5W – 150W	81% - 100%	12%

TABLA VIII. Reglas y resultados obtenidos por el algoritmo.

Regla	GR	TPr	FPr
R1:IF DNI=Very Low THEN P_M =2	5,30	0,524	0,098
R2:IF DNI=Low THEN P_M =2	75,89	0,362	0,004
R3:IF G=Medium THEN P_M =3	1,35	0,889	0,656
R4:IF APE=Low THEN P_M =3	1,05	0,993	0,942
R5:IF DNI=Medium THEN P_M =3	4,33	0,397	0,091
R6:IF DNI=High AND APE=Low AND T_a =Medium AND W_S=Medium THEN P_M =4	3,87	0,037	0,009
R7:IF DNI=High AND APE=Low THEN P_M =4	9,92	0,134	0,013
R8:IF APE=Low AND T_a =Low AND W_S =Medium AND SMR=High AND G=High THEN P_M =4	31,00	0,033	0,001
R9:IF APE=Low AND T_a =Low AND WS =Low AND SMR=High AND G=High THEN P_M =4	5,81	0,025	0,004
R10:IF APE=Low AND T_a =Very Low AND SMR=High THEN P_M =4	21,31	0,046	0,002

4

CONCLUSIONES Y LÍNEAS FUTURAS DE INVESTIGACIÓN

En primer lugar, en este capítulo se resumen las principales conclusiones derivadas de la Tesis Doctoral. Posteriormente, se proponen futuras líneas de trabajo o investigación que, sin duda, pueden complementar los resultados obtenidos en la misma.

Los trabajos desarrollados han permitido validar las hipótesis principales que dieron origen al presente documento. Se han diseñado y ejecutado plataformas de caracterización de sistemas fotovoltaicos usando plataformas de hardware libre con los requisitos planteados durante el capítulo 2, tales como la flexibilidad en los rangos de medida, procesamiento en tiempo real de los datos, etc. Además, a partir de éstas, ha sido posible analizar algunos aspectos del comportamiento de tecnologías FV emergentes como es la CPV.

Las **principales conclusiones** de la presente Tesis Doctoral se pueden describir de manera resumida en los siguientes hitos:

- *Conclusiones relacionadas con el objetivo 1.*

1.- **Se pueden desarrollar sistemas de caracterización de dispositivos fotovoltaicos modulares, flexibles y de relativo coste a partir de instrumentación de laboratorio de propósito general y plataformas de hardware libre.** Este es el resultado se ha alcanzado modificando diseños previos del grupo IDEA e incorporando algunos bloques funcionales desarrollados con plataformas de hardware libre, además del desarrollo de un software de control y procesamiento de datos más potente. El sistema desarrollado utiliza para la medida multímetros comerciales que podrían ser adquiridos con certificado de calibración del fabricante. Un estudio en detalle de la arquitectura propuesta se ha publicado en el artículo "*Photovoltaic Device Performance Evaluation Using an Open-Hardware System and Standard Calibrated Laboratory Instruments*".

2.- **Se pueden desarrollar sistemas de caracterización de dispositivos fotovoltaicos de alta precisión y muy bajo coste usando exclusivamente plataformas de hardware libre y diseños electrónicos fácilmente replicables**. Este prototipo, que parte de las conclusiones del punto 1, se ha diseñado, construido y validado experimentalmente entre dos grupos de investigación de distintas universidades (Universidad de Jaén y Universidad Nacional del Nordeste). Además, ha sido validado en dos laboratorios independientes acreditados (LABSOL y

CIEMAT), certificando que el equipo presenta una baja incertidumbre en la medida de la curva I-V. Este sistema y su proceso de validación se presenta en el artículo "*Low cost I-V curve tracer for PV modules under real operation conditions*". Los certificados de medida obtenidos por el CIEMAT y LABSOL se adjuntan en los Anexos I y II.

- *Conclusiones relacionadas con el objetivo 2.*

3.- **Los métodos clásicos de extracción de parámetros son válidos para caracterizar sistemas fotovoltaicos de 3ª generación basados en células tándem**. Se han ejecutado campañas experimentales de caracterización de módulos FV en las que se han aplicado distintos métodos de extracción de parámetros. En concreto, se han estudiado cuatro métodos: Phang, Blas, Khan y Almonacid.. Este estudio se presenta en el artículo "*Comparative study of methods for the extraction of concentrator photovoltaic module parameters*", e indica que los métodos de Phang, Almonacid y Blas presentan un error similar, mientras que el método de Khan arroja un error superior a los demás.

4.- **Los métodos de extracción de parámetros muestran un comportamiento similar en las tecnologías FV, basadas en m-Si, y CPV, basadas en células multiunión.** En el artículo "Comparative analysis of parameter extraction techniques for the electrical characterization of multi-junction CPV and m-Si technologies" se presenta un análisis del comportamiento de cada uno de los parámetros extraídos por los métodos de extracción en función de la irradiancia incidente para módulos de dos tecnologías FV distintas (m-Si y CPV). Se obtienen tendencias, tanto en los errores como en los parámetros característicos, similares entre ambas tecnologías frente a esta magnitud. También se aplicaron distintos ajustes a los parámetros y la irradiancia para estudiar qué tipo de tendencia sigue cada uno. Se concluye que el parámetro R_s decrece de forma logarítmica, R_{sh} decrece de forma exponencial e I_{ph} crece de forma lineal con la radiación. Tanto m como I_0 muestran una tendencia creciente y se ajustan de forma lineal con dicha magnitud, aunque sin ninguna relación directa tal y como señala el índice R^2.

El presente trabajo doctoral ha permitido alcanzar resultados y conclusiones de gran relevancia en al ámbito de la caracterización de los sistemas FV. Además, durante la realización de su Tesis, el autor ha colaborado activamente con otros grupos y centros de investigación, tanto nacionales como extranjeros, que tienen líneas de investigación comunes. Gracias a todo esto, se han abierto nuevas y prometedoras **líneas futuras de investigación** que se detallan continuación:

- *Líneas futuras relacionadas con el objetivo 1.*

EL Grupo de Ciencia de Materiales y Energías Renovables de la Pontificia Universidad Católica del Perú (MatER-PUCP), en colaboración con el Grupo IDEA de la Universidad de Jaén, está realizando los primeros avances para que el Perú cuente con un laboratorio de análisis y calibración de módulos FV a sol real. Este laboratorio sería el primero del país que contaría con la instrumentación adecuada para realizar: (a) procesos de calibración y certificación de módulos FV que podrían ser ofertados a empresas u otras instituciones públicas, (b) estudios detallados del comportamiento y degradación de las diferentes tecnologías FV comerciales en función de las condiciones climáticas de operación particulares de la ciudad de Lima (niveles de irradiancia, temperatura de operación, humedad, distribución espectral, etc.).

El doctorando ha participado activamente durante más de un año en su diseño, construcción, montaje y calibración, y se puede afirmar que una parte del laboratorio de caracterización en

potencia de módulos FV se encuentra a pleno funcionamiento desde finales de abril de este año. Disponer del citado laboratorio permitirá al tesitando, en su etapa Postdoctoral, profundizar sus investigaciones en el marco de los dos objetivos específicos propuestos en esta Tesis.

Con respecto a la caracterización de tecnologías FV, la zona ecuatorial y tropical de la costa pacífica de Sudamérica, y por ende Lima, es una región totalmente inexplorada en lo que respecta a la medida experimental de la operación real de las distintas tecnologías. Es evidente que, para un correcto desarrollo de una tecnología en un país, es necesario un estudio detallado del comportamiento de la misma en sus diferentes versiones comerciales. Para ello, es imprescindible que se cuenten con laboratorios de investigación locales que permitan su estudio in situ basándose en la realización de campañas experimentales de medida, su posterior análisis y la publicación de resultados y, que los mismos, puedan servir de referencia para otros investigadores de la zona y de guía para los diferentes actores del tejido industrial y organismos y entidades públicas con capacidad de decisión en política energética, etc.

Por otro lado, al ser un laboratorio en el que su diseño ha partido desde cero, está siendo diseñado con el objetivo de responder a algunas nuevas preguntas de investigación que han surgido durante el periodo de realización de la presente Tesis y que no eran objeto de la misma. En la Figura 24 se muestra el esquemático general del sistema planteado. Algunas de estas nuevas preguntas están relacionadas con los siguientes tópicos:

- Los fabricantes de instrumentación "Solar" están migrando de dispositivos que ofrecían una salida analógica proporcional al parámetro medido a nuevos sensores con salida tipo digital en formato bus serie normalizado. ¿Cómo afecta este hecho a los diseños propuestos en esta Tesis? ¿Qué modificaciones habría que incluir en la arquitectura global para adaptarse a esta nueva realidad? ¿Es una oportunidad para reducir costes o un inconveniente?

- El sistema de caracterización diseñado para en la PUCP ha sido pensado para una medida secuencial de hasta 16 módulos FV, aunque, el número de módulos FV a ensayo, podría ser ampliado fácilmente. El sistema sigue utilizando un único bloque variador de impedancia, sistema de control y medida. Sería necesario un análisis detallado de los tiempos de muestreo máximos que podrían asumirse en un sistema de caracterización con esta arquitectura y cuáles serían sus límites de aplicación en función de las condiciones de medida.

- Una novedad del sistema es la incorporación de microinversores de conexión a red, que permitirán realizar comparaciones entre una caracterización en potencia y una caracterización en energía de una misma tecnología bajo idénticas condiciones de operación. Normalmente, cuando se caracteriza un módulo FV trazando de manera repetida su curva I-V, los especímenes a ensayo, permanecen en circuito abierto la mayor parte del tiempo. ¿Qué resultado de P^*_M se obtendría si el módulo FV estuviera trabajando en punto de máxima potencia durante todo el tiempo? Si el fin último del sistema de caracterización no tuviera fines científicos, solo industriales o comerciales, ¿Con qué grado de fiabilidad se podría construir un sistema de caracterización de módulos FV, que permita la obtención de su $P^*_{M,}$ basado simplemente en un microinversor comercial?

Todas estas preguntas, a las que los investigadores de ambos grupos están ya trabajando para darles respuesta, serán objeto de futuras Tesis Doctorales y nuevas publicaciones.

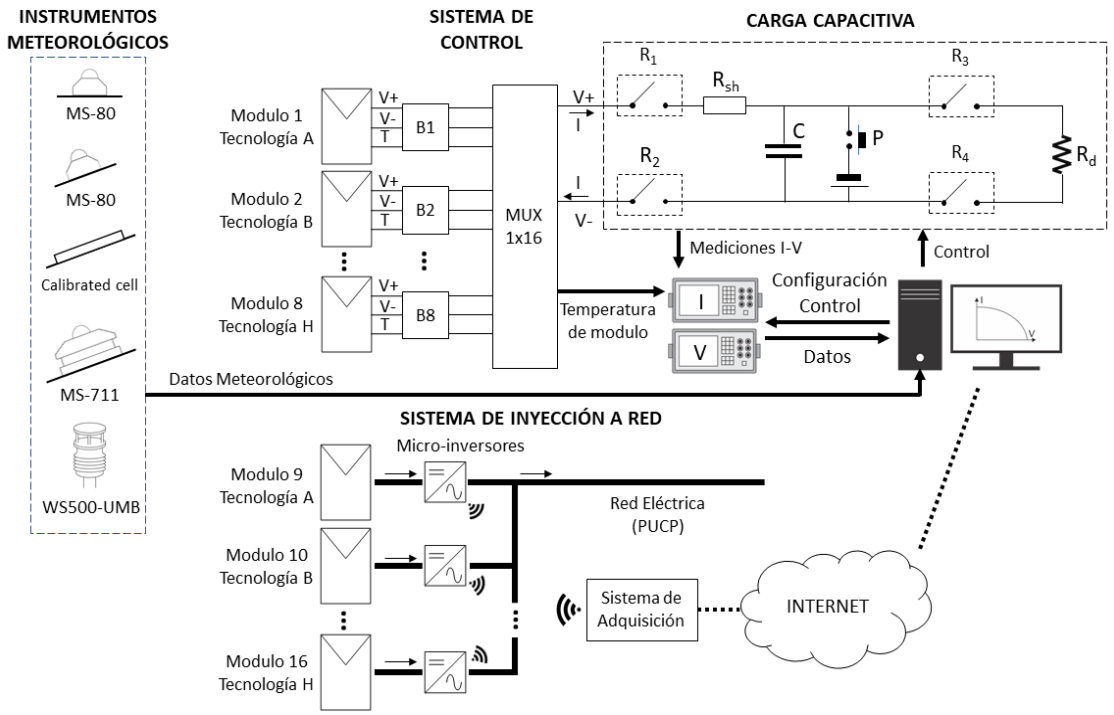

FIGURA 24. Esquemático general del sistema de caracterización implementado en la PUCP.

La segunda vertiente en la que se espera el desarrollo de sistemas de bajo coste, se pretende realizar mejoras a lo ya expuesto, fijando objetivos como la implementación de comunicaciones inalámbricas, la sustitución del PC como elemento de control por plataformas "*Internet of Things* (IoT)" que almacenen datos en la Nube y se puedan visualizar vía web, modificar el sistema para que sea autónomo energéticamente, la inclusión del sistema en módulos FV conectados a red, etc. En este sentido, se pretende trabajar con empresas privadas para conseguir dichos objetivos.

Aparte de los resultados científicos, esta Tesis ha realizado aportes de carácter netamente tecnológicos. El diseño y desarrollo de un prototipo de muy bajo coste que permite el trazado de curvas I-V, junto con las relaciones mantenidas con investigadores del CIEMAT durante el proceso de validación del mismo en un laboratorio certificado, han dado como fruto, a fecha de redacción de este documento, que una empresa española de amplia implantación en el sector de la operación y mantenimiento de grandes plantas fotovoltaicas se haya interesado por el mismo. Originalmente, el sistema estaba pensado como un equipo de laboratorio, por lo que la empresa ha solicitado un proyecto de desarrollo e innovación empresarial a la Comunidad Autónoma de Castilla-La Mancha que le permita asumir los costes necesarios para convertir el prototipo en un producto comercial que pueda ser utilizado en labores de mantenimiento de sistemas. De culminarse con éxito este propósito, se habría alcanzado un nuevo hito no previsto en los planes de investigación originales como sería el logro de la transferencia de resultados al tejido productivo.

A modo de **resumen**, se indican de forma concisa las líneas de investigación futuras relacionadas con este prometedor objetivo de la tesis:

- Diseño, implementación y evaluación del sistema de caracterización propuesto para la PUCP con las nuevas características técnicas planteados por los requisitos de la investigación.

- Analizar el comportamiento eléctrico de distintas tecnologías FV frente a las particulares condiciones ambientales de la ciudad de Lima.

- Evaluar las diferencias existentes entre la caracterización mediante el trazado de la curva I-V y mediante el sistema conectado a red con micro inversores.

- Diseño y desarrollo de un sistema prototipo de bajo coste para el trazado de curvas I-V que incluya comunicaciones inalámbricas, autonomía energética y conecte con un servicio web para el almacenamiento y visualización de los datos.

- Estudiar y evaluar la posibilidad de incluir un sistema de trazado I-V a un módulo FV perteneciente a un *string* conectado a un inversor central.

Aparte de los resultados científicos, esta Tesis ha realizado aportes de carácter netamente tecnológicos. El diseño y desarrollo de un prototipo de muy bajo coste que permite el trazado de curvas I-V, junto con las relaciones mantenidas con investigadores del CIEMAT durante el proceso de validación del mismo en un laboratorio certificado, han dado como fruto, a fecha de redacción de este documento, que una empresa española de amplia implantación en el sector de la operación y mantenimiento de grandes plantas fotovoltaicas se haya interesado por el mismo. Originalmente, el sistema estaba pensado como un equipo de laboratorio, por lo que la empresa ha solicitado un proyecto de desarrollo e innovación empresarial a la Comunidad Autónoma de Castilla-La Mancha que le permita asumir los costes necesarios para convertir el prototipo en un producto comercial que pueda ser utilizado en labores de mantenimiento de sistemas. De culminarse con éxito este propósito, se habría alcanzado un nuevo hito no previsto en los planes de investigación originales como sería el logro de la transferencia de resultados al tejido productivo. Para ello, ya se está trabajando en: (a) implementación de comunicaciones inalámbricas, (b) la sustitución del PC como elemento de control por plataformas "*Internet of Things* (IoT)" que almacenen datos en la Nube y permiten su visualización vía web, (c) modificar el sistema para que sea autónomo energéticamente, alimentándose del propio dispositivo FV a estudio, (d) etc…

- *Líneas futuras relacionadas con el objetivo 2.*

Por otra parte, se pretende continuar con la línea de trabajos expuestos referentes al objetivo específico 2, donde se analiza y modela el comportamiento de las distintas tecnologías FV por medio de métodos de extracción de parámetros. En este campo, tanto la tecnología CPV como la FV requieren aún de estudios detallados de su comportamiento frente a distintas condiciones ambientales. En el transcurso de la presente Tesis se ha analizado la influencia de la irradiancia frente a los parámetros que marcan el comportamiento de la tecnología. Sin embargo, se desconoce con precisión cómo y en qué medida afectan otros parámetros ambientales al comportamiento de estas tecnologías. En este sentido, se destacan las siguientes líneas de investigación destinadas a mejorar las actuales herramientas de modelización y evaluación:

- **Estudiar, modelar y comparar la influencia del espectro en los parámetros característicos de distintas tecnologías.** El espectro ha demostrado tener una influencia relevante en el comportamiento de la tecnología CPV y FV. Debido a esto, es más que

probable que este influya en los parámetros fundamentales de ambas tecnologías. Sin embargo, esto todavía no ha sido abordado por ningún grupo de investigación y permanece por lo tanto desconocido.

- **Estudiar, modelar y comparar la influencia de la temperatura en los parámetros característicos de distintas tecnologías.** La temperatura de operación de los sistemas FV modifica las propiedades físicas de los semiconductores que lo componen, y por lo tanto, sus parámetros fundamentales. Esto aún no ha sido estudiado de forma profunda en la actualidad, tanto en el caso de la tecnología FV como CPV. Debido a esto, la capacidad de modelar el impacto de la temperatura en los parámetros característicos todavía no es posible.

- **Evaluar, modelar y comparar el efecto de la no uniformidad en los parámetros característicos de distintas tecnologías.** Además de las variables señaladas, la no uniformidad, causada por el polvo y suciedad o por el sombreado de otros módulos u objetos, influye en la distribución de la radiación sobre la superficie de los sistemas FV. Esto se ha demostrado influye en el rendimiento de las distintas tecnologías FV, y, por lo tanto, se espera influya en sus parámetros característicos. Sin embargo, a día de hoy, todavía se desconoce cuál es la influencia de estas variables, y la capacidad de evaluar y modelar su efecto de forma precisa permanece desconocida.

- **Estudiar la degradación de diversas tecnologías usando los parámetros característicos.** La modelización más precisa de los parámetros fundamentales permitirá cuantificar de forma univoca cual es el impacto de la degradación en las distintas tecnologías. Esto cobra aún más significado en la tecnología CPV, donde este tipo de estudios son muy escasos.

- **Comparar y modelar el comportamiento de los parámetros característicos en varios emplazamientos.** Las variables comentadas en los puntos anteriores van a depender fuertemente de las condiciones ambientales del emplazamiento de los sistemas FV. En este sentido, se pretende comparar la evolución de los mismos en varias localizaciones. Esto se llevará a cabo gracias a dos sistemas experimentales, desarrollados en el ámbito de esta tesis, de iguales características situados en la Universidad de Chipre y de Jaén, y que se muestran en la Figura 25.

(a) (b)

FIGURA 25. Sistemas experimentales instalados en: (a) Universidad de Chipre; (b) Universidad de Jaén

Alcanzar estos nuevos objetivos permitirá mejorar de forma significativa las herramientas destinadas a modelar y evaluar las distintas tecnologías FV. Además, permitiría comparar su rendimiento de forma más precisa en función de las características ambientales del emplazamiento bajo estudio. Esto ayudará a mejorar la competitividad de las tecnologías FV en general, lo que servirá de gran ayuda para promover la transición energética a un sistema basado en tecnologías no contaminantes.

4

CONCLUSIONS AND FUTURE RESEARCH LINES

In this section, the main conclusions derived from this Doctoral Thesis are summarized. Secondly, future lines of work or research are proposed which, undoubtedly, can complement the results obtained.

The work carried out has validated the main initial hypothesis. Photovoltaic system characterization platforms have been designed and executed using free hardware platforms with the requirements stated in chapter 2, such as flexibility in measurement ranges, real-time data processing, etc. In addition, from these, it has been possible to analyze some aspects of the behavior of emerging PV technologies such as the CPV. The work carried out in these areas has led to four publications in prestigious journals and three in congresses.

The **main conclusions** of this Doctoral Thesis can be summarized under the following points:

- *Conclusions related to objective 1.*

1.- **Modular and flexible characterization systems of photovoltaic devices can be developed using general purpose laboratory instrumentation and free hardware platforms.** This result has been achieved by modifying previous designs of the IDEA group and incorporating some functional blocks developed with free hardware platforms. In addition, a more powerful control and data processing software has been achieved. The system developed uses commercial multimeters that can be acquired with the manufacturer's calibration certificate. A detailed study of the proposed architecture has been published in the article "*Photovoltaic Device Performance Evaluation Using an Open-Hardware System and Standard Calibrated Laboratory Instruments*".

2.- **High-precision and very low-cost photovoltaic device characterization systems can be developed exclusively using free hardware platforms and electronic designs.** This prototype, which is based on the conclusions of point 1, has been designed, built and experimentally validated between two research groups from different universities (University of Jaen and National University of the Northeast). In addition, it has been validated in two independent accredited laboratories (LABSOL and CIEMAT), certifying that the equipment presents a low uncertainty in the measurement of the I-V curve. This system and its validation process is presented in the article "Low cost I-V curve tracer for PV modules under real operation conditions". The measurement certificates obtained by CIEMAT and LABSOL are attached in Annexes I and II.

- *Conclusions related to objective 2.*

3.- **The classical methods of parameter extraction are valid to characterize 3rd generation photovoltaic systems based on tandem cells**. Experimental campaigns have been carried out to characterize PV modules where different parameter extraction methods have been applied. Specifically, four methods were studied: Phang, Blas, Khan and Almonacid. This study is described in the article "*Comparative study of methods for the extraction of concentrator photovoltaic module parameters*", and indicates that Phang, Almonacid and Blas methods show a similar error, while Khan's method presents a higher error.

4.- **Parameter extraction methods show similar behaviour in m-Si and CPV based PV technologies based on multiunion cells.** In the article "Comparative analysis of parameter extraction techniques for the electrical characterization of multi-junction CPV and m-Si technologies" an analysis of the behaviour of each of the parameters extracted by the extraction methods as a function of the incident irradiance for modules of two different PV technologies (m-Si and CPV) is presented. Similar trends are obtained from both technologies. Different fits were applied to the parameters and irradiance in order to study what kind of trend follows each one. It is concluded that the parameter R_s decreases logarithmically, R_{sh} decreases exponentially and I_{ph} grows linearly with irradiance. Both m and I_0 show an increasing trend and they are adjusted in a linear fit, although without any direct relation as the index R^2 indicates.

This work has led to highly relevant results and conclusions in the field of PV system characterisation. Furthermore, during the preparation of his Thesis, the author has actively collaborated with other groups and research centres, both national and international, that have common research lines. As a result, new and promising future lines of research have been initiated.

- *Future lines related to Objective 1.*

The Materials Science and Renewable Energies Group of the Pontificia Universidad Católica del Perú (MatER-PUCP), in collaboration with the IDEA Group of the University of Jaén, is conducting the first advances to provide a laboratory for the analysis and calibration of PV modules in real sunlight in Peru. This laboratory would be the first in the country to have the appropriate instrumentation to carry out both calibration and certification processes of PV modules that could be offered to companies or other public institutions. Furthermore, detailed studies of the behavior and degradation of the different commercial PV technologies depending on the particular climatic operating conditions of the city of Lima (irradiance levels, operating temperature, humidity, spectral distribution, etc.) can be carried out.

The doctoral student has been actively involved for more than a year in the design, construction, assembly and calibration of the equipment, and part of the PV module characterization laboratory has been fully operational since the end of April this year. Having the above mentioned laboratory will allow the author in his Postdoctoral stage to deepen his research in the framework of the two specific objectives proposed in this Thesis.

Regarding the characterization of PV technologies, the equatorial and tropical zone of the Pacific coast of South America, and thus Lima, is a totally unexplored region in terms of the experimental measure of the actual operation of the different technologies. It is evident that, for a correct development of a technology in a country, a detailed study of the behavior of the technology in its different commercial versions is necessary. Therefore, it is essential to have local research laboratories that allow its study in situ based on the conduct of experimental measurement campaigns, analysis and publication of results. They can serve as a reference for

other researchers in the area and guide for the different actors of the industrial sector and public institutions.

On the other hand, since it is a laboratory designed from the beginning, it is being built with the aim of answering some new research questions that have emerged during the period of the Thesis but were not the object of it. Figure 24 shows the general schematic of the proposed system. Some of these questions are related to the following aspects:

- The instrumentation manufacturers are changing from devices that offered an analogical output proportional to the measured parameter to new sensors with digital type output in standardized serial bus format. How does this fact affect the designs proposed in this Thesis? What modifications should be included in the global architecture to adapt to this new reality? Is it an opportunity to reduce costs or an inconvenience?

- The characterization system developed for the PUCP has been designed for sequential measurement of up to 16 PV modules, although the number of PV modules to be tested could easily be expanded. The system still uses sweep, control and measurement system blocks. A detailed analysis of the maximum sampling times that could be assumed in a characterization system with this architecture would be necessary.

- A new feature of the system is the incorporation of micro-inverters for grid connection, which will allow comparisons to be made between a power characterization and an energy characterization of the same technology under identical operation conditions. When a PV module is characterised by repeatedly plotting its I-V curve, the specimens under test normally remain in open circuit most of the time. What P^*_M result would be obtained if the PV module were working at maximum power point all the time? If the ultimate purpose of the characterisation system was not scientific, but only industrial or commercial, how reliable could the PV module characterisation system be for obtaining P^*_M using only a commercial microinverter?

The researchers of both groups are already working to provide answers to these questions and will be the subject of future Doctoral Theses.

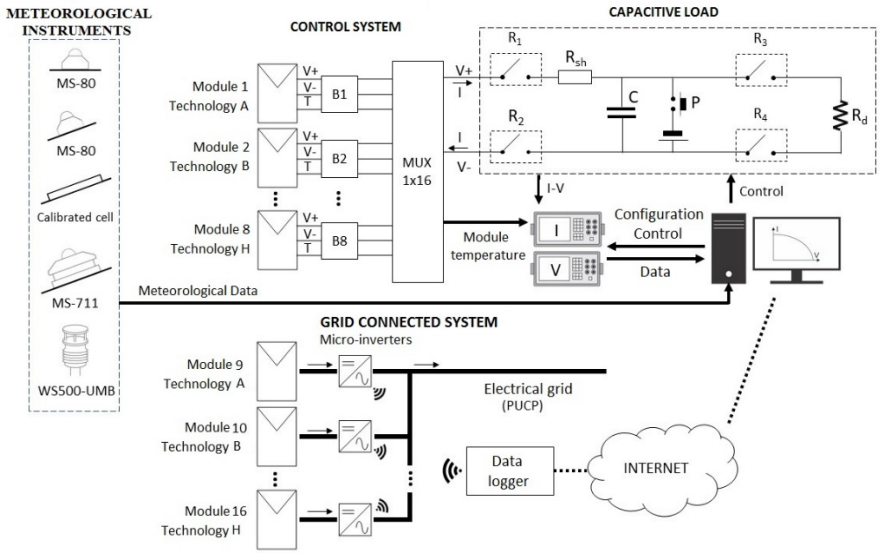

FIGURE 24. General schematic of the characterization system implemented at the PUCP.

The second aspect in which the development of low-cost systems is expected, we plan to make improvements setting objectives such as the implementation of wireless communications, the replacement of the PC as a control element for " Internet of Things (IoT)" platforms that store data in the Cloud and can be visualized through web, the modification of the system to make it energetically autonomous, the inclusion of the system into the PV string, etc. In this sense, it is intended to work with private companies to achieve these objectives.

Apart from the scientific results, this thesis has made contributions of a purely technological nature. The design and development of a very low-cost prototype that allows the drawing of I-V curves, together with the relations maintained with CIEMAT researchers during the validation process, have resulted in the interest of a Spanish company widely established in the sector of operation and maintenance of large photovoltaic plants. Originally, the system was designed as a laboratory equipment, so the company has requested a project of business development and innovation to the Autonomous Community of Castilla-La Mancha that will assume the necessary costs to convert the prototype into a commercial product that can be used in system maintenance. If this project is successful, a new goal not contemplated in the original research plans will be achieved as the transfer of results to the productive sector.

- *Future lines related to Objective 2.*

On the other hand, it is intended to continue with the line of work presented in relation to objective 2, where the behavior of the different PV technologies is analyzed and modeled by means of parameter extraction methods. In this field, both CPV and PV technologies still require detailed studies of their behavior under different environmental conditions. In the course of this Thesis, the influence of irradiance on the parameters that define the behavior of the technology has been analyzed. However, it is unknown accurately how and in which degree, other environmental parameters affect the behavior of these technologies. In this sense, the following research lines aimed at improving the existing modeling and evaluation tools are highlighted:

- **Study, model and compare the influence of the spectrum on the characteristic parameters of different technologies.** Solar spectrum has been proved to influence the behaviour of CPV and PV technology. For this reason, it is highly possible that it influences the fundamental parameters of both technologies. However, this has not been addressed by any research group yet and therefore remains unknown.

- **Study, model and compare the influence of temperature on the characteristic parameters of different technologies.** The operating temperature of PV systems modifies the physical properties of the semiconductors that compose the system, and therefore their fundamental parameters. This has not been extensively studied at present, either in the case of PV and CPV technology. Because of this, the capability of modeling the impact of temperature on characteristic parameters is still not possible.

- **Evaluate , model and compare the effect of non-uniformity on the characteristic parameters of different technologies.** In addition to the above variables, non-uniformity, caused by dust or dirt or by the shading of other modules, influences the distribution of radiation on the surface of PV systems. This has been shown to influence the performance of the various PV technologies, and is therefore expected to influence their characteristic parameters. However, at present, the influence of these variables is

still unknown, and the ability to evaluate and model their effect accurately remains unpredictable.

- **Study the degradation of various technologies using the characteristic parameters.** More precise modeling of the fundamental parameters will make it possible to quantify unequivocally what the impact of degradation is on the different technologies. This becomes even more significant in CPV technology, where this sort of study is very limited.

- **Compare and model the behavior of characteristic parameters at various locations**. The variables discussed in the previous points will depend significantly on the environmental conditions of the PV system site. In this sense, the aim is to compare the evolution of the parameters at various locations. This will be carried out thanks to two experimental systems, developed within the scope of this thesis, with the same characteristics located at the University of Cyprus and Jaén, and shown in Figure 25.

(a) (b)

FIGURE 25. Experimental systems installed in: (a) University of Cyprus; (b) University of Jaen

Achieving these new objectives will significantly improve the tools for modeling and evaluating the various PV technologies. In addition, it would allow their performance to be compared more precisely according to the environmental characteristics of the site under study. This will help to improve the competitiveness of PV technologies in general, which will greatly assist in promoting the energy transition to a system based on clean technologies.

5

BIBLIOGRAFÍA

Alaaeddin, M.H., Sapuan, S.M., Zuhri, M.Y.M., Zainudin, E.S., AL-Oqla, F.M., 2019. Photovoltaic applications: Status and manufacturing prospects. Renew. Sustain. Energy Rev. 102, 318–332. https://doi.org/10.1016/j.rser.2018.12.026

Almonacid, F., Rodrigo, P., Fernández, E.F., 2016. Determination of the current-voltage characteristics of concentrator systems by using different adapted conventional techniques. Energy 101, 146–160. https://doi.org/10.1016/j.energy.2016.01.082

Analog Devices, 2011. Instrumentation Amplifier AD620 20.

Appelbaum, J., Peled, A., 2014. Parameters extraction of solar cells - A comparative examination of three methods. Sol. Energy Mater. Sol. Cells 122, 164–173. https://doi.org/10.1016/j.solmat.2013.11.011

Araujo, G.., Sánchez, E., 1982. Analytical expressions for the determination of the maximum power point and the fill factor of a solar cell. Sol. Cells 5, 377–386. https://doi.org/10.1016/0379-6787(82)90008-4

ASTM International, 2019. ASTM E927 - 19, Standard Classification for Solar Simulators for Electrical Performance Testing of Photovoltaic Devices.

Azaklar, S., Korkmaz, H., 2010. A remotely accessible and configurable electronics laboratory implementation by using LabVIEW. Comput. Appl. Eng. Educ. 18, 709–720. https://doi.org/10.1002/cae.20276

Bello, C., Jimenez, V., Toranzos, V., Busso, A., Vera, L.H., Cadena, C., 2009. RELEVADOR PORTATIL DE CURVAS I-V DE PANELES FOTOVOLTAICOS COMO HERRAMIENTA DE DIAGNOSTICO IN SITU DE SISTEMAS DE GENERACION FOTOVOLTAICA. Av. en Energías Renov. y Medio Ambient. 13, 77–83.

Bertolín, J.C., Fuentes, M., Muñoz, J.V., Casa, J. de la, 2012. Applications of DC/DC converters for obtaining characteristic curves of PV generators, in: 27th European Photovoltaic Solar Energy Conference. Frankfurt, Germany, pp. 3254–3258. https://doi.org/10.4229/27thEUPVSEC2012-4BV.2.13

Blaesser, G., Munro, D., 1995a. Guidelines for the Assessment of Photovoltaic Plants Document A Photovoltaic System Monitoring, Commission of the European Communities, Joint Research Centre. Ispra, Italy.

Blaesser, G., Munro, D., 1995b. Guidelines for the Assessment of Photovoltaic Plants Document B Analysis and Presentation of Monitoring Data. Ispra, Italy.

BP, 2018. Statistical Review of World Energy 2018 1–53.

Cariou, R., Benick, J., Feldmann, F., Höhn, O., Hauser, H., Beutel, P., Razek, N., Wimplinger,

M., Bläsi, B., Lackner, D., Hermle, M., Siefer, G., Glunz, S.W., Bett, A.W., Dimroth, F., 2018. III-V-on-silicon solar cells reaching 33% photoconversion efficiency in two-terminal configuration. Nat. Energy 3, 326–333. https://doi.org/10.1038/s41560-018-0125-0

Casa, J. De, Fuentes, M., Muñoz, J. V, Talavera, D.L., Nofuentes, G., Aguilera, J., 2012. Herramientas para la docencia de créditos prácticos en asignaturas directamente relacionadas con la energía solar fotovoltaica ., in: TAEE 2012. pp. 168–173.

Chan, D.S.H., Phillips, J.R., Phang, J.C.H., 1986. A comparative study of extraction methods for solar cell model parameters. Solid. State. Electron. 29, 329–337. https://doi.org/10.1016/0038-1101(86)90212-1

De Blas, M.A., Torres, J.L., Prieto, E., García, A., 2002. Selecting a suitable model for characterizing photovoltaic devices. Renew. Energy 25, 371–380. https://doi.org/10.1016/S0960-1481(01)00056-8

Duran, E., Piliougine, M., Sidrach-De-Cardona, M., Galan, J., Andujar, J.M., 2008. Different methods to obtain the I-V curve of PV modules: A review, in: Conference Record of the IEEE Photovoltaic Specialists Conference. https://doi.org/10.1109/PVSC.2008.4922578

EKO Instruments, 2017. EKO Instruments [WWW Document]. URL https://eko-eu.com/

ENE 2008-05098, 2009. Estimación de la energía generada por módulos fotovoltaicos de capa delgada: influencia del espectro.

ENE2009-08302, 2009. Análisis y caracterización de un Sistema Fotovoltaico de Concentración a sol real. Comparativa con otras tecnologías fotovoltaicas.

Erkaya, Y., Flory, I., Marsillac, S.X., 2014. Development of a String Level I-V Curve Tracer, in: Photovoltaic Specialist Conference (PVSC), 2014 IEEE 40th. Denver, CO, USA.

Erkaya, Y., Moses, P., Marsillac, S., 2016. On-Site Characterization of PV Modules Using a Portable , MOSFET- Based Capacitive Load 3119–3122.

Fernández, E.F., 2012. Modelización y caracterización de células solares III-V multiunión y de módulos de concentración. Universidad de Santiago de Compostela.

Fernández, E.F., Ferrer-Rodríguez, J.P., Almonacid, F., Pérez-Higueras, P., 2017. Current-voltage dynamics of multi-junction CPV modules under different irradiance levels. Sol. Energy 155, 39–50. https://doi.org/10.1016/J.SOLENER.2017.06.012

Fernández, E.F., Montes-Romero, J., de la Casa, J., Firman, A., Cáceres, M., Vera, L.H., 2018. Contributions to the design and construction of characteristic curve tracers for photovoltaic devices, in: Proceedings of 2018 Technologies Applied to Electronics Teaching, TAEE 2018. https://doi.org/10.1109/TAEE.2018.8476093

Fernández, E.F., Montes-Romero, J., de la Casa, J., Rodrigo, P., Almonacid, F., 2016. Comparative study of methods for the extraction of concentrator photovoltaic module parameters. Sol. Energy 137, 413–423. https://doi.org/10.1016/j.solener.2016.08.046

Fernandez, E.F., Seoane, N., Almonacid, F., Garcia-Loureiro, A.J., 2018. Vertical-tunnel-junction (VTJ) solar cell for ultra-high light concentrations (>2000 suns). IEEE Electron Device Lett. https://doi.org/10.1109/LED.2018.2880240

Ferrer-Rodríguez, J.P., 2018. Contribución al desarrollo de sistemas fotovoltaicos de alta concentración. Análisis de nuevas configuraciones de módulos. Universidad de Jaén.

Firman, A., Toranzos, V., Busso, A., Cadena, C., Vera, L., 2011. Determinación del punto de trabajo de sistemas fotovoltaicos conectados a red: metodo simplificado de traslacion punto a punto a condiciones estandar de medida. Av. en Energías Renov. y Medio

Ambient. 15, 1–8.

Frankfurt School, UNEP, 2016. Global Trends In Renewable Energy Investment.

Fraunhofer Institute for Solar Energy Systems (ISE), 2018. Photovoltaics report. Photovoltaics Rep. 1, 1–45. https://doi.org/20.10.2016

García-Domingo, B., 2014. Análisis , caracterización y modelado del comportamiento en exterior de módulos de concentración fotovoltaica. Universidad de Jaén.

García-Valverde, R., Chaouki-Almagro, S., Corazza, M., Espinosa, N., Hösel, M., Søndergaard, R.R., Jørgensen, M., Villarejo, J.A., Krebs, F.C., 2016. Portable and wireless IV-curve tracer for >5kV organic photovoltaic modules. Sol. Energy Mater. Sol. Cells 151, 60–65. https://doi.org/10.1016/j.solmat.2016.02.012

García, M., Maruri, J.M., Marroyo, L., Lorenzo, E., Pérez, M., 2008. Partial Shadowing, MPPT Performance and Inverter Configurations: Observations at Tracking PV Plants. Prog. Photovolt Res. Appl. 15, 659–676. https://doi.org/10.1002/pip

Garrido, G.E.N., 2000. Contribución al desarrollo de aplicaciones fotovoltáicas en edificios.

Ghani, F., Fernandez, E.F., Almonacid, F., O'Donovan, T.S., 2017. The numerical computation of lumped parameter values using the multi-dimensional Newton-Raphson method for the characterisation of a multi-junction CPV module using the five-parameter approach. Sol. Energy 149, 302–313. https://doi.org/https://doi.org/10.1016/j.solener.2017.04.024

Guzmán Martínez, E.J., 2000. Diseño de interruptor electrónico para carga de ensayo de módulos fotovoltáicos. Universidad de Jaén.

Hammoumi, A.E., Motahhir, S., Chalh, A., Ghzizal, A.E., Derouich, A., 2018. Real-time virtual instrumentation of Arduino and LabVIEW based PV panel characteristics, in: IOP Conference Series: Earth and Environmental Science. https://doi.org/10.1088/1755-1315/161/1/012019

Hemza, A., Abdeslam, H., Rachid, C., Pasquinelli, M., Barakel, D., 2015. Tracing current-voltage curve of solar panel Based on LabVIEW Arduino Interfacing. BİLİŞİM Teknol. DERGİSİ 3, 117–123. https://doi.org/10.17671/btd.39450

Hossain, M.I., Qarony, W., Ma, S., Zeng, L., Knipp, D., Tsang, Y.H., 2019. Perovskite/Silicon Tandem Solar Cells: From Detailed Balance Limit Calculations to Photon Management. Nano-Micro Lett. 11. https://doi.org/10.1007/s40820-019-0287-8

Humada, A.M., Hojabri, M., Mekhilef, S., Hamada, H.M., 2016. Solar cell parameters extraction based on single and double-diode models: A review. Renew. Sustain. Energy Rev. 56, 494–509. https://doi.org/10.1016/j.rser.2015.11.051

International Electrotechnical Commission, 2007a. IEC 60891, Photovoltaic Devices. Procedures for Temperature and Irradiance Corrections to Measure I-V Characteristics. Geneva, Switzerland.

International Electrotechnical Commission, 2007b. IEC 60904-9, Photovoltaic Devices, Part 9: Solar simulator performance requirements. Geneva, Switzerland.

International Electrotechnical Commission, 2006. IEC 60904-1, Photovoltaic Devices, Part 1: Measurement of Photovoltaic Current–Voltage Characteristics. Geneva, Switzerland.

International Energy Agency, 2017. World Energy Outlook 2017. Int. ENERGY AGENCY Together Secur. Sustain. Executive, 13. https://doi.org/10.1016/0301-4215(73)90024-4

IPT-2011-1468-920000, n.d. SIGMAPLANTAS: La innovación en las plantas y modelos de sistemas de Concentración Fotovoltaica en España.

Khan, F., Baek, S.H., Park, Y., Kim, J.H., 2013. Extraction of diode parameters of silicon solar cells under high illumination conditions. Energy Convers. Manag. 76, 421–429. https://doi.org/10.1016/j.enconman.2013.07.054

Lazard, 2018. Lazard's Levelized Cost of Energy Analysis - Version 12.0.

Leite, V., Batista, J., Chenlo, F., Afonso, J.L., 2012. Low-Cost Instrument for Tracing Current-Voltage Characteristics of Photovoltaic Modules, in: International Conference on Renewable Energies and Power Quality. pp. 1012–1017.

Leite, V., Chenlo, F., 2010. An improved electronic circuit for tracing the IV characteristics of photovoltaic modules and strings, in: International Conference on Renewable Energies and Power Quality. pp. 1224–1228.

Lorenzo, E., 2006. Volumen II--Radiación Solar y Dispositivos Fotovoltaicos. Univ. Politec. Madrid.

Martin, S.S., Chebak, A., Barka, N., 2016. Concept of educational renewable energy laboratory integrating wind, solar and biodiesel energies. Int. J. Hydrogen Energy 41, 21036–21046. https://doi.org/10.1016/j.ijhydene.2016.06.102

Montes-Romero, J., Piliougine, M., Muñoz, J., Fernández, E., de la Casa, J., 2017. Photovoltaic Device Performance Evaluation Using an Open-Hardware System and Standard Calibrated Laboratory Instruments. Energies 10, 1869. https://doi.org/10.3390/en10111869

Montes Romero, J., 2014. Sistema automatizado para el trazado de curvas características de módulos FV. Universidad de Jaén.

Moya, A.S., 2017. Análisis de la influencia espectral en dispositivos de alta concentración fotovoltaica: desarrollo de técnicas para su evaluación bajo diferentes condiciones atmosféricas y temporales.

Muñoz, J., Lorenzo, E., 2006. Capacitive load based on IGBTs for on-site characterization of PV arrays. Sol. Energy 80, 1489–1497. https://doi.org/10.1016/j.solener.2005.09.013

Muñoz, J.V.., Torres-Ramírez, M.., García-Domingo, B.., Fuentes, M.., de la Casa, J.., Nofuentes, G.., Aguilera, J.., 2014. Automatic monitoring system to assess the outdoor behaviour of photovoltaic modules, in: 29th European Photovoltaic Solar Energy Conference and Exhibition. pp. 2654–2657.

Muñoz, J.V., de la Casa, J., Fuentes, M., Aguilera, J., Bertolín, J.C., 2011. New portable capacitive load able to measure PV modules, PV strings and large PV generators, in: 26th European Photovoltaic Solar Energy Conference and Exhibition. pp. 4276–4280. https://doi.org/10.4229/26thEUPVSEC2011-5BV.2.23

Munoz, M.A., Alonso-García, M.C., Vela, N., Chenlo, F., 2011. Early degradation of silicon PV modules and guaranty conditions. Sol. Energy 85, 2264–2274. https://doi.org/10.1016/j.solener.2011.06.011

Neuenstein J., P.C., 2009. Los módulos y sus curvas. Photon. La Rev. fotovoltaica 54–71.

Nofuentes, G., Aguilera, J., Álvarez, E., Hontoria, L., de la Casa, J., 2003. Estimación de la potencia máxima media en condiciones estándares de medida de un módulo fotovoltaico de silicio cristalino, in: X Simposio Peruano de Energía Solar.

Nofuentes, G., de la Casa, J., Solís-Alemán, E.M., Fernández, E.F., 2017. Spectral impact on PV performance in mid-latitude sunny inland sites: Experimental vs. modelled results. Energy 141, 1857–1868. https://doi.org/10.1016/j.energy.2017.11.078

Or, A. Ben, Appelbaum, J., 2013. Estimation of multi-junction solar cell parameters. Prog. Photovolt Res. Appl. https://doi.org/10.1002/pip.2158

Osterwald, C.R., 1986. Translation of device performance measurements to reference conditions. Sol. Cells,18,3-4,Pages 269-279 80401, 269–279.

Pam, M., Bogdanov, D., Aghahosseini, A., Oyewo, S., Gulagi, A., Child, M., Fell, H.-J., Breyer, C., 2017. Global energy system based on 100% renewable energy - power sector.

Phang, J.C.H., Chan, D.S.H., Phillips, J.R., 1984. Accurate analytical method for the extraction of solar cell model parameters. Electron. Lett. 20, 406. https://doi.org/10.1049/el:19840281

Picault, D., Raison, B., Bacha, S., de la Casa, J., Aguilera, J., 2010. Forecasting photovoltaic array power production subject to mismatch losses. Sol. Energy 84, 1301–1309. https://doi.org/10.1016/j.solener.2010.04.009

Piliougine, M., Cañete, C., Moreno, R., Carretero, J., Hirose, J., Ogawa, S., Sidrach-de-Cardona, M., 2013. Comparative analysis of energy produced by photovoltaic modules with anti-soiling coated surface in arid climates. Appl. Energy 112, 626–634. https://doi.org/10.1016/j.apenergy.2013.01.048

Piliougine, M., Carretero, J., Mora-Lõpez, L., Sidrach-De-Cardona, M., 2011. Experimental system for current-voltage curve measurement of photovoltaic modules under outdoor conditions. Prog. Photovoltaics Res. Appl. 19, 591–602. https://doi.org/10.1002/pip.1073

Publicover, B., 2019. IHS Markit: la demanda solar global alcanzará 129 GW en 2019. PV-Magazine.

PV-Engineering GmbH, 2016. pve Photovoltaik Engineering [WWW Document]. https://www.pv-engineering.de/en/home/. URL https://www.pv-engineering.de/en/home/

Rivai, A., Rahim, N.A., 2014. Binary-based tracer of photovoltaic array characteristics. IET Renew. Power Gener. 8, 621–628. https://doi.org/10.1049/iet-rpg.2013.0111

Rodrigo Cruz, P.M., 2013. Contribución al desarrollo de los sistemas fotovoltaicos de concentración. Estudio de las pérdidas de energía por sombreado. Universidad de Jaén.

Rodrigo, P., Fernández, E.F., Almonacid, F., Pérez-Higueras, P.J., 2013. Models for the electrical characterization of high concentration photovoltaic cells and modules: A review. Renew. Sustain. Energy Rev. 26, 752–760. https://doi.org/10.1016/j.rser.2013.06.019

Sanchis, P., López, J., Ursúa, A., Gubía, E., Marroyo, L., 2007. On the Testing, Characterization, and Evaluation of PV Inverters and Dynamic MPPT Performance Under Real Varying Operating Conditions. Prog. Photovolt Res. Appl. 15, 659–676. https://doi.org/10.1002/pip

Schneider Electric, 2018. Schneider Electric Leadership Series: Digital Grid Unleashed.

Silvestre, S., Kichou, S., Guglielminotti, L., Nofuentes, G., Alonso-Abella, M., 2016. Degradation analysis of thin film photovoltaic modules under outdoor long term exposure in Spanish continental climate conditions. Sol. Energy 139, 599–607. https://doi.org/10.1016/J.SOLENER.2016.10.030

Smith, R.M., Jordan, D.C., Kurtz, S.R., 2012. Outdoor PV module degradation of current-voltage parameters, in: World Renewable Energy Forum. pp. 1–9.

SolarPower Europe, 2019. Global Market Outlook For Solar Power: 2018 - 2022 1–81.

TEP2009-5045M, n.d. Análisis y caracterización de un Sistema Fotovoltaico de Concentración. Comparativa con otras tecnologías fotovoltaicas.

Texas Instruments, 2019. ARM® Cortex®-M4F Based MCU TM4C123G LaunchPad™ Evaluation Kit [WWW Document]. URL http://www.ti.com/tool/EK-TM4C123GXL

Torres-Ramírez, M., 2015. Contribución al modelado del comportamiento eléctrico en exterior de módulos fotovoltaicos de capa delgada. Universidad de Jaén.

Tossa, A.K., Soro, Y.M., Azoumah, Y., Yamegueu, D., 2014. A new approach to estimate the performance and energy productivity of photovoltaic modules in real operating conditions. Sol. Energy 110, 543–560. https://doi.org/10.1016/j.solener.2014.09.043

TRITEC Group, 2008. Tritec [WWW Document]. URL http://www.tritec-energy.com/

WILLUHN, M., 2019. Brazil A-4 auction signs 211 MW of solar for record-low price of $0.0175 kWh. PV-Magazine.

Yandt, M.D., Cook, J.P.D., Kelly, M., Schriemer, H., Hinzer, K., 2015. Dynamic Real-Time I – V Curve Measurement System for Indoor / Outdoor Characterization of Photovoltaic Cells and Modules. IEEE J. Photovoltaics 5, 337–343. https://doi.org/10.1109/JPHOTOV.2014.2366690

Yu, K., Chen, X., Wang, X., Wang, Z., 2017. Parameters identification of photovoltaic models using self-adaptive teaching-learning-based optimization. Energy Convers. Manag. 145, 233–246. https://doi.org/10.1016/j.enconman.2017.04.054

CEAEMA- Ujaen ,2014:

Título del proyecto: Acciones de cooperación al desarrollo en el marco de la transferencia del conocimiento a universidades iberoamericanas. caso de estudio: caracterización a sol real de módulos FV utilizando equipamiento de bajo coste.
Entidad/es financiadora/s: CEAEMA – Universidad de Jaén.
Entidades participantes: Universidad de Jaén – Universidad Nacional del Nordeste (Argentina).
Investigador/es responsable/es: Juan de la Casa Higueras.
Número de investigadores/as: 5
Nombre del programa: Plan Plurianual de I+D del Centro de Estudios Avanzados en Energía y Medio Ambiente
Código según financiadora: CG 03.11.02
Fecha de inicio: 1/06/2014 hasta: 31/12/2015
Cuantía total: 10.000 Euros

6

PUBLICACIONES

PUBLICACIONES EN REVISTAS INDEXADAS EN JCR

Listado de publicaciones aceptadas o en estado de revisión, en orden cronológico:

[I] Fernández, E.F., Montes-Romero, J., de la Casa, J., Rodrigo, P., Almonacid, F., 2016. Comparative study of methods for the extraction of concentrator photovoltaic module parameters. Sol. Energy 137, 413–423. https://doi.org/10.1016/j.solener.2016.08.046

[II] Montes-Romero, J., Piliougine, M., Muñoz, J., Fernández, E., de la Casa, J., 2017. Photovoltaic Device Performance Evaluation Using an Open-Hardware System and Standard Calibrated Laboratory Instruments. Energies 10, 1869. https://doi.org/10.3390/en10111869

[III] Montes-Romero, J., Almonacid, F., Theristis, M., de la Casa, J., Georghiou, G.E., Fernández, E.F., 2018. Comparative analysis of parameter extraction techniques for the electrical characterization of multi-junction CPV and m-Si technologies. Sol. Energy 160, 275–288. https://doi.org/10.1016/j.solener.2017.12.011

[IV] *M. Cáceres, A. Firman, J. Montes-Romero, A. Raúl, G. Mayans, L. Horacio, E. F. Fernández, J. de la Casa, "Low cost I-V curve tracer for PV modules under real operation conditions." IEEE Instrumentation and Measurements.* ***EN REVISIÓN***

PUBLICACIONES EN REVISTAS INDEXADAS EN SJR

[V] García-Vico, A.M., Montes, J., Aguilera, J., Carmona, C.J., del Jesus, M.J., 2016. Analysing Concentrating Photovoltaics Technology Through the Use of Emerging Pattern Mining, in: Advances in Intelligent Systems and Computing book series, AISC, volume 527. Springer International Publishing, Cham, pp. 334–344. https://doi.org/10.1007/978-3-319-47364-2_32

COMUNICACIONES A CONGRESOS CON VISIBILIDAD SCOPUS

[VI] Montes-Romero, J., Torres-Ramírez, M., De La Casa, J., Firman, A., Cáceres, M., 2016. Software tool for the extrapolation to Standard Test Conditions (STC) from experimental curves of photovoltaic modules, in: IEEE XPlore. Proceedings of 2016 Technologies Applied to Electronics Teaching, TAEE 2016. https://doi.org/10.1109/TAEE.2016.7528252

[VII] Fernández, E.F., Montes-Romero, J., de la Casa, J., Firman, A., Cáceres, M., Vera, L.H., 2018. Contributions to the design and construction of characteristic curve tracers for photovoltaic devices, in: IEEE XPlore. Proceedings of 2018 Technologies Applied to Electronics Teaching, TAEE 2018. https://doi.org/10.1109/TAEE.2018.8476093

[VIII] Montes-Romero, J., Micheli, L., Theristis, M., Fernández-Solas, Á., De La Casa, J., Georghiou, G.E., Almonacid, F., Fernández, E.F., 2019. Impact of soiling on the outdoor performance of CPV modules in Spain, in: 15th International Conference on Concentrator Photovoltaic Systems. Fes, Morocco. https://doi.org/10.1063/1.5124197

[IX] *Conde, L.A., Montes-Romero, J., Carhuavilca, A., Perich, R., Jorge, A., Angulo, J., Muñoz, E., Töfflinger, J.A., Casa, J. De, 2019. Performance evaluation and characterization of different photovoltaic technologies under the coastal , desertic climate conditions of Lima , Peru, in: Solar World Congress. Santiago, Chile.* ***ACEPTADO, EN PROCESO DE PUBLICACIÓN***

PUBLICACIÓN I

Título	**"Comparative study of methods for the extraction of concentrator photovoltaic module parameters"**
Autores	F. Fernández, E.; Montes-Romero, J.; de la Casa, J.; Rodrigo, P.; Almonacid, F.
Revista	Solar Energy
Volumen, páginas, año	137, 413-423, 2016
Categoría y posición	ENERGY AND FUELS (21/92)
Factor de impacto	4.018 (2016)
DOI	10.1016/j.solener.2016.08.046

Solar Energy 137 (2016) 413–423

Contents lists available at ScienceDirect

Solar Energy

journal homepage: www.elsevier.com/locate/solener

Comparative study of methods for the extraction of concentrator photovoltaic module parameters

Eduardo F. Fernández [a,*], Jesús Montes-Romero [a], Juan de la Casa [a], Pedro Rodrigo [b], Florencia Almonacid [a]

[a] IDEA Solar Energy Research Group, University of Jaen, Jaen 23071, Spain
[b] Universidad Panamericana, Campus Aguascalientes, Facultad de Ingeniería, Josemaría Escrivá de Balaguer 101, Aguascalientes, Aguascalientes 20290, Mexico

ARTICLE INFO

Article history:
Received 22 July 2016
Received in revised form 24 August 2016
Accepted 26 August 2016
Available online 31 August 2016

Keywords:
Concentrator photovoltaics
IV parameters
Extracting methods

ABSTRACT

The modelling and outdoor evaluation of high concentrator photovoltaic (HCPV) systems is complex due to the use of multi-junction solar cells and optical devices. At the same time, the single exponential model (SEM) is widely used for predicting the IV characteristics of PV systems. In this paper, several conventional analytical methods for extracting the five parameters of the SEM model of non-concentrating PV devices are applied and evaluated for the electrical characterization of a HCPV module for the first time. Among the different approaches, three simple analytical methods have been selected with the aim of offering rapid and easy solutions for the characterization of HCPV systems. The selected methods are: the method of Phang et al., the method of Blas et al. and the method of Khan et al. In addition, these methods are compared with a numerical extraction method previously introduced by the authors. Results show that all the methods investigated can be valid for predicting the IV curve of a HCPV module except the method of Khan et al., which tends to underestimate the IV curve and maximum power of the module. The dependence of the extracted SEM model parameters with the input irradiance is also discussed.

1. Introduction

The most widely used approach for the electrical characterization of photovoltaic (PV) solar cells and modules is based on the equivalent circuit shown in Fig. 1. From this circuit, the relation between the current (I) and the voltage (V) is given by the so-called single exponential model (SEM) according to the following mathematical expression:

$$I = I_{ph} - I_o\left(\exp\left(\frac{V+IR_s}{mV_T}\right) - 1\right) - \frac{(V+IR_s)}{R_{sh}} \quad (1)$$

where the solar cell or module is characterized by a set of 5 parameters, namely: the photo-generated current (I_{ph}), the diode saturation current (I_o), the diode ideality factor (m), the series resistance (R_s) and the shunt (or parallel) resistance (R_{sh}). V_T in Eq. (1) is the thermal voltage of the PV device, given by $V_T = kT/q$, being k the Boltzmann constant with a value of 1.38E−23 J/K and q the electron or elementary charge with a value of 1.60E−19 C.

The current-voltage (IV) characterization provides the most information of the performance of any type of PV device (Almonacid et al., 2015). In this context, the accurate estimation of the characteristic parameters of Eq. (1) is crucial for the modelling, evaluation, quality control concerns, degradation studies, optimization of fabrication process and for scientific research in general (Kichou et al., 2016a,b; Ishibashi et al., 2008; Lo Brano et al., 2010; Celik and Acikgoz, 2010; Gasparin et al., 2016). Bearing this in mind, the scientific community have devoted big efforts in developing tools capable to estimate the characteristic parameters of solar cells and modules for decades (Cotfas et al., 2013; Ciulla et al., 2014; Humada et al., 2016; Li et al., 2013). The different extraction methods can be divided in analytical or semi-analytical methods (Chegaar et al., 2006; Ishibashi et al., 2008; Tivanov et al., 2005; Wolf and Benda, 2013) and in numerical methods (Ghani et al., 2014, 2016) such as vertical optimization (Easwarakhanthan et al., 1986), electric conductance optimization (Chegaar et al., 2004), co-content function (Ortiz-Conde et al., 2006), Lambert-W function (Zhang et al., 2011; Ghani and Duke, 2011), genetic algorithms (Sellami and Bouaïcha, 2011) or particle swarm optimization algorithms (Ye et al., 2009). The numerical methods are supposed to be more accurate and adaptable to the particular solar cells and modules under study. Despite of this, Chan et al. (1986) have pointed out that the analytical methods can be more accurate than sophisticated curve fitting and numerical methods under the normal operating conditions of PV devices.

High Concentrator Photovoltaics (HCPV) is considered as one of the most promising research avenues to produce more

* Corresponding author at: Centre for Advanced Studies in Energy and Environment, University of Jaen, Jaen 23071, Spain.
E-mail address: fenandez@ujaen.es (E.F. Fernández).

http://dx.doi.org/10.1016/j.solener.2016.08.046
0038-092X/

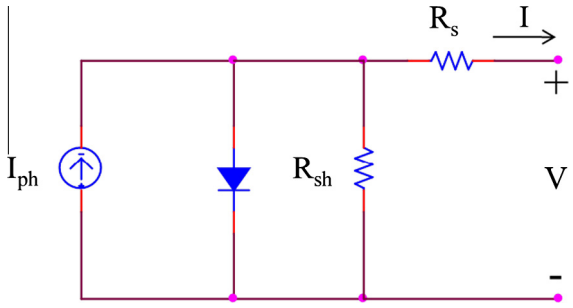

Fig. 1. Equivalent circuit of the single exponential model of a PV device.

cost-effective electricity than PV technology by replacing the amount of semiconductor material by using less expensive optical elements (Friedman et al., 2013; Perez-Higueras and Fernández, 2015) and has already shown promising results at locations with high solar resource (Talavera et al., 2015; Haysom et al., 2015; Fernández et al., 2016a). The HCPV module is the fundamental unit of HCPV technology to convert the direct non-concentrated sunlight into electricity and, nowadays, largely consists of (Rodrigo et al., 2015b): high efficiency multi-junction III–V solar cells made up of several p-n junctions to increase the absorption of the incident solar spectrum (Fernández et al., 2013a; Yamaguchi et al., 2008), and therefore, the efficiency of the system (Fernández et al., 2015a; Yamaguchi et al., 2005), a primary optical concentrator element, a secondary optical element to homogenize the luminous power on the solar cell surface and to improve the acceptance angle of the system (Shanks et al., 2016), and a passive cooling mechanism able to dissipate the heat produced by the high energy fluxes impinging on the solar cells surface (Micheli et al., 2016). Due to the features commented above, the modelling and electrical characterization of HCPV devices is inherently different and more complex than in conventional PV systems (Rodrigo et al., 2013, 2014; Theristis and O'Donovan, 2015) and the understanding of the performance of HCPV modules when operating in real world conditions is clearly lower than conventional PVs (Soria-Moya et al., 2015; Kurtz et al., 2015; Fernández et al., 2013b).

At the present, the studies concerning the extraction of the five parameters of Eq. (1) in HCPV technology are essentially limited to the work presented in (Segev et al., 2012; Ben Or and Appelbaum, 2013; Appelbaum and Peled, 2014; Almonacid et al., 2016). Segev et al. (2012) proposed a semi-empirical numerical method to extract the characteristics parameters of triple-junction InGaP/InGaAs/Ge solar cells under different concentrations and temperatures. The study of the Newton-Raphson method, the Levenberg-Marquardt method combined with Lambert-W function and a Genetic-Algorithm for the extraction of the key parameters of a triple-junction InGaP/InGaAs/Ge solar cell under different concentration levels was conducted by Ben Or and Appelbaum (2013) and Appelbaum and Peled (2014). Recently, Almonacid et al. (2016) proposed a numerical method to extract the parameters of a whole HCPV module under real different operating conditions of irradiance and temperature.

This paper goes deep in the previous study of the authors commented above. For the first time, the simple conventional analytical solutions for the extraction of the five parameters of non-concentrating PV devices are applied and analysed for HCPV technology. The selected extraction methods have been chosen according to the two following criteria: (a) easy and fast to implement and (b) extract the five parameters of the SEM model. Moreover, the methods under study are compared with the numerical method previously introduced by the authors. The final aim of this work is to examine simple and rapid solutions for the modelling and evaluation of HCPV technology. In addition, the dependence of the extracted parameters with the incident irradiance is investigated to contribute to the discussion of the fundamental dependencies of concentrator solar cells with light intensity (Fernández et al., 2015b; Kinsey et al., 2008; Siefer and Bett, 2014). These topics are critical to achieve a better understanding of this technology under real working scenarios, and then, to help in its market expansion and large scale deployment.

2. Experimental set-up

To conduct this study, the data available of a HCPV module monitored during six months from July to December 2013 at the Centre for Advanced in Energy and Environment at the University of Jaen in Southern Spain have been used. Jaen is a non-industrialised medium size city with low-medium values of precipitable water and turbidity, periodically affected by Saharan dust and burning of olives trees branches. It also has a high annual energy resource, more than 2000 kW h/m^2, and an extreme range of air temperatures that usually go from around 5 °C in winter to more than 40 °C in summer. Thus, it is possible to evaluate the performance of PV and HCPV devices under a wide range of atmospheric conditions. The HCPV module, see Fig. 2, is formed by 20 triple-junction lattice-matched GaInP/GaInAs/Ge solar cells interconnected in series. The primary optics consists of silicone-on-glass Fresnel lenses and the secondary optics of reflective truncated pyramids. The efficiency of this optical configuration is 80%. The module has also a geometric concentration of 700× and uses natural convective finned aluminium heat exchangers to ensure that the cells are working on their recommended temperature range, which is usually within 50–80 °C (Fernández et al., 2014a). Fig. 3 shows a schematic diagram of a single solar receiver integrated with the primary and secondary optics, as well as the different materials that compose the different layers of the solar receiver. It is worth mentioning that the features of the module described above represent the most wide-spread concentrator nowadays (Rodrigo et al., 2015b). Hence, the results of this work can be considered representative of the current HCPV technology.

The HCPV module was mounted of a high-accurate pedestal two-axis solar tracker designed by BSQ Company, see Fig. 2, for point focus Fresnel Lenses. The current-voltage characteristics were recorded with a high-precise four-wire PVPV 1000 C40 IV tracer (less than 1 s and 100 points per IV curve for the electrical range of the module under study). Also, two four-wire PT100 temperature sensors were installed on the back of the module and on a solar cell receiver to record, respectively, the heat-sink and cell temperature, as previously discussed in (Fernández et al., 2014b). In addition, an atmospheric station MTD 3000 from Geonica Company equipped with different sensors recorded all the relevant parameters necessary for the outdoor evaluation of concentrator photovoltaic modules. All the parameters were monitored every 5 min. The days on which the system was stopped by failure, maintenance or because an experiment was carried out have not been considered to avoid any distortion on the data. Also, the module was cleaned once a week and after rainy days, and the alignment of the tracker was periodically calibrated to avoid possible electrical losses and noise in the recorded data. Further information of the experimental set-up above can be found, for instance, in (Fernández et al., 2013b).

Table 1 shows the maximum, minimum and average values of cell temperature (T_C) and spectrally corrected direct normal irradiance (DNI_C), or simply effective irradiance, gathered during the experiment. This irradiance may be defined as the portion of the spectrum that the HCPV module is able to convert into electricity

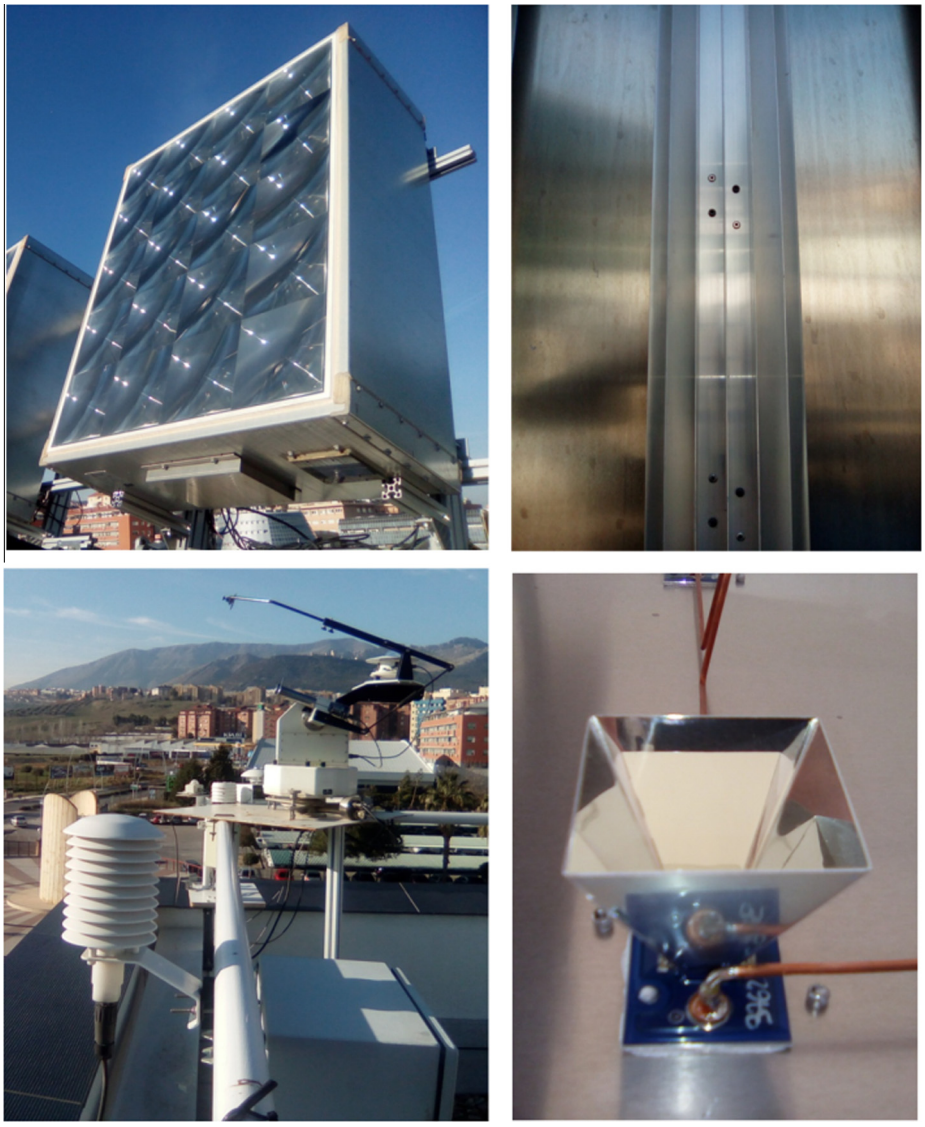

Fig. 2. Top-left: front of the HCPV module, top-right: back of the HCPV module, bottom-left: atmospheric station and bottom-right: detail of a solar receiver with secondary optics.

by considering its spectral response. It is a more appropriate magnitude than the broadband direct normal irradiance (DNI) for the electrical characterization of HCPV systems since it contains the strong spectral dependence of the device (Theristis et al., 2016a; Peharz et al., 2009). Detailed information of this magnitude and its estimation from atmospheric variables can be found in (Fernández and Almonacid, 2014; Fernández et al., 2015c, 2016b). It should be also remarked that sensor previously commented to measure T_C was placed on a solar receiver close to one of the solar cells of the module by using a high conductivity thermal paste (thermal conductivity > 3.5 W/m K). This receiver was located between the centre and the border of the module, so that, this temperature should be considered as the average cell temperature of the module due to the temperature distribution of HCPV modules (Ota et al., 2012). This approach has been previously discussed by the authors and demonstrated to be valid for approximating the cell temperature and the electrical characterization of HCPV modules (Fernández et al., 2014b, 2015d; Fernández and Almonacid, 2015). In addition, Fig. 4 shows the data distribution as a function of the DNI_C and T_C recorded during the whole experimental campaign.

3. Extraction methods

In this section, the main features of the selected extraction methods are described. The mathematical expressions and the main procedures necessary for the estimation of the five characteristic parameters of Eq. (1) are provided. The methods selected in this study are: the method of Phang et al. (1984), the method of Blas et al. (2002), the method of Khan et al. (2013) and the method of Almonacid et al. (2016). Among the different methods available in the literature, and as previously commented, these methods have been select according to the following two criteria: (a) they are easy and fast to implement and (b) they extract the five parameters of the single exponential model. Therefore, they would allow the complete IV characteristics of HCPV systems to be modelled by using simple mathematical procedures.

3.1. Method of Phang et al.

A simple analytical method for extracting the five parameters of several single-junction solar cells under different irradiance and temperature levels was proposed by Phang et al. (1984). First,

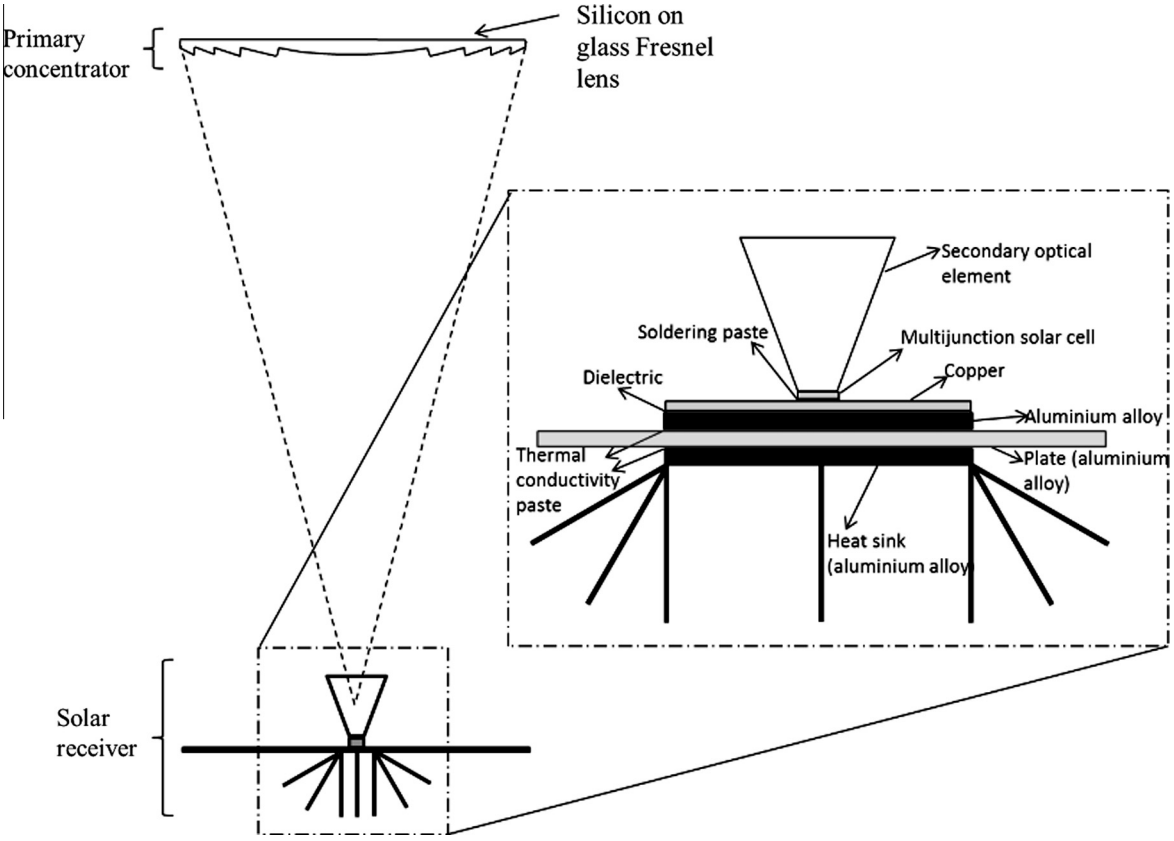

Fig. 3. Schematic detailed diagram of a single receiver integrated with the primary and secondary optics of the HCPV module under study.

Table 1
Maximum, minimum and average values of T_c (cell temperature) and DNI_c (effective direct normal irradiance) recorded during the experiment.

Value	T_C (°C)	DNI_C (W/m^2)
Maximum	89.2	972.3
Minimum	32.4	250.2
Average	57.3	637.6

the values of R_{so} and R_{sho} are estimated by performing a linear fit of the IV curve around the open-circuit voltage and the short-circuit current, respectively, according to:

$$R_{so} = -\left(\frac{dV}{dI}\right)_{V=V_{oc}} \tag{2}$$

$$R_{sho} = -\left(\frac{dV}{dI}\right)_{I=I_{sc}} \tag{3}$$

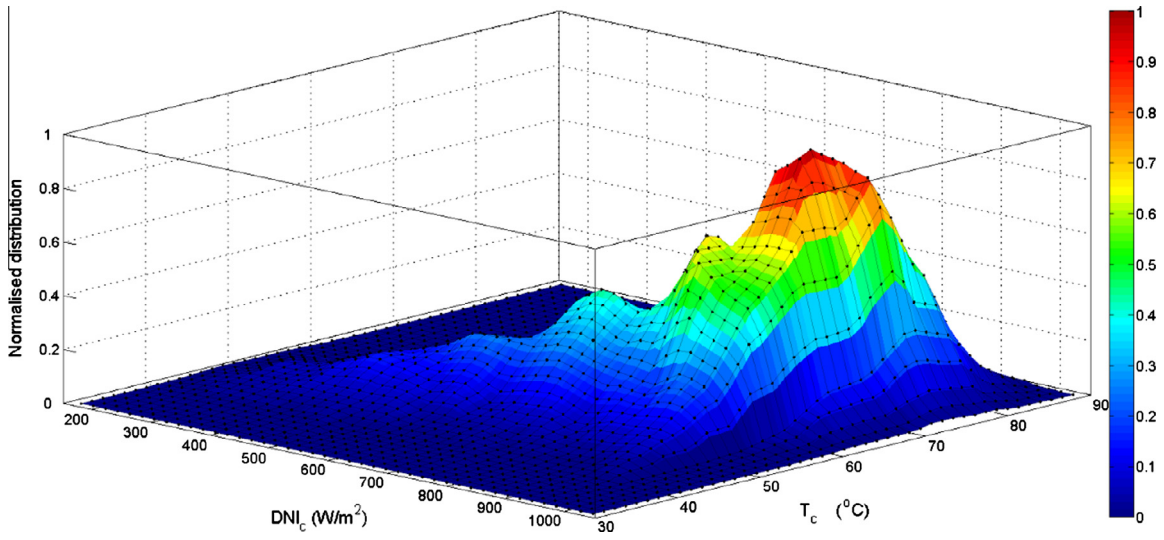

Fig. 4. Normalised data distribution as a function of the measured T_c (cell temperature) and DNI_c (effective direct normal irradiance).

After that, the five parameters of Eq. (1) are estimated from the experimental values of I_{sc}, V_{oc}, I_{mpp}, V_{mpp}, R_{so} and R_{sho} by means of the following expressions:

$$I_{ph} = I_{sc}\left(1 + \frac{R_s}{R_{sh}}\right) + I_o\left(\exp\left(\frac{I_{sc}R_s}{mV_T}\right) - 1\right) \quad (4)$$

$$I_o = \left(I_{sc} - \frac{V_{oc}}{R_{sh}}\right)\exp\left(-\frac{V_{oc}}{mV_T}\right) \quad (5)$$

$$m = \frac{V_{mpp} + R_{so}I_{mpp} - V_{oc}}{V_T\left[\ln\left(I_{sc} - \frac{V_{mpp}}{R_{sh}} - I_{mpp}\right) - \ln\left(I_{sc} - \frac{V_{oc}}{R_{sh}}\right) + \frac{I_{mpp}}{I_{sc} - \frac{V_{oc}}{R_{sh}}}\right]} \quad (6)$$

$$R_s = R_{so} - \frac{mV_T}{I_o}\exp\left(-\frac{V_{oc}}{mV_T}\right) \quad (7)$$

$$R_{sh} = R_{sho} \quad (8)$$

3.2. Method of Blas et al.

The aim of the method proposed by Blas et al. (2002) was to develop a simple procedure able to extract the five parameters of a PV module with a satisfactory degree of accuracy. As in the previous method, the characteristic parameters of Eq. (1) are estimated for the desired levels of irradiance and temperature from the experimental values of I_{sc}, V_{oc}, I_{mpp} and V_{mpp}, R_{so} and R_{sho}. The proposed equations are:

$$I_{ph} = I_o\left(\exp\left(\frac{V_{oc}}{mV_T}\right) - 1\right) + \frac{V_{oc}}{R_{sh}} \quad (9)$$

$$I_o = \left(I_{sc}\left(1 + \frac{R_s}{R_{sh}}\right) - \frac{V_{oc}}{R_{sh}}\right)\exp\left(-\frac{V_{oc}}{mV_T}\right) \quad (10)$$

$$m = \frac{V_{mpp} + R_sI_{mpp} - V_{oc}}{V_T ln\left[\frac{(I_{sc} - I_{mpp})\left(1 + \frac{R_s}{R_{sh}}\right) - \frac{V_{mpp}}{R_{sh}}}{I_{sc}\left(1 + \frac{R_s}{R_{sh}}\right) - \frac{V_{oc}}{R_{sh}}}\right]} \quad (11)$$

$$R_s = \frac{R_{so}\left(\frac{V_{oc}}{mV_T} - 1\right) + R_{sho}\left(1 - \frac{I_{sc}R_{so}}{mV_T}\right)}{\frac{V_{oc} - I_{sc}R_{sho}}{mV_T}} \quad (12)$$

$$R_{sh} = R_{sho} - R_s \quad (13)$$

On the contrary than the methods of Phang et al. and Khan et al., to solve the equations of this method, is necessary to follow a simple algorithm in which an initial value of R_s has to be assumed. The steps to solve the system of equations are as follows: (1) set an initial value of R_s, (2) estimate the values of R_{sh} and m, (3) recalculate R_s, (4) repeat steps (2) and (3) until the value of R_s converges, (4) calculate I_{ph}, I_o, m and R_{sh} from this last value of R_s and the rest of the experimental data previously commented.

3.3. Method of Khan et al.

An analytical method to extract the parameters of silicon solar cells under different concentration levels has been recently reported by Khan et al. (2013). This method allows the parameters of a PV cell under high fluxes to be obtained from the experimental measurements of I_{sc}, V_{oc}, I_{mpp} and V_{mpp}, R_{so} and R_{sho} by means of the following set of equations:

$$m = \frac{V_{mpp} + R_sI_{mpp} - V_{oc}}{V_T\left[\ln(I_{sc} - I_{mpp}) - \ln(I_{sc})\right]} \quad (14)$$

$$I_o = \frac{mV_T}{(R_{so} - R_s)}\exp\left(-\frac{V_{oc}}{mV_T}\right) \quad (15)$$

$$R_s = R_{so} - \frac{V_{mpp} + R_{so}I_{mpp} - V_{oc}}{I_{mpp} + \left[\ln(I_{sc} - I_{mpp}) - \ln(I_{sc})\right]I_{sc}} \quad (16)$$

The values of I_{ph} and R_{sh} are estimated, respectively, as previously defined in Eqs. (9) and (8).

3.4. Method of Almonacid et al.

A numerical method to extract the parameters of HCPV modules was presented by Almonacid et al. (2016). The method is based on building a system of five non-linear implicit equations derived from Eq. (1). This system is then solved for the five unknown parameters by a trust-region optimization algorithm (Powell, 1970).

The points on the IV curve required to build the system of equations are: (0, I_{sc}), (V_{mpp}, I_{mpp}), (V_{oc}, 0) and two additional points (V_x, I_x) and (V_{xx}, I_{xx}), where $V_x = V_{oc}/2$ and $V_{xx} = (V_{mpp} + V_{oc})/2$. By applying Eq. (1) to these points, the system of five equations with five unknowns is obtained.

The trust-region algorithm searches a numerical solution of the system. This technique improves robustness when starting far from the solution and is able to handle the case when the Jacobian at a specific iteration is singular. However, as other optimization algorithms, it requires an initial set of parameter values. This initial set is calculated from R_{so}, R_{sho}, I_{sc} and V_{oc} by the following equations:

$$R_{sh} = R_{sho} \quad (17)$$

$$R_s = R_{so} - \frac{mV_T}{I_{sc} - V_{oc}/R_{sh}} \quad (18)$$

$$I_{ph} = \left(1 + \frac{R_s}{R_{sh}}\right)I_{sc} \quad (19)$$

$$I_0 = \left(I_{sc} - \frac{V_{oc} - R_sI_{sc}}{R_{sh}}\right)\exp\left(-\frac{V_{oc}}{mV_T}\right) \quad (20)$$

As the m parameter is unknown, seven attempts of solving the system are run for the values m = 1.0, 1.5, 2.0, 2.5, 3.0, 3.5, 4.0,. . .. The solution that minimizes the sum of squares of current errors is then selected as the best solution of the system, and results of this solution are considered as the extracted parameters of the IV curve.

4. Results

In this section, the analysis of results of the methods described in the previous section is carried out. To achieve this, several IV curves covering the full operating range of the HCPV module were selected. First, an analysis of the recorded IV curves as a function of the cell temperature and effective irradiance was conducted, see Fig. 4. Based on this distribution, the six IV curves shown in Table 2 have been considered as a representative set of data of the HCPV module under real working conditions, see also Table 1. Curves 1 and 2 represent IV curves with low effective irradiance, and low and high cell temperatures, respectively. Curves 3 and 4 represent IV curves with high effective irradiance, and low and high cell temperatures. Finally, curves 5 and 6 represent IV curves around the maximum of the data distribution which represent the typical working conditions of the HCPV module. The criteria above, as well as the IV curves shown in Table 2, are the same previously considered by the authors to validate the models analysed in (Almonacid et al., 2016).

Table 2
Effective normal irradiance, cell temperature and main electrical parameters of the IV curves used to evaluate the methods.

Curve	DNI_C (W/m^2)	T_C (°C)	I_{sc} (A)	V_{oc} (V)	I_{mpp} (A)	V_{mpp} (V)
1	253	39.9	1.49	60.35	1.33	54.76
2	352	65.5	2.07	57.46	1.86	51.65
3	905	48.7	5.33	59.54	4.84	49.50
4	928	86.7	5.47	55.06	4.98	45.90
5	665	56.4	3.92	58.56	3.69	49.80
6	814	70.5	4.79	56.96	4.43	46.65

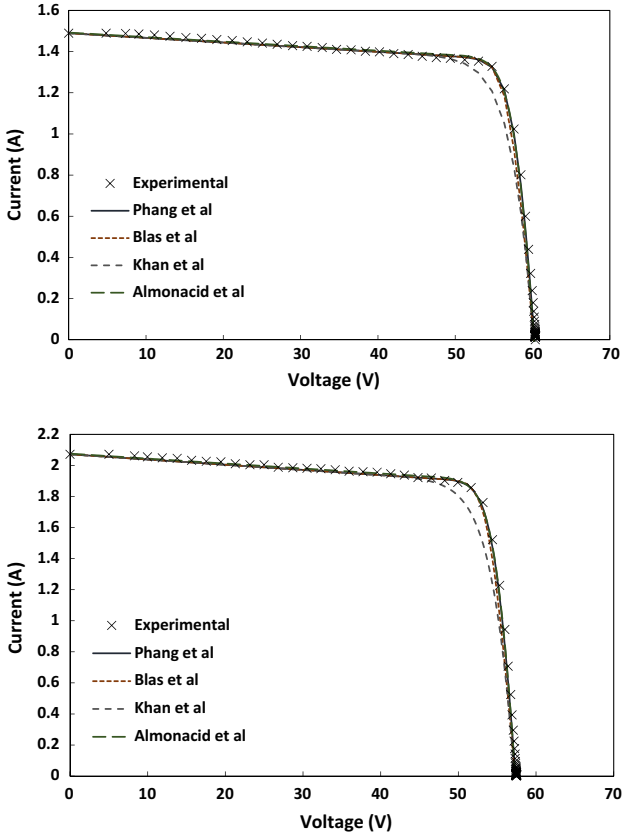

Fig. 5. Measured and modelled IV curve for low effective irradiance, and low (top) and high (bottom) cell temperatures (curves 1 and 2).

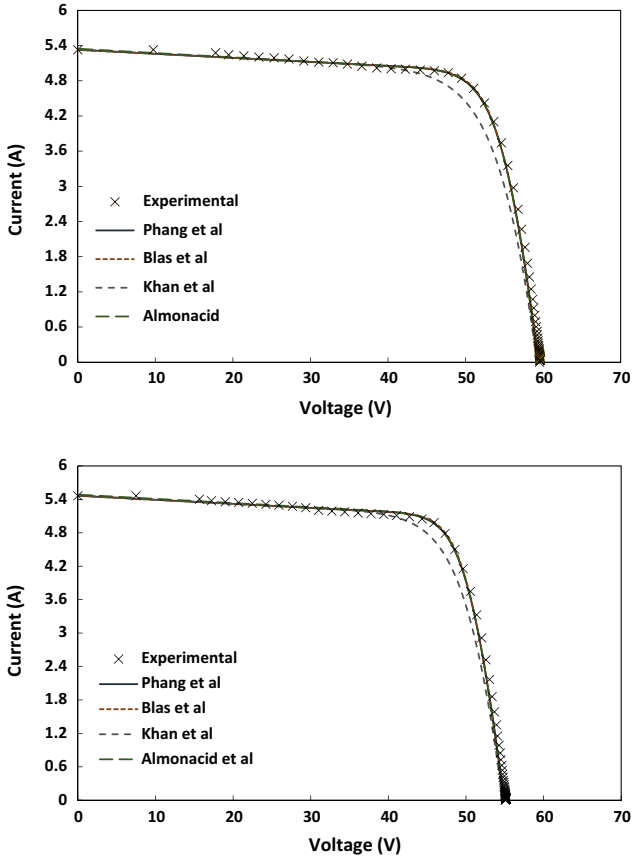

Fig. 6. Measured and modelled IV curve for high effective irradiance, and low (top) and high (bottom) cell temperatures (curves 3 and 4).

Figs. 5–7 show the six selected and modelled IV curves with the four methods under study. Different statistical indexes have been calculated to analyse the quality of the methods for the modelling of these representative IV curves. Fig. 8 shows the root means square error (RMSE) and the mean bias error (MBE) between actual and modelled IV curves for the four methods under study obtained as (Rodrigo et al., 2015a):

$$RMSE = \sqrt{\frac{1}{N}\sum_{i=1}^{N} RE(V)_i^2} \tag{21}$$

$$MBE = \frac{1}{N}\sum_{i=1}^{N} RE(V)_i \tag{22}$$

where N is the number of samples on the curve taken at small voltage steps and $RE(V)_i$ is the relative error between the modelled and the measured current at a voltage V. This relative error is calculated for each value of voltage by means of the following expression:

$$RE(V) = \frac{I_{modelled}(V) - I_{measured}(V)}{I_{sc,measured}} \tag{23}$$

Results show that all the methods predict the IV curve of the HCPV module with a high quality except the method of Khan et al., see also Figs. 5–7. The methods of Phang et al. and Almonacid et al. give the best and similar results with an average RMSE of 1.22% and 1.35%, and an average MBE of −0.46% and −0.40% respectively. The method of Blas et al. gives slightly poorer results with an average RMSE of 1.71% and an average MBE of −0.66%. The method of Khan et al. gives the poorest results with an average RMSE of 3.53% and an average MBE of −1.81%, which indicates that this method tends to underestimate the IV curve of the HCPV module. This underestimation is mainly located around the maximum power point of the IV curve, as can be clearly seen in the examples shown in Figs. 5–7. This effect has found to be because of the higher predicted values of I_o and m compared with the other methods, as discussed below. The methods of Phang et al., Almonacid et al. and Blas et al. predict the maximum power of the HCPV module with a high quality with an average absolute relative error of 0.3%, 0.0% and 0.1% respectively. On the contrary, the underestimation of the method of Khan et al. around the maximum power point of the IV curve leads to an average absolute relative error of 5.4%. In

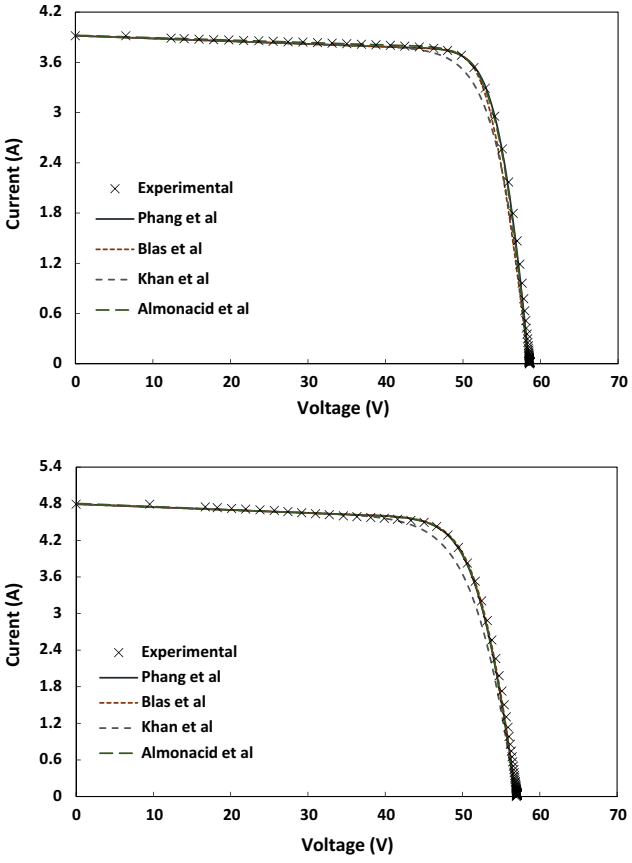

Fig. 7. Measured and modelled IV curve for typical observed values of effective irradiance and cell temperature (curves 5 and 6).

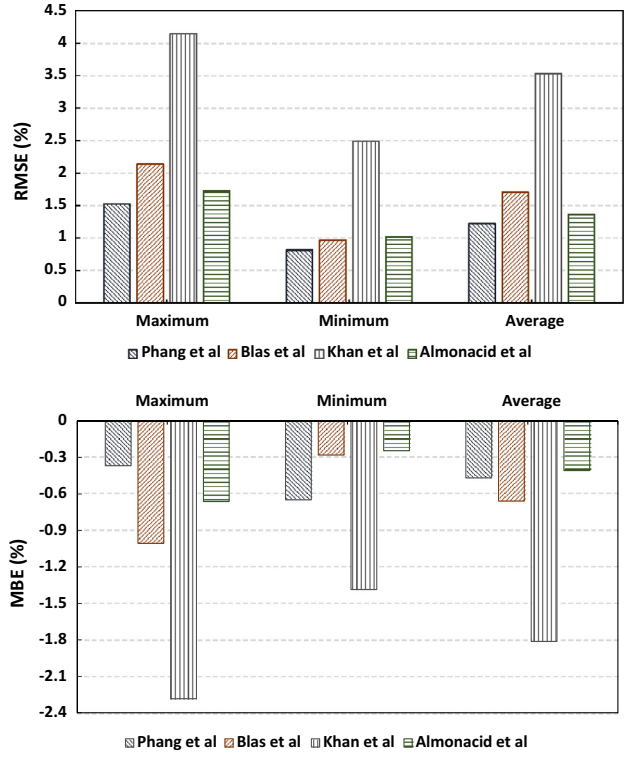

Fig. 8. Root means square error (RMSE), top, and mean bias error (MBE), bottom, between actual and predicted IV curves for the four analysed methods.

addition to the commented above, it is worth mentioning that the performance of all the methods has found to be independent of the operating conditions, cell temperature and effective irradiance, of the HCPV module.

In addition, the determination coefficient (R^2) between actual and modelled current at each voltage step for the six IV curves and the four methods has been also calculated, see Fig. 9. The R^2 values are close to 1 for all the methods which indicates the good match between the measured and modelled current. In any case, the methods of Phang et al. and Almonacid et al. show once again the best results with values of R^2 of 0.99. The method of Blas et al. gives slightly poorer results with an average R^2 of 0.99, but values ranging from 0.98 to 0.99. As in the previous cases, the method of Khan et al. shows the poorest results with an average R^2 of 0.97, and values ranging from 0.96 to 0.99. Despite this good linear behaviour, it is important to mention that all the methods tend to underestimate the current and increase the errors in the estimation of the IV characteristics of the module for low current values close to V_{oc}, as is shown in the example IV curve plotted in Figs. 9 and 10. This can be explained due to the fact that all the methods slightly underestimate the V_{oc} of the IV curve of the HCPV module. The methods of Phang et al., Blas et al. and Almonacid et al. show almost the same performance with an average absolute relative error of 0.3%, 0.3% and 0.4% respectively, while the method of Khan et al. shows once again a worse performance with an average absolute relative error of 0.6%.

The extracted characteristic parameters of the HCPV module obtained with each of the methods for the data set considered are shown in Table 3. Based on these values, several general conclusion can be found. As can be seen, the four methods predict almost the same values of I_{ph}. Regarding $I_{o,}$ the methods of Blas et al. and Khan et al. tend to predict the lowest and highest values respectively, with a difference ranging from around 9E−17 A to 4E−4 A. The methods of Phang et al. and Almonacid et al. predict closer results, although the last always leads to higher values, with a difference ranging from around 2E−3 A to 8E−1 A. With regards to m, the methods of Blas et al. and Khan et al. also tend to predict the lowest and highest values respectively, with a difference ranging from around 1.8 (32%) to 2.8 (43%). The methods of Phang et al. and Almonacid et al. predict almost the same values of m with a difference ranging from around 0.03 (1%) to 0.3 (14%). Regarding R_s, the methods of Blas et al. and Khan et al. tend to predict the highest and lowest values, respectively, with a difference ranging from around 0.2 Ω (36%) to 1.2 Ω (74%). The methods of Phang et al. and Almonacid et al. offer again similar results with a difference ranging from around 0.04 Ω (8%) to 0.2 Ω (22%). Finally, all

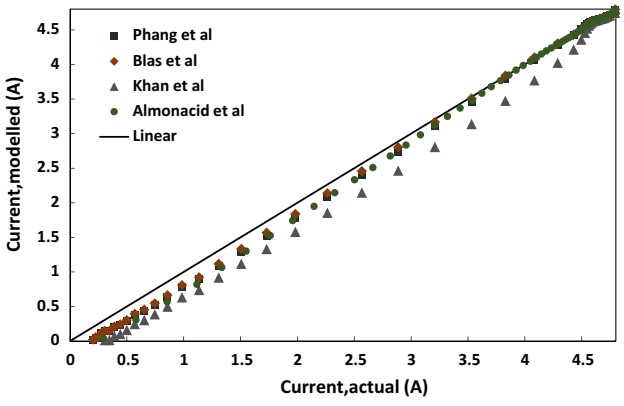

Fig. 9. Actual vs. modelled current of an IV curve for typical observed values of effective irradiance and cell temperature (curve 6).

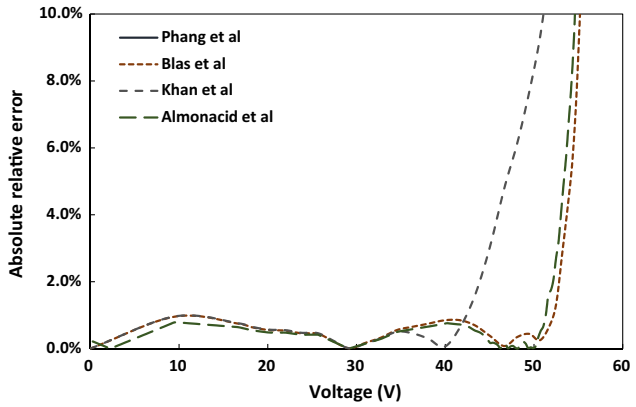

Fig. 10. Absolute relative error between actual and modelled current vs. voltage of an IV curve for typical observed values of effective irradiance and cell temperature (curve 6).

the methods yield to similar results in the estimation of R_{sh} with a difference ranging from 0.6 Ω (0.6%) to 71 Ω (19%).

4.1. Dependence of parameters with input irradiance

The direct normal irradiance is the main driver of the electrical output of concentrator photovoltaic devices. So, it is also interesting to study the relationship between the results obtained with the different methods and the incident irradiance. This is basic to gather a better understanding of the technology and to help in the prediction of the parameters of the SEM model. At the present, the only study regarding the dependencies of the parameters of Eq. (1) for HCPV technology is limited to the work conducted by Ben Or and Appelbaum (2014). They studied the dependence of the parameters of a triple-junction InGaP/InGaAs/Ge solar cells with concentration and temperature. In any case, the dependence of the SEM model parameters with irradiance at HCPV module level when operating in outdoors still remains unknown.

The six IV curves previously selected for the analysis above are not adequate for this study since they have different operating cell temperatures. Under real operating conditions, is extremely complex to control the cell temperature since this is mainly dominated by the incident irradiance (Almonacid et al., 2012). Hence, it is not usually possible to have IV data from low to high irradiance levels to any desired cell temperature. In this case, a new data set of six IV curves, evenly distributed from a low to high effective irradiance, operating at a cell temperature of around 65 °C has been used to diminish as much as possible the thermal effects. This temperature has been chosen for two reasons, namely: (a) IV data from low to high effective irradiance levels were available, and (b) is usually considered as the typical operating cell temperature of HCPV systems in outdoors (Fernández et al., 2014a; Kinsey and Edmondson, 2009; Philipps et al., 2010).

Fig. 11 shows the dependence of I_{ph} with effective irradiance. As can be seen, all the methods predict almost the same results. Moreover, the I_{ph} shows a clear linear tendency with the effective irradiance since DNI_C quantifies the strong spectral dependence of the system. Fig. 12 shows the dependence of I_o and m with effective irradiance. As can be see, both parameters show a similar behaviour for all the methods. The I_o tends to grow with the effective irradiance from minimum values of 7.0E−26 A (Phang et al.), 1.60E−28 A (Blas et al.), 1.15E−14 A (Khan et al.) and 3.21E−25 A (Almonacid et al.), to maximum values of 5.64E−09 A (Phang et al.), 1.18E−08 A (Blas et al.), 8.47E−07 A (Khan et al.) and 1.66E−08 A (Almonacid et al.). The m also tends to grow with the input effective irradiance from minimum values of 1.72 (Phang et al.), 1.56 (Blas et al.), 3.08 (Khan et al.) and 1.77 (Almonacid et al.), to maximum values of 4.68 (Phang et al.), 4.85 (Blas et al.), 6.16 (Khan et al.) and 4.93 (Almonacid et al.). Finally, Fig. 13 shows the dependence of R_s and R_{sh} with effective irradiance. As in the previous case, both magnitudes present a similar behaviour. The R_s shows a clear tendency to decrease with the incident effective irradiance from maximum values of 0.91 Ω (Phang et al.), 1.10 Ω (Blas et al.), 0.46 Ω (Khan et al.) and 0.95 Ω (Almonacid et al.), to minimum values of 0.47 Ω (Phang et al.), 0.39 Ω (Blas et al.), 0.33 Ω (Khan et al.) and 0.34 Ω (Almonacid et al.). At the same time, the R_{sh} also tends to decrease with the effective irradiance. It varies from maximum values of 430.0 Ω (Phang et al. and Khan et al.), 427.9 Ω (Blas et al.) and 475.0 Ω (Almonacid et al.), to minimum values of 148.7 Ω (Phang et al. and Khan et al.), 148.1 Ω (Blas et al.) and 148.8 Ω (Almonacid et al.).

It is important to mention that the dependencies above are in agreement with the findings previously reported by Ben Or and Appelbaum (2014) for a triple-junction solar cell under different concentration levels. In addition, it is also worth mentioning that the same trends have been found by Khan et al. (2014) for the case

Table 3
Single exponential model parameters determined by the four analysed methods.

Method	Parameter	Curve 1	Curve 2	Curve 3	Curve 4	Curve 5	Curve 6
Phang et al.	I_{ph} (A)	1.49	2.08	5.35	5.49	3.92	4.81
	I_o (A)	1.72E−22	5.29E−22	7.69E−12	5.42E−13	4.03E−15	8.22E−11
	m	2.22	1.99	3.96	2.98	3.00	3.90
	R_s (Ω)	1.06	0.84	0.53	0.57	0.61	0.58
	R_{sh} (Ω)	453.6	306.7	150.4	142.6	320.3	219.3
Blas et al.	I_{ph} (A)	1.49	2.08	5.35	5.49	3.93	4.81
	I_o (A)	4.41E−28	2.56E−27	1.42E−12	8.18E−14	3.51E−19	7.87E−11
	m	1.77	1.59	3.72	2.80	2.36	3.89
	R_s (Ω)	1.61	1.20	0.56	0.59	0.93	0.54
	R_{sh} (Ω)	452.0	305.5	149.8	142.0	319.4	218.7
Khan et al.	I_{ph} (A)	1.49	2.07	5.34	5.48	3.92	4.80
	I_o (A)	4.71E−12	3.01E−11	4.11E−07	6.31E−08	7.09E−10	2.22E−07
	m	4.23	3.95	6.57	4.86	4.60	5.70
	R_s (Ω)	0.41	0.34	0.29	0.38	0.39	0.38
	R_{sh} (Ω)	453.6	306.7	150.4	142.6	320.3	219.3
Almonacid et al.	I_{ph} (A)	1.49	2.08	5.35	5.48	3.92	4.80
	I_o (A)	3.30E−21	2.59E−19	1.18E−11	2.21E−12	1.15E−13	1.03E−10
	m	2.36	2.26	4.01	3.12	3.31	3.92
	R_s (Ω)	1.00	0.65	0.49	0.52	0.54	0.52
	R_{sh} (Ω)	481.2	330.9	149.9	147.2	385.2	213.2

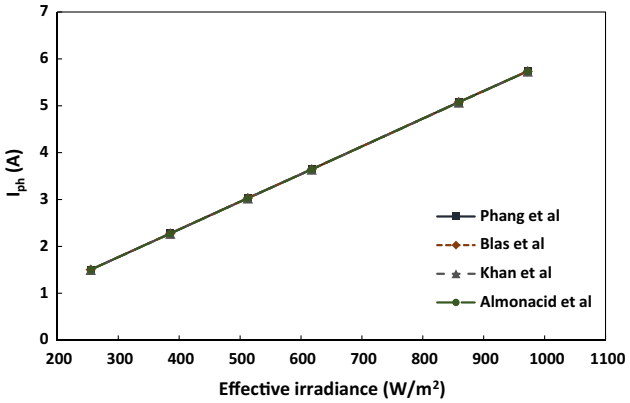

Fig. 11. Dependence of the photo-generated current (I_{ph}) with spectrally corrected direct normal irradiance (DNI_C). The operating cell temperature (T_C) is 65 °C ± 3.5 °C.

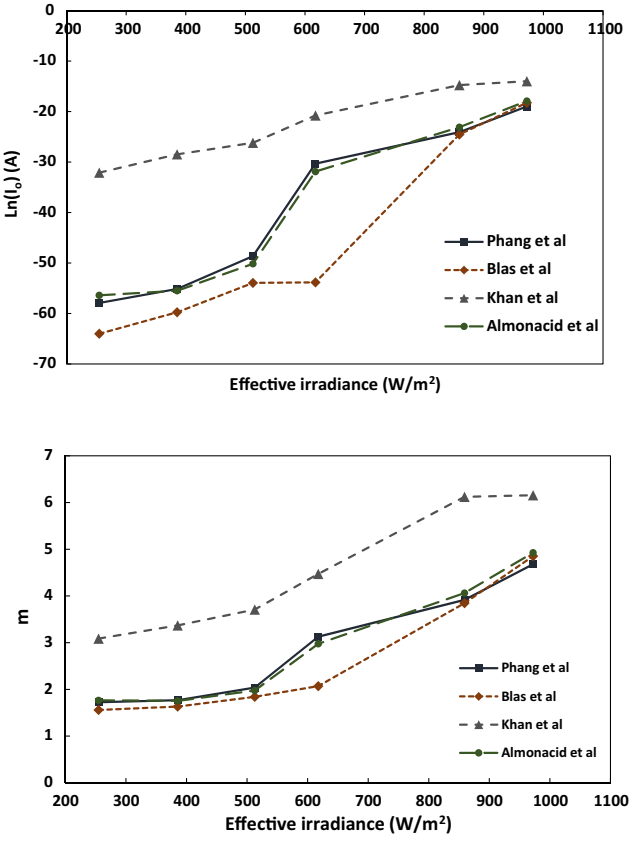

Fig. 12. Dependence of the diode saturation current (I_o) and the diode ideality factor (m) with spectrally corrected direct normal irradiance (DNI_C). The operating cell temperature (T_C) is 65 °C ± 3.5 °C.

of concentrator Si solar cells. The results of this work clearly signal the importance of considering the behaviour of the key parameters of concentrator modules as a function of irradiance to accurately evaluate and model their electrical performance under real operating conditions.

5. Conclusions

In this paper, four methods for extracting the five parameters of the single exponential model of a high concentrator photovoltaic module are analysed. For the first time, simple analytical solutions,

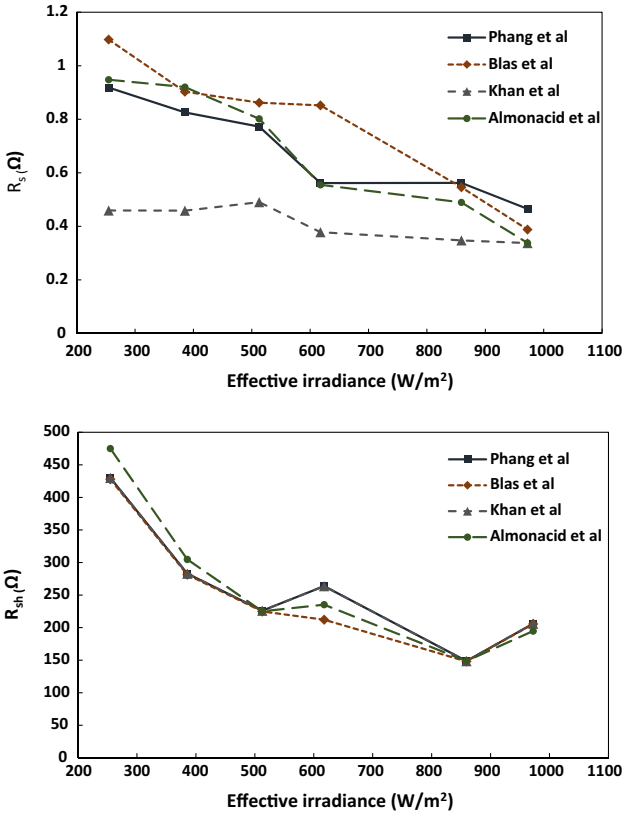

Fig. 13. Dependence of the series resistance (R_s) and the shunt (or parallel) resistance (R_{sh}) with spectrally corrected direct normal irradiance (DNI_C). The operating cell temperature (T_C) is 65 °C ± 3.5 °C.

widely used for the extraction of the five parameters of photovoltaic (PV) devices, are implemented and evaluated for a high concentrator photovoltaic (HCPV) module. The methods analysed are: the method of Phang et al., the method of Blas et al. and the method of Khan et al. In addition, these analytical procedures are compared with a numerical method, previously introduced by the authors (Almonacid et al.), for extracting the characteristic parameters of a HCPV module.

Results show that the analytical methods of Phang et al. and Blas et al. present a high quality, an almost the same performance than the numerical method of Almonacid et al., in the prediction of the current-voltage (IV) curve of the HCPV module under study. In any case, the methods of Phang et al. and Almonacid et al. present the best and almost the same performance. On the contrary, the method of Khan et al. always tends to underestimate the IV curve of the HCPV module. Also, it is important to mention that the performance of the studied methods can be considered independent of the operating conditions of the HCPV module.

Regarding the obtained values of the characteristic parameters, it can be concluded that the methods of Phang et al. and Almonacid et al. present the closest predicted results. On the contrary, the methods of Blas et al. and Khan et al. show the maximum difference in the calculated values of the characteristic parameters. It is also worth mentioning that the method of Khan et al. tends to underestimate the values of the diode saturation current (I_o) and the diode ideality factor (m) when compared with the other methods. Also, among the different parameters, all the methods tend to predict almost the same values of shunt resistance (R_{sh}), while the differences are higher for the rest of parameters.

Future works should analyse sophisticated numerical procedures, such as numerical analysis using the Lambert-W function or the Newton-Raphson method, for extraction the parameters of

the single exponential model of HCPV modules. The quality of the double exponential model, characterized by a set of 7 parameters, should be also studied for the case of HCPV modules. Moreover, the analysis and physical meaning of the single and double exponential models parameters for various modules with different characteristics, under different controlled irradiance and temperature levels, should be also carefully studied.

Acknowledgments

This work has partially being supported by the Spanish Ministry of Economy and Competitiveness under the project ENE2013-45242-R and by FEDER funds and by the "Plan de Apoyo a la Investigación de la Universidad de Jaén y la Caja Rural de Jaén" (UJA2015/07/01). Eduardo F. Fernández thanks the Spanish Ministry of Economy and Competitiveness for the Juan de la Cierva 2013 programme.

References

Almonacid, F., Fernández, E., Mallick, T., Pérez-Higueras, P., 2015. High concentrator photovoltaic module simulation by neuronal networks using spectrally corrected direct normal irradiance and cell temperature. Energy 84, 336–343.
Almonacid, F., Pérez-Higueras, P., Fernández, E., Rodrigo, P., 2012. Relation between the cell temperature of a HCPV module and atmospheric parameters. Sol. Energy Mater. Sol. Cells 105, 322–327.
Almonacid, F., Rodrigo, P., Fernández, E.F., 2016. Determination of the current–voltage characteristics of concentrator systems by using different adapted conventional techniques. Energy 101, 46–160.
Appelbaum, J., Peled, A., 2014. Parameters extraction of solar cells – a comparative examination of three methods. Sol. Energy Mater. Sol. Cells 122, 164–173.
Ben Or, A., Appelbaum, J., 2013. Estimation of multi-junction solar cell parameters. Prog. Photovoltaics Res. Appl. 21 (4), 713–723.
Ben Or, A., Appelbaum, J., 2014. Dependence of multi-junction solar cells parameters on concentration and temperature. Sol. Energy Mater. Sol. Cells 130, 234–240.
Blas, M.A., Torres, J.L., Prieto, E., García, A., 2002. Selecting a suitable model for characterizing photovoltaic devices. Renewable Energy 25, 371–380.
Celik, A., Acikgoz, N., 2010. Modelling and experimental verification of the operating current of mono-crystalline photovoltaic modules using four- and five-parameter models. Appl. Energy 84 (1), 1–15.
Chan, D.S.H., Phillips, J.R., Phang, J.C.H., 1986. A comparative study of extraction methods for solar cell model parameters. Solid-State Electron. 29, 329–337.
Chegaar, M., Azzouzi, G., Mialhe, P., 2006. Simple parameter extraction method for illuminated solar cells. Solid-State Electron. 50, 234–237.
Chegaar, M., Ouennoughia, Z., Guechi, F., 2004. Extracting dc parameters of solar cells under illumination. Vacuum 75, 367–372.
Ciulla, G., Lo Brano, V., Di Dio, V., Cipriani, G., 2014. A comparison of different one-diode models for the representation of I-V characteristic of a PV cell. Renew. Sustain. Energy Rev. 32, 684–696.
Cotfas, D.T., Cotfas, P.A., Kplanis, S., 2013. Methods to determine the dc parameters of solar cells: a critical review. Renew. Sustain. Energy Rev. 28, 588–596.
Easwarakhanthan, T., Bottin, J., Bouhouch, I., Boutrit, C., 1986. Non linear minimization algorithm for determining the solar cell parameters with microcomputers. Int. J. Solar Energy 4, 1–12.
Fernández, E., Almonacid, F., 2015. A new procedure for estimating the cell temperature of a high concentrator photovoltaic grid connected system based on atmospheric parameters. Energy Convers. Manage. 103, 1031–1039.
Fernández, E., Almonacid, F., Garcia-Loureiro, A., 2015b. Multi-junction solar cells electrical characterization by neuronal networks under different irradiance, spectrum and cell temperature. Energy 90, 846–856.
Fernández, E.F., Almonacid, F., 2014. Spectrally corrected direct normal irradiance based on artificial neural networks for high concentrator photovoltaic applications. Energy 74 (C), 941–949.
Fernández, E.F., Almonacid, F., Rodrigo, P., Pérez-Higueras, P., 2014a. Calculation of the cell temperature of a high concentrator photovoltaic (HCPV) module: a study and comparison of different methods. Sol. Energy Mater. Sol. Cells 121, 144–151.
Fernández, E.F., Almonacid, F., Soria-Moya, A., Terrados, J., 2015c. Experimental analysis of the spectral factor for quantifying the spectral influence on concentrator photovoltaic systems under real operating conditions. Energy 90, 1878–1886.
Fernández, E.F., García-Loureiro, A.J., Smestad, G.P., 2015a. Multijunction concentrator solar cells: analysis and fundamentals. In: Pérez-Higueras, Pedro, Fernández, Eduardo F. (Eds.), High Concentrator Photovoltaics: Fundamentals, Engineering and Power Plants. s.l.: Springer, pp. 9–37.
Fernández, E.F., Pérez-Higueras, P., Garcia Loureiro, A., Vidal, P., 2013b. Outdoor evaluation of concentrator photovoltaic systems modules from different manufacturers: first results and steps. Prog. Photovoltaics Res. Appl. 21 (4), 693–701.
Fernández, E.F., Rodrigo, P., Almonacid, F., Pérez-Higueras, P., 2014b. A method for estimating cell temperature at the maximum power point of a HCPV module under actual operating conditions. Sol. Energy Mater. Sol. Cells 124, 159–165.
Fernández, E. et al., 2015d. Model for estimating the energy yield of a high concentrator photovoltaic system. Energy 87, 77–85.
Fernández, E. et al., 2013a. A two subcell equivalent solar cell model for III-V triple junction solar cells under spectrum and temperature variations. Sol. Energy 92, 221–229.
Fernández, E., Soria-Moya, A., Almonacid, F., Aguilera, J., 2016a. Comparative assessment of the spectral impact on the energy yield of high concentrator and conventional photovoltaic technology. Sol. Energy Mater. Sol. Cells 147, 185–197.
Fernández, E., Talavera, D., Almonacid, F., Smestad, G., 2016b. Investigating the impact of weather variables on the energy yield and cost of energy of grid-connected solar concentrator systems. Energy 106, 790–801.
Friedman, D.J., King, R.K., Swanson, R.M., 2013. Toward 100 Gigawatts of concentrator photovoltaics. IEEE J. Photovoltaics 3 (4), 1460–1463.
Gasparin, F., Bühler, A., Rampinelli, G., Krenzinger, A., 2016. Statistical analysis of I-V curve parameters from photovoltaic modules. Sol. Energy 131, 30–38.
Ghani, F., Duke, M., 2011. Numerical determination of parasitic resistances of a solar cell using the Lambert W-function. Sol. Energy 85 (9), 2386–2394.
Ghani, F., Rosengarten, G., Duke, M., 2016. The characterisation of crystalline silicon photovoltaic devices using the manufacturer supplied data. Sol. Energy 132, 15–24.
Ghani, F., Rosengarten, G., Duke, M., Carson, J.K., 2014. The numerical calculation of single-diode solar-cell modelling parameters. Renewable Energy 72, 105–112.
Haysom, J. et al., 2015. Learning curve analysis of concentrated photovoltaic systems. Prog. Photovoltaics Res. Appl. 23 (11), 1678–1686.
Humada, A., Hojabri, M., Mekhilef, S., Hamada, H., 2016. Solar cell parameters extraction based on single and double-diode models: a review. Renew. Sustain. Energy Rev. 56, 494–509.
Ishibashi, K., Kimura, Y., Niwano, M., 2008. An extensively valid and stable method for derivation of all parameters of a solar cell from a single current-voltage characteristic. J. Appl. Phys. 103, 094507.
Khan, F., Baek, S., Kim, J., 2014. Intensity dependency of photovoltaic cell parameters under high illumination conditions: an analysis. Appl. Energy 133, 356–362.
Khan, F., Baek, S., Park, Y., Kim, J., 2013. Extraction of diode parameters of silicon solar cells under high illumination conditions. Energy Convers. Manage. 76, 421–429.
Kichou, S. et al., 2016a. Study of degradation and evaluation of model parameters of micromorph silicon photovoltaic modules under outdoor long term exposure in Jaén, Spain. Energy Convers. Manage. 120, 109–119.
Kichou, S. et al., 2016b. Characterization of degradation and evaluation of model parameters of amorphous silicon photovoltaic modules under outdoor long term exposure. Energy 96, 231–241.
Kinsey, G., Edmondson, K., 2009. Spectral response and energy output of concentrator multijunction solar cells. Prog. Photovoltaics Res. Appl. 17 (5), 279–288.
Kinsey, G. et al., 2008. Concentrator multifunction solar cell characteristics under variable intensity and temperature. Prog. Photovoltaics Res. Appl. 16 (6), 503–508.
Kurtz, S. et al., 2015. Key parameters in determining energy generated by CPV modules. Prog. Photovoltaics Res. Appl. 23 (10), 1250–1259.
Li, Y. et al., 2013. Evaluation of methods to extract parameters from current-voltage characteristics of solar cells. Sol. Energy 90, 51–57.
Lo Brano, V., Orioli, A., Ciulla, G., Di Gangi, A., 2010. An improved five-parameter model for photovoltaic modules. Sol. Energy Mater. Sol. Cells 94 (8), 1358–1370.
Micheli, L. et al., 2016. Performance, limits and economic perspectives for passive cooling of High Concentrator Photovoltaics. Sol. Energy Mater. Sol. Cells 153, 164–178.
Ortiz-Conde, A., Sánchez, F.J.G., Muci, J., 2006. New method to extract the model parameters of solar cells from the explicit analytic solutions of their illuminated I-V characteristics. Sol. Energy Mater. Sol. Cells 90, 352–361.
Ota, Y., Nagai, H., Araki, K., Nishioka, K., 2012. Temperature distribution in 820X CPV module during outdoor operation. AIP Conf. Proc. 1477, 364–367.
Peharz, G., Siefer, G., Bett, A., 2009. A simple method for quantifying spectral impacts on multi-junction solar cells. Sol. Energy 83 (9), 1588–1598.
Perez-Higueras, P., Fernández, E.F., 2015. High Concentrator Photovoltaics: Fundamentals, Engineering and Power Plants. s.l.: Springer.
Phang, J.C.H., Chan, D.S.H., Phillips, J.R., 1984. Accurate analytical method for the extraction of solar cell model parameters. Electron. Lett. 20 (10), 406–408.
Philipps, S. et al., 2010. Energy harvesting efficiency of III-V triple-junction concentrator solar cells under realistic spectral conditions. Sol. Energy Mater. Sol. Cells 94 (5), 869–877.
Powell, M.J.D., 1970. A Fortran subroutine for solving systems of nonlinear algebraic equations. In: Numerical Methods for Nonlinear Algebraic Equations. s.l.: P. Rabinowitz.
Rodrigo, P., Fernández, E., Almonacid, F., Pérez-Higueras, P., 2013. Models for the electrical characterization of high concentration photovoltaic cells and modules: a review. Renew. Sustain. Energy Rev. 26, 752–760.
Rodrigo, P., Fernández, E., Almonacid, F., Pérez-Higueras, P., 2014. Review of methods for the calculation of cell temperature in high concentration photovoltaic modules for electrical characterization. Renew. Sustain. Energy Rev. 38, 478–488.
Rodrigo, P. et al., 2015a. A methodology for the electrical characterization of shaded high concentrator photovoltaic modules. Energy 89, 768–777.

Rodrigo, P., Micheli, L., Almonacid, F., 2015b. The high-concentrator photovoltaic module. In: Perez-Higueras, P., Fernández, Eduardo, F. (Eds.), High Concentrator Photovoltaics: Fundamentals, Engineering and Power Plants. s.l.: Springer, pp. 115–151.
Segev, G., Mittelman, G., Kribus, A., 2012. Equivalent circuit models for triple-junction concentrator solar cells. Sol. Energy Mater. Sol. Cells 98, 57–65.
Sellami, A., Bouaïcha, M., 2011. Application of the genetic algorithms for identifying the electrical parameters of PV solar generators. In: Kosyachenko, L.A. (Ed.), Solar Cells -Silicon Wafer-Based Technologies. s.l.: InTech, pp. 349–364.
Shanks, K. et al., 2016. Theoretical investigation considering manufacturing errors of a high concentrating photovoltaic of cassegrain design and its experimental validation. Sol. Energy 131, 235–245.
Siefer, G., Bett, A., 2014. Analysis of temperature coefficients for III-V multi-junction concentrator cells. Prog. Photovoltaics Res. Appl. 22 (5), 515–524.
Soria-Moya, A. et al., 2015. Performance analysis of models for calculating the maximum power of high concentrator photovoltaic modules. IEEE J. Photovoltaics 5 (3), 947–955.
Talavera, D.L., Pérez-Higueras, P., Ruíz-Arias, J., Fernández, E.F., 2015. Levelised cost of electricity in high concentrated photovoltaic grid connected systems: spatial analysis of Spain. Appl. Energy 151, 49–59.
Theristis, M., Fernández, E., Stark, C., O'Donovan, T., 2016a. A theoretical analysis of the impact of atmospheric parameters on the spectral, electrical and thermal performance of a concentrating III-V triple-junction solar cell. Energy Convers. Manage. 117, 218–227.
Theristis, M., O'Donovan, T., 2015. Electrical-thermal analysis of III-V triple-junction solar cells under variable spectra and ambient temperatures. Sol. Energy 118, 533–546.
Tivanov, M. et al., 2005. Determination of solar cell parameters from its current–voltage and spectral characteristics. Sol. Energy Mater. Sol. Cells 87, 457–465.
Wolf, P., Benda, V., 2013. Identification of PV solar cells and modules parameters by combining statistical and analytical methods. Sol. Energy 93, 151–157.
Yamaguchi, M.N.K.-I.S.T. et al., 2008. Novel materials for high-efficiency III-V multi-junction solar cells. Sol. Energy 82 (2), 173–180.
Yamaguchi, M., Takamoto, T., Araki, K., Ekins-Daukes, N., 2005. Multi-junction III-V solar cells: current status and future potential. Sol. Energy 79 (1), 78–85.
Ye, M., Wang, X., Xu, Y., 2009. Parameter extraction of solar cells using particle swarm optimization. J. Appl. Phys. 105, 094502–8.
Zhang, C. et al., 2011. A simple and efficient solar cell parameter extraction method from a single current-voltage curve. J. Appl. Phys. 110, 064504.

PUBLICACIÓN II

Título	**"Photovoltaic Device Performance Evaluation Using an Open-Hardware System and Standard Calibrated Laboratory Instruments"**
Autores	Montes-Romero, Jesús; Piliougine, Michel; Muñoz, José Vicente; F. Fernández, Eduardo; de la Casa, Juan
Revista	Energies
Volumen, número, año	10, 1869, 2017
Categoría y posición	ENERGY AND FUELS (48/97)
Factor de impacto	2,676 (2017)
DOI	10.3390/en10111869

energies

MDPI

Article

Photovoltaic Device Performance Evaluation Using an Open-Hardware System and Standard Calibrated Laboratory Instruments

Jesús Montes-Romero [1], Michel Piliougine [2], José Vicente Muñoz [1], Eduardo F. Fernández [1,*] and Juan de la Casa [1]

[1] IDEA Research Group, Universidad de Jaén, Campus de Las Lagunillas, 23071 Jaén, Spain; jmontes@ujaen.es (J.M.-R.); jmunoz@ujaen.es (J.V.M.); delacasa@ujaen.es (J.d.l.C.)

[2] Dpto. de Lenguajes y Ciencias de la Computación, Universidad de Málaga, Bulevar Louis Pasteur 35, 29071 Málaga, Spain; michel@uma.es

* Correspondence: fenandez@ujaen.es; Tel.: +34-953-213-520

Received: 1 October 2017; Accepted: 10 November 2017; Published: 15 November 2017

Abstract: This article describes a complete characterization system for photovoltaic devices designed to acquire the current-voltage curve and to process the obtained data. The proposed system can be replicated for educational or research purposes without having wide knowledge about electronic engineering. Using standard calibrated instrumentation, commonly available in any laboratory, the accuracy of measurements is ensured. A capacitive load is used to bias the device due to its versatility and simplicity. The system includes a common part and an interchangeable part that must be designed depending on the electrical characteristics of each PV device. Control software, developed in LabVIEW, controls the equipment, performs automatic campaigns of measurements, and performs additional calculations in real time. These include different procedures to extrapolate the measurements to standard test conditions and methods to obtain the intrinsic parameters of the single diode model. A deep analysis of the uncertainty of measurement is also provided. Finally, the proposed system is validated by comparing the results obtained from some commercial photovoltaic modules to the measurements given by an independently accredited laboratory.

Keywords: *I-V* curve; outdoor measurements; uncertainty analysis; characterization system

1. Introduction

The generation of electricity using photovoltaic (PV) technology has been the most successful renewable energy source in the last decade. Specifically, during the 2005–2015 period, the average annual growth rate of investment in this type of system was 27% [1]. In addition, over the year 2016, 75 GWp were installed [2], and at the mid-year of 2017, the globally installed capacity exceeds 320 GWp [3].

Currently, four countries clearly lead the accumulated power ranking: China, Japan, the USA, and Germany. However, for the last three years, and due to lower prices, a lot of countries have been including photovoltaic technology in their energy production matrix. At the end of 2016, every continent has at least 1 GWp installed: 24 countries have more than 1 GWp and 114 countries have at least 10 MWp [4].

As a consequence of the globalization of solar photovoltaic energy, universities, investigation centers, and research groups along the world have joined those already working in this field of science to contribute current knowledge about this technology. Therefore, they must have scientific instruments to perform the required experiments. Usually, this specific instrumentation is expensive and not flexible.

A valid option is a self-built system based on general purpose measurement instrumentation, such as multimeters, scopes, electronic loads, etc.

Undoubtedly, the trace of the characteristic current-voltage (*I-V*) curve [5] of a photovoltaic device is the most important and basic experiment that should be performed in any laboratory—educational or research—related to photovoltaic technology to obtain information about its behavior. The most economical way—the only viable way in some cases—is to perform this experiment in outdoor conditions [6–8]. The *I-V* curve is composed off the current-voltage pairs, in which the photovoltaic device can operate. From this set of points, all the interesting electrical parameters under exposure conditions can be obtained. Therefore, during the sweep of the *I-V* curve, the operation conditions, such as the irradiance (G), the ambient temperature (T_a), the cell temperature (T_c), the wind speed (W_s), and the spectral distribution, must be recorded.

Besides, to the electrical characteristic parameters, the shape of the *I-V* curve provides useful information about the possible anomalies of a PV device, such as partial shadowing [9], degradation [10], mismatch [11], and influence of dust [12]. Deformation of the *I-V* curve may be related to failures of the maximum power point tracking system [13,14] when the modules are connected to the grid, causing an improper operation.

In addition to the *I-V* curve, it is essential to have high level software to carry out automatic data-processing of the experimental measurements. Data analysis tools, such as parameter extraction methods [15], are interesting because these parameters characterize the behavior of any photovoltaic module or cell [16] and allow a theoretical reconstruction of the *I-V* curve. Definitely, characterizing the electrical behavior of current and underdeveloped technologies is of great importance due to the fact that not all technologies act equally under similar environmental conditions [17].

From the electronic point of view, an *I-V* curve tracer is a system capable of emulating an impedance variation from zero to infinite to achieve a sweep across the complete working range of the PV device [18]. There are some desired features of an *I-V* curve tracer, including scalability and accuracy. Different *I-V* tracers can be found on the market and also in the literature: there are many research papers describing hand-made tracers [19–31]. However, these works only deal with a small part of the problem. None of them provides a framework capable of controlling the recording of the *I-V* curves, obtaining the electrical parameters to extrapolate the measurements for the standard test conditions (STC), or extracting the internal intrinsic parameters. Besides, most of the commercial *I-V* tracers [32,33] are mostly prepared for on-site characterization. In any case, this kind of equipment presents the same drawbacks as the ones found in the literature: a high price exceeding $3000, a very restrictive measurement range, and a very reduced set of analog channels to measure the ambient parameters—principally limited to one irradiance and one temperature. Moreover, the control software of commercial *I-V* tracers is not prepared for an automatic experimental campaign of measurements. The commercial *I-V* tracers usually offer insufficient characteristics for research purposes.

The proposed system uses general-purpose instrumentation, which can be acquired with a respective calibration certificate from the manufacturer. In this way, the accuracy and precision of the measurements is ensured. The use of the same framework to measure single cells, modules, strings, or a whole PV generator has been another goal of the *I-V* characterization system. In this sense, interchangeable parts can be easily replaced to adjust the system to the power of the device under test using the same software. Lastly, both hardware and software are open, and can therefore be modified according to the specific requirements of the user.

Summarizing, the aim of the work presented by the IDEA research group is the construction of a complete *I-V* characterization system using open hardware and a software framework widely used by the scientific community, such as LabVIEW. The system will be able to measure the *I-V* curve and the meteorological sensors using general purpose instrumentation. Moreover, the system includes automatic data treatment for the extrapolation to STC and parameter extraction methods.

The paper is arranged as follows: firstly, a review of the most recent related works is provided (Section 2). Next, the proposed approach is described in detail (Section 3). A complete analysis

about the uncertainty of the measurements is developed (Section 4). Then, the performed experiment (Section 5) and the results (Section 6) are presented. Finally, the conclusions and future work are presented (Section 7).

2. Previous Works

Durán et al. [18] propose a classification of the *I-V* curve tracers depending on the principle used to bias the module throughout all the possible states in which a photovoltaic device could operate. Several different ways to sweep all the points between the short circuit current (I_{SC}) and the open circuit voltage (V_{OC}) have been identified: variable resistor, capacitive load, electronic load, four-quadrant power supply, and DC-DC converter.

A complete literature review of examples for each type of system can be found in Piliougine et al. [19]. That paper, like many others [20–22], proposes a system that uses a four-quadrant power supply to bias the module. This accurate way of plotting the *I-V* curve has the inconvenience of its price. Indeed, in most of these works, the objective was to design an accurate system to obtain *I-V* curves of PV cells or modules without paying attention to the cost of the used equipment. However, for the last five years, many works are aimed to reduce the final price of the system.

At first sight, a variable resistive load could be a very cheap way to bias a photovoltaic device [23]. However, the *I-V* tracers based on this principle present a complexity drawback associated with the control of the load. Rivai and Rahim [24] propose a resistive load composed by a small set of resistors, combined in series, using binary codification with the help of a microcontroller. In this way, it is possible to accurately assess some commercial systems [34].

Leite et al. [25] propose a low-cost electronic load *I-V* curve tracer for modules and strings based on a MOSFET transistor electronic load to bias the device and control it using an application programmed in LabVIEW [26]. Another example of the use of an electronic load combined with low-cost acquisition hardware is pointed out in the work carried out by Hemza et al. [27], where the acquisition of the current-voltage pairs is performed by an Arduino board governed by a personal computer also running a LabVIEW application.

Another widely reported principle used for tracing the *I-V* curve of a PV device is based on the charge of a capacitor bank (a capacitor bank is a single capacitor or a parallel/series combination of several capacitors. In the article by Vargas and Abrahamse [28], open-source hardware is used to reduce the final price of the system. In this case, the PV device is biased by capacitors, whereas the *I-V* curve is acquired by a low-cost, analog-to-digital converter with two independent channels.

The experimental setup presented in this paper is intended to assist technical staff or engineers with basic knowledge about photovoltaic and electronic design in the construction of a hand-made *I-V* curve tracer system using the provided software to process the data. One of the most remarkable features is that the accuracy of the obtained curves is ensured because the measurements are performed using standard calibrated instruments. Finally, the presented scheme can be used when the results must be reported with their respective uncertainties.

3. Description of the System

3.1. General Block Diagram

The proposed characterization system consists on an open platform employed according to the schematic diagram exhibited in Figure 1. This system consists of three blocks: *I-V* sweep, measurement, and control.

The *I-V* sweep block is an electronic system able to reproduce a variable impedance from zero to infinite in order to perform the *I-V* sweep of a PV module. Amongst all the available methods [18], this block is based on a capacitive load. Therefore, it includes a power stage and the capacitor bank. The power stage is a circuit board addressed to control the process of charge and discharge of the capacitor bank. This power stage was designed by the IDEA research group [29–31].

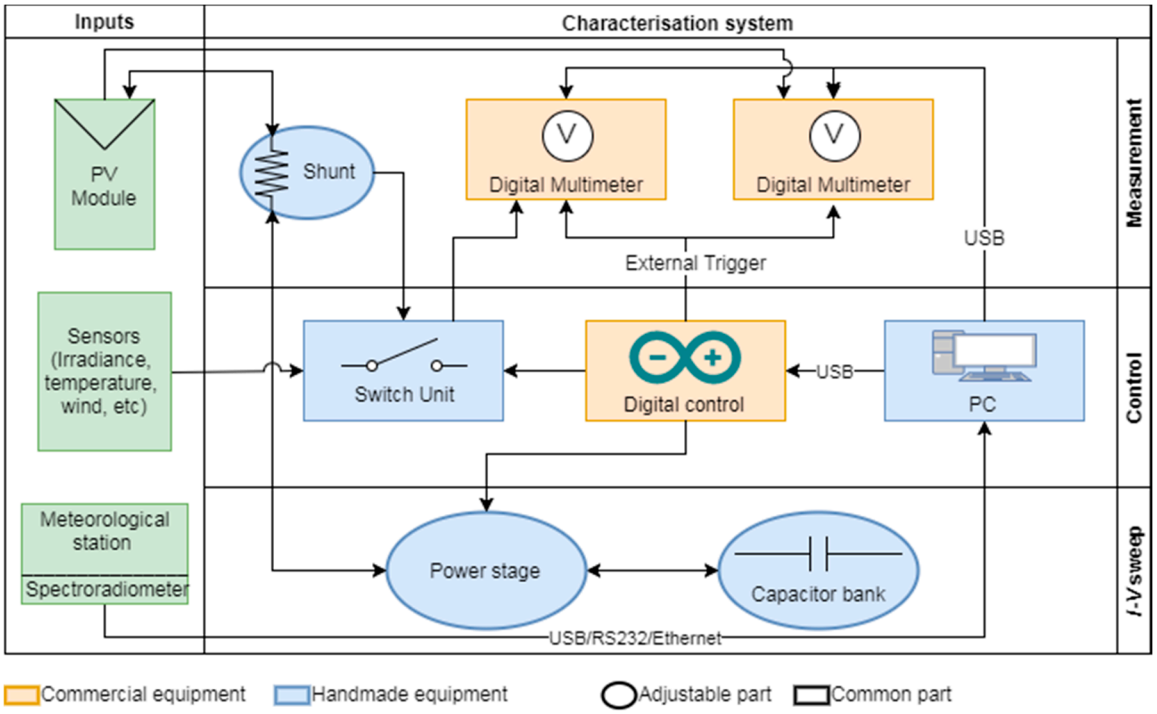

Figure 1. General scheme of the proposed system.

The measurement block includes specific instrumentation with calibration certificates, which delimits the error associated with the measurement and it is generated as a result of the periodic calibration. Any specific instrumentation can be used for this purpose. It only has to include a series of characteristics to be satisfactory: (a) communication to the PC through any kind of communication protocol; (b) the use of an external trigger to synchronize the voltage and current measurements; (c) enough buffer to store the measurement of each *I-V* curve; (d) enough sampling frequency to measure the desired number of points during the charge of the capacitor; and (e) the capacity of measuring different types of temperature sensors. Definitely, any mid- to top-range multimeter of any recognized brand can fulfill the necessary requirements. In the proposed set-up, the measurement block is composed off two Agilent 34411A multimeters to record the voltage and the current values simultaneously. One of them is used to measure the voltage across the terminals of the PV device. The second one is used to measure the current by means of the voltage drop across a shunt resistor between the device and the capacitor. In addition, the second multimeter also measures the operation conditions. Both multimeters are synchronized by a shared external trigger signal generated by the digital control system.

The control block carries out the management of the *I-V* sweep block and the synchronization, configuration, and communication of the measurement block. The control block is composed of a switch unit, a digital control, and a PC. As the second multimeter is used to measure several signals (including the voltage drop across the shunt resistor), a relay board that multiplexes the different signals is required. The digital control is responsible for generating the signals that control the power stage, synchronizing the measurements through the external trigger and controlling the switch unit that allows the measurement of several sensors. For this purpose, an Arduino board has been installed in the proposed experimental set-up. This board and both multimeters are connected to the PC by USB ports in order to be controlled by the application. Optionally, a meteorological station or a specific equipment, such as a spectroradiometer, can be connected directly to the PC by a standard communication port. The software, in our case programmed in LabVIEW, offers the flexibility of adding any number and type of sensors. It is also able to perform an automatic experimental measurement campaign where the obtained data are processed in real time. Another important feature

is the centralization and synchronization of the data. Also, the obtained parameters are synchronized with the sweep of the *I-V* curve and recorded at the same time. Since the complete system is open, it can be modified to implement new data treatment techniques on each measured *I-V* curve that may emerge in future researches.

Most of the equipment included is common and independent of the size of the photovoltaic device to be characterized. The common part of the system includes both multimeters, the switch unit, the digital control board, and the PC with the control software. However, other parts of the system, such as the capacitor bank, the shunt resistor, and the power stage, must be designed and replaced depending on the specifications of the PV generator in terms of maximum current and voltage. In this way, the *I-V* curve tracer can be scaled to measure from a single cell to a power plant generator by selecting a suitable power stage, shunt resistor, and capacitor bank.

In Figure 2, an image of the system employed to perform the experimental campaign of measurement is exposed.

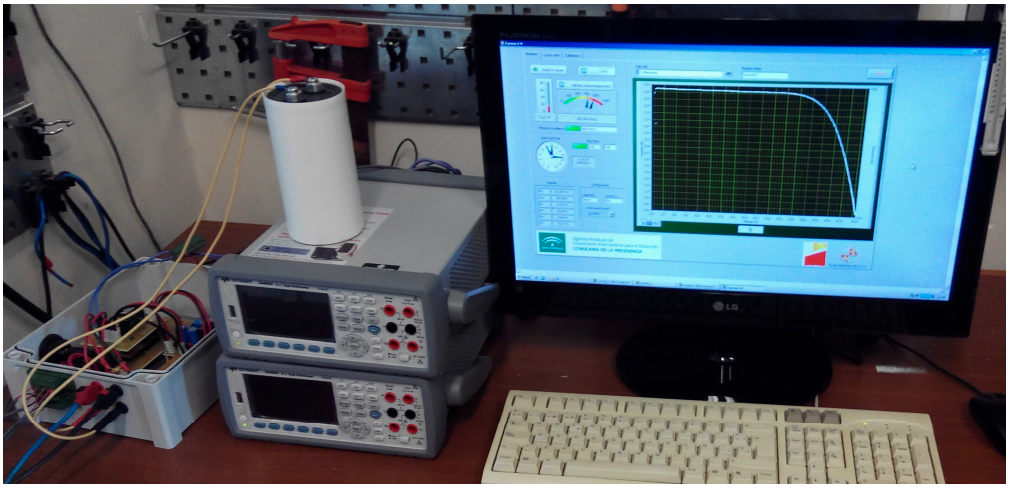

Figure 2. Image of the complete proposed system.

3.2. Hardware Description and Design

In Figure 3, the schematic of the hand-made equipment and its connections are presented. As was mentioned previously, the power stage controls the charge and discharge process of the capacitor bank. Three procedures are required—in this order—to plot the *I-V* curve: pre-charge, charge, and discharge. The pre-charge process negatively charges the capacitor bank to ensure that the PV device starts biased at the second quadrant ($V < 0$; $I > 0$) and the sweep passes through the short-circuit point during the charging process. The pre-charge voltage is set at 5 V, and it must be taken into account that high-reversed voltages at the capacitor may damage this component. Secondly, the charge process sweeps the *I-V* curve of the PV device during the charging time of the capacitor. The measurements of current and voltage of the PV device must be taken during this process to obtain the *I-V* curve. Finally, the capacitor must be discharged. To achieve this process, the stored energy at the capacitor is consumed by a power resistor.

In order to control the mentioned process, four switches—labelled as *Sw*1, *Sw*2, *Sw*3, and *Sw*4—are used. Switches *Sw*1 and *Sw*2 regulate the connection of the pre-charge source labelled as *Vp*. To avoid a short circuit at the pre-charge source at the beginning of this process, a resistor R_p is introduced. *Sw*3 switch governs the discharge procedure of the capacitor bank through the resistor R_d. Finally, the most critical element of this circuit is the switch *Sw*4, which is addressed to connect and disconnect the photovoltaic device to the capacitor bank.

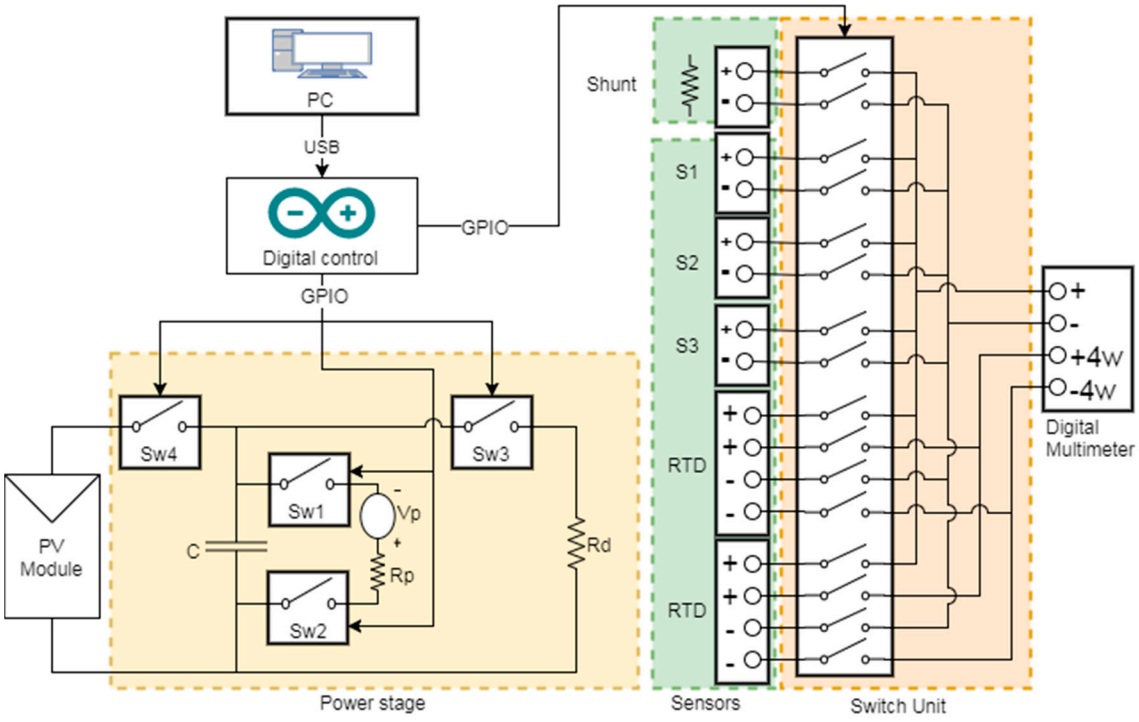

Figure 3. Schematic diagram of the handmade equipment.

The switches must be selected according to the PV device under test: the maximum voltage provided by the PV generator must be tolerated by all switches. Switch *Sw*4 must also allow the maximum current generated by the PV device, and it is also recommended to have a low serial resistance value. Therefore, technologies such as SCR, IGBT, or MOSFET are the most suitable for this task. Switches *Sw*1 and *Sw*2 should allow the current provided by the pre-charge source. Finally, switch *Sw*3 must tolerate the discharge current, which depends on the resistor R_d. All the control signals used to trigger the switches are generated by the digital control board and commanded by the LabVIEW application.

The design of the capacitor bank—labelled as C inside the power stage—must have a maximum permissible voltage superior to the voltage of the PV generator. For example, the capacitor bank shown in Figure 4a was employed to measure a single module up to 100 V. A capacitor bank—composed by 24 capacitors—that can perform the *I-V* curve of a 900 V PV generator is also shown in Figure 4b. The capacitance of the capacitor bank has to be selected to fit in the desired charging time range [35], which is delimited by the multimeters integration time. The charging time depends on the capacitance of the capacitor bank and the voltage and current provided by the PV generator. The integration time is a configurable parameter of the multimeters that adjusts the required time to perform a single measure. Therefore, the integration time is set depending on the number of points to capture and the required time to charge the capacitor bank. In the same way, the value of the discharging resistor influences the time that is necessary to discharge the capacitor. The maximum power dissipation of the discharge resistor must be also considered. A balance between the discharge time and the power dissipation should be sought. Different implementations of the power stage are shown in Figure 5. They were used for several tests depending on the power (voltage and current) of the PV device. In Figure 5a, a PV module power stage design is presented. This design is based on an SCR to control the charging process of the capacitor, low power relays to perform the negative pre-charge of the capacitor, and a solid state relay to control the discharge of the capacitor process. This power stage design has been used to measure PV modules up to 400 Wp. In Figure 5b, a large PV generator power stage is shown.

This design is based on IGBG technology and allows the measurement of high power PV generators from 20 kWp to 200 kWp.

Figure 4. Two capacitor banks used to measure photovoltaic generators of different sizes: (**a**) a single capacitor able to measure any commercial module; (**b**) a capacitor bank used to measure PV generators up to 200 kWp.

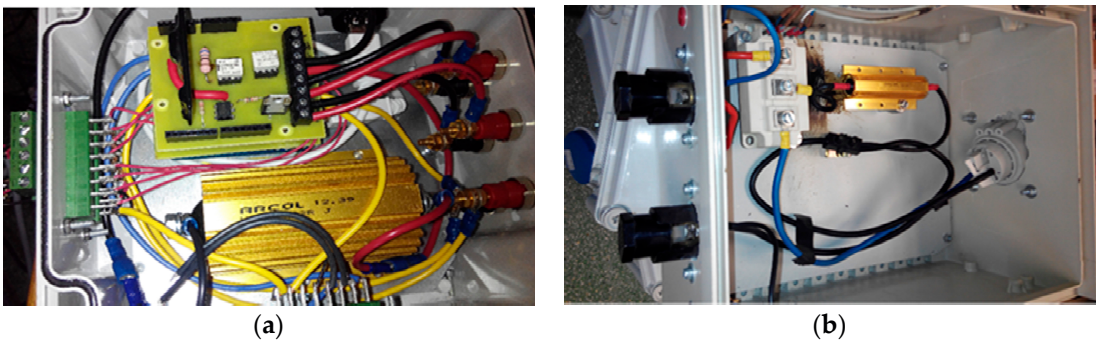

Figure 5. Different designs of the power stage to be used as a function of the size of photovoltaic generator: (**a**) based on Silicon-Controlled Rectifier (SCR) for charge process, low power electromechanical relays for pre-charge, and solid-state relays for discharge; (**b**) based on high power Insulated Gate Bipolar Transistors (IGBT) to measure photovoltaic (PV) generators from 20 to 200 kWp.

3.3. Control, Processing, and Storing Software

A personal computer is necessary to control the Arduino board and to process the measurements performed by the multimeters. The Arduino board and multimeters are connected to the PC by USB ports, so the PC must count with at least three USB ports. The use of this port—widely present on the PC market—rather than other ports such as GPIB or PXI makes the experimental set-up more suitable for laboratories with a reduced budget. As was mentioned before, a software application developed using LabVIEW from National Instruments [36] will run in the computer. The general schematic is presented in Figure 6, in which the principal control processes are activated by three

user buttons. The main function of this software is to control the acquisition of the *I-V* curve and perform campaigns of measurements automatically. A campaign of measurements will be carried out, as this program can be easily configured to manage different PV devices—and consequently, different capacitors banks. The application is capable of processing measurements to obtain the main electrical parameters of the PV device (I_{SC}, V_{OC}, P_{max}, current at the maximum power point (IP_{max}), voltage at the maximum power point (VP_{max}) and *FF*), extrapolating them to STC using different methods [37–40], and extracting different intrinsic parameters from the single-diode model (photo-generated current (I_{ph}), saturation current (I_0), serial resistance (R_s), ideality factor (m), parallel resistance (R_{sh})) using the methods described in [41–43]. All the acquired data are shown on screen and saved when the *I-V* curve is validated, that is, when the ambient parameters have no significant differences before and after the trace of the curve.

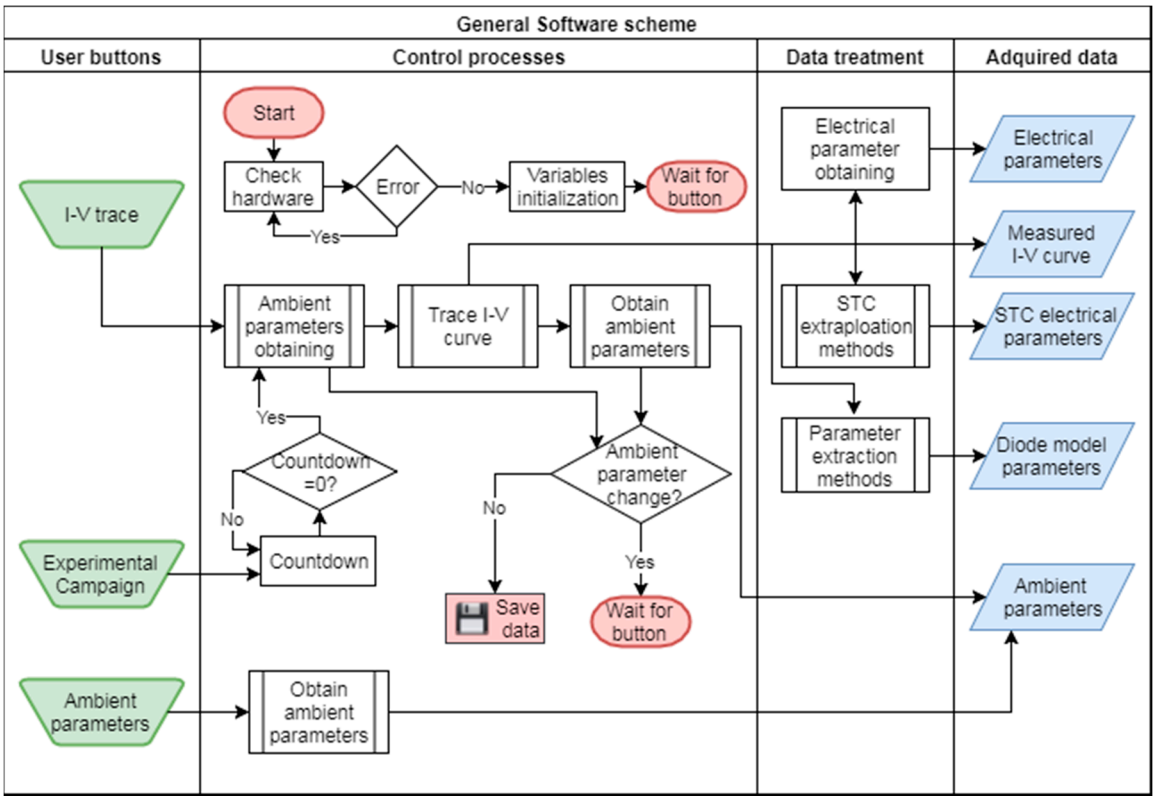

Figure 6. General schematic of the developed software.

In Figure 7, a screenshot of the user panel from the implemented application is shown. The resulting *I-V* curve of a PV module under specific ambient conditions is displayed on the screen after performing a voltage sweep. Another remarkable feature of the software application is the possibility to perform—from among the data previously collected—charts where the variables to plot can be chosen by the user. Thus, the application allows the variable for abscissa and ordinate to be selected, which is a valuable characteristic for researchers and students [44] due to the fact that it makes feasible correlations between recorded variables. For example, in Figure 8a, the dependency on the temperature for the open circuit voltage of the PV module is shown. Other plots can represent the STC values obtained in comparison with any parameter as they are presented in Figure 8b. Also, linear fits can be done between the represented variables and provide some statistical parameters, such as the standard deviation, variance, coefficient of determination, or root mean square deviation. The representation of the extracted parameters from the single diode model can also be represented in the function of the other parameters, as can be seen in Figure 9. Filters of all parameters can be implemented in the plots.

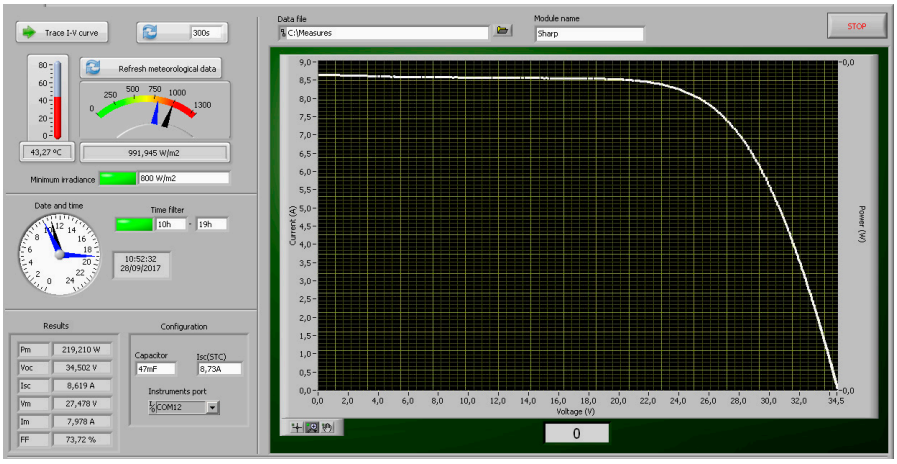

Figure 7. Main window of the software module for the *I-V* curve trace.

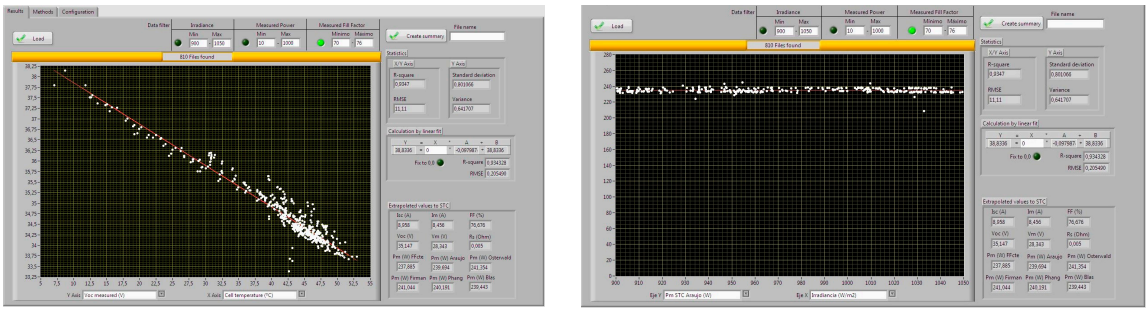

(**a**) (**b**)

Figure 8. Window for the representation of standard test conditions (STC) values, representing: (**a**) *V*oc parameter (Y-axis) measured from several *I-V* curves as a function of the measured cell temperature (X-axis); (**b**) maximum power extrapolated to STC (Y-axis) vs. global irradiance at operating conditions (X-axis).

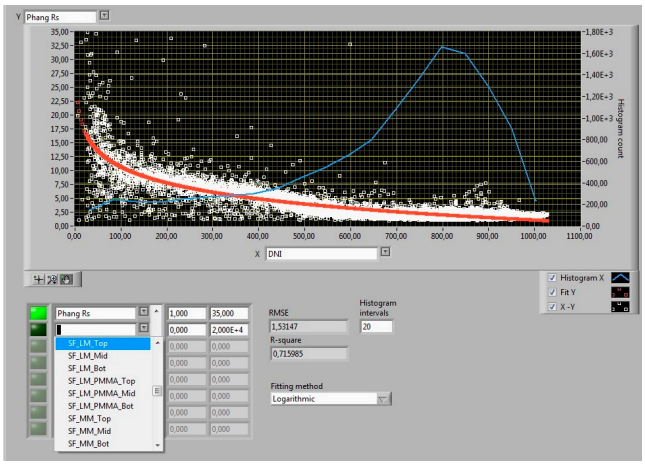

Figure 9. Window for using the parameter extraction methods. Example of serial resistance (Y-axis) parameter as a function of the direct irradiance (X-axis) in white points, logarithmic fit in red line, and data histogram in blue line.

4. Estimation of Uncertainty

All measurement equipment must display the results providing a value of the measured magnitude and an estimation of its uncertainty. The measurement system proposed in this paper is based on a pair of multimeters with their respective calibration certificates from the manufacturer. Thus, an uncertainty study for the obtained results can be easily performed. An estimation of the inherent uncertainty associated with the multimeter is provided in the first part of this section. Furthermore, these uncertainties can be combined in order to determine the uncertainty associated with the *I-V* pairs and will be explained in the second part of this section. The third part explains how the uncertainty of the main electrical parameters: short-circuit current I_{SC}, open circuit voltage V_{OC}, maximum power P_{max}, and fill factor *FF*, is calculated. Finally, those expressions are put into practice for a commercial module measured at three different irradiance levels, giving for each example curve the uncertainty associated with the main electrical parameters.

This uncertainty analysis is based on concepts defined in the guide JCGM GUM [45]. In the literature, there are some works where an analogous analysis has been applied to determine the uncertainty of measurement systems in the field of photovoltaic systems [19,46].

4.1. Uncertainty Associated to the Multimeter

All the measurements are performed by the Agilent 34411A [47]. There are three sources of uncertainty associated with this instrument: accuracy (*A*), resolution (*B*), and calibration standard (*C*).

The uncertainty due to the accuracy depends on the selected measurement range; for this analysis, the PV device to be characterized has been assumed to have, at most, 100 V of open-circuit voltage and 10 A of short-circuit current to fit into the worst case possible for the PV device used.

The accuracy of the multimeter can be computed as the addition of two terms: a percentage of the measured value and another percentage of the selected range:

$$A = (\%\ \text{reading}) \times (\text{outputvalue}) + (\%\ \text{range}) \times (\text{selected range}) \quad (1)$$

where the (% reading) and (% range) to apply are provided by the manufacturer as a table of coefficients (see Table 1, Column 1).

Table 1. Accuracy coefficients for an Agilent 34411A multimeter (% of reading + % of range).

	Range	Integration Time	Column 1	Column 2	Column 3	Column 4
Module Voltage	100 V	0.02 PLCs	0.0040 + 0.0006	0.0005 + 0.0001	0.0 + 0.0030	0.0 + 0.0003
Module Current	1 V	0.02 PLCs	0.0035 + 0.0007	0.0005 + 0.0001	0.0 + 0.0030	0.0 + 0.0003

Mainly, there are two types of measurement: voltage component of each *I-V* point, and the current component of each one measured through a shunt resistor. The values given in Column 1 must be incremented if the temperature of the multimeters is beyond a specific range. For each additional degree outside the range [18 °C, 28 °C], the value in Column 1 should be incremented by the value in Column 2. Finally, another additional term should be added if the integration time is set to a value different to 100 Power Line Cycles (PLC). The integration time used to capture the current-voltage pairs of the *I-V* curve will be 0.02 PLCs. Due to the integration time, the noise adder term can be seen in Table 1, Column 3. Several cases will be considered, and thus different expressions of the uncertainty will be obtained according to the accuracy with which measurements were recorder. Another source of uncertainty comes from the resolution of analog to digital conversion, so the last parameter is given in Column 4.

$$A_V(\text{V}) = 0.00009\,|V| + 0.0046 \quad (2)$$

$$A_{V_S}(\mathrm{V}) = 0.000085\, V_S + 0.000047 \tag{3}$$

where A_V is the uncertainty due to accuracy of a measurement V of the voltage between the terminals of the PV device and A_{V_S} is the uncertainty associated with the reading of the voltage drop across the shunt used to measure the current by the PV device.

The uncertainty associated with the resolution can be estimated as one-half of the resolution given in Table 1, Column 4. Therefore, the values of uncertainty B due to resolution are: B_V = 0.00015 V for the module voltage and B_{V_S} = 0.0000015 V for voltage drop in the shunt.

The third source of uncertainty is associated with the calibration standard used to calibrate the Agilent 34411A. The calibration certificate states that the multimeter was calibrated using a multimeter Fluke 5720A. On the Service Manual [48] of this second multimeter, the absolute uncertainty (with a 95% confidence level and k = 2) is provided giving two parameters, a ppm of the reading and an offset value (see Table 2). For each case of measurement, this uncertainty could be calculated as follows in the Equation (4):

$$C = (\text{ppm of reading}) \times (\text{calibrated value}) + (\text{offset}) \tag{4}$$

Performing the required calculations, the obtained uncertainty is C_V = 0.00054 V (module voltage) and = 0.0000057 V (voltage drop in the shunt resistor).

Table 2. Absolute uncertainties of Fluke 5720A (95% confidence level, k = 2).

	Calibrated Value	**Fluke 5720A Range**	**Absolute Calibration Uncertainty**	
			ppm × Reading	**+ offset**
Module Voltage	100 V	220 V	5 ppm	40 µV
Module Current	1 V	2.2 V	5 ppm	0.7 µV

The acquired uncertainties for module voltage and current will have a confidence level of 95% with k = 2. To obtain the standard uncertainty of resolution and accuracy, both terms are divided by $\sqrt{3}$ due to the fact that nothing is known about the error distribution. The calibration uncertainty is provided by Fluke—with a 95% of confidence level and coverage factor k = 2, which implies a normal distribution of the error—and to compute the standard uncertainty, the value C should be divided by 2. Then, the combined uncertainty of a measurement of module voltage using Agilent 34411A can be computed using the following expression:

$$U_V(\mathrm{V}) = 2\sqrt{\left(\frac{A_V}{\sqrt{3}}\right)^2 + \left(\frac{B_V}{\sqrt{3}}\right)^2 + \left(\frac{C_V}{2}\right)^2} = 2\sqrt{2.7 \times 10^{-9} V^2 + 2.8 \times 10^{-7}|V| + 7.1 \times 10^{-6}} \tag{5}$$

In case of the measurement of the module current, there is another source of uncertainty related to the quality of the shunt resistor itself. For the experimental setup, the shunt class is 0.5. This means that it could be a maximum error of 0.5% of the measured value:

$$E_S = 0.5\% \cdot V_S = 0.005 \cdot V_S \tag{6}$$

Again, nothing should be supposed about the distribution associated with E_S, so this error must be divided by $\sqrt{3}$ to get the standard uncertainty. The combined uncertainty for the current measurement is given by:

$$\begin{aligned} U_{V_S}(V) \quad &= 2\sqrt{\left(\frac{A_{V_S}}{\sqrt{3}}\right)^2 + \left(\frac{B_{V_S}}{\sqrt{3}}\right)^2 + \left(\frac{C_{V_S}}{2}\right)^2 + \left(\frac{E_S}{\sqrt{3}}\right)^2} \\ &= 2\sqrt{8.3 \cdot 10^{-6} V_{S^2} + 2.7 \cdot 10^{-9} V_S + 7.5 \cdot 10^{-10}} \end{aligned} \tag{7}$$

In fact, U_{V_S} is the uncertainty of the voltage measurement from the shunt resistor. The current value should be computed by the shunt specification: 10 A/150 mV. Therefore, the uncertainty expressed in amperes will be:

$$U_I(A) = \frac{10\text{ A}}{150\text{ mV}} \cdot U_{V_S} = 2\sqrt{8.3 \cdot 10^{-6} I^2 + 1.8 \cdot 10^{-7} I + 3.3 \cdot 10^{-6}} \tag{8}$$

For each current-voltage point of the *I-V* curve, the value of power is calculated as $P = VI$. According to Piliougine et al. [14], the uncertainty of a calculated value can be estimated by propagating the uncertainties using the partial derivatives of the formula of the power. Hence, the expanded uncertainty of the power value of each point of the curve can be calculated by:

$$\begin{aligned} U_P(W) &= 2\sqrt{\left(\frac{\mathrm{dP}}{\mathrm{dV}}\right)^2\left(\frac{U_V}{2}\right)^2 + \left(\frac{\mathrm{dP}}{\mathrm{dI}}\right)^2\left(\frac{U_I}{2}\right)^2} = 2\sqrt{I^2 \cdot \left(\frac{U_V}{2}\right)^2 + V^2 \cdot \left(\frac{U_I}{2}\right)^2} \\ &= 2\sqrt{8.3 \cdot 10^{-6} V^2 I^2 + 2.8 \cdot 10^{-7} |V| I^2 + 7.1 \cdot 10^{-6} I^2 + 1.8 \cdot 10^{-7} V^2 I + 3.3 \cdot 10^{-6} V^2} \end{aligned} \tag{9}$$

4.2. Uncertainty of the Main Electrical Parameters

In order to calculate the short circuit current I_{SC}, the linear interpolation of the point immediately before the zero voltage axis (V_0, I_0) and the point immediately after it (V_1, I_1) should be done. Therefore, I_{SC} can be estimated using the following expression:

$$I_{SC} = I_1 - V_1 \frac{I_1 - I_0}{V_1 - V_0} \tag{10}$$

The Equation (10) used to calculate I_{SC} has its own uncertainties that should be propagated to estimate the uncertainty of I_{SC} using this formula:

$$\begin{aligned} U_{I_{SC}} &= 2\sqrt{\left(\frac{dI_{SC}}{dV_0}\right)^2\left(\frac{U_{V_0}}{2}\right)^2 + \left(\frac{dI_{SC}}{dI_0}\right)^2\left(\frac{U_{I_0}}{2}\right)^2 + \left(\frac{dI_{SC}}{dV_1}\right)^2\left(\frac{U_{V_1}}{2}\right)^2 + \left(\frac{dI_{SC}}{dI_1}\right)^2\left(\frac{U_{I_1}}{2}\right)^2} \\ &= 2\sqrt{\left(\frac{V_1(I_1-I_0)}{(V_1-V_0)^2}\right)^2\left(\frac{U_{V_0}}{2}\right)^2 + \left(\frac{V_1}{V_1-V_0}\right)^2\left(\frac{U_{I_0}}{2}\right)^2 + \left(\frac{V_0(I_1-I_0)}{(V_1-V_0)^2}\right)^2\left(\frac{U_{V_1}}{2}\right)^2 + \left(\frac{V_0}{V_1-V_0}\right)^2\left(\frac{U_{I_1}}{2}\right)^2} \end{aligned} \tag{11}$$

In addition, to estimate V_{OC}, the set of points $\{(V_k, I_k) \mid I_k < U_I\,(0)\}$ must be taken into account, where $U_I\,(0)$ is the uncertainty of a current measurement equal to zero amperes. The estimated value of V_{OC} can be calculated as the mean value of all the points in that set. The standard uncertainty is computed as the standard deviation of the voltage values around that mean value. Therefore, the value of V_{OC} and its expanded uncertainty due to the approximation procedure can be estimated using the following expressions:

$$V_{OC}(V) = \frac{1}{n}\sum_{k=1}^{n} V_k \tag{12}$$

$$U_{I\approx 0}(V) = 2\sqrt{\frac{1}{n-1}\sum_{k=1}^{n}(V_k - V_{OC})^2} \tag{13}$$

where n is the number of points of the set.

In addition, the last voltage uncertainty due to the approximation procedure must be combined to the uncertainty due to a single measurement of voltage around the calculated value of V_{OC}:

$$U_{V_{OC}} = 2\sqrt{\left(\frac{U_V(V_{OC})}{2}\right)^2 + \left(\frac{U_{I\approx 0}}{2}\right)^2} \tag{14}$$

The maximum power P_{max} is computed as maximum value of $V_k \cdot I_k$ among all discrete points of the curve, but this is an underestimation of the actual value of P_{max}, and hence an additional source

of uncertainty is added. This uncertainty can be neglected if there is a high density of points around the knee of the curve, as stated in [19]. This fact can be ensured if the difference in power between two consecutive points is much less than the uncertainty in power of a single point: $|P_{i+1} - P_i| <<< U_P(P_i)$. For example, in the checked case $|P_{i+1} - P_i| < 0.2\ U_P(P_i)$, and if the last expression is not satisfied, the *I-V* curve should be discarded and the speed of the multimeters should be increased to acquire more points at the same time. Therefore, the uncertainty of the value of P_{max} will be the uncertainty in power of a single measured point provided by the next equation:

$$U_{P_{max}}(\mathrm{W}) = 2\sqrt{IP_{max}^2 \cdot \left(\frac{U_{VP_{max}}}{2}\right)^2 + VP_{max}^2 \cdot \left(\frac{U_{IP_{max}}}{2}\right)^2} = \\ = 2\sqrt{8.3 \cdot 10^{-6} VP_{max}^2 IP_{max}^2 + 1.8 \cdot 10^{-7} VP_{max}^2 I_{P_{max}} 2.8 \cdot 10^{-7} VP_{max} IP_{max}^2 + 3.3 \cdot 10^{-6} VP_{max}^2 + 7.1 \cdot 10^{-6} IP_{max}^2} \quad (15)$$

Finally, for each measured *I-V* curve, its fill factor will be computed using the following expression:

$$\mathrm{FF} = \frac{P_{max}}{I_{\mathrm{SC}} \cdot V_{\mathrm{OC}}} = \frac{\mathrm{IP}_{max} \cdot \mathrm{VP}_{max}}{I_{\mathrm{SC}} \cdot V_{\mathrm{OC}}} \quad (16)$$

Therefore, the uncertainty associated to each value of FF can be computed as:

$$U_{FF} = 2\sqrt{\left(\frac{d\,FF}{dP_{max}}\right)^2 \cdot \left(\frac{U_{P_{max}}}{2}\right)^2 + \left(\frac{d\,FF}{dI_{\mathrm{SC}}}\right)^2 \left(\frac{U_{I_{\mathrm{SC}}}}{2}\right)^2 + \left(\frac{d\,FF}{dV_{\mathrm{OC}}}\right)^2 \left(\frac{U_{V_{\mathrm{OC}}}}{2}\right)^2} = \\ = 2\frac{1}{I_{\mathrm{SC}} \cdot V_{\mathrm{OC}}} \sqrt{\left(\frac{U_{P_{max}}}{2}\right)^2 + \frac{P_{max}^2}{I_{\mathrm{SC}}^2}\left(\frac{U_{I_{\mathrm{SC}}}}{2}\right)^2 + \frac{P_{max}^2}{V_{\mathrm{OC}}^2}\left(\frac{U_{V_{\mathrm{OC}}}}{2}\right)^2} \quad (17)$$

4.3. Practical Case of Uncertainty Estimation

In order to illustrate the practical use of the expressions previously described, three examples of *I-V* curves under different weather conditions are measured for a commercial photovoltaic module Sharp NU245J5 and the results are exposed in Figure 10. In addition, the values of the irradiance *G*, the cell temperature T_c, the short circuit current I_{SC}, the open circuit voltage V_{OC}, the maximum power P_{max}, and the fill factor FF are obtained for each measured curve and their respective uncertainties are calculated accordingly to the set of expressions provided previously. The results are shown in Table 3. Moreover, the specifications of the PV modules are shown in Table 4.

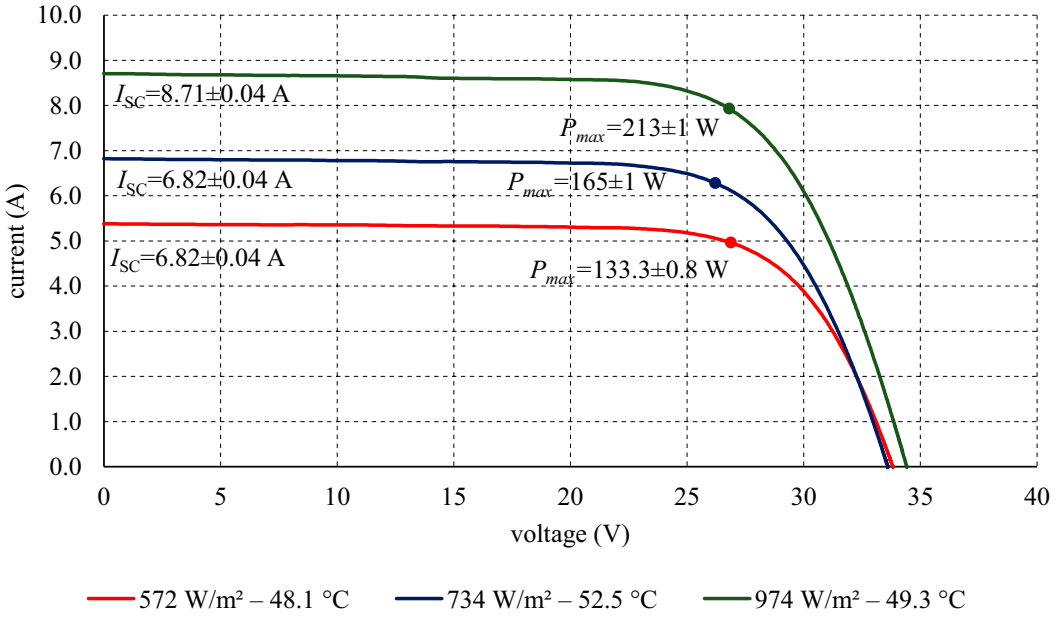

Figure 10. Current-voltage curves for Sharp NU245J5 module under different weather conditions.

Table 3. Electrical parameters extracted from curves shown in Figure 9 for Sharp NU245J5 module.

	Curve 1	**Curve 2**	**Curve 3**
G (W/m^2)	572 ± 24	734 ± 30	974 ± 40
T_m (°C)	48.1 ± 1.3	52.5 ± 1.3	52.5 ± 1.3
I_{SC} (A)	5.38 ± 0.03	6.82 ± 0.04	8.71 ± 0.04
V_{OC} (V)	33.81 ± 0.01	33.60 ± 0.01	34.41 ± 0.01
P_{max} (W)	133.3 ± 0.8	165 ± 1	213 ± 1
FF (%)	73.3 ± 0.6	71.9 ± 0.6	70.9 ± 0.5

Table 4. Specifications of the photovoltaic modules at STC.

	#1	**#2**	**#3**
Technology	mono-Si	multi-Si	HIT
Manufacturer	Sharp	Suntech	Sanyo
Model	NU245J5	STP-160	HIT-240HDE4
Num. of cells	60	72	60
Coeffcient α	+0.053%/°C	+0.06%/°C	+2.21 mA/°C
Coeffcient β	−130 mV/°C	−155 mV/°C	−109 mV/°C
Coeffcient γ	−0.485%/°C	−0.47%/°C	−0.30%/°C
Main Electrical Parameters at STC (Manufacturer)			
I_{SC} (A)	8.73	5.12	7.37
V_{OC} (V)	37.5	42.4	43.6
P_{max} (W)	245	160	240
IP_{max} (A)	8.04	4.78	6.77
VP_{max} (V)	30.5	33.5	35.5
Main Electrical Parameters at STC (IAL, Solar Simulator)			
I_{SC} (A)	8.68	5.03	7.45
V_{OC} (V)	37.4	43.6	42.8
P_{max} (W)	241	165	242
IP_{max} (A)	7.92	4.75	7.07
VP_{max} (V)	30.4	34.8	34.2
FF (%)	74.1	75.4	75.9

5. Experimental Design

The components that compose the experimental design and the methodology will be exposed in this section. Three commercial modules from different photovoltaic technologies—monocrystalline silicon, polycrystalline silicon and CIGS—have been characterized by measuring their *I-V* curves and computing their main electrical parameters. The modules and the necessary sensors for the experiment were located in an outdoor solar tracker placed on the terrace of the Engineering Building of the University of Jaen. The main electrical specifications in STC provided by the manufacturer are summarized in Table 4. In order to compare the obtained results to a true value, the modules were previously sent to an independent, accredited laboratory (IAL). The IAL (Centro de Investigaciones Energéticas, Medioambientales y Tecnológicas (CIEMAT), Madrid, Spain) performs characterizations under standard test conditions in a solar simulator. The electrical parameters given by the IAL are also exposed in Table 4. The system has been tested using a predetermined configuration suitable to measure a single commercial photovoltaic module. The selected configuration is summarized in Table 5. In addition, the sensors connected to the system are shown in Table 6. As an approximated budget of the system, the total material cost reached a value of $3000, while the value of two multimeters from the top range was approximately $2800, plus $200 of electronic material costs.

Table 5. Components used on the interchangeable part of the system.

Component	Manufacturer/Model	Characteristics
Capacitor bank	Kermet PEH200	V = 100 V C = 47 mF
Switch	TYN640	V_{DRM} = 640 V I_T = 40 A
Shunt	Kainos	I = 10 A V = 150 mV
Resistor	Arcol HS200	R = 22 Ω P = 200 W
Precharge source	Arduino	V = 5 V I = 50 mA

Table 6. Sensors connected to the system.

Sensor	Manufacturer/Model	Parameter
Pyranometer	Kipp & Zonen CMP21	Global normal irradiance
Spectroradiometer	EKO MS-700	Solar spectrum
Platinum RTD	PT100	Cell temperature
Platinum RTD	PT100	Air temperature
Anemometer	Young 05305VM	Wind direction
Anemometer	Young 05305VM	Wind speed

With the aim of quantifying the closeness of agreement of the proposed system, 50 curves per module have been selected under irradiance ranges between 950 W/m^2 and 1050 W/m^2. In order to compare the results obtained by the proposed system and the results given by the IAL, the *I-V* curves must be extrapolated into STC. For this, three extrapolation methods have been used. On the first hand, the model of Osterwald [39] is employed to estimate the value of P_{max} under STC for each measured curve. Besides, the method described by Araujo et al. [38] and the one published by Firman et al. [40] have been applied to determine also the value of I_{SC}, V_{OC}, and P_{max} at STC conditions; the FF is also computed using those parameters. In order to know the closeness of agreement between the measurements taken by experimental set-up and those ones recorded by the IAL, the RMSE (Equation (18)) and the relative error (Equation (19)) have been computed. It must be taken into account that the error is produced by the sum of two factors: the error generated from the measurement system and from the extrapolation method.

$$RMSE = \sqrt{\frac{1}{N}\sum_{i=1}^{N}\Re(V)_i^2} \tag{18}$$

$$\Re(V) = \frac{IALparameter - Measuredparameter}{IALparameter} \tag{19}$$

6. Results

The comparison between the obtained results by the proposed system and the results from an Independent Accredited Laboratory (IAL) will be exposed in this section. For each electrical parameter, the mean value, RMSE, and relative error of the set on STC from all the curves is computed and the results can be seen in Tables 7–9, and in Tables 8 and 9 for Sharp NU245J5, Suntech STP-160, and Sanyo HIT240, respectively.

Table 7. Measurement of the CIEMAT vs. measurement of the proposed system over Sharp NU245J5.

	CIEMAT	Corrected to STC by Araújo			Corrected to STC by Firman			Corrected to STC by Osterwald		
		MEAN	RMSE	Relative Error	MEAN	RMSE	Relative Error	MEAN	RMSE	Relative Error
I_{SC} (A)	8.74	9.02	0.28	3.2%	9.02	0.29	3.3%			
V_{OC} (V)	37.4	37.57	0.20	0.5%	37.45	0.12	0.3%			
P_{max} (W)	241	236	5	2.1%	245	4	1.7%	249	9	3.6%
FF (%)	73.7	70.5	3.2	4.3%	72.6	1.2	1.7%			

Table 8. Measurement of the CIEMAT vs. measurement of the proposed system over Suntech STP-160.

	CIEMAT	Corrected to STC by Araújo			Corrected to STC by Firman			Corrected to STC by Osterwald		
		MEAN	RMSE	Relative Error	MEAN	RMSE	Relative Error	MEAN	RMSE	Relative Error
I_{SC} (A)	5.03	5.26	0.23	4.6%	5.26	0.23	4.6%			
V_{OC} (V)	43.6	43.46	0.16	0.4%	43.52	0.21	0.5%			
P_{max} (W)	165	161	4	2.4%	168	3	1.8%	172	7	4.2%
FF (%)	75.4	71.4	4.0	5.3%	73.3	2.1	2.8%			

Table 9. Measurement of the CIEMAT vs. measurement of the proposed system over Sanyo HIT240.

	CIEMAT	Corrected to STC by Araújo			Corrected to STC by Firman			Corrected to STC by Osterwald		
		MEAN	RMSE	Relative Error	MEAN	RMSE	Relative Error	MEAN	RMSE	Relative Error
I_{SC} (A)	7.45	7.42	0.04	0.5%	7.43	0.04	0.5%			
V_{OC} (V)	42.8	42.63	0.18	0.4%	42.63	0.18	0.5%			
P_{max} (W)	242	233	10	4.1%	236	6	2.5%	237	7	2.9%
FF (%)	75.9	74.4	1.9	2.5%	74.5	1.4	1.8%			

After analyzing the parameters used for establishing the closeness of agreement between the measured system and the IAL, the worst results obtained correspond to *FF,* which were less than 5.3%. The *FF* is the most difficult parameter to predict for the selected STC methods, since its value is highly affected by the parasitic resistances (serial and shunt resistances), which depend on the ambient conditions. Low differences were found on this parameter between the value measured at real conditions and the value extrapolated to STC. In terms of the short circuit current, the relative error was slightly higher than 3% for the Sharp NU245J5 (mono-Si), around 4.6% for the SunTech STP-160 (multi-Si), and only 0.5% for the Sanyo HIT. The I_{SC} value extrapolation to STC is very sensitive to the irradiance sensor measure and a slightly different α value (for these specific modules). Also, the uncertainties produced by the shunt resistor can be a great source of error. The error in the estimation of the open circuit voltage is different in the three cases, but never greater than 0.5%. In contrast to the previous parameter, this value is mainly affected by the temperature value. The β value is also a source of error in the extrapolation to STC. A lower error value may be justified for the higher stability of this parameter in outdoor conditions. Regarding the maximum power, for the Sharp NU245J5 using models by Araújo or Firman, the error in power is around 2–2.1% and 1.7%, respectively, whereas the Osterwald's method has an error of 3.6%. In the same way, for the module Suntech STP-160, the error using the Osterwald's method is more than 4%, while the error of the Araújo's model is 2.4% and the error the of Firman's model is only 1.8%. However, in case of the Sanyo HIT module, the model of Araújo, with a relative error of 4.1%, behaves worse than the other two models (2.5% for the Firman's model and 2.9% for the Osterwald model). Surprisingly, the method of Osterwald—which is employed only to estimate the maximum power value—obtained the highest error results.

7. Conclusions

A complete system to measure the *I-V* curves of any photovoltaic device has been implemented. The system is based on three principles: the use of general purpose instrumentation to perform the measurements, which ensures accuracy and precision; the use of open-hardware, which allows

the reproduction of the system in any laboratory; and scalability, which measures any PV device. These characteristics also reduce the final budget of the system.

The hardware is composed of a common part, which can be used to measure any PV generator, and an interchangeable part, which must be designed taking into account the specifications of the PV device under test. This way, the proposed system can be used to measure any PV generator. The provided software allows the process of measurement to be configured and controlled to automatically take *I-V* curves at regular intervals of time. In addition, the program offers a set of tools to perform data processing from the obtained *I-V* curves such as extrapolation to STC.

A deep study of the uncertainties associated with the measuring process was done. Thus, the reported *I-V* curves for the modules under test include their respective uncertainty.

A campaign of measurements was carried out. Three commercial modules of different photovoltaic technologies were characterized by the system. These modules were previously sent to an independent accredited laboratory in order to compare the results obtained by the proposed system to those given by the IAL. The obtained results prove that the relative error when measuring the main electrical parameters and performing the extrapolation to STC is less than 5%. In short-circuit the error is never greater than 5%, in open-circuit voltage is less than 0.5%, and in maximum power it is around 4% in the worst case. Thus, the obtained results suggest that the proposed system is suitable and can be profitable for laboratories with reduced budget or for educational applications.

Acknowledgments: This work has been supported by Andalusian International Cooperation Agency (Agencia Andaluza de Cooperación Internacional para el Desarrollo, AACID) in the framework of the project: "Emergiendo con el sol. Apoyo institucional al centro de energías renovables de la Universidad Nacional de Ingeniería en el campo de la generación de energía eléctrica empleando tecnología fotovoltaica" and the University of Jaén in the program "Incentivos a la Excelencia de I+D+I. Grupos de Investigación. Acción 2 del Plan de Apoyo a la I+D+I (convocatoria 2015)". In addition, the work is also partially funded by "Junta de Andalucía", (grant P11-RNM-7115), co-financed with FEDER (European Fund for Regional Development) funds by the EU. Eduardo F. Fernández acknowledges the Spanish Ministry of Economy and Competitiveness for the Juan de la Cierva 2015—Incorporation fellowship and the FEDER funds under the project ENE2016-78251-R.

Author Contributions: All authors have contributed actively to the work that has resulted in this paper. The authors are especially grateful to the researchers of the IDEA group for their contributions, reflections and scientific support during the more than 20 years that the line of research has been active within the work of the group. Jesús Montes-Romero and Michel Piliougine wrote the paper. Jesús Montes-Romero performed the experiments. Michel Piliougine carried out the uncertainty analysis. Juan de la Casa conceived the idea and design of the device. Juan de la Casa, José Vicente Muñoz and Eduardo F. Fernández revised the paper and provided suggestions in the implementation and validation of the electronic device.

Conflicts of Interest: The authors declare no conflict of interest.

References

1. Bloomberg New Energy Finance. *Global Trends in Clean Energy Investment*; Bloomberg New Energy Finance: New York, NY, USA, 2017.
2. SolarPower Europe. *Global Market Outlook for Solar Power 2017–2021*; SolarPower Europe: Brussels, Belgium, 2017.
3. Fraunhofer Institute for Solar Energy Systems. *Photovoltaics Report*; Fraunhofer Institute for Solar Energy Systems: Munich, Germany, 2017.
4. REN 21. *Renewables 2017: Global Status Report*; REN 21: Paris, France, 2017.
5. International Electrotechnical Commission. *IEC 60904-1, Photovoltaic Devices, Part 1: Measurement of Photovoltaic Current–Voltage Characteristics*; International Electrotechnical Commission: Geneva, Switzerland, 2006.
6. Virtuani, A.; Müllejans, H.; Dunlop, E.D. Comparison of indoor and outdoor performance measurements of recent commercially available solar modules. *Prog. Photovolt. Res. Appl.* **2011**, *19*, 11–20. [CrossRef]
7. Fernández, E.F.; Pérez-Higueras, P.; Garcia Loureiro, A.J.; Vidal, P.G. Outdoor evaluation of concentrator photovoltaic systems modules from different manufacturers: First results and steps. *Prog. Photovolt. Res. Appl.* **2013**, *21*, 693–701. [CrossRef]

8. Kichou, S.; Abaslioglu, E.; Silvestre, S.; Nofuentes, G.; Torres-Ramírez, M.; Chouder, A. Study of degradation and evaluation of model parameters of micromorph silicon photovoltaic modules under outdoor long term exposure in Jaen, Spain. *Energy Convers. Manag.* **2016**, *120*, 109–119. [CrossRef]
9. García, M.; Maruri, J.M.; Marroyo, L.; Lorenzo, E.; Pérez, M. Partial Shadowing, MPPT Performance and Inverter Configurations: Observations at Tracking PV Plants. *Prog. Photovolt. Res. Appl.* **2008**, *15*, 659–676. [CrossRef]
10. Smith, R.M.; Jordan, D.C.; Kurtz, S.R. Outdoor PV module degradation of current-voltage parameters. In *World Renewable Energy Forum*; National Renewable Energy Laboratory: Denver, CO, USA, 2012; pp. 1–9.
11. Picault, D.; Raison, B.; Bacha, S.; de la Casa, J.; Aguilera, J. Forecasting photovoltaic array power production subject to mismatch losses. *Sol. Energy* **2010**, *84*, 1301–1309. [CrossRef]
12. Piliougine, M.; Cañete, C.; Moreno, R.; Carretero, J.; Hirose, J.; Ogawa, S.; Sidrach-de-Cardona, M. Comparative analysis of energy produced by photovoltaic modules with anti-soiling coated surface in arid climates. *Appl. Energy* **2013**, *112*, 626–634. [CrossRef]
13. Sanchis, P.; López, J.; Ursúa, A.; Gubía, E.; Marroyo, L. On the Testing, Characterization, and Evaluation of PV Inverters and Dynamic MPPT Performance Under Real Varying Operating Conditions. *Prog. Photovolt. Res. Appl.* **2007**, *15*, 659–676. [CrossRef]
14. Munoz, M.A.; Alonso-García, M.C.; Vela, N.; Chenlo, F. Early degradation of silicon PV modules and guaranty conditions. *Sol. Energy* **2011**, *85*, 2264–2274. [CrossRef]
15. Humada, A.M.; Hojabri, M.; Mekhilef, S.; Hamada, H.M. Solar cell parameters extraction based on single and double-diode models: A review. *Renew. Sustain. Energy Rev.* **2016**, *56*, 494–509. [CrossRef]
16. Fernández, E.F.; Montes-Romero, J.; de la Casa, J.; Rodrigo, P.; Almonacid, F. Comparative study of methods for the extraction of concentrator photovoltaic module parameters. *Sol. Energy* **2016**, *137*, 413–423. [CrossRef]
17. Ogbomo, O.O.; Amalu, E.H.; Ekere, N.N.; Olagbegi, P.O. A review of photovoltaic module technologies for increased performance in tropical climate. *Renew. Sustain. Energy Rev.* **2016**, *75*, 1225–1238. [CrossRef]
18. Duran, E.; Piliougine, M.; Sidrach-De-Cardona, M.; Galan, J.; Andujar, J.M. Different methods to obtain the I-V curve of PV modules: A review. In Proceedings of the 33rd IEEE Photovoltaic Specialists Conference, San Diego, CA, USA, 11–16 May 2008.
19. Piliougine, M.; Carretero, J.; Mora-Lõpez, L.; Sidrach-De-Cardona, M. Experimental system for current-voltage curve measurement of photovoltaic modules under outdoor conditions. *Prog. Photovolt. Res. Appl.* **2011**, *19*, 591–602. [CrossRef]
20. Hecktheuer, L.A.; Krenzinger, A.; Prieb, C.W.M. Methodology for Photovoltaic Modules Characterization and Shading Effects Analysis. *J. Braz. Soc. Mech. Sci.* **2002**, *24*, 26–32. [CrossRef]
21. Granek, F.; Danowicz, T. Advanced system for calibration and characterization of solar cells. *Optoelectron. Rev.* **2004**, *12*, 57–67.
22. Yandt, M.D.; Cook, J.P.D.; Kelly, M.; Schriemer, H.; Hinzer, K. Dynamic Real-Time I-V Curve Measurement System for Indoor / Outdoor Characterization of Photovoltaic Cells and Modules. *IEEE J. Photovolt.* **2015**, *5*, 337–343. [CrossRef]
23. Willoughby, A.A.; Omotosho, T.V.; Aizebeokhai, A.P. A simple resistive load I-V curve tracer for monitoring photovoltaic module characteristics. In Proceedings of the IREC 2014—5th International Renewable Energy Congress, Hammamet, Tunisia, 25–27 March 2014; pp. 1–6.
24. Rivai, A.; Rahim, N.A. Binary-based tracer of photovoltaic array characteristics. *IET Renew. Power Gener.* **2014**, *8*, 621–628. [CrossRef]
25. Leite, V.; Batista, J.; Chenlo, F.; Afonso, J.L. Low-Cost Instrument for Tracing Current-Voltage Characteristics of Photovoltaic Modules. In Proceedings of the International Conference on Renewable Energies and Power Quality, Santiago de Compostela, Spain, 28–30 March 2012; Volume 1, pp. 1012–1017.
26. Leite, V.; Chenlo, F. An improved electronic circuit for tracing the IV characteristics of photovoltaic modules and strings. In Proceedings of the International Conference on Renewable Energies and Power Quality, Granada, Spain, 23–25 March 2010; Volume 1, pp. 1224–1228.
27. Hemza, A.; Abdeslam, H.; Rachid, C.; Pasquinelli, M.; Barakel, D. Tracing current-voltage curve of solar panel Based on LabVIEW Arduino Interfacing. *BİLİŞİM Teknol. DERGİSİ* **2015**, *3*, 117–123. [CrossRef]
28. Vargas, T.; Abrahamse, A. An open-source hardware IV curve tracer for monitoring PV output in Bolivia. *Investig. Y Desarro.* **2014**, *1*, 100–114. [CrossRef]

29. Muñoz, J.V.; de la Casa, J.; Fuentes, M.; Aguilera, J.; Bertolín, J.C. New portable capacitive load able to measure PV modules, PV strings and large PV generators. In Proceedings of the 26th European Photovoltaic Solar Energy Conference and Exhibition, Hamburg, Germany, 5–9 September 2011; Volume 1, pp. 4276–4280.
30. Bertolín, J.C.; Fuentes, M.; Muñoz, J.V.; de la Casa, J. Applications of DC/DC converters for obtaining characteristic curves of PV generators. In Proceedings of the 27th European Photovoltaic Solar Energy Conference, Frankfurt, Germany, 24–28 September 2012.
31. Muñoz, J.V.; Torres-Ramírez, M.; García-Domingo, B.; Fuentes, M.; de la Casa, J.; Nofuentes, G.; Aguilera, J. Automatic monitoring system to assess the outdoor behaviour of photovoltaic modules. In Proceedings of the 29th European Photovoltaic Solar Energy Conference and Exhibition, Amsterdam, The Netherlands, 22–26 September 2014; pp. 2654–2657.
32. Podewils, C.; Bosworth, M. The learning curve. *Photon* **2012**, 52–72.
33. Hernday, P. Field Applications for I-V Curve Tracers. *SolarPro*, September 2011, pp. 76–106.
34. Tritec. *Operating Instructions Tri-ka*; Tritec: Basel, Switzerland, 2010.
35. Erkaya, Y.; Flory, I.; Marsillac, S.X. Development of a String Level I-V Curve Tracer. In Proceedings of the 2014 IEEE 40th Photovoltaic Specialist Conference (PVSC), Denver, CO, USA, 8–13 June 2014.
36. National Instruments. *LabVIEW User Manual*; National Instruments: Austin, TX, USA, 2003.
37. International Electrotechnical Commission. *IEC 60891, Photovoltaic Devices. Procedures for Temperature and Irradiance Corrections to Measure I-V Characteristics*; International Electrotechnical Commission: Geneva, Switzerland, 2007.
38. Araujo, G.; Sánchez, E. Analytical expressions for the determination of the maximum power point and the fill factor of a solar cell. *Sol. Cells* **1982**, *5*, 377–386. [CrossRef]
39. Osterwald, C.R. Translation of device performance measurements to reference conditions. *Sol. Cells* **1986**, *18*, 269–279. [CrossRef]
40. Firman, A.; Toranzos, V.; Busso, A.; Cadena, C.; Vera, L. Determinación del punto de trabajo de sistemas fotovoltaicos conectados a red: Metodo simplificado de traslacion punto a punto a condiciones estandar de medida. *Av. en Energías Renov. y Medio Ambient.* **2011**, *15*, 1–8.
41. Phang, J.C.H.; Chan, D.S.H.; Phillips, J.R. Accurate analytical method for the extraction of solar cell model parameters. *Electron. Lett.* **1984**, *20*, 406. [CrossRef]
42. Khan, F.; Baek, S.-H.; Kim, J.H. Intensity dependency of photovoltaic cell parameters under high illumination conditions: An analysis. *Appl. Energy* **2014**, *133*, 356–362. [CrossRef]
43. De Blas, M.A.; Torres, J.L.; Prieto, E.; García, A. Selecting a suitable model for characterizing photovoltaic devices. *Renew. Energy* **2002**, *25*, 371–380. [CrossRef]
44. Montes-Romero, J.; Torres-Ramírez, M.; De La Casa, J.; Firman, A.; Cáceres, M. Software tool for the extrapolation to Standard Test Conditions (STC) from experimental curves of photovoltaic modules. In Proceedings of the 2016 Technologies Applied to Electronics Teaching, Seville, Spain, 22–24 June 2016.
45. Evaluation of measurement data—Guide to the expression of uncertainty in measurement. *JCGM* **2008**, *50*, 134. [CrossRef]
46. Whitfield, K.; Osterwald, C.R. Procedure for determining the uncertainty of photovoltaic module outdoor electrical performance. *Prog. Photovolt. Res. Appl.* **2001**, *9*, 87–102. [CrossRef]
47. Agilent Technologies. *34410A/11A 6-1/2 Digit Multimeter User's Guide*; Editi, F., Ed.; Agilent Technologies: Santa Clara, CA, USA, 2012.
48. Fluke Corporation. *Fluke 5700A/5720A Series II. Service Manual*; Fluke Corporation: Everett, WA, USA, 2005.

PUBLICACIÓN III

Título	**"Comparative analysis of parameter extraction techniques for the electrical characterization of multi-junction CPV and m-Si technologies"**
Autores	Montes-Romero, Jesús; Almonacid, Florencia; Theristis, Marios; de la Casa, Juan; E. Georghiou, George; F. Fernández, Eduardo
Revista	Solar Energy
Volumen, páginas, año	160, 275-288, 2018
Categoría y posición	ENERGY AND FUELS (23/97)
Factor de impacto	4,374 (2017)
DOI	10.1016/j.solener.2017.12.011

Solar Energy 160 (2018) 275–288

Contents lists available at ScienceDirect

Solar Energy

journal homepage: www.elsevier.com/locate/solener

Comparative analysis of parameter extraction techniques for the electrical characterization of multi-junction CPV and m-Si technologies

Jesús Montes-Romero[a], Florencia Almonacid[a], Marios Theristis[b], Juan de la Casa[a], George E. Georghiou[b], Eduardo F. Fernández[a,*]

[a] Centre for Advanced Studies on Energy and Environment (CEAEMA), IDEA Solar Energy Research Group, Electronics and Automation Engineering Department, University of Jaén, Las Lagunillas Campus, Jaén 23071, Spain
[b] PV Technology Laboratory, FOSS Research Centre for Sustainable Energy, Department of Electrical and Computer Engineering, University of Cyprus, Nicosia 1678, Cyprus

ARTICLE INFO

Keywords:
Concentrating photovoltaics
Monocrystalline silicon
Single-diode model
Outdoor characterisation

ABSTRACT

Modelling the current-voltage (*I-V*) characteristics of photovoltaic (PV) modules under real operating conditions is crucial for the better understanding of each technology. The most commonly used model for the electrical characterization of PV is the single-diode model where the five parameters are extracted through a variety of techniques. Although numerous extraction methods were developed for conventional PV technologies, the studies concerning the concentrating photovoltaic (CPV) technology are still limited. In this work, three analytical parameter extraction methods (Phang et al., Blas et al. and Khan et al.) are applied and compared for a multi-junction (MJ) CPV and a monocrystalline (m-Si) module based on long-term outdoor measurements in Jaén, Spain. The sensitivity of the models against the dominant parameters that influence the behaviour of PV and CPV (i.e. irradiance, module temperature and air mass) is also investigated. Furthermore, the effect of irradiance on the extracted parameters is discussed including the derivation of the corresponding fitting equations and errors. The results indicate that the most robust method is the one proposed by Phang et al. for the CPV module (normalised root mean square error, *NRMSE*, of 1.55%) and the one proposed by Blas et al. for the m-Si module (*NRMSE* of 0.58%). The method of Khan et al. resulted the highest error values for every case (*NRMSE* of 4.5% and 1.74% for CPV and m-Si respectively) while the Phang et al. method exhibited a similar error for both technologies. The main outcome of this work contributes to the optimum selection of parameter extraction techniques depending on the technology and the desired associated errors while the analysis of the dependence of the parameters on irradiance provides a better understanding of each technology's behaviour in the field.

1. Introduction

Concentrating photovoltaics (CPV) are considered as one of the most promising photovoltaic (PV) technology (Talavera et al., 2017, 2016). This technology employs optics to concentrate the direct sunlight onto a smaller area, most often made of high efficiency multi-junction (MJ) solar cells. Due to the combination of different components and the requirement for solar tracking, such systems are characterised by a multiphysics behaviour that makes the performance assessment more complex and inherently different than conventional photovoltaic devices (Rodrigo et al., 2013). Therefore, the CPV behaviour under actual operating conditions is not as clear as in conventional PV, which are very well understood and predictable nowadays (Fernández et al., 2013b; Kurtz et al., 2015; Theristis et al., 2018). This fact triggered important efforts within the last decade to analyse the behaviour and to develop models tailored to the special features of CPV technology at cell (Domínguez et al., 2010; Fernández et al., 2013; Theristis and O'Donovan, 2015), module (Fernández et al., 2013a; Steiner et al., 2015; Theristis et al., 2017b) and system level (Fernández et al., 2015; Kim et al., 2013; Strobach et al., 2015). Knowledge of the current-voltage (*I-V*) output of CPV, as a function of the relevant input parameters, is crucial for the understanding of the CPV performance. This, in turn, can lead to a reduction in investment risk and increase in bankability and therefore contribute to the market expansion of the technology (Fernández et al., 2016a; Kurtz et al., 2015; Leloux et al., 2014).

The *I-V* curve provides valuable information about the operational characteristics of a PV cell, module or array (Almonacid et al., 2015). The *I-V* curve of such devices is defined by the equivalent circuit models. A frequently used equivalent circuit model is the single-diode

* Corresponding author.
E-mail address: fenandez@ujaen.es (E.F. Fernández).

https://doi.org/10.1016/j.solener.2017.12.011
Received 7 August 2017; Received in revised form 7 November 2017; Accepted 5 December 2017

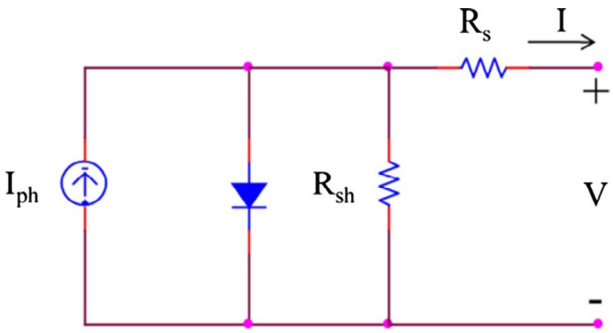

Fig. 1. Equivalent circuit of the single-diode model.

model (or single exponential model, SEM) illustrated in Fig. 1 for a single solar cell. The circuit is formulated using Kirchoff's current law where the current equals the photocurrent (I_{ph}) subtracted by the voltage-dependent current lost to recombination and the current lost due to shunt resistances:

$$I = I_{ph} - I_0\left(\exp\left(\frac{V + IR_s}{mV_T}\right) - 1\right) - \frac{V + IR_s}{R_{sh}} \quad (1)$$

where the current through the diode is modelled using the Shockley equation for an ideal diode, I_0 is the diode's saturation current, R_s is the series resistance, m is the diode's ideality factor, R_{sh} is the shunt resistance and V_T is the thermal voltage given by $V_T = kT/q$, where k is Boltzmann's constant (1.38E-23 J/K), T is the cell temperature and q is the elementary charge (1.6E-19C).

The estimation of the five characteristic parameters of the single-diode model (i.e. I_{ph}, I_0, R_s, m, R_{sh}) are of great importance for the modelling and evaluation of PV systems but also for degradation studies or other related scientific research in general (Celik and Acikgoz, 2007; Emery and Osterwald, 1987; Gasparin et al., 2016; Ishibashi et al., 2008; Kichou et al., 2016a,b; Sharma et al., 2014). Numerous studies in the literature developed and presented appropriate techniques capable of estimating and extracting the characteristic parameters of PV cells and modules (Ciulla et al., 2014; Cotfas et al., 2013; Humada et al., 2016; Li et al., 2013). The extraction methods presented in the literature can be divided into three main categories: a) the analytical methods (Chegaar et al., 2006; Tivanov et al., 2005; Wolf and Benda, 2013), b) the numerical methods such as the Lambert W functions (Ghani and Duke, 2011; Ortiz-Conde et al., 2006; Zhang et al., 2011) and Newton-Raphson method (Easwarakhanthan et al., 1986; Ghani et al., 2014) and c) the heuristic methods (Jamadi et al., 2016; Zagrouba et al., 2010; Ye et al., 2009; Yu et al., 2017). Numerical methods require suitable initial values in order to converge and can therefore result in a lower efficiency when the initial conditions are far from the optimal conditions (Yu et al., 2017). On the other hand, heuristic algorithms such as genetic, particle swarm optimisation, neural networks etc. have proven to be an alternative to numerical methods since they impose no restriction on the problem formulation. Furthermore, analytical methods are usually more preferable because such techniques are simpler to use and are able to provide comparable results under the normal operating conditions of PV devices (Chan et al., 1986; Ghani et al., 2017).

Although various parameter extraction techniques have been developed for conventional PV technologies, not much work has been done for CPV (Almonacid et al., 2016; Appelbaum and Peled, 2014; Ben Or and Appelbaum, 2013; Segev et al., 2012). In addition to this, all the parameter extraction methods related to CPV are based on numerical or heuristic modelling. The sole study applying analytical modelling techniques for CPV was recently published by the authors elsewhere (Fernández et al., 2016b) where, due to the aforementioned complexity of such systems, only a number of representative *I-V* curves was selected to conduct the study. This work however, moves one step beyond our previous study and long-term data (from Jaén, Spain) are accumulated using an in-house design for the *I-V* tracing. It is the first time that analytical methods used for the extraction of the five parameters in PV are applied in CPV and their performance is compared using long-term data of a monocrystalline Silicon (m-Si) and a CPV module, installed side-by-side. Such experiments can provide useful information about the applicability of simple analytical techniques, widely used in PV, on a more complicated technology such as the CPV eventually leading to improved energy yield predictions. Moreover, the sensitivity of the models against the dominant parameters that influence the behaviour of PV and CPV (i.e. irradiance, module temperature, T_{mod}, and air mass, *AM*) is also investigated for the first time. Finally, the influence of irradiance on the extracted parameters is analysed and the corresponding fitting equations and errors are derived; such analysis has been conducted only by Fernández et al. (2017) using indoor measurements under controlled environment for the case of CPV modules. The outcome of this research enables the selection of the most appropriate parameter extraction method in order to compare both technologies, and therefore, contribute to the optimum selection of PV technology according to the solar resource and atmospheric conditions of the site under consideration.

2. Materials and methods

In this section, the experimental campaign and methods used to conduct this study are presented. Initially, all the instrumentation used to collect the operational, meteorological and irradiance data is described. The methodology and chosen analytical methods are then presented along with their selection criteria.

2.1. Experimental campaign

The study was carried out at the University of Jaén in Southern Spain (N 37°27′36″, W 03°28′12″) from January to December 2016. This area is non-industrialized with low to medium values of precipitable water and aerosol content. The annual global solar irradiation is greater than 2000 kW h/m^2 and the annual direct normal irradiation is around 1800 kW h/m^2. The ambient temperature ranges from approximately 5 °C in winter to 40 °C in summer.

Two modules were installed side-by-side on a two-axis solar tracker designed by BSQ Solar as it is presented in the upper left picture of Fig. 2. The MJ-based CPV module manufactured by Daido Co. (model DACPV-150W25) and the m-Si module manufactured by Sharp Co. (model NU-E245) are shown on the left and right side of the upper left picture in Fig. 2, respectively. The CPV module consists of 25 triple-junction lattice-matched GaInP/GaInAs/Ge solar cells interconnected in series. The primary optics are PMMA dome-shaped lenses and the secondary optics are refractive pyramids. The geometric concentration is 550× and it is cooled passively without employing any extended surfaces (i.e. heat sink) (Theristis et al., 2012). The nominal output power of the module is 150 W. The maximum recommended temperature is 80 °C (Fernández et al., 2014; Micheli et al., 2016). On the other hand, the m-Si module is formed by 60 solar cells interconnected in series with a nominal output power of 245 W.

The irradiance was monitored using a Kipp & Zonen CMP11 pyranometer for the global normal irradiance (*GNI*) and a Kipp & Zonen CHP1 pyrheliometer for the direct normal irradiance (*DNI*). A four-wire PT100 was also placed at the centre of each module's back surface to measure a representative module temperature (i.e. the T_{mod}). A weather station, installed on the site, was measuring all the relevant meteorological parameters such as the ambient temperature, wind speed and direction, and relative humidity.

In order to obtain the five parameters of the single-diode model, a characterisation system consisting of an open platform was employed according to the schematic diagram exhibited in Fig. 2 (Montes-Romero et al., 2017). The monitoring and characterisation system in the

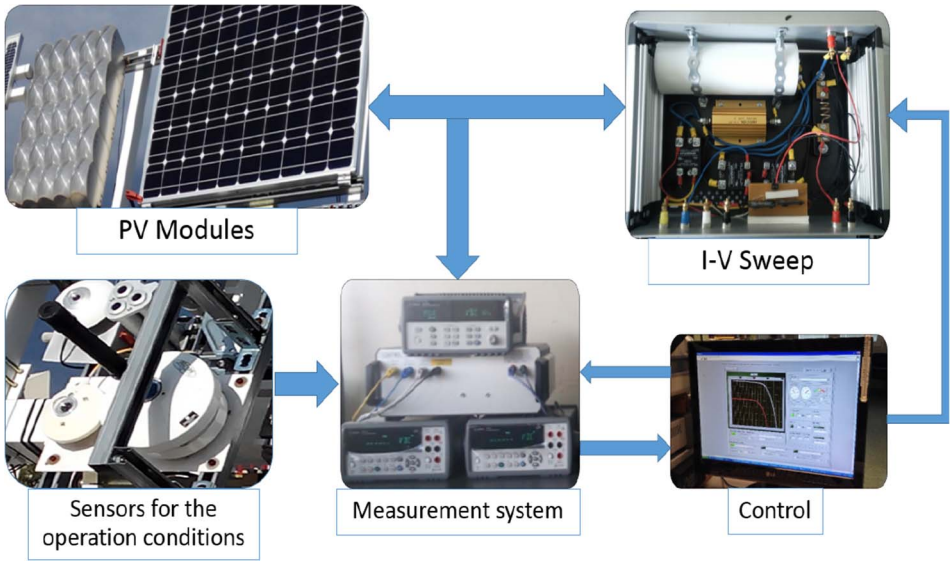

Fig. 2. Schematic diagram of the measurement system.

schematic consists of three blocks: *I-V* sweep, measurement and control. The *I-V* sweep block is an electronic system able to reproduce a variable impedance from zero to infinite in order to perform the *I-V* sweep of a PV module. This block was designed by the IDEA research group (Bertolín et al., 2012; Muñoz et al., 2014, 2011) and, amongst all the available methods (Duran et al., 2008), it is based on a capacitive load. In its features, the system is modular and scalable offering the flexibility to measure a wide range of modules. Also, the system is customizable to the specific requirements or conditions of the application. In this case, a sequential measurement of up to four modules was carried out by this system.

The measurement block includes specific instrumentation with the corresponding calibration certificates which delimit the errors associated with the measurement and allow a periodic calibration by the manufacturer. This block is composed of two Agilent 34411A multimeters that recorded the *I-V* pairs obtained during the *I-V* sweep and a data logger Agilent 34970A that recorded the meteorological and irradiance parameters from the sensors described above. As presented in Fig. 3, voltage measurements are performed using a four-wire configuration in order to neglect any voltage drops that can occur by connection resistances such as wires, connectors, and switches. The current measurements are obtained through a shunt resistor, where a voltage drop is produced as a function of the current that passes through this element.

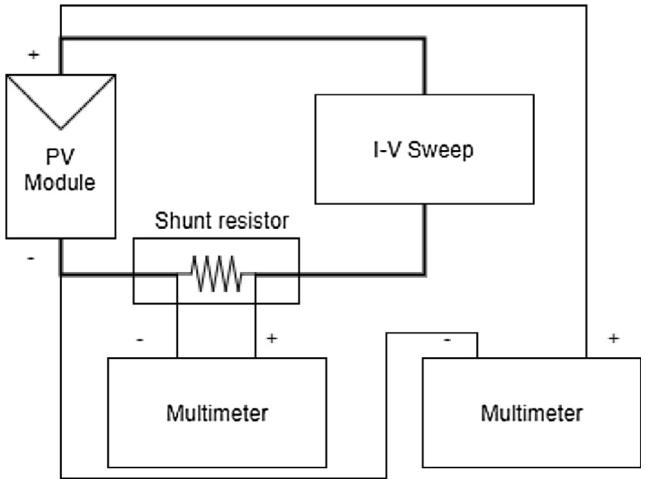

Fig. 3. Wiring diagram of the *I-V* tracing part of the system.

The control block carries out the control of the *I-V* sweep and the synchronization and configuration of the measurement block. The data treatment is also performed by the control block which, basically, consists of a software developed in LabVIEW. The software offers the flexibility of adding any number of sensors. It is also able to perform an automatic measurement campaign where the obtained data can be treated in real time. Another important feature is the centralisation and synchronisation. All the data are stored in the same file and the obtained parameters are synchronized with the sweep of the *I-V* curve. Since the system is open, it was modified in a specific way to simultaneously implement the extraction techniques on each measured *I-V* curve.

Each measurement was obtained every 5 min. To ensure quality of measurements, and since the irradiance is the most variable parameter, only the *I-V* curves with an irradiance variation lower than 1% between the first and the second *I-V* trace were recorded. It should also be noted that all sensors were within the calibration period and all sensors and modules were cleaned once a week.

2.2. Methodology

As mentioned in the introduction, a number of parameter extraction techniques were reported in the literature. In this study, three techniques were adapted based on: a) the capability of extracting the five parameters of the single-diode model, b) the simplicity and relatively good accuracy and c) the easiness and speed of implementation. Following these criteria, the methods of Phang et al. (1984), De Blas et al. (2002) and Khan et al. (2013) were selected.

A common procedure of these methods falls into the estimation of R_{so} and R_{sho}. These values are obtained by applying a linear fit on the *I-V* curve data close to the open-circuit voltage (0%–30% of I_{sc}) and the short-circuit current (0%–30% of V_{oc}) for the R_{so} and R_{sho}, respectively. The absolute value of the slope of the linear fit becomes the value of the corresponding parameter:

$$R_{so} = -\left(\frac{dV}{dI}\right)_{V=V_{oc}} \tag{2}$$

$$R_{sho} = -\left(\frac{dV}{dI}\right)_{I=I_{sc}} \tag{3}$$

2.2.1. Parameter extraction method by Phang et al.

The first simple analytical method analysed is the one proposed by Phang et al. After applying Eqs. (2) and (3), the five parameters of Eq.

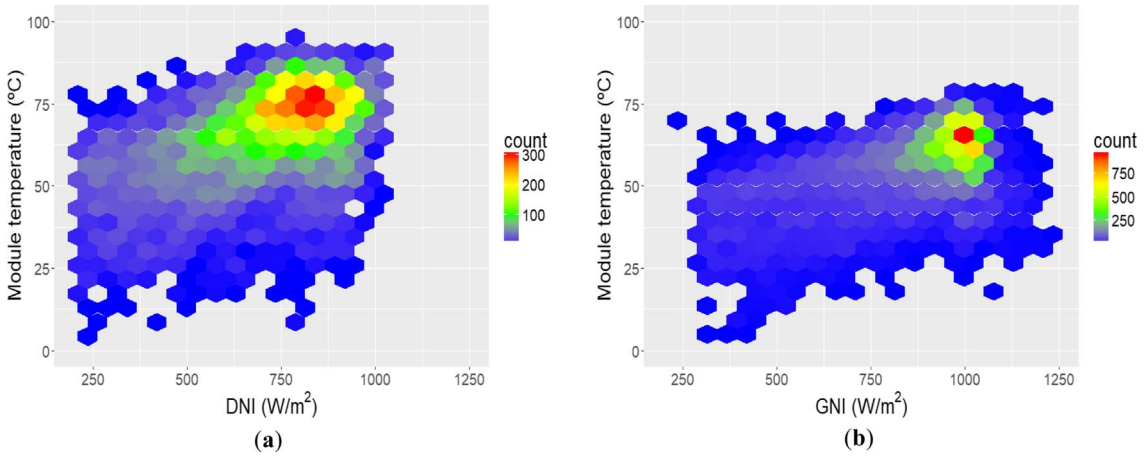

Fig. 4. Data distribution of module temperature as a function of irradiance for: (a) CPV module and (b) m-Si module.

(1) are estimated using the following expressions:

$$I_{ph} = I_{sc}\left(1 + \frac{R_s}{R_{sh}}\right) + I_0\left(\exp\left(\frac{I_{sc}R_s}{mV_T}\right) - 1\right) \tag{4}$$

$$I_0 = \left(I_{sc} - \frac{V_{oc}}{R_{sh}}\right)\exp\left(-\frac{V_{oc}}{mV_T}\right) \tag{5}$$

$$m = \frac{V_{mpp} + R_{so}I_{mpp} - V_{oc}}{V_T\left[\ln\left(I_{sc} - \frac{V_{mpp}}{R_{sh}} - I_{mpp}\right) - \ln\left(I_{sc} - \frac{V_{oc}}{R_{sh}}\right) + \frac{I_{mpp}}{I_{sc} - \frac{V_{oc}}{R_{sh}}}\right]} \tag{6}$$

$$R_s = R_{so} - \frac{mV_T}{I_0}\exp\left(-\frac{V_{oc}}{mV_T}\right) \tag{7}$$

$$R_{sh} = R_{sho} \tag{8}$$

2.2.2. Parameter extraction method by Blas et al.

The method proposed by Blas et al. is implemented using the following steps: a) set an initial R_s value, b) estimate the values of R_{sh} and m, c) recalculate R_s and repeat until the initial and recalculated values of R_s converge. Once the convergence is achieved, I_{ph}, I_0, m and R_{sh} can be calculated as follow:

$$I_{ph} = I_0\left(\exp\left(\frac{V_{oc}}{mV_T}\right) - 1\right) + \frac{V_{oc}}{R_{sh}} \tag{9}$$

$$I_0 = \left(I_{sc}\left(1 + \frac{R_s}{R_{sh}}\right) - \frac{V_{oc}}{R_{sh}}\right)\exp\left(-\frac{V_{oc}}{mV_T}\right) \tag{10}$$

$$m = \frac{V_{mpp} + R_{so}I_{mpp} - V_{oc}}{V_T \ln\left[\frac{(I_{sc} - I_{mpp})\left(1 + \frac{R_s}{R_{sh}}\right) - \frac{V_{mpp}}{R_{sh}}}{I_{sc}\left(1 + \frac{R_s}{R_{sh}}\right) - \frac{V_{oc}}{R_{sh}}}\right]} \tag{11}$$

$$R_s = \frac{R_{so}\left(\frac{V_{oc}}{mV_T} - 1\right) + R_{sho}\left(1 - \frac{I_{sc}R_{so}}{mV_T}\right)}{\frac{V_{oc} - I_{sc}R_{sho}}{mV_T}} \tag{12}$$

$$R_{sh} = R_{sho} - R_s \tag{13}$$

2.2.3. Parameter extraction method by Khan et al.

The method proposed by Khan et al. is implemented using experimental measurements of V_{oc}, I_{sc}, V_{mpp}, I_{mpp}, R_{so} and R_{sho}. The value of R_{sh} is estimated as in Phang et al. by applying Eq. (8) and the I_{ph} is calculated according to Blas et al. using Eq. (9). The remaining parameters are calculated by:

$$m = \frac{V_{mpp} + R_s I_{mpp} - V_{oc}}{V_T\left[\ln(I_{sc} - I_{mpp}) - \ln(I_{sc})\right]} \tag{14}$$

$$I_0 = \frac{mV_T}{(R_{so} - R_s)}\exp\left(-\frac{V_{oc}}{mV_T}\right) \tag{15}$$

$$R_s = R_{so} - \frac{V_{mpp} + R_{so}I_{mpp} - V_{oc}}{I_{mpp} + \left[\ln(I_{sc} - I_{mpp}) - \ln(I_{sc})\right]I_{sc}} \tag{16}$$

2.2.4. Accuracy estimation

In order to quantify the accuracy of each parameter extraction technique, different statistical indexes were used to estimate the associated errors produced by the reproduction of the *I-V* curve. In this sense, the normalised root mean square error ($NRMSE_{IV}$) and mean bias error (MBE_{IV}) were obtained as in (Rodrigo et al., 2015) using the following equations:

$$NRMSE_{IV} = \sqrt{\frac{1}{N}\sum_{i=1}^{N}\left(\frac{I_{modelled}(V)_i - I_{measured}(V)_i}{I_{sc,measured}}\right)^2} \tag{17}$$

$$MBE_{IV} = \frac{1}{N}\sum_{i=1}^{N}\left(\frac{I_{modelled}(V)_i - I_{measured}(V)_i}{I_{sc,measured}}\right) \tag{18}$$

where N is the number of samples on the curve taken at small voltage steps and $I(V)$ is the current at voltage V for both modelled and measured data. In order to obtain the error tendencies in relation to the irradiance, an average filter was implemented to the error data set. The average filter took all the data in small intervals: 50 W/m^2 for irradiance, 5 °C for temperature and 0.5 for *AM*; the data within the ranges were averaged. As such, the data dispersion was removed and the relationships between the parameters could be observed.

3. Results

The frequency distribution of module temperature as a function of irradiance is presented for a) the MJ-based CPV and b) the m-Si technology, in Fig. 4a and b respectively. It can be seen that the most common conditions for CPV can be found at approximately 750 W/m^2 and 75 °C. On the other hand, it is clear that the m-Si module operates at lower temperatures compared to the CPV with around 60 °C at 1000 W/m^2. Similarly, the data distribution of *AM* –calculated through Eq. (19)-against irradiance is presented in Fig. 5a and b for CPV and m-Si modules respectively where the majority of data points fall within *AM* values of around 1.25.

$$AM = \frac{1}{\cos(\theta) + 0.50572(96.07995 - \theta)^{-1.6364}} \tag{19}$$

where θ is the zenith angle.

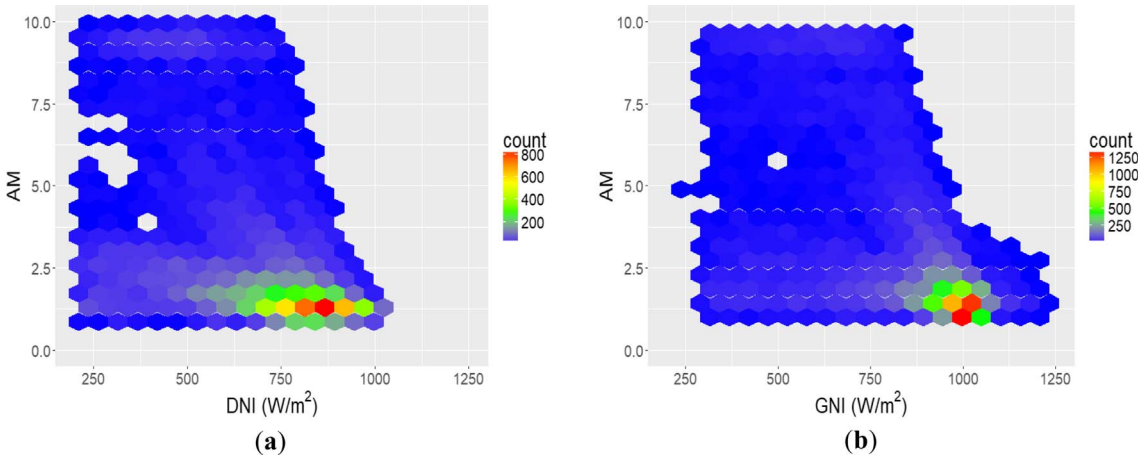

Fig. 5. Data distribution of air mass as a function irradiance for: (a) CPV module and (b) m-Si module.

3.1. Analysis of errors on the I-V curves

Initially, the obtained error in the reproduction of the complete *I-V* curve for both modules is analysed using the complete dataset. As can be seen in Figs. 6a and 7a, the $NRMSE_{IV}$ values are significantly lower for the m-Si module compared to the CPV module with average $NRMSE_{IV}$ differences between both modules of 0.01%, 2.76% and 1.59% for Phang et al., Khan et al. and Blas et al. respectively. These figures also show that the less dispersed data and hence the most stable method can be considered to be the one proposed by Phang et al. for CPV and Blas et al. for m-Si. These dispersion results coincide with the minimum average errors for those methods in their respective technologies. It is also interesting to highlight that the method proposed by Phang et al. provides similar $NRMSE_{IV}$ values for the two modules analysed. In terms of the MBE_{IV}, it can be pointed out that all three methods underestimate the *I-V* curve of the m-Si module practically in any case. For the CPV module two cases can be found; while the Khan et al. method tends to underestimate the *I-V* curve in all cases, the other two methods tend to overestimate it for irradiance levels lower than 500 W/m^2 and underestimate it for irradiance levels above that. It is interesting to notice that the Phang et al. method provides similar results for both modules. The obtained results show that the most accurate method for m-Si is the Blas et al. method with an average $NRMSE_{IV}$ of 0.58% and an MBE_{IV} of −0.27%. In the case of CPV the minimum average error of 1.55% was found using the Phang et al. method.

In order to investigate the performance of each method, the $NRMSE_{IV}$ was plotted against the main parameters that affect the output of any PV device (i.e. irradiance, temperature and *AM*). The results are shown in Figs. 8–10 for irradiance, temperature and *AM* respectively. Fig. 8a and b shows the $NRMSE_{IV}$ of the three methods versus the irradiance, for the CPV and m-Si respectively. In the case of the CPV module, (i.e. Fig. 8a), it can be observed that the Phang et al. method provides the best results with a relatively constant behaviour and values ranging from 1.48% to 1.92%. The other two methods exhibit a similar behaviour with a tendency to increase the $NRMSE_{IV}$ with irradiance. It is also shown that the Khan et al. method is the worst performing technique with $NRMSE_{IV}$ values ranging from 3.32% to 5.38%. In the case of the Blas et al. method, a slight decrement can be observed in the range of 200 W/m^2–500 W/m^2 (with a minimum $NRMSE_{IV}$ value of 1.52%) whereas it increases with higher irradiance to reach its maximum value at 2.95%. On the other hand, the $NRMSE_{IV}$ versus the irradiance plot of the m-Si module (i.e. Fig. 8b) shows that the Blas et al. method provides the best results, with $NRMSE_{IV}$ values around 0.75% at irradiance levels above 700 W/m^2, reaching a maximum of 1.35% at around 400 W/m^2. The other two methods show similar trends where the $NRMSE_{IV}$ values decrease until a certain irradiance level (400 W/m^2 for Phang et al. method and 500 W/m^2 for Khan et al. method); a steady state is achieved at higher irradiance levels. As in CPV, the Khan et al. method exhibits the highest errors with values ranging from 1.55% to 3.20% while the Phang et al. method falls within 2.20%. It is interesting to highlight, again, that the Phang et al. method tends to give similar results for the two modules under study.

Similar to the irradiance, the performance of the methods was also examined against the module temperatures. In the case of the CPV

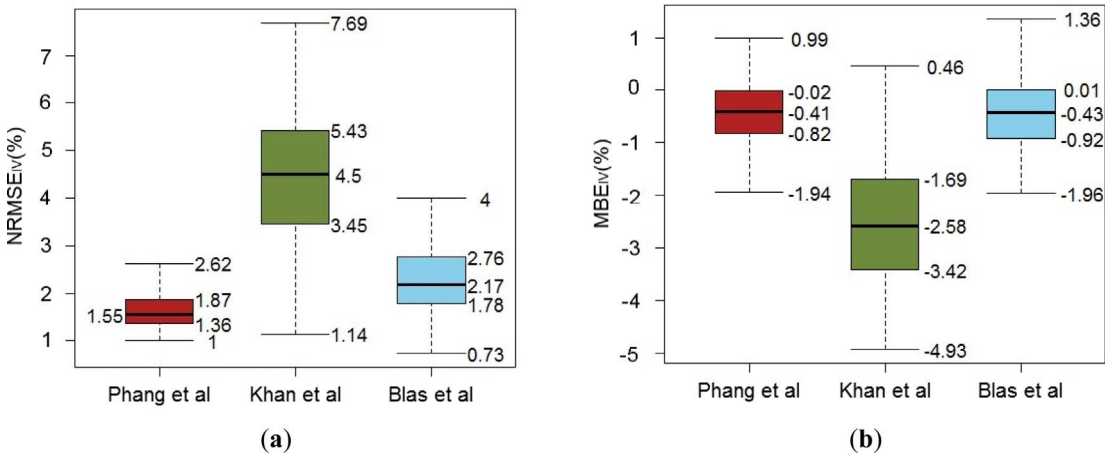

Fig. 6. (a) $NRMSE_{IV}$ and (b) MBE_{IV} dispersion for the complete dataset of CPV.

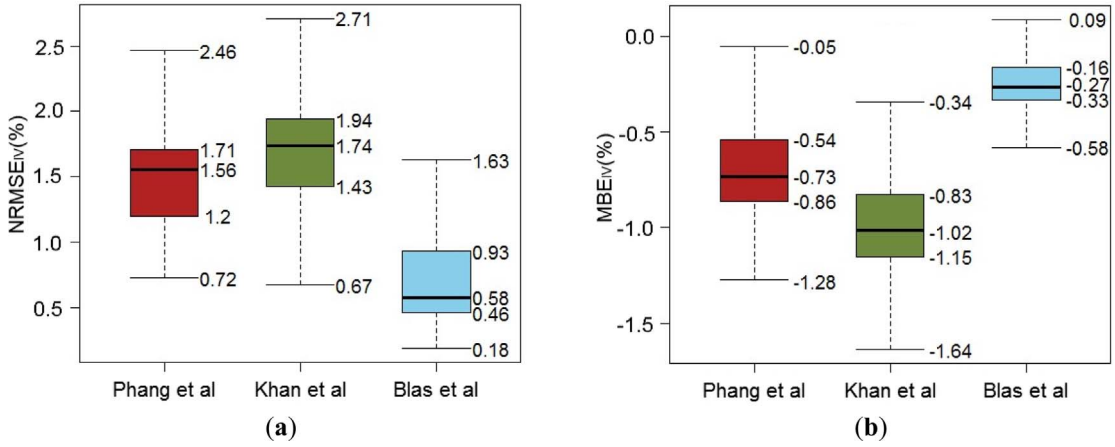

Fig. 7. (a) $NRMSE_{IV}$ and (b) MBE_{IV} dispersion for the complete dataset of m-Si.

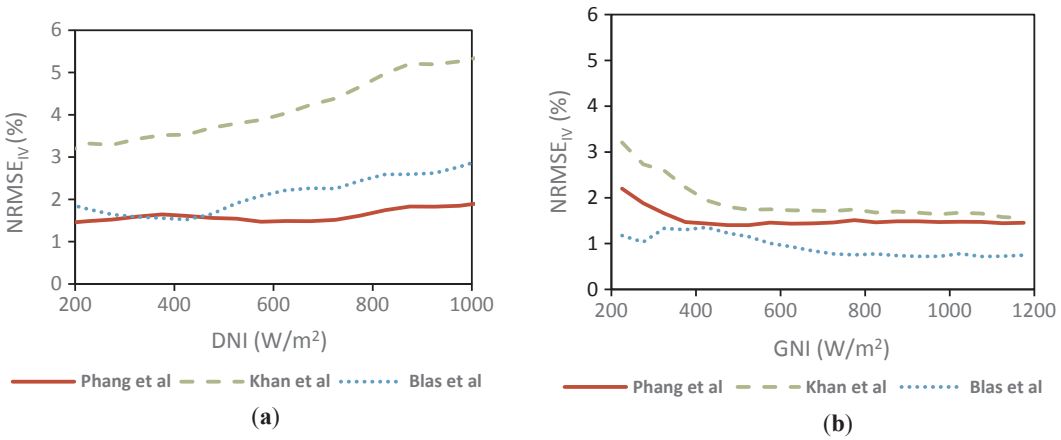

Fig. 8. $NRMSE_{IV}$ values in comparison with irradiance for: (a) CPV module; (b) m-Si module.

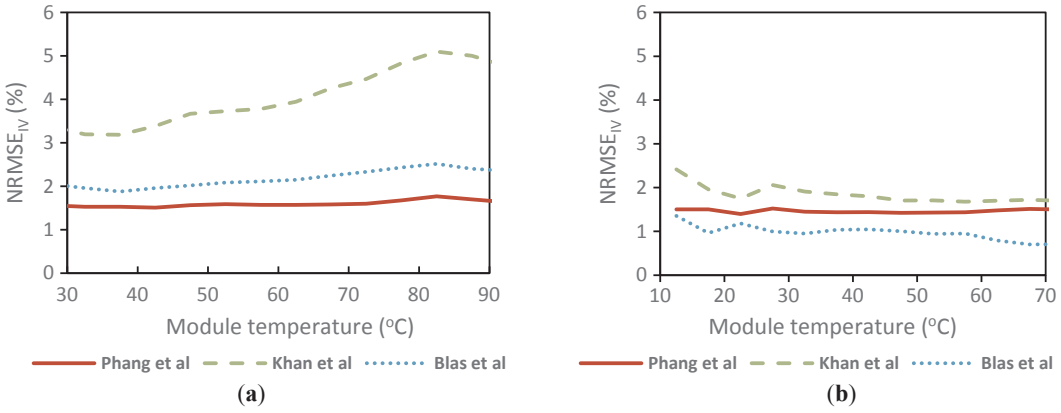

Fig. 9. $NRMSE_{IV}$ values in comparison with module temperature for: (a) CPV module; (b) m-Si module.

module (see Fig. 9a), the Phang et al. method seems to have a relatively negligible change with increasing temperature ($NRMSE_{IV}$ around 1.55%) whereas the other two methods exhibit a relatively similar behaviour where the trends seem to increase until 80 °C. This trend is more pronounced in the Khan et al. method, which presents the highest $NRMSE_{IV}$ values ranging from 3.18 to 5.10%. In Fig. 9b the same approach is illustrated for m-Si. The Phang et al. method exhibits, again, a relatively negligible behaviour with temperature ($NRMSE_{IV}$ values around 1.5%). The other methods present a similar behaviour with higher $NRMSE_{IV}$ values at lower temperatures. In this sense, a decrement of 0.65% is achieved by the *Blas* et al. method along the temperature range whereas Khan et al. method decreases by a 0.63% absolute. Similarly to the case of irradiance, it is interesting to notice that the Phang et al. method tends to give similar results for both the CPV and m-Si modules.

Finally, Fig. 10a and b show the $NRMSE_{IV}$ of the three methods versus the *AM* for the CPV and the m-Si modules, respectively. In the case of the CPV module (Fig. 10a), unclear trends are observed for the Khan et al. and Blas et al. methods, while the Phang et al. method exhibits an almost constant behaviour. The worst performing method (Khan et al.), presents $NRMSE_{IV}$ values ranging from 3.65% to 4.66%. The best results are obtained by the Phang et al. method with $NRMSE_{IV}$

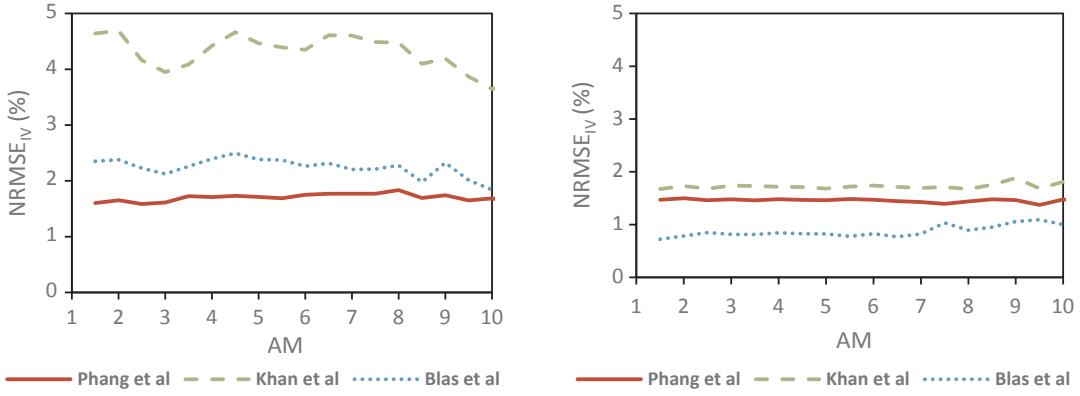

Fig. 10. $NRMSE_{IV}$ values in comparison with air mass for: (a) CPV module; (b) m-Si module.

values around 1.7% for all *AM* values. At last, the $NRMSE_{IV}$ values for the Blas et al. method are in the range of 1.84% to 2.5%. In the case of the m-Si module (Fig. 10b), all methods exhibit a relatively constant behaviour for *AM* values up to around 5. The highest errors are observed for the Khan et al. method with $NRMSE_{IV}$ values ranging from 1.63% to 1.88%. On the other hand, the best results are given by the Blas et al. method with $NRMSE_{IV}$ values in the range of 0.72%–1.09%. Furthermore, the $NRMSE_{IV}$ values for the Phang et al. method are around 1.45% for all *AM* values. Similarly to our previous investigations against irradiance and temperature, the Phang et al. method tends to give similar results for both modules.

To summarise, it can be concluded that the error analysis points out that the highest quality extraction method for the CPV module is the one proposed by Phang et al. with an average $NRMSE_{IV}$ value of 1.55% and an average MBE_{IV} value of −0.41%. This method also achieved the lowest error dispersion when the results of the two modules were compared. For the m-Si module, the best method is the one proposed by Blas et al. with an average $NRMSE_{IV}$ and MBE_{IV} of 0.58% and −0.27% respectively. In this case, the data dispersion are similar for all methods. Generally, taking into account both modules, the Khan et al. method proved to be the least robust method with more notorious errors in the case of the CPV module.

The analysis of the $NRMSE_{IV}$ in relation with irradiance and module temperature showed that, in the case of the CPV module, all methods exhibited a tendency to increase with irradiance and temperature. In the case of m-Si technology, the opposite trend can be observed where the $NRMSE_{IV}$ values decrease with irradiance and module temperature. The error follows the same principle to CPV, in the case of *AM*, but the values are significantly less affected. This could be attributed to the large temperature gradient between the cell and the backplate of the CPV module (Theristis et al., 2017b), where the temperature sensor is located. The gradient becomes greater with increasing irradiance levels and the thermal resistance follows an approximately linear behaviour (Fernández et al., 2014) and may contribute to the higher errors found for the CPV models; this is because the thermal resistance of CPV modules is greater than the one of PV modules.

3.2. Impact of irradiance on the five parameters of the single-diode model

In this section, the extracted parameters are analysed in order to observe their dependence on irradiance since this parameter is, by far, the dominant magnitude affecting the performance of solar systems. By applying the average filter, discussed in Section 2, the tendencies of the parameters in relation with the irradiance are analysed. It should be noted that the parameters are discussed on the single-cell level by means of the following expressions:

$$I_{ph,c} = \frac{I_{ph}}{N_P} \tag{20}$$

$$I_{o,c} = \frac{I_o}{N_P} \tag{21}$$

$$m_c = \frac{m}{N_s} \tag{22}$$

$$R_{s,c} = \frac{R_s}{N_s} \tag{23}$$

$$R_{sh,c} = \frac{R_{sh}}{N_P} \tag{24}$$

where the subscript "*c*" refers to the values at cell level, while N_s and N_p is the number of cells connected in series and parallel respectively. In this work, the CPV module consists of 25 series connected (i.e. $N_s = 25$, $N_p = 1$) solar cells while the m-Si consists of 60 solar cells connected in series (i.e. $N_s = 60$, $N_p = 1$). The use of normalized values is more appropriate since it allows the direct comparison of the SEM's extracted parameters. It is also important to mention that these equations assume that all the solar cells within a module have identical electrical characteristics, but also same (i.e. uniform) incident irradiance and temperature. Therefore, all the cells will perform with the same behaviour and the voltage and current will increase depending on the number of series and parallel cells respectively.

The evolution of the parameters in respect to irradiance can be observed in Figs. 11 and 12 for the CPV and m-Si modules respectively. The behaviour of $R_{sh,c}$ and $I_{ph,c}$ are practically the same for all methods, therefore, no differences can be found between them.

In the case of the CPV module, Fig. 11a shows the evolution of the series resistance with irradiance where the tendency is similar in the three methods. Values obtained with the Khan et al. method are constantly lower compared to the other two methods. For irradiance levels greater than 600 W/m^2 the $R_{s,c}$ values tend to stabilise whereas at values lower than 600 W/m^2, a high slope is observed. Fig. 11b shows that the $R_{sh,c}$ decreases with increasing irradiance as a power function. In terms of the *m* parameter (see Fig. 11c), the behaviour of Phang et al. and Khan et al. methods is relatively similar: at around 500 W/m^2 of irradiance, a positive slope splits the values until around 700 W/m^2 where the Khan et al. becomes relatively constant and the Phang et al. decreases almost linearly. Using the Blas et al. method, the *m* parameter has a slight trend to decrease with irradiance. The logarithm of $I_{0,c}$ in Fig. 11d, shows that the behaviour of this parameter is analogous to the m_c parameter. As expected, the last parameter analysed, $I_{ph,c}$, increases linearly with irradiance in all methods (see Fig. 11e).

In the case of the m-Si module, the differences between all the parameter extraction techniques are significantly lower, compared to

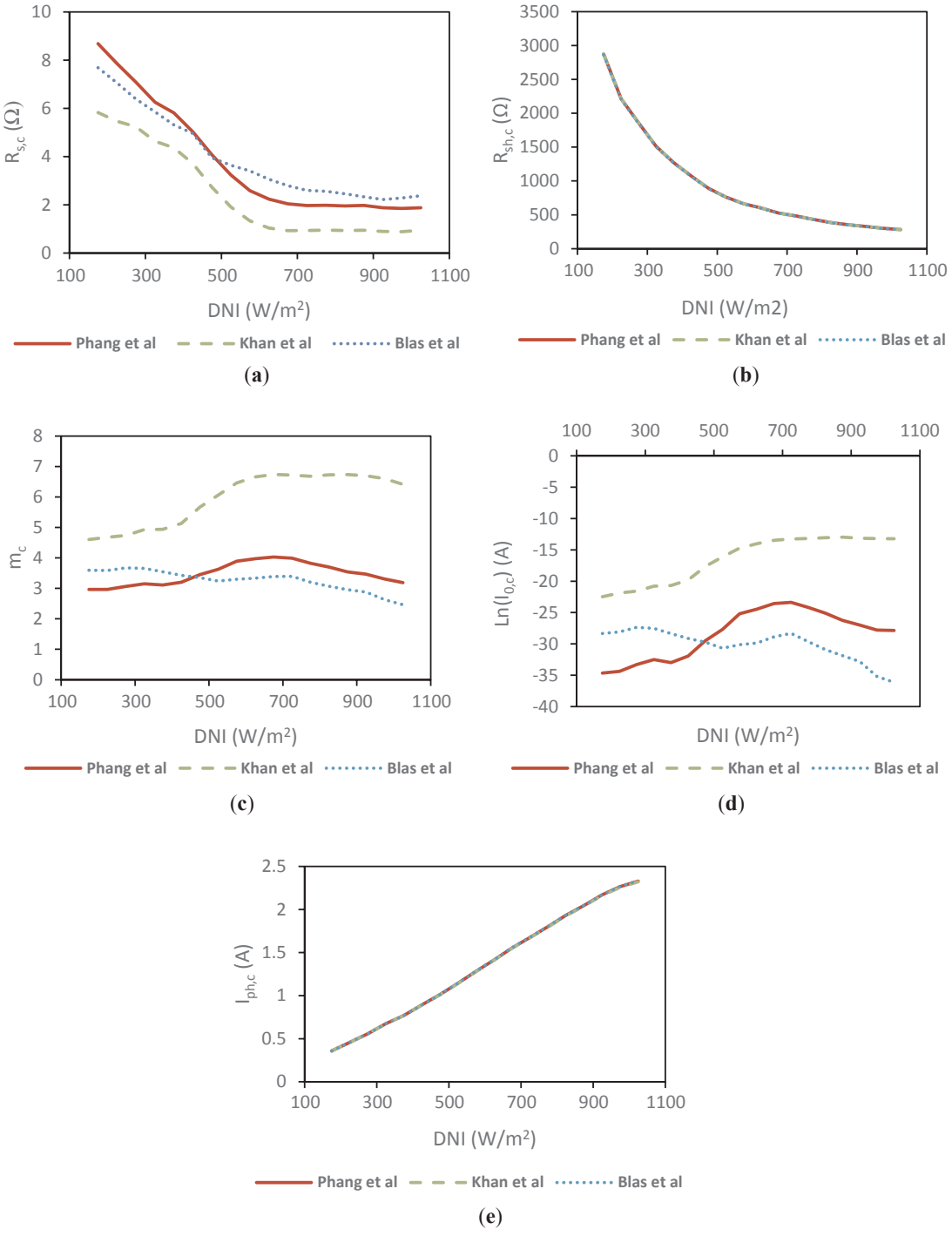

Fig. 11. Influence of direct normal irradiance on the extracted parameters of the CPV module using all the investigated methods.

the CPV module. Qualitatively speaking, the behaviour of all the parameters can be considered similar for the three methods. In Fig. 12a, the $R_{s,c}$ values tend to be constant above 500 W/m^2 and a growing slope is found below this irradiance value. The tendency of $R_{sh,c}$ is relatively similar to the CPV, but the values are considerably lower for the m-Si module as it is shown in Fig. 12b. The m values, in Fig. 12c, have almost a constant behaviour for irradiance above 400 W/m^2 with a reduced value at lower irradiances. Similar to the CPV module, Fig. 12d shows that the trends of $I_{0,c}$'s logarithm and m_c are comparable. Finally, as expected, the $I_{ph,c}$ increases linearly with irradiance for all methods as it is presented in Fig. 12e.

3.3. Modelling the five extracted parameters of the single-diode model with irradiance

The dependence of the five extracted parameters on irradiance was analysed in the previous subsection. In this subsection, analytical equations that predict the *I-V* parameters of both modules as a function of irradiance are introduced. In order to obtain the equations that fit the behaviour of each extracted parameter, the Phang et al. method was used. This method proved to be the most robust achieving lower errors and data dispersion. Moreover, the average $NRMSE_{IV}$ differences between the two PV modules was 0.01%. The equations were obtained without applying any filter and, therefore, the complete dataset was

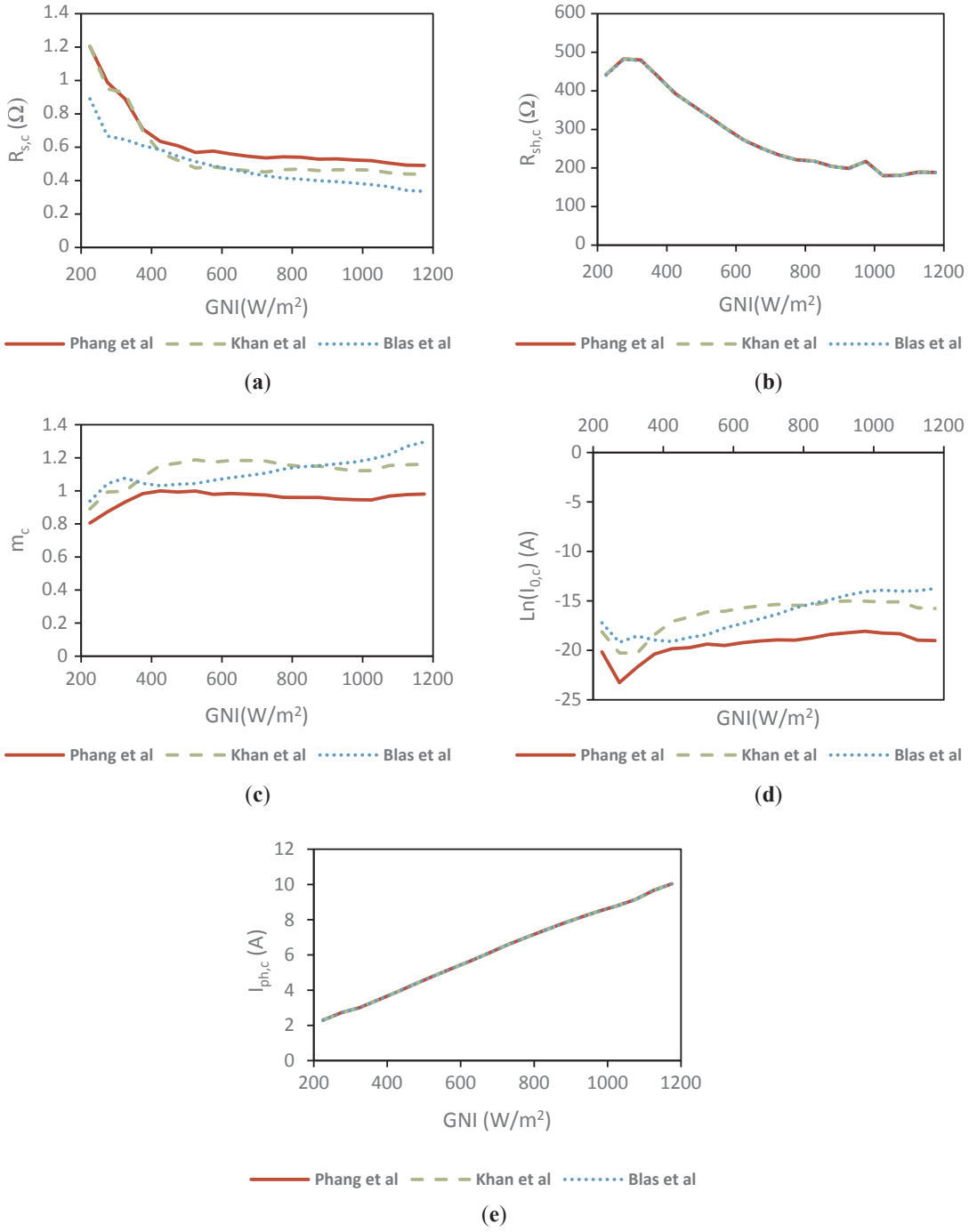

Fig. 12. Influence of global normal irradiance on the extracted parameters of the m-Si module using all the investigated methods.

used. As such, the scatter shown in the figures could be attributed to other parameters such as temperature and spectrum variations. Dealing with these effects should be the topic of future research activities. With the purpose of limiting the error, the *NRMSE* and *MBE* equations proposed in (Fernández and Almonacid, 2015) were used as criteria.

In Figs. 13 and 14, the five extracted parameters are presented as a function of irradiance for the CPV and m-Si modules respectively. A similar behaviour was observed for both modules and therefore, the same type of fitting equations could be applied. In the case of $R_{s,c}$ (see Figs. 13a and 14a), two possible equations were analysed, hence, both logarithmic and power fitting functions could be used to obtain its tendency. The $R_{sh,c}$ exhibited a power function behaviour and $I_{ph,c}$ can be considered linear. The remaining parameters (i.e. m_c and $I_{o,c}$) did not exhibit any trends and the close to zero R^2 proved that irradiance has a negligible effect on them.

The $R_{s,c}$ data of the CPV module presented in Fig. 13, point out that the series resistance fits as a power function and appears to have a better adjustment at higher irradiance, an underestimation between 200 W/m^2 and 500 W/m^2 and an overestimation at values below 200 W/m^2. On the other hand, the logarithmic function fits the data well at lower irradiances but slightly worse for high irradiances. In order to quantify the differences, the logarithmic function performed better exhibiting lower errors (*NRMSE* of −4.22% and *MBE* of 0.01%) compared to the 8.54% of the power function (*NRMSE* of 8.54% and *MBE* of 0.25%). In respect to the power fitting of $R_{sh,c}$, no significant differences were found along the irradiance values. As a result, the

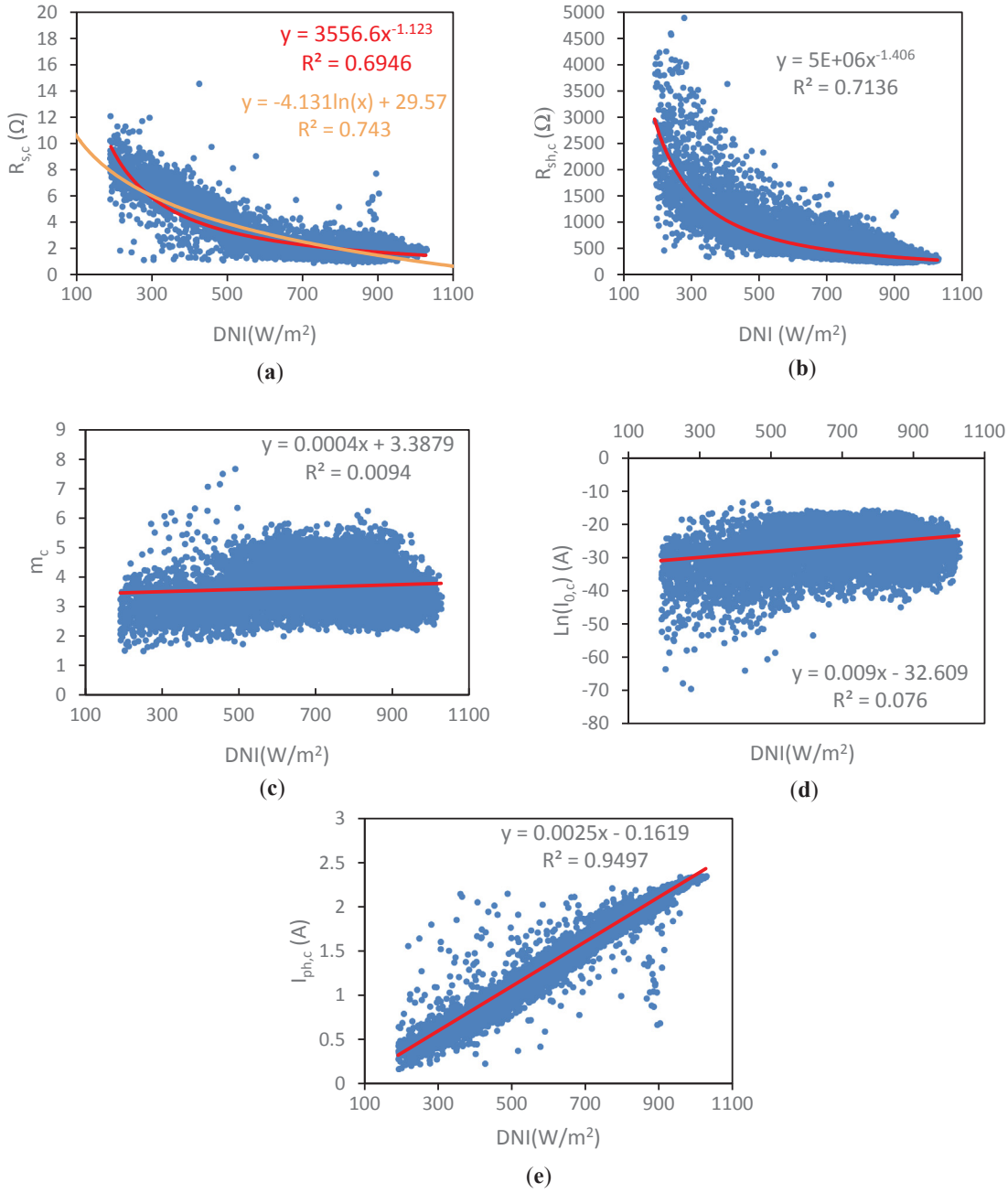

Fig. 13. Data of each parameter of the CPV module obtained by the Phang et al. method as a function of irradiance. The fitting functions are also shown.

power function reached a *NRMSE* and *MBE* value of 3.79% and −0.4% respectively. The m_c parameter showed a relatively constant value. Therefore, this parameter could be considered as a constant value of 3.39 which is relatively close to the value recommended in the IEC 62670-3 for triple-junction solar cells. Due to the scattered behaviour of this parameter, the *NRMSE* reached the highest value of 11.73% among the remaining parameters and the *MBE* was −0.35%. The logarithm of the saturation current ($I_{0,c}$) exhibited a similar behaviour to the m parameter with an almost constant value of −32.61 A. The *NRMSE* and *MBE* values reached 10.12% and −0.002% respectively. Finally, the $I_{ph,c}$ value increases linearly with the irradiance. A *NRMSE* value of 0.12% was obtained for this parameter and a *MBE* of 1.06%, which indicates that this parameter tends to be overestimated using this fitting. A summary of all errors for the CPV module is given in Table 1.

In the case of the m-Si module, similar fitting functions were found and the associated errors are presented in Table 2. The $R_{s,c}$ exhibited a logarithmic and power fit behaviour similar to the CPV case (see Fig. 14a). The *NRMSE* of the fitting functions were 5.93% and 5.96% for the logarithmic and power functions, respectively. The *MBE* value was found to be −0.05% (logarithmic function) and −0.54% (power function). The power fit of the $R_{sh,c}$ exhibited a higher *NRMSE* (7.46%) compared to the CPV module (3.79%) whereas the *MBE* was -0.62%. In respect to m_c, a constant value of 1.01 was found for a *NRMSE* of 11.53% which is comparable to the error found in CPV (11.73%). The constant value of m_c agrees with the assumption used in literature, for silicon solar cells. The logarithm of $I_{0,c}$ has a similar behaviour to the one extracted from the CPV module. A constant value of −21.44 A was found corresponding to a *NRMSE* and *MBE* of 8.09% and 0.01% respectively. Finally, the $I_{ph,c}$ whose behaviour is linear exhibited a *NRMSE* and *MBE* of 2.65% and −0.37% respectively. Although the *MBE* values, in general, can point out either underestimation or overestimation of a prediction, it was found that for both the CPV and m-Si

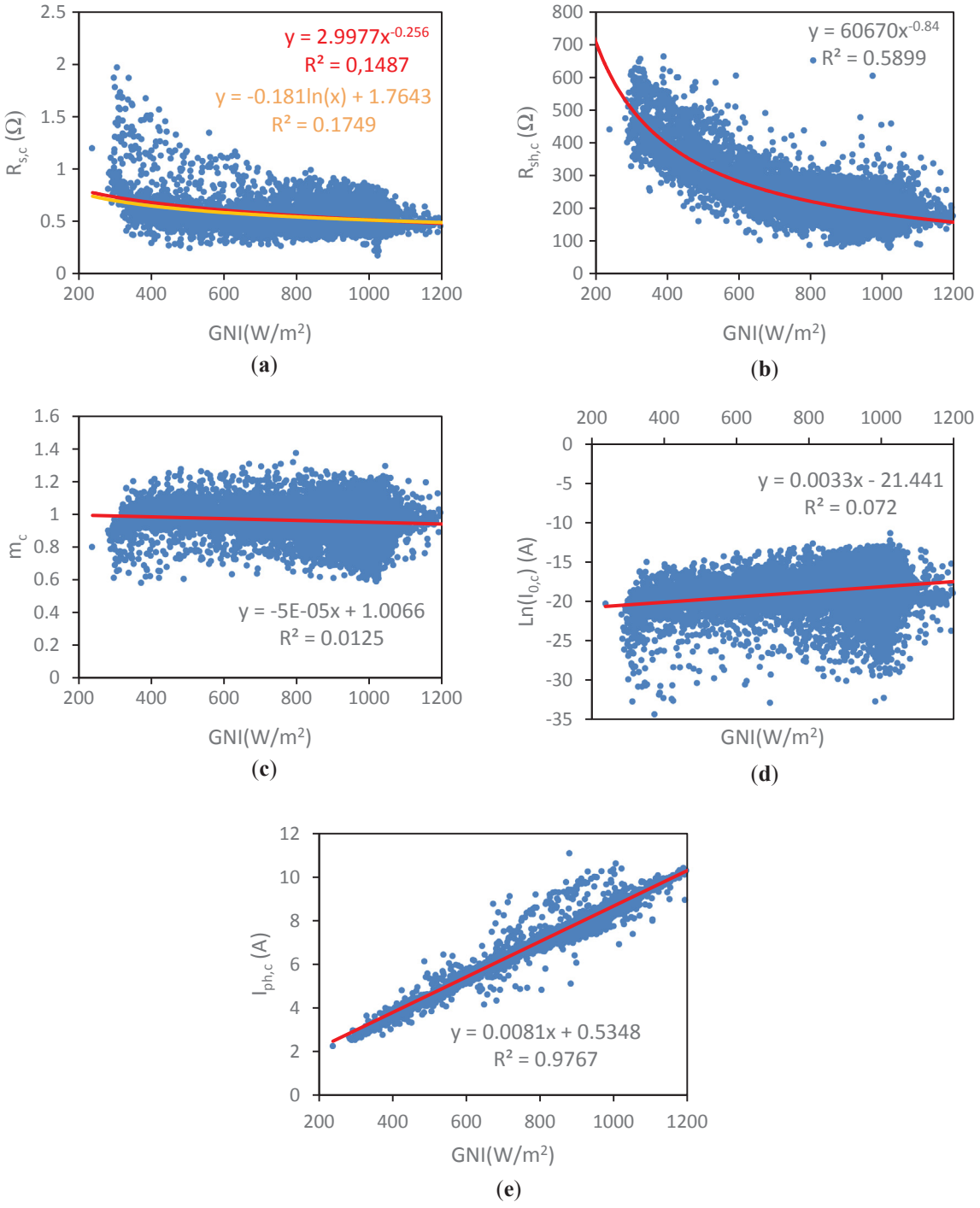

Fig. 14. Data of each parameter of the m-Si module obtained by the Phang et al. method as a function of irradiance. The fitting functions are also shown.

Table 1
NRMSE and *MBE* values obtained for each parameter of the CPV module.

Parameter	*NRMSE*	*MBE*
$R_{s,c}$ (logarithmic fit)	4.23%	0.007%
$R_{s,c}$ (power fit)	8.54%	−0.25%
$R_{sh,c}$	3.79%	0.40%
m_c	11.73%	−0.35%
$I_{0,c}$	10.12%	−0.002%
$I_{ph,c}$	0.12%	1.06%

Table 2
NRMSE and *MBE* values obtained for each parameter of the CPV module.

Parameter	*NRMSE*	*MBE*
$R_{s,c}$ (logarithmic fit)	5.93%	−0.05%
$R_{s,c}$ (power fit)	5.96%	−0.54%
$R_{sh,c}$	7.46%	−0.62%
m_c	11.53%	0.55%
$I_{0,c}$	8.09%	0.007%
$I_{ph,c}$	2.65%	−0.37%

modules, the *MBE* values of all the parameters (except $I_{ph,c}$ of CPV) were near zero; this can allow the conclusion that for the majority of the parameters, the fitting equations neither overestimate nor underestimate the predicted parameter except in the case of the CPV's $I_{ph,c}$ where an overestimation of 1.06% was observed.

Overall, the equations proposed could be considered as a first step towards an analytical approach for the prediction of the SEM's parameters as a function of the most relevant factors. However, the prediction errors of some of the parameters are probably not acceptable in practice. This is clear when analyzing the prediction errors of m and I_0 for both modules. Indeed, the small slopes of these magnitudes clearly suggest that these parameters show an almost negligible dependence on irradiance. As a result of this study, it can could be considered that, although the irradiance is the main driver of the PV technology, the impact of other parameters such as the temperature and spectral conditions (Rodrigo et al., 2017; Stark and Theristis, 2015; Theristis et al., 2017a, 2016) should be taken into account in order to accurately estimate the SEM's parameters.

As a summary of this section and in respect to the $I_{ph,c}$ of MJ solar cells, the linear behaviour was expected (Kinsey et al., 2008), although the parameter could be also affected by intrinsic mismatches between the different receivers (Vorster and Van Dyk, 2005). These expectations were cross-checked in the obtained results. The values of $\ln(I_{0,c})$ and m can provide information about the rate and type of recombination mechanism that occurs within the solar cells (i.e. Radiative, Auger and Shockley-Read-Hall) (Nelson, 2014). Hence, they were expected to be influenced by the incident irradiance since it affects the injection level. In the results, these values presented a similar behaviour however, not a significant relationship with irradiance was found. In CPV, an increment of these values was observed for irradiance values greater than 500 W/m^2, although in the case of the m-Si module, the value was constant along the irradiance values. The $R_{s,c}$ parameter of a solar cell is mainly determined by the corresponding resistance of the semiconductor layers, the front metal grid resistance, the metallic contact resistance (Vossier et al., 2012) and also the resistance of the wires of the modules. The $R_{s,c}$ and $R_{sh,c}$ tend to decrease with irradiance intensity. This tendency can be understood by considering the increase of the conductivity of the semiconductor layers with the number of charge carriers, and therefore with the input irradiance (Grundmann, 2010), as well as the higher shunt leakage current as a function of the growing irradiance (Khan et al., 2014). As expected, these parameters increase their values substantially at lower irradiance levels.

Finally, fitting equations for each parameter, were introduced. The Phang et al. method was selected for this task due to its minimum difference between both technologies and the quality of results for the CPV module. The series resistance presents a logarithmic function with a *NRMSE* value of 4.23% and 5.93% for CPV and m-Si modules respectively. The shunt resistance fits as a power function with a *NRMSE* of 3.79% and 7.46% for these technologies. The photo-generated current clearly showed a linear behaviour with a *NRMSE* of 0.12% for m-Si and 2.65% for CPV. The rest of the parameters (m_c and $I_{o,c}$) did not show any trends with irradiance at neither of the investigated technologies. The error values increase for m_c and $I_{o,c}$, but reach their minimum for the $I_{ph,c}$.

4. Conclusions

Three methods for the extraction of the five parameters of the single exponential model of a concentrator photovoltaic module were analysed in this work. These methods aimed to achieve simple and quality analytical solutions for the extraction of the five parameters of photovoltaic devices. The methods analysed were the ones from: a) Phang et al., b) Blas et al. and c) Khan et al. The parameters were obtained for two different photovoltaic technologies: a multi-junction concentrator photovoltaic module and a monocrystalline silicon module, in order to compare the performance of all methods.

The results indicated that the most robust and less dispersed method is the one proposed by Phang et al. for the CPV module and the one proposed by Blas et al. for the m-Si module. These two methods exhibited a low error for both technologies. The method of Khan et al. reached the highest error values at every case while the Phang et al. method exhibited a similar error for both technologies.

The *RMSE* results obtained by each parameter were also studied in relation to three parameters: irradiance, module temperature and air mass. Similar tendencies were obtained by each method for their respective technology. Moreover, fitting functions and their equations were proposed in order to model the behaviour of the five extracted parameters in relation to irradiance. This analysis was performed for the Phang et al. method due to the lower error differences for both technologies. The fitting functions pointed out that the series resistance ($R_{s,c}$) follows a logarithmic function, shunt resistance ($R_{sh,c}$) fits with a power function and the photo-generated current ($I_{ph,c}$) follows a linear function; the remaining parameters (i.e. ideality factor and saturation current) did not exhibit any trends. Although the constant values of ideality factor were relatively close to the assumptions reported in literature, this parameter along with the saturation current demonstrated the highest error values of their respective fitting functions. As expected, the photo-generated current exhibited the lowest error values.

Future work should allow an in-depth study of the parameter extraction techniques as a function of temperature and air mass. To perform this, filters must be applied to the data in order to seek a relationship between the investigated parameters.

Acknowledgments

Eduardo F. Fernández acknowledges the Spanish Ministry of Economy and Competitiveness for the Juan de la Cierva – Incorporación 2015 fellowship. The authors also thank the Spanish Ministry of Economy and Competitiveness and FEDER funds for the project ENE2016-78251-R and the "Plan de Apoyo a la Investigación de la Universidad de Jaén y la Caja Rural de Jaén" (UJA2015/07/01).

References

Almonacid, F., Fernández, E.F., Mallick, T.K., Pérez-Higueras, P.J., 2015. High concentrator photovoltaic module simulation by neuronal networks using spectrally corrected direct normal irradiance and cell temperature. Energy 84, 336–343. http://dx.doi.org/10.1016/j.energy.2015.02.105.

Almonacid, F., Rodrigo, P., Fernández, E.F., 2016. Determination of the current-voltage characteristics of concentrator systems by using different adapted conventional techniques. Energy 101, 146–160. http://dx.doi.org/10.1016/j.energy.2016.01.082.

Appelbaum, J., Peled, A., 2014. Parameters extraction of solar cells? A comparative examination of three methods. Sol. Energy Mater. Sol. Cells 122, 164–173. http://dx.doi.org/10.1016/j.solmat.2013.11.011.

Ben Or, A., Appelbaum, J., 2013. Estimation of multi-junction solar cell parameters. Prog. Photovoltaics Res. Appl. 21, 713–723. http://dx.doi.org/10.1002/pip.2158.

Bertolín, J.C., Fuentes, M., Muñoz, J.V., Casa, J.de la, 2012. Applications of DC/DC converters for obtaining characteristic curves of PV generators. In: 27th European Photovoltaic Solar Energy Conference. Frankfurt, http://dx.doi.org/10.1017/CBO9781107415324.004.

Celik, A.N., Acikgoz, N., 2007. Modelling and experimental verification of the operating current of mono-crystalline photovoltaic modules using four- and five-parameter models. Appl. Energy 84, 1–15. http://dx.doi.org/10.1016/j.apenergy.2006.04.007.

Chan, D.S.H., Phillips, J.R., Phang, J.C.H., 1986. A comparative study of extraction methods for solar cell model parameters. Solid State Electron. 29, 329–337. http://dx.doi.org/10.1016/0038-1101(86)90212-1.

Chegaar, M., Azzouzi, G., Mialhe, P., 2006. Simple parameter extraction method for illuminated solar cells. Solid State Electron. 50, 1234–1237. http://dx.doi.org/10.1016/j.sse.2006.05.020.

Ciulla, G., Lo Brano, V., Di Dio, V., Cipriani, G., 2014. A comparison of different one-diode models for the representation of I-V characteristic of a PV cell. Renew. Sustain. Energy Rev. 32, 684–696. http://dx.doi.org/10.1016/j.rser.2014.01.027.

Cotfas, D.T., Cotfas, P.A., Kaplanis, S., 2013. Methods to determine the dc parameters of solar cells: A critical review. Renew. Sustain. Energy Rev. 28, 588–596. http://dx.doi.org/10.1016/j.rser.2013.08.017.

De Blas, M.A., Torres, J.L., Prieto, E., García, A., 2002. Selecting a suitable model for characterizing photovoltaic devices. Renew. Energy 25, 371–380. http://dx.doi.org/10.1016/S0960-1481(01)00056-8.

Domínguez, C., Antón, I., Sala, G., 2010. Multijunction solar cell model for translating I-V characteristics as a function of irradiance, spectrum, and cell temperature. Prog.

Photovoltaics Res. Appl. 18http://dx.doi.org/10.1002/pip.965. n/a-n/a.
Duran, E., Piliougine, M., Sidrach-De-Cardona, M., Galan, J., Andujar, J.M., 2008. Different methods to obtain the I-V curve of PV modules: A review. In: Conference Record of the IEEE Photovoltaic Specialists Conference, http://dx.doi.org/10.1109/PVSC.2008.4922578.
Easwarakhanthan, T., Bottin, J., Bouhouch, I., Boutrit, C., 1986. Nonlinear minimization algorithm for determining the solar cell parameters with microcomputers. Int. J. Sol. Energy 4, 1–12. http://dx.doi.org/10.1080/01425918608909835.
Emery, K., Osterwald, C., 1987. Measurement of photovoltaic device current as a function of voltage, temperature, intensity and spectrum. Sol. Cells 21, 313–327. http://dx.doi.org/10.1016/0379-6787(87)90130-X.
Fernández, E.F., Almonacid, F., 2015. A new procedure for estimating the cell temperature of a high concentrator photovoltaic grid connected system based on atmospheric parameters. Energy Convers. Manage. 103, 1031–1039. http://dx.doi.org/10.1016/j.enconman.2015.07.034.
Fernández, E.F., Almonacid, F., Rodrigo, P., Pérez-Higueras, P., 2013a. Model for the prediction of the maximum power of a high concentrator photovoltaic module. Sol. Energy 97, 12–18. http://dx.doi.org/10.1016/j.solener.2013.07.034.
Fernández, E.F., Ferrer-Rodríguez, J.P., Almonacid, F., Pérez-Higueras, P., 2017. Current-voltage dynamics of multi-junction CPV modules under different irradiance levels. Sol. Energy 155, 39–50. http://dx.doi.org/10.1016/j.solener.2017.06.012.
Fernández, E.F., Montes-Romero, J., de la Casa, J., Rodrigo, P., Almonacid, F., 2016a. Comparative study of methods for the extraction of concentrator photovoltaic module parameters. Sol. Energy 137, 413–423. http://dx.doi.org/10.1016/j.solener.2016.08.046.
Fernández, E.F., Pérez-Higueras, P., Almonacid, F., Ruiz-Arias, J.A., Rodrigo, P., Fernandez, J.I., Luque-Heredia, I., 2015. Model for estimating the energy yield of a high concentrator photovoltaic system. Energy 87, 77–85. http://dx.doi.org/10.1016/j.energy.2015.04.095.
Fernández, E.F., Pérez-Higueras, P., Garcia Loureiro, A.J., Vidal, P.G., 2013b. Outdoor evaluation of concentrator photovoltaic systems modules from different manufacturers: First results and steps. Prog. Photovoltaics Res. Appl. 21, 693–701. http://dx.doi.org/10.1002/pip.1262.
Fernández, E.F., Rodrigo, P., Almonacid, F., Pérez-Higueras, P., 2014. A method for estimating cell temperature at the maximum power point of a HCPV module under actual operating conditions. Sol. Energy Mater. Sol. Cells 124, 159–165. http://dx.doi.org/10.1016/j.solmat.2014.01.050.
Fernández, E.F., Siefer, G., Almonacid, F., Loureiro, A.J.G., Pérez-Higueras, P., 2013. A two subcell equivalent solar cell model for III–V triple junction solar cells under spectrum and temperature variations. Sol. Energy 92, 221–229. http://dx.doi.org/10.1016/j.solener.2013.03.012.
Fernández, E.F., Talavera, D.L., Almonacid, F., Smestad, G.P., 2016b. Investigating the impact of weather variables on the energy yield and cost of energy of grid-connected solar concentrator systems. Energy 106, 790–801. http://dx.doi.org/10.1016/j.energy.2016.03.060.
Gasparin, F.P., Bühler, A.J., Rampinelli, G.A., Krenzinger, A., 2016. Statistical analysis of I-V curve parameters from photovoltaic modules. Sol. Energy 131, 30–38. http://dx.doi.org/10.1016/j.solener.2016.01.061.
Ghani, F., Duke, M., 2011. Numerical determination of parasitic resistances of a solar cell using the Lambert W-function. Sol. Energy 85, 2386–2394. http://dx.doi.org/10.1016/j.solener.2011.07.001.
Ghani, F., Fernandez, E.F., Almonacid, F., O'Donovan, T.S., 2017. The numerical computation of lumped parameter values using the multi-dimensional Newton-Raphson method for the characterisation of a multi-junction CPV module using the five-parameter approach. Sol. Energy 149, 302–313. http://dx.doi.org/10.1016/j.solener.2017.04.024.
Ghani, F., Rosengarten, G., Duke, M., Carson, J.K., 2014. The numerical calculation of single-diode solar-cell modelling parameters. Renew. Energy 72, 105–112. http://dx.doi.org/10.1016/j.renene.2014.06.035.
Grundmann, M., 2010. The Physics of Semiconductors. Springer, Berlin Heidelberg.
Humada, A.M., Hojabri, M., Mekhilef, S., Hamada, H.M., 2016. Solar cell parameters extraction based on single and double-diode models: A review. Renew. Sustain. Energy Rev. 56, 494–509. http://dx.doi.org/10.1016/j.rser.2015.11.051.
Ishibashi, K., Kimura, Y., Niwano, M., 2008. An extensively valid and stable method for derivation of all parameters of a solar cell from a single current-voltage characteristic. J. Appl. Phys. 103, 94507. http://dx.doi.org/10.1063/1.2895396.
Jamadi, M., Merrikh-Bayat, F., Bigdeli, M., 2016. Very accurate parameter estimation of single- and double-diode solar cell models using a modified artificial bee colony algorithm. Int. J. Energy Environ. Eng. 7, 13–25. http://dx.doi.org/10.1007/s40095-015-0198-5.
Khan, F., Baek, S.-H., Kim, J.H., 2014. Intensity dependency of photovoltaic cell parameters under high illumination conditions: An analysis. Appl. Energy 133, 356–362. http://dx.doi.org/10.1016/j.apenergy.2014.07.107.
Khan, F., Baek, S.H., Park, Y., Kim, J.H., 2013. Extraction of diode parameters of silicon solar cells under high illumination conditions. Energy Convers. Manage. 76, 421–429. http://dx.doi.org/10.1016/j.enconman.2013.07.054.
Kichou, S., Abaslioglu, E., Silvestre, S., Nofuentes, G., Torres-Ramírez, M., Chouder, A., 2016a. Study of degradation and evaluation of model parameters of micromorph silicon photovoltaic modules under outdoor long term exposure in Jaen, Spain. Energy Convers. Manage. 120, 109–119. http://dx.doi.org/10.1016/j.enconman.2016.04.093.
Kichou, S., Silvestre, S., Nofuentes, G., Torres-Ramírez, M., Chouder, A., Guasch, D., 2016b. Characterization of degradation and evaluation of model parameters of amorphous silicon photovoltaic modules under outdoor long term exposure. Energy 96, 231–241. http://dx.doi.org/10.1016/j.energy.2015.12.054.
Kim, Y.S., Kang, S.-M., Winston, R., 2013. Modeling of a concentrating photovoltaic system for optimum land use. Prog. Photovoltaics Res. Appl. 21, 240–249. http://dx.doi.org/10.1002/pip.1176.
Kinsey, G.S., Hebert, P., Barbour, K.E., Krut, D.D., Cotal, H.L., Sherif, R.A., 2008. Concentrator multijunction solar cell characteristics under variable intensity and temperature. Prog. Photovoltaics Res. Appl. 16, 503–508. http://dx.doi.org/10.1002/pip.834.
Kurtz, S., Muller, M., Jordan, D., Ghosal, K., Fisher, B., Verlinden, P., Hashimoto, J., Riley, D., 2015a. Key parameters in determining energy generated by CPV modules. Prog. Photovoltaics Res. Appl. 23, 1250–1259. http://dx.doi.org/10.1002/pip.2544.
Leloux, J., Lorenzo, E., García-Domingo, B., Aguilera, J., Gueymard, C.A., 2014. A bankable method of assessing the performance of a CPV plant. Appl. Energy 118, 1–11. http://dx.doi.org/10.1016/j.apenergy.2013.12.014.
Li, Y., Huang, W., Huang, H., Hewitt, C., Chen, Y., Fang, G., Carroll, D.L., 2013. Evaluation of methods to extract parameters from current-voltage characteristics of solar cells. Sol. Energy 90, 51–57. http://dx.doi.org/10.1016/j.solener.2012.12.005.
Zagrouba, M., Sellami, A., Bouaïcha, M., Ksouri, M., 2010. Identification of PV solar cells and modules parameters using the genetic algorithms: Application to maximum power extraction. Sol. Energy 84, 860–866. http://dx.doi.org/10.1016/J.SOLENER.2010.02.012.
Micheli, L., Fernández, E.F., Almonacid, F., Mallick, T.K., Smestad, G.P., 2016. Performance, limits and economic perspectives for passive cooling of high concentrator photovoltaics. Sol. Energy Mater. Sol. Cells 153, 164–178. http://dx.doi.org/10.1016/j.solmat.2016.04.016.
Muñoz, J.V., de la Casa, J., Fuentes, M., Aguilera, J., Bertolín, J.C., 2011. New portable capacitive load able to measure PV modules, PV strings and large PV generators. In: 26th European Photovoltaic Solar Energy Conference and Exhibition, pp. 4276–4280. http://dx.doi.org/10.4229/26thEUPVSEC2011-5BV.2.23.
Muñoz, J.V., Torres-Ramírez, M., García-Domingo, B., Fuentes, M., de la Casa, J., Nofuentes, G., Aguilera, J., 2014. Automatic monitoring system to assess the outdoor behaviour of photovoltaic modules. In: 29th European Photovoltaic Solar Energy Conference and Exhibition, pp. 2654–2657.
Montes-Romero, J., Piliougine, M., Muñoz, J.V., Fernández, E.F., de la Casa, J., 2017. Photovoltaic Device Performance Evaluation Using an Open-Hardware System and Standard Calibrated Laboratory Instruments. Energies 10 (11), 1869. http://dx.doi.org/10.3390/en10111869.
Nelson, J., 2014. The Physics of Solar Cells. Imperial College Press, London.
Ortiz-Conde, A., García-Sánchez, F., Muci, J., 2006. New method to extract the model parameters of solar cells from the explicit analytic solutions of their illuminated characteristics. Sol. Energy Mater. Sol. Cells 90, 352–361. http://dx.doi.org/10.1016/j.solmat.2005.04.023.
Phang, J.C.H., Chan, D.S.H., Phillips, J.R., 1984. Accurate analytical method for the extraction of solar cell model parameters. Electron. Lett. 20, 406. http://dx.doi.org/10.1049/el:19840281.
Rodrigo, P., Fernández, E.F., Almonacid, F., Pérez-Higueras, P.J., 2013. Models for the electrical characterization of high concentration photovoltaic cells and modules: A review. Renew. Sustain. Energy Rev. 26, 752–760. http://dx.doi.org/10.1016/j.rser.2013.06.019.
Rodrigo, P., Gutiérrez, S., Velázquez, R., Fernández, E.F., Almonacid, F., Pérez-Higueras, P.J., 2015. A methodology for the electrical characterization of shaded high concentrator photovoltaic modules. Energy 89, 768–777. http://dx.doi.org/10.1016/j.energy.2015.05.143.
Rodrigo, P.M., Fernández, E.F., Theristis, M., Cruz, F.A., 2017. Characterization of the spectral matching ratio and the Z-parameter from atmospheric variables for CPV spectral evaluation. IEEE J. Photovoltaics 7, 1802–1809. http://dx.doi.org/10.1109/JPHOTOV.2017.2747156.
Segev, G., Mittelman, G., Kribus, A., 2012. Equivalent circuit models for triple-junction concentrator solar cells. Sol. Energy Mater. Sol. Cells 98, 57–65. http://dx.doi.org/10.1016/j.solmat.2011.10.013.
Sharma, V., Sastry, O.S., Kumar, A., Bora, B., Chandel, S.S., 2014. Degradation analysis of a-Si, (HIT) hetro-junction intrinsic thin layer silicon and m-C-Si solar photovoltaic technologies under outdoor conditions. Energy 72, 536–546. http://dx.doi.org/10.1016/j.energy.2014.05.078.
Stark, C., Theristis, M., 2015. The impact of atmospheric parameters on the spectral performance of multiple photovoltaic technologies. In: 2015 IEEE 42nd Photovoltaic Specialist Conference (PVSC), pp. 1–5. http://dx.doi.org/10.1109/PVSC.2015.7355836.
Steiner, M., Siefer, G., Hornung, T., Peharz, G., Bett, A.W., 2015. YieldOpt, a model to predict the power output and energy yield for concentrating photovoltaic modules. Prog. Photovoltaics Res. Appl. 23, 385–397. http://dx.doi.org/10.1002/pip.2458.
Strobach, E., Faiman, D., Kabalo, S., Bokobza, D., Melnichak, V., Gombert, A., Gerstmaier, T., Ruttger, M., 2015. Modeling a grid-connected concentrator photovoltaic system. Prog. Photovoltaics Res. Appl. 23, 582–592. http://dx.doi.org/10.1002/pip.2467.
Talavera, D.L., Ferrer-Rodríguez, J.P., Pérez-Higueras, P., Terrados, J., Fernández, E.F., 2016. A worldwide assessment of levelised cost of electricity of HCPV systems. Energy Convers. Manage. 127, 679–692. http://dx.doi.org/10.1016/j.enconman.2016.09.054.
Talavera, D.L., Pérez-Higueras, P., Almonacid, F., Fernández, E.F., 2017. A worldwide assessment of economic feasibility of HCPV power plants: Profitability and competitiveness. Energy 119, 408–424. http://dx.doi.org/10.1016/j.energy.2016.12.093.
Theristis, M., Fernández, E.F., Almonacid, F., Georghiou, G.E., 2017a. Spectral correction of CPV modules equipped with GaInP/GaInAs/Ge solar cells and Fresnel lenses. Appl. Sci. 7.
Theristis, M., Fernández, E.F., Almonacid, F., Pérez-Higueras, P., 2016. Spectral corrections based on air mass, aerosol optical depth, and precipitable water for CPV performance modeling. IEEE J. Photovoltaics 6, 1598–1604. http://dx.doi.org/10.1109/JPHOTOV.2016.2606702.

Theristis, M., Fernández, E.F., Sumner, M., O'Donovan, T.S., 2017b. Multiphysics modelling and experimental validation of high concentration photovoltaic modules. Energy Convers. Manage. 139, 122–134. http://dx.doi.org/10.1016/j.enconman.2017.02.044.

Theristis, M., O'Donovan, T.S., 2015. Electrical-thermal analysis of III-V triple-junction solar cells under variable spectra and ambient temperatures. Sol. Energy 118, 533–546. http://dx.doi.org/10.1016/j.solener.2015.06.003.

Theristis, M., Sarmah, N., Mallick, T.K., O'Donovan, T.S., 2012. Design and numerical analysis of enhanced cooling techniques for a high concentration photovoltaic (HCPV) system. In: 27th European Photovoltaic Solar Energy Conference and Exhibition, pp. 260–265. http://dx.doi.org/10.4229/27thEUPVSEC2012-1AV.3.35.

Theristis, M., Venizelou, V., Makrides, G., Georghiou, G.E., 2018. Chapter II-1-B - energy yield in photovoltaic systems. In: Kalogirou, S.A. (Ed.), McEvoy's Handbook of Photovoltaics, third ed. Academic Press, pp. 671–713. http://dx.doi.org/10.1016/B978-0-12-809921-6.00017-3.

Tivanov, M., Patryn, A., Drozdov, N., Fedotov, A., Mazanik, A., 2005. Determination of solar cell parameters from its current-voltage and spectral characteristics. Sol. Energy Mater. Sol. Cells 87, 457–465. http://dx.doi.org/10.1016/j.solmat.2004.07.033.

Vorster, F.J., Van Dyk, E.E., 2005. Current-voltage characteristics of high-concentration, photovoltaic arrays. Prog. Photovoltaics Res. Appl. 13, 55–66. http://dx.doi.org/10.1002/pip.563.

Vossier, A., Chemisana, D., Flamant, G., Dollet, A., 2012. Very high fluxes for concentrating photovoltaics: Considerations from simple experiments and modeling. Renew. Energy 38, 31–39. http://dx.doi.org/10.1016/j.renene.2011.06.036.

Wolf, P., Benda, V., 2013. Identification of PV solar cells and modules parameters by combining statistical and analytical methods. Sol. Energy 93, 151–157. http://dx.doi.org/10.1016/j.solener.2013.03.018.

Ye, M., Wang, X., Xu, Y., 2009. Parameter extraction of solar cells using particle swarm optimization. J. Appl. Phys. 105, 94502. http://dx.doi.org/10.1063/1.3122082.

Yu, K., Chen, X., Wang, X., Wang, Z., 2017. Parameters identification of photovoltaic models using self-adaptive teaching-learning-based optimization. Energy Convers. Manage. 145, 233–246. http://dx.doi.org/10.1016/j.enconman.2017.04.054.

Zhang, C., Zhang, J., Hao, Y., Lin, Z., Zhu, C., 2011. A simple and efficient solar cell parameter extraction method from a single current-voltage curve. J. Appl. Phys. 110, 64504. http://dx.doi.org/10.1063/1.3632971.

PUBLICACIÓN IV

Título	**"Low cost I-V curve tracer for PV modules under real operation conditions"**
Autores	Caceres, M.; Firman, A.; Montes-Romero, J.; González Mayans, A.R.; Vera, L.; Fernández, E.F.; de la Casa, J.
Revista	**En fase de revisión** en IEEE Transactions on Instrumentation and Measurement
Categoría y posición	INSTRUMENTS & INSTRUMENTATION (14/58) ENGINEERING, ELECTRICAL & ELECTRONIC (88/266)
Factor de impacto	3,067 (2018)

Low cost I-V curve tracer for PV modules under real operation conditions

Manuel Cáceres, Andrés Firman, Jesús Montes Romero, Alexis Raúl González Mayans, Luis Horacio Vera, Eduardo F. Fernández, Juan de la Casa Higueras

***Abstract*— Photovoltaic generation has a broad scientific development. In order to ensure the transfer of knowledge through the training of qualified staff, didactic tools are necessary. Most training centers have restrictions to acquire specific equipment due to its cost. In this sense, the development and transference of a low cost I-V curve tracer acquisition system are presented in this article. This system is based on embedded systems together with all the hardware and software necessary for its operation. The hardware and software that involves the system are open and free, and with very low cos, i.e. the estimated cost of the components is 163€. Four institutions from three different countries have participated in the project. Measurement uncertainties associated to the developed equipment are estimated using three different PV technologies. In addition, the developed system can be transferred for its use as an academic tool in the teaching of photovoltaic solar technology. The instrument presents low error values on the measurement of the *I-V* curve. These errors have been certificated by an accredited laboratory. The system can be implemented at low cost. Also, the access to the required tools for the correct learning of this topic is ensured.**

***Index Terms*— Current-voltage characteristics, Photovoltaic systems, Solar energy.**

I. Introduction

RENEWABLE energies have enjoyed an important development during the last decades. These kind of systems have been incorporated as an alternative energy source. Also, from the technological point of view, the development of more efficient and sustainable systems has been achieved [1]-[3].

In this context, the production of electrical energy through the photovoltaic (PV) conversion of the incoming sunlight is signaled as an important alternative due to its inherent characteristics. Compared to other generation methods, the large number of applications and its high reliability can be highlighted as some of the most outstanding features [4], [5].

Therefore, systematic studies are required in order to determine and explain the operation principles of the different technologies [6]-[8] –existing or in development–. This is relevant to maximize the operation efficiency and to elaborate methods of exploitation of the electric energy produced [9].

Currently, the study of photovoltaic technology is a subject of broad scientific interest. The transfer of the knowledge acquired from these investigations to the society is one of the most relevant challenges of this topic. This transfer can be carried out through the training of qualified human resources in academic environments.

However, most of these training centers have significant access restrictions to the equipment required for the testing, evaluation and diagnosis of PV devices. The high cost of this equipment can only be assumed by specialized centers in this area. As a consequence, developing tools that allow the educational and scientific objectives to be fulfilled is necessary. This is fundamental to achieve the transfer of knowledge at an affordable cost. Design, implement and transfer equipment destined to characterize the photovoltaics devices must be developed to ensure the development of this technology [10].

In this context, as a contribution to the exposed problem, the present article proposes the development of a low cost *I-V* curve tracer system for PV modules under real operation conditions. An *I-V* tracer system is a device used for the evaluation and diagnosis of the PV technology. Also, this tool is essential for teaching purposes because it permits the characterization of the PV generator.

A. I-V curve of a photovoltaic device

The *I-V* curve of a PV cell, module or array under a determined operation conditions, gives information related to its electrical behavior –normal or anomalous- and its energy generation capacity [11]. It is the most important and widely used metric to describe the electrical output of a PV device [12] - [14].

PV modules and arrays are built through the serial or parallel connection of several number of cells. In normal operation conditions, the *I-V* curve presents a similar morphology at any association. The normalized *I-V* curve of a PV device is shown in Fig. 1. Any *I-V* curve presents characteristic points such as short-circuit current (*Isc*), open-circuit voltage (*Voc*) and maximum power point (*Pm*). The latter is defined by the voltage at the maximum power point (*Vm*) and the current at the maximum power point (*Im*).

M. Cáceres, A. Firman, A.R. González Mayans and L. Vera are with the Group of Renewable Energies (GER), National University of the Northeast, Argentina. (email: drmanu.caceres@gmail.com; andresfirman@gmail.com; raulgonzalezmayans@gmail.com ; luis.horacio.vera@comunidad.unne.edu.ar)

J. Montes-Romero, E.F. Fernández and J. de la Casa are with the IDEA research group, University of Jaén, Spain. (email: jmontes@ujaen.es; eduardo.fernandez@ujaen.es; delacasa@ujaen.es)

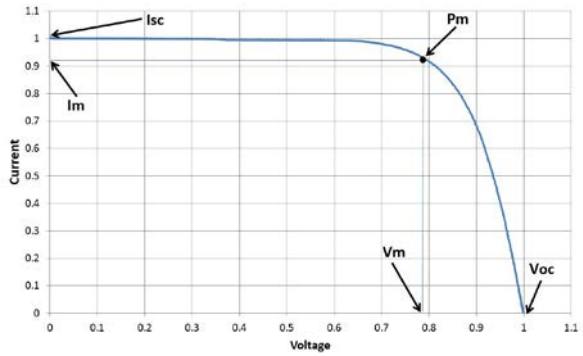

Fig. 1. Normalized *I-V* curve of a photovoltaic device.

The value of those parameters depends on the size of the PV generator and the operation conditions, usually irradiance and temperature- [15]. The variations of the parameters can be described and represented by using multiple mathematical models [16]–[19]. The necessary data to use those methods can be experimentally obtained from the *I-V* curve of the technology under investigation. This fact reinforces the need of the *I-V* tracers in the study and learning of the PV technology.

The system presented in this study is capable of accomplishing this task and its use is focused on the characterization of PV modules.

II. Operation Principle of the Developed System

In the following section, a general description of the main components of the system is presented. This also includes the ~~in~~ details of the analog signal conditioning circuits. The calibration process carried out to develop and validate the presented prototype is exposed. A simplified material budget that allows the system to be replicated, is also presented.

A. System description

The proposed system performs the measurement, acquisition, sweep and analysis of the voltage and current values of a PV module under real operation conditions. The variation of the working point is done connecting the PV module to a capacitor with a small negative residual charge and exposing the PV module to the solar radiation. This connection causes a current flux on the capacitor, which varies from the short-circuit value at the initial moment of the connection, to zero when the capacitor voltage reaches the open-circuit voltage value. During this electrical transient, the system simultaneously measures the voltage and current values. The sampling rate of the system allows a correct construction of the *I-V* curve for the actual outdoor operation conditions.

In Fig. 2, the electrical diagram of the *I-V* sweeping circuit is presented. This process is based on a capacity load, among all the possible methods [20]. The switch S_1 is a relay that controls the negative pre-charge of the capacitor. This process must be done before connecting the PV module to the capacitor in order to obtain the *Isc* point during the charging process. The switch S_2 is an electronic switching device –a MOSFET transistor is used– with a control stage that connects the capacitor to the PV module. Finally, the switch S_3 performs the discharge of the capacitor, dissipating the stored energy on a power resistor *Rd* after the charging process is complete.

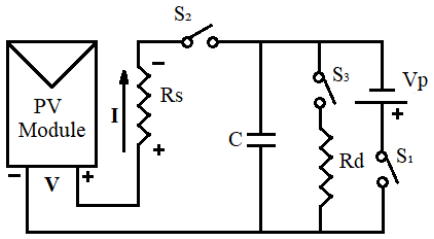

Fig. 2. Electrical diagram of the proposed I-V curve tracer.

In order to measure the current, a shunt resistor *Rs* is used [21]. The device used in the experimental setup is classified as 0.5 class and has a scale of 15A/150mV. This resistor is connected in series with the capacitive load. The voltage measurement is done with a four-wire configuration in order to remove the voltage drop produced at the wires and connections. Therefore, the voltage measurement is done on the PV generator terminals.

In addition to the *I-V* curve, it is necessary to define the present operation conditions during the experiment. In this sense, irradiance and cell temperature are the basic parameters that have to be acquired. In addition, the developed system considers the use of a reference cell, [22], composed by two polycrystalline silicon photovoltaic cells. One of the cells is used as an irradiance transducer –operating at *Isc* point with a shunt resistor-, and the other cell is used to measure the cell temperature –operating at *Voc* point-. The temperature can also be acquired by a resistance temperature detector (RTD) PT100 [23], [24].

Due to the requirements of this project –measurement, acquisition, and processing of four variables-, an evaluation of low-cost embedded systems was carried out. In this sense, four systems with similar features were studied: PSoC 5LP, NUCLEO-F411RE, LPCXpresso18 and TivaC Series Launchpad. Table I shows the main technical-economic characteristics of the considered systems. Because of the optimal features for analog signal acquisition, i.e. 2 independent ADC of 12 bits and a maximum sampling rate of 1Ms/s, potential for digital signal processing and low cost, the TivaC Series LaunchPad was selected [25].

TABLE I
Technical-economic characteristics of 4 commercial embedded systems under analysis

Commercial Embbeded System	Cores and Memories	Digital peripherals	Analog peripherals	Price
CY8CKIT-059 PsoC 5LP Prototyping Kit from Cypress	ARM Cortex-M3 Flash: 256 kB SRAM: 64 kB EEPROM: 2 kB	24 universal digital blocks	2 SAR 12 bits 1kS/s; 20 bits 180 S/s	11,5 €
NUCLEO-F411RE from ST Microelectronics	ARM Cortex-M4 Flash: 256 kB SRAM: 128 kB	50 GPIO	1 ADC 12 bits 2,4 MS/s	11,7 €
LPCXpresso18S37 from NXP	ARM Cortex-M3 Flash: 1 MB SRAM: 136 kB EEPROM: 16 kB	49 GPIO	2 ADC 10 bits 400 kS/s	24,3 €

Tiva C Series LaunchPad from Texas Instruments	ARM Cortex-M4 Flash: 256 kB SRAM: 32 kB EEPROM: 2 kB	48 GPIO	2 ADC 12 bits 1 MS/s	11,5 €

The measurement of the physical variables required is done by voltage signal transducers of different magnitude and with a determined bandwidth. For this reason, conditioning and filtering stages must be included to suit the requirements of the A/D converters. In Fig. 3, an image of the developed boards is shown. The bottom plate corresponds to the analog signal conditioning stages, the middle to the commercial board TIVA and the top to the power board that controls the capacitive load.

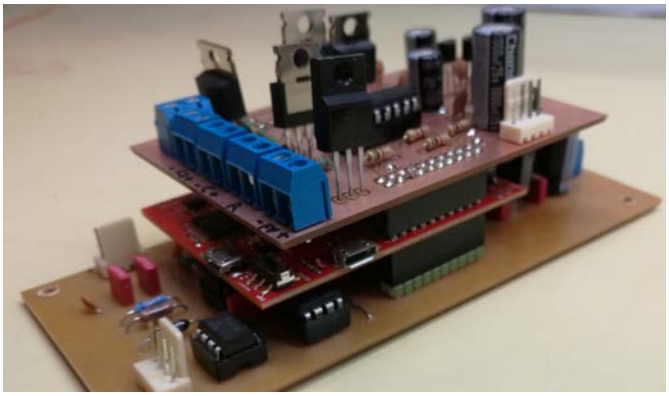

Fig. 3. Last version of the prototype boards built at the University of Jaén. Signal conditioning stage at bottom, commercial embedded system board atthe middle and power stage at top.

Furthermore, the measurement system was designed for its use as a test, evaluation and characterization instrument for academic environments. A simple software was implemented to control the measurement system and performs the subsequent analysis of the acquired data. This software was developed on LabVIEW environment due to its simplicity and intuitive characteristics. The main window of the developed software is shown in Fig. 4.

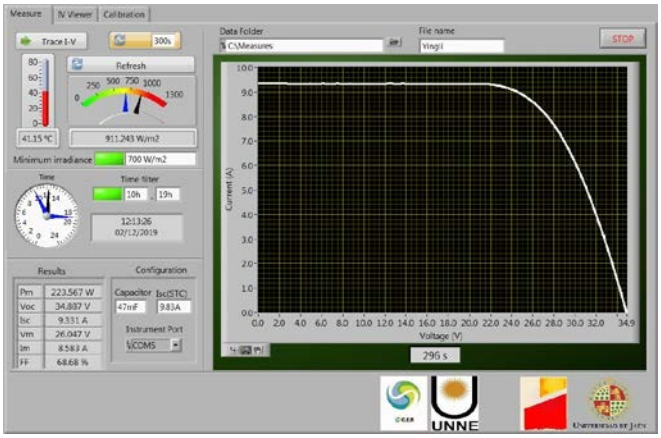

Fig. 4. Main windows of the developed control software.

B. *Analog signal conditioning*

As previously explained, the system is designed to measure four voltage signal variables of different magnitudes. Two of them must be acquired simultaneously. The design of the amplification stages was carried out as a function of the transducers employed in the proposed system [26]. These devices are summarized in Table II.

TABLE II
TECHNICAL CHARACTERISTICS OF TRANSDUCERS USED IN THE MEASUREMENT OF THE VARIABLES.

Channel	Measurement Range	Transducer	Transducer Operation Range
PV module current (I)	0 to 12 A	Shunt Resistor Class 0.5	0 to 15 A / 150 mV
PV module voltage (V)	-10 to 100 V	Attenuator 120 V/ 1.6 V	0 to 1.6 V
Irradiance (G)	0 to 1300 W/m²	Class 0.5 shunt connected Poly-Si cell	0 to 3.5 A / 42 mV
Cell temperature (T)	0 to 100 °C	Open circuit Poly-Si Cell	0.5 to 0.8 V
Cell temperature (T)	0 to 100 °C	PT100 resistor	0.5 V to 0.7 V (with 5 mA constant current source)

Based on the analog inputs, different signal conditioning were elaborated in order to maximize the precision of the measurements. In this sense, amplification stages were developed for the current, irradiance and temperature channels. For the voltage channel, an attenuation stage with low impedance at the output was implemented. The instrumentation operational amplifier AD620BNZ by Analog Devices is employed to perform the conditioning of the signals. The electrical schematic of the current and voltage stages can be seen in Fig. 5 and Fig. 6. The amplification stage for irradiance and temperature is similar to the current channel~~, adapting~~. The gain resistance is adapted to the required values by the transducer. The analogical stages are powered by a symmetrical source stabilized at ±12 V.

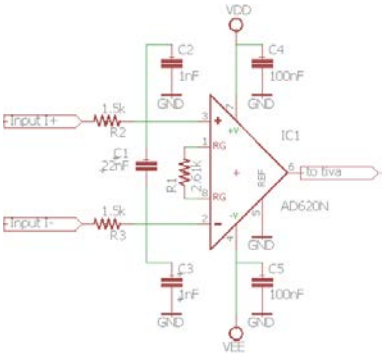

Fig. 5. Amplification stage. Current measurement.

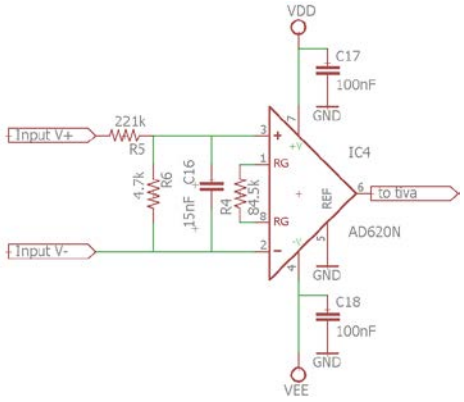

Fig. 6. Amplification stage. Voltage measurement.

The differential inputs bandwidth was limited by antialiasing filters with a cutoff frequency of 2.36 kHz. This is key to simplify the digital signal processing and avoid erroneous results. The acquisition of 500 points in a time less than 100 ms -5 kS/s equivalent sample rate- ensures the correct representation of the *I-V* curve [27]. Taking into account that the embedded system admits a sampling rate of 1 MS/s, the cutoff frequency selected is considered appropriate for the filters. The calculations conducted to select the appropriate filters were done according to the equations presented in [28].

In addition, to enable the measurement of the cell temperature through a four wires PT100, a constant current source was implemented to the respective channel. This source was built from a reference signal generated by a CI MAX6350, an operational amplifier LM358 and a 1kΩ resistor. This is shown in Fig. 7.

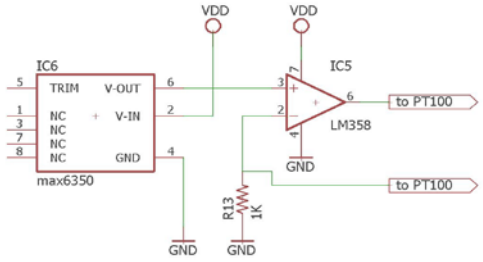

Fig. 7. Constant current source employed to enable the four-wire measurement of the PT100 sensor.

In order to avoid inferences between the conditioning stage and the power stage, the system was designed with optocouplers and an independent symmetrical source of ±5V. The power stage is employed to control the process of precharge, charge and discharge of the capacitor. Its electrical schematic is shown in Fig. 8.

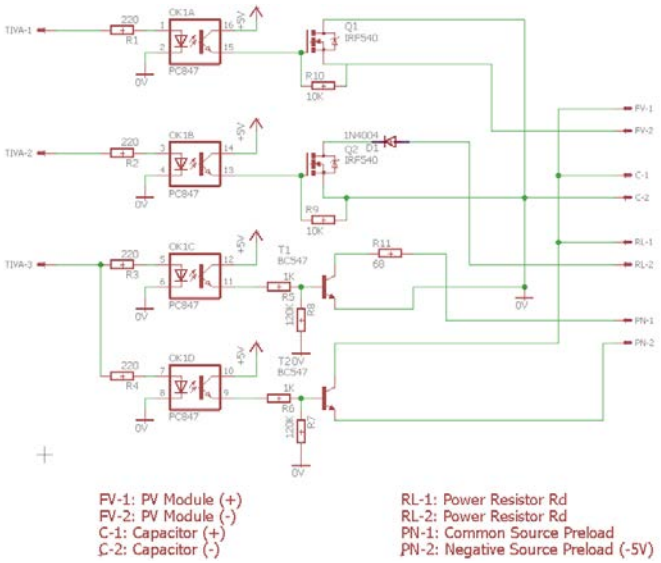

Fig. 8. Power stage and symmetrical source for its supply.

C. *Instrument cost*

One of the objectives of this project is the possibility of transferring the developed system to the academic units interested in its implementation. This transference will be also done through the publication of all the details of the project on a website. All the hardware and software are open and free. In this sense, the final budget of materials involved in the system is relevant. The material costs are presented in Table IV. The associated cost to the fabrication, mounting, calibration and setup were ignored. It is expected that the academic units interested will involve their personal staff to perform the activities related to the implementation of the system. Fig. 9 shows the prototype version used for the experimental campaign.

TABLE IV
PARTIAL COSTS AND TOTAL COST OF THE MATERIALS AND COMPONENTS ASSOCIATED TO THE PROJECT

System Stage	Price
Analog signal Processing	75.00 €
Power Drive	48.50 €
Embedded System	11.50 €
Miscellaneous	28.00 €
Total Project Price	**163.00** €

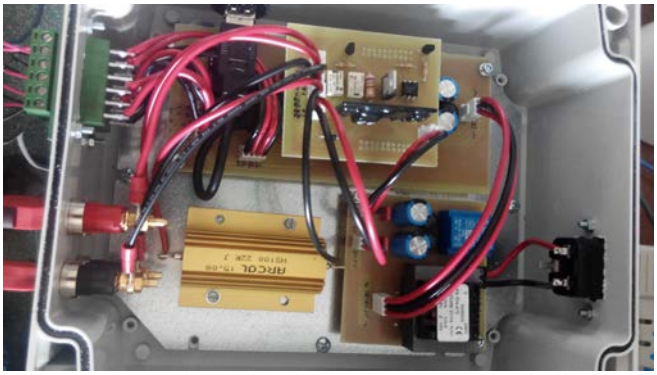

Fig. 9. Prototype version used for the experimental campaign developed at the University of Jaén.

D. Instrument calibration

The developed instrument was subjected to a calibration process at the University of Jaen. This calibration consists on the acquisition of discrete values applied by a power supply or voltage reference device, in contrast with a calibrated instrument considered as pattern. The reference signal has been generated using a process signal calibrator C.A.1631 from Chauvin Arnoux. This instrument has a resolution of 0.01mV in the range of 100mV, and of 1mV in the range of 20V. The uncertainty given by the manufacturer is 0.02%. In this case, the pattern measurement system employed was a Keysight multimeter 34465A. The process was carried out throughout the complete operation range established for each measurement channel. Then, the calibration equations were obtained by a linear fit.

III. Methodology of the Experimental Campaign

In this section, the methodology followed to estimate the error committed by the developed instrument will be explained. This methodology was carried out in the four laboratories that collaborates in this work: The Research and Development in Solar Energy (IDEA) research group of the University of Jaén (Spain), The Renewable Energy Group (GER) of the National University of the Northeast (Argentina), the Solar Energy Laboratory (LABSOL) of the Federal University of Rio Grande do Sul (Brazil) and the Centre for Energy, Environmental and Technological Research (CIEMAT) (Spain).

A. Experimental setup

The developed instrument was connected in parallel with other measurement systems used as patterns during the *I-V* curve tracing. In Table V, the measurement system used on each laboratory is shown.

TABLE V
PATTERN SYSTEM USED ON EACH LABORATORY

Laboratory	Pattern instrument
IDEA	Keysight 34465A
GER	Keysight 34410A
CIEMAT	Yokogawa WT3000
LABSOL	Agilent 3458A

The developed system produces a trigger signal in order to synchronize both the developed and pattern systems. For the IDEA [29] and GER laboratories, the measurements were ~~as~~ configured to obtain the voltage and current values with the same sampling rate on both systems. As a consequence, the measured values were obtained simultaneously at the same time base. Because the voltage and current samples of both equipment are equi-temporal, a point-by-point comparison of the measurements can be done. On the other hand, the CIEMAT and LABSOL laboratories measure at different time bases. Therefore, the comparison is only done for the main characteristic *I-V* points.

For a deeper contrast test, commercial PV modules of three different technologies were used at the IDEA laboratory: monocrystalline silicon, polycrystalline silicon and thin film. Table VI presents the electrical characteristics of each module at Standard Test Conditions (STC) -1000 W/m^2 of irradiance, 25ºC of cell temperature and AM1.5G of spectral distribution - . Those electrical characteristics were certified by the CIEMAT.

TABLE VI
ELECTRICAL CHARACTERISTICS OF THE MODULES AT STC CERTIFIED BY CIEMAT.

PV Technology	Pm (W)	Voc (V)	Isc (A)	Vm (V)	Im (A)
Thin-Film (120 Wp)	112.7	59	3.09	41.9	2.69
Poly-Si (160 Wp)	165.4	43.61	5.03	34.8	4.75
Mono-Si (245 Wp)	243.4	37.44	8.74	30.2	8.07

B. Error estimation

In order to estimate the error produced by each channel - voltage and current-, the absolute error for each of the *N* data pairs is obtained by using equation (1). It is calculated by the difference between the measured value by the developed system and the value by the pattern system under consideration.

$$Ea(n) = |Xm(n) - Xp(n)| \quad (1)$$

where,

Ea(n) = Absolute error at time instant *n*.

Xm(n) = Voltage or current value measured by the developed instrument at time instant *n*.

Xp(n) = Voltage or current value measured by the pattern instrument at time instant *n*.

Depending on the number of samples and the electrical characteristics of the PV device, a set of absolute error values is obtained in different places of the scale. As expected, the channel present different errors depending on the measurement range. Therefore, the absolute error values obtained will be different along the measurement range. However, this error distribution is inherent to the acquisition process of the *I-V* curve and must be taken into account to quantify the deviation between the measured and real curve.

The error can be analyzed by statistic tools. In this sense, a representative value can be obtained by a mean value and the standard deviation value of the distribution. This way, the sum of the mean value mentioned, and the standard deviation becomes the mean error committed for each channel, as expressed in equation (2). Also, in order to normalize this value, it can be divided by the full scale (FS) value of each channel, equation (3). In the case of the developed system, the FS of the current value is 12A and the FS of the voltage is 100V.

$$Ear = |\overline{Ea}| + |\sigma| \quad (2)$$

where,

Ear = Representative absolute error.

$\overline{Ea}$ = Mean value of the error distribution.

σ = Standard deviation of the error distribution.

$$E\% = \frac{Ear.100}{FS} \quad (3)$$

where,
$E\%$ = Normalized percentage error.
FS = Full Scale.

Both the voltage and current are involved in the measurement of the *I-V* curve. The multiplication of these values represent the power of the PV module. As proposed in [30], to estimate the error committed by the instrument on the acquisition of the *I-V* curve, the sum of the normalized percentage error of each channel is done by using equation (4).

$$E_{IV}\% = E_V\% + E_I\% \quad (4)$$

where,
$E_{IV}\%$ = Percentage error in the acquisition of the *I-V* curve.
$E_V\%$ = Percentage error in the voltage cannel.
$E_I\%$ = Percentage error in the current channel.

This way, it is possible to obtain a unique value that represents the error committed on the acquisition of the *I-V* curve.

IV. Results

The following results correspond to the experimental campaign carried out at the IDEA laboratories. This represents the experimental campaign that involved the largest number of PV technologies and in which the *I-V* curves were measured at the same sampling rate. More than 50 curves were obtained for each PV module.

The results shown include the *I-V* curve percentage error ($E_{IV}\%$), the percentage error in the voltage channel ($E_V\%$) and the percentage error in the current channel ($E_I\%$). These magnitudes have been evaluated as a function of the irradiance since is the most relevant parameters of PV technology.

The variation of the errors for the curves of Thin Film technology are presented in Fig. 10. As can be seen, the values remain below 1% for irradiances between 550 and 1000 W/m². The voltage channel is the most influenced by the error. The values stay practically constant for the different values of irradiance. Nevertheless, the error committed by the current channel slightly increases with irradiance, but the value is lower in comparison with the voltage channel. This increment is produced by the current value. High irradiance values generate higher current on PV modules. This implies a lower charging time on the capacitor. In the tests, the sampling rate was fixed to a mean value, producing a constant measuring time. For higher irradiance values, the *I-V* sweep time decreases and an accumulation of data points on the *Voc* point is produced. The percentage error on the current channel for the *Voc* point tends to increase due to an offset value in the developed instrument versus a null offset value on the reference system.

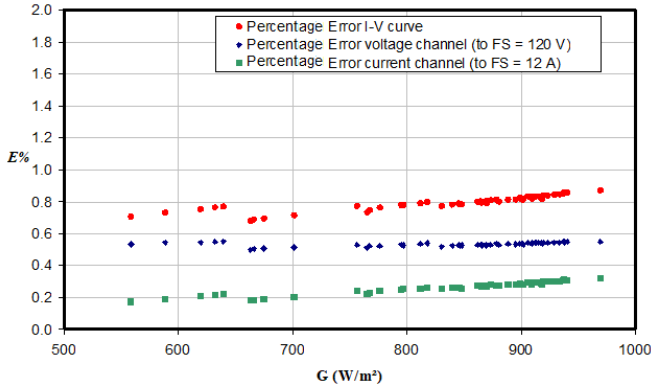

Fig. 10. Variation of percentage error of the *I-V* curves, the voltage channel and the current channel for the Thin Film PV module.

The percentage error values obtained for the polycrystalline silicon PV module are presented in Fig. 11. The maximum error is obtained for an irradiance equal to 1000 W/m² with a value of 1.37%. Again, the error on the voltage remains constant and the current error increases with irradiance. In this case, the increment of the current error is higher in comparison with the Thin Film module. Now the error produced in the voltage is lower than that produced in the current. This can be explained considering the higher *Isc* value of this module in comparison with the previous case, see Table VI.

The trends of the percentage errors commented above are also repeated for the case of the monocrystalline silicon module. This is shown in Fig. 12. This module presents a higher error value at the current channel, resulting in a total error equal to 1.58% at 970 W/m² of irradiance. This is the highest error obtained at this channel among all the PV technologies investigated. As also previously commented, this can be understood considering that this module presents the highest *Isc* value, see Table VI.

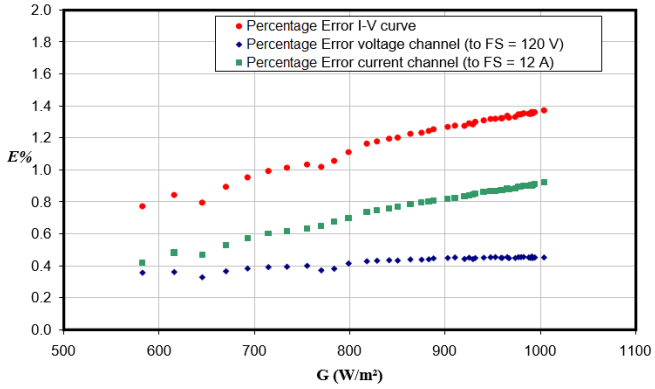

Fig. 11. Variation of percentage error of the *I-V* curves, the voltage channel and the current channel for the polycrystalline silicon PV module.

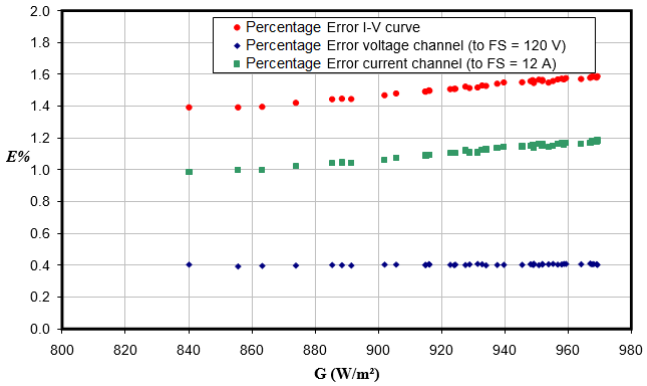

Fig. 12. Variation of percentage error of the I-V curves, the voltage channel and the current channel for the monocrystalline silicon PV module.

The variation error on the current channel above can be explained due to fixed sampling rate on the test conditions. This can be decreased adapting the measurement times to the PV module connected and to the irradiance value. This adjustment can be done in two different ways: adapting the sampling rate to the measurement time or changing the capacitor.

As presented in Table I, the embedded system allows a maximum sampling rate of 1 MS/s to be achieved. This value is much higher than the chosen value for the tests - approximately 5kS/s-. By modifying the control software, an appropriate sampling rate can be estimated in order to avoid the sample accumulation on the *Voc* point.

In order to present a graphic comparison of the *I-V* curves obtained by both the developed and the reference systems, Fig. 13, 14 and 15 are shown. The curves were taken for irradiances close to 900 W/m². In the figures, an almost perfect match between the points taken by both systems can be seen. This visually shows the low error values obtained in the analysis, where the highest error was 1.6%.

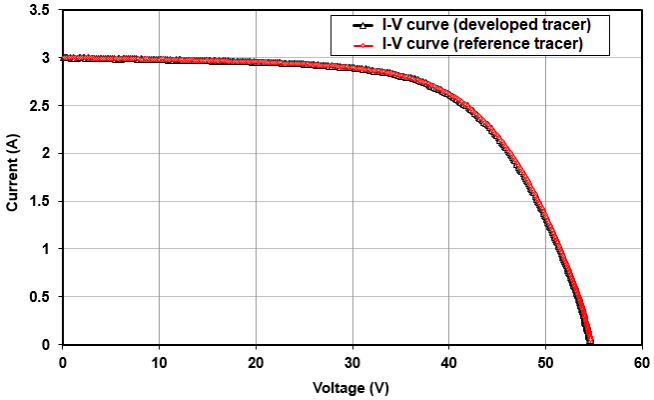

Fig. 13. I-V curves obtained simultaneously between the developed tracer and the reference tracer for the Thin Film PV module.

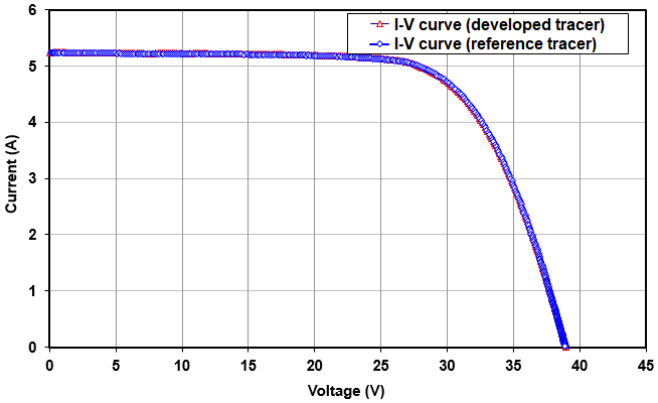

Fig. 14. I-V curves obtained simultaneously between the developed tracer and the reference tracer for the polycrystalline silicon PV module.

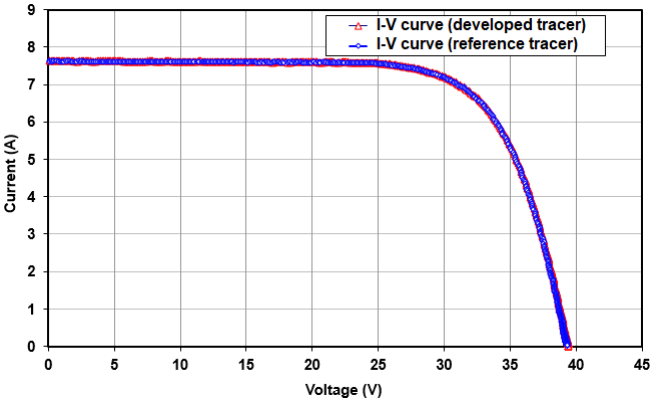

Fig. 15. I-V curves obtained simultaneously between the developed tracer and the reference tracer for the monocrystalline silicon PV module.

The tests above were repeated in four different laboratories of the institutions previously mentioned. The results obtained by the IDEA and GER laboratories are summarized in Table VII. The results obtained at the GER laboratory are analogoues to the obtained at ~~for~~ the IDEA laboratory previously discussed. The voltage error is similar for the measured modules and the current error increases for higher current, or irradiance, values. The maximum error values for the voltage, current and *I-V* were 0.08%, 0.78% and 0.85% respectively. On the other hand, while

minimum error values were 0.04%, 0.67% and 0.72% for the voltage, current and *I-V*, respectively.

The photovoltaic solar energy laboratory from CIEMAT is the reference institution of Spain in terms of calibration and certification of any instrument related to this technology. The pattern instrument used for the test of this work has a certified precision of 0.05% in the measurement. The test carried out in this institution was done for 30 *I-V* curves, obtaining maximum

TABLE VII
SUMMARY OF ERRORS TESTED GER AND IDEA LABORATORIES

PV Technology	Laboratory	E_V%	E_I%	E_{IV}%
Thin-Film (120 Wp)	IDEA	0.55	0.32	0.87
Poly-Si (160 Wp)	IDEA	0.45	0.92	1.37
Mono-Si (245 Wp)	IDEA	0.45	1.23	1.58
Poly-Si (50 Wp)	GER	0.11	0.26	0.37
Poly-Si (140 Wp)	GER	0.1	0.8	0.9

errors of 1.50% for the current channel, 0.65% for the voltage channel and 2.13% for the whole *I-V* curve. On the other hand, the minimum error values were 0.02%, 0.01% and 0.2% respectively. The average deviation obtained for the I_{SC}, V_{OC} and P_M are -0.1%, -0.4% and +0.35% respectively. The uncertainties given by the CIEMAT are, ±0.02A for the I_{SC}, ±0.2V for the V_{OC} and ±2W for the P_M. The presented values include the deviations and uncertainties produced by instant irradiance variations during the measurements, and the errors on the estimation of the parameters. The LABSOL certification is in agreement with these results and show similar error ranges. The results show an average deviation of 0.58%, 0.23% and 0.05% in the estimation of the ~~on~~ I_{SC}, V_{OC} and P_M respectively.

V. CONCLUSIONS

An *I-V* curve tracer of PV modules was developed for testing under real operation conditions. The equipment has a high degree of accuracy at a very low cost, a budget lower than 170€. Four institutions were involved on the experimental campaign conduced to check the quality of the new device. Three PV modules from different technologies –monocrystaline silicon, polycrystaline silicon and thin film- were tested. The statistical error obtained on the acquisition of the *I-V* curve is lower than 1.6% when compared to commercial instruments. This error can be lowered by modifying the control software to adapt the sampling rate as a function of the PV module characteristics and the test conditions irradiance and temperature-. The CIEMAT laboratory certified average deviations lower than 0.4%. The system can be implemented without the need of expensive instruments, ensuring access to the technology for correct learning of the PV area.

ACKNOWLEDGEMENTS

The authors would like to thanks the laboratory staff from the LABSOL laboratory in Brazil and the CIEMAT staff in Spain for their collaboration in the experiments carried out in the project presented in this article.

This work has been supported by Andalusian International Cooperation Agency (Agencia Andaluza de Cooperación Internacional para el Desarrollo, AACID) in the framework of the project: "Emergiendo con el sol. Apoyo institucional al centro de energías renovables de la Universidad Nacional de Ingeniería en el campo de la generación de energía eléctrica empleando tecnología fotovoltaica" and "Plan Plurianual de I+D" from "Centro de Estudios Avanzados en Energía y Medio Ambiente" of the University of Jaen in the framework of the project: Acciones de cooperación al desarrollo en el marco de la transferencia del conocimiento a universidades iberoamericanas. Caso de estudio: caracterización a sol real de módulos FV utilizando equipamiento de bajo coste"

REFERENCES

[1] O. Ellabban, H. Abu-Rub, & F. Blaabjerg. "Renewable energy resources: Current status, future prospects and their enabling technology". Renewable and Sustainable Energy Reviews, vol. 39, pp. 748-764, 2014.

[2] M. Alonso, H. Amaris, C. Alvares-Ortega. Integration of Renewable Energy Sources in Smart Grids by Means of Evolutionary Optimization Algorithms. Expert Systems with Applications, Vol 57, pp. 195-204. 2012.

[3] A. Bayod-Rujula. "Future Development of the Electricity Systems with Distributed Generation". Energy, vol 39, pp. 5513-5522. 2009.

[4] G. Adinolfi, G. Graditi, P. Siano, & A. Piccolo. "Multiobjective optimal design of photovoltaic synchronous boost converters assessing efficiency, reliability, and cost savings". IEEE Transactions on Industrial Informatics, vol. 11(5), pp. 1038-1048. 2015.

[5] P. Denholm, R. Margolis. "Evaluating the Limits of Solar Photovoltaics (PV) in Traditional Electric Power Systems". Energy Policy, vol 35, pp. 2852-2861. 2007.

[6] EN 61646:2008. "Thin-Film Terrestrial Photovoltaic (PV) Modules – Design Qualification and Type Approval". 2008.

[7] EN 60904-1:2006. "Photovoltaic Devices: Measurement of Photovoltaic Current –Voltage Characteristics". 2006.

[8] IEC. IEC 60904-1. "IEC 60904-1, Photovoltaic Devices, Part 1: Measurement of Photovoltaic Current–Voltage Characteristics". 2006.

[9] J.V. Muñoz, G. Nofuentes, M. Fuentes, J. de la Casa and J. Aguilera. "DC energy yield prediction in large monocrystalline and polycrystalline PV plants: Time-domain integration of Osterwald's model". Energy, vol. 114, pp. 951–960. 2016.

[10] F. J. Sánchez-Pacheco, P. J. Sotorrío-Ruiz, J. R. Heredia-Larrubia, F. Pérez-Hidalgo, and M. S. De Cardona, "PLC-based PV plants smart monitoring system: Field measurements and uncertainty estimation," *IEEE Trans. Instrum. Meas.*, vol. 63, no. 9, pp. 2215–2222, 2014.

[11] C. Schuss *et al.*, "Detecting Defects in Photovoltaic Cells and Panels and Evaluating the Impact on Output Performances," *IEEE Trans. Instrum. Meas.*, vol. 65, no. 5, pp. 1108–1119, 2016.

[12] F. Almonacid, E. F. Fernández, T. K. Mallick, and P. J. Pérez-Higueras, "High concentrator photovoltaic module simulation by neuronal networks using spectrally corrected direct normal irradiance and cell temperature," Energy, vol. 84, pp. 336–343, May

[13] F. P. Gasparin, A. J. Bühler, G. A. Rampinelli, and A. Krenzinger, "Statistical analysis of I–V curve parameters from photovoltaic modules," Sol. Energy, vol. 131, pp. 30–38, Jun. 2016.

[14] J. Montes-Romero, F. Almonacid, M. Theristis, J. de la Casa, G. E. Georghiou, and E. F. Fernández, "Comparative analysis of parameter extraction techniques for the electrical characterization of multi-junction CPV and m-Si technologies," Sol. Energy, vol. 160, no. December 2017, pp. 275–288, 2018.

[15] A. Luque, S. Hegedus. Handbook of Photovoltaic Science and Engineering. John Wiley and Sons, Second Edition, pp. 112. 2011.

[16] A. Abbassi, R. Gammoudi, M. A. Dami, O. Hasnaoui, & M. Jemli. "An improved single-diode model parameters extraction at different operating conditions with a view to modeling a photovoltaic generator: A comparative study". Solar Energy, vol. 155, pp. 478-489. 2017.

[17] K. Ishaque, Z. Salam, H. Taheri. “Simple, Fast and Accurate Two-Diode Model for Photovoltaic Modules”. Solar Energy Materials and Solar Cells, vol 95, pp. 586-594. 2011.
[18] A. Celik, N. Acikgoz. “Modellig and Experimental Verification of the Operating Current of Mono-Crystalline Photovoltaic Modules Using Four and Five Parameter Models”. Applied Energy, vol 84, pp. 1-15. 2007.
[19] F. Attivissimo, A. Di Nisio, M. Savino, and M. Spadavecchia, “Uncertainty analysis in photovoltaic cell parameter estimation,” IEEE Trans. Instrum. Meas., vol. 61, no. 5, pp. 1334–1342, 2012.
[20] E. Duran, M. Piliougine, M. Sidrach-de-Cardona, J. Galan and J. M. Andujar, "Different methods to obtain the I–V curve of PV modules: A review," in 33rd IEEE Photovoltaic Specialists Conference, San Diego, CA, USA, 2008, pp. 1-6.
[21] A. Di Nisio, T. Di Noia, C. G. C. Carducci, and M. Spadavecchia, “High dynamic range power consumption measurement in microcontroller-based applications,” *IEEE Trans. Instrum. Meas.*, vol. 65, no. 9, pp. 1968–1976, 2016.
[22] A. Firman, L. Zini, R. Sanchez, L. Vera. “Desarrollo y Calibración de Dispositivos Fotovoltaicos Para Determinar el Recurso Solar Utilizable por SFCR”. Avances en Energías Renovables y Medio Ambiente, Vol 18, pp. 04.09-04.17, ISSN 2314-1433. 2014.
[23] F. Almonacid, P. Rodrigo, E. F. Fernández. “Determination of the current–voltage characteristics of concentrator systems by using different adapted conventional techniques”. Energy, vol. 101, pp. 146-160. 2016.
[24] L. De Bernardez, R. Buitrago, M. Battioni, M. Cutrera, G. Risso. “Estudio de la curva IV de celdas individuales en paneles fotovoltaicos”. Avances en Energías Renovables y Medio Ambiente, vol 9, pp. 04.44-04.47, ISSN 2314-1433. 2005.
[25] F. Salvadori, C. S. Gehrke, L. V Hartmann, E. T. Macedo, A. L. de Lima, and S. L. Maia, “Design of an intelligent electronic device based on TivaC platform for smart grid applications,” in *2016 IEEE International Instrumentation and Measurement Technology Conference Proceedings*, 2016, pp. 1–6.
[26] A. Giordani and L. Mari, “Measurement, Models , and Uncertainty,” *IEEE Trans. Instrum. Meas.*, vol. 61, no. 8, pp. 2144–2152, 2012.
[27] F. Martínez-Moreno, E. Lorenzo, J. Muñoz, R. Moretón. “On the testing of large PV arrays”. Progress in photovoltaics: Research and Applications, vol. 20(1), pp. 100–105. 2012.
[28] Analog Devices. “AD620 Low Cost Low Power Instrumentation Amplifier Datasheet”. Rev. H, pp. 15-16. 2011.
[29] J. Montes-Romero, M. Piliougine, J.V. Muñoz, E.F. Fernández, J. de la Casa. “Photovoltaic Device Performance Evaluation Using an Open-Hardware System and Standard Calibrated Laboratory Instruments”. Energies, vol. 10. n. 11 2017.
[30] J.R. Taylor. “An Introduction to Error Analysis”, 327 pp. Books, Sausalito, Calif. 1997.

Cáceres, Manuel. (M’80) received the B.S. degree in electronics engineering from National University of Northeast, Corrientes, Argentina, in 2009 and the Ph.D. degree from National University of Salta, Salta, Argentina, in 2014. Since 2014 he’s leading Photovoltaic Systems Lab depending on Renewable Energy Group from National University of Northeast, Corrientes, Argentina. His research interest includes photovoltaic systems applications, electronics applied to instrumentation and digital signal processing, power electronics, industrial electric installations, automation, control and power systems simulation and analysis.

Firman, Andrés D. (M’77) was born in Reconquista, Santa Fé, Argentina in 1977. He received the B.S. degree in Electronics Engineering from the National University of Northeast, Corrientes, Argentina in 2006 and the Ph.D. degree in Renewal Energy Area from Salta National University, Salta, Argentina, in 2014. From 2009 to date, he participated actively in the Renewable Energy Group of the University of Northeast, Corrientes, working on various applied engineering projects related to renewable energies. His main areas of expertise are the electrical characterization of photovoltaic modules and the monitoring of large photovoltaic power plants. He is also a professor at the National University of the Northeast and he has been a professor at the de la Cuenca del Plata University since 2016.

González Mayans, Alexis Raúl. (M’93) received degree in electronics engineering from National University of Northeast, Corrientes, Argentina, in 2017. Since 2016 he’s leading Photovoltaic Systems Lab depending on Renewable Energy Group from National University of Northeast, Corrientes, Argentina. His research interest includes photovoltaic systems applications, electronics applied to instrumentation and digital signal processing, power electronics and power systems simulation and analysis

Luis H. Vera. He was born in Machagai, Argentina in 1976. He received his degree in Mechanical Engineering from the National University of Northeast in 2000; Master's Degree in Engineering Sciences from the Federal University of Rio Grande do Sul, Brazil, in 2004; PhD in Engineering Sciences from the Federal University of Rio Grande do Sul, Brazil, in 2009 and his degree of Specialization in Technological Linkage from the National University of the Northeast in 2013. His fields of research are related to the application of systems of energy use. Renewable Energy and Energy Efficiency.

Eduardo F. Fernández received his B.S. in physics from University of Oviedo, Spain, in 2004, and the M. S. in physics, the M.S. in renewables energies, and the Ph.D. in the area of solar energy from University of Santiago de Compostela, Spain, respectively in 2006, 2008 and 2012. He is currently Ramón y Cajal researcher at the Centro de Estudios Avanzados en Energía y Medio Ambiente (CEAEMA) of the University of Jaén. His research interest covers the developing, characterization and modelling of photovoltaic devices and systems.

Juan de la Casa (M’68) received his Bachelor’s Degree (Technical Industrial Engineer Specialized in Electricity) in 1991 and he completed a Master of Electronics Engineering from the University of Granada (Spain) in 2002. He holds a Ph.D. in Engineering from the University of Jaén (Spain) since 2008. He serves as a teacher and researcher at the University of Jaén since 1992 and currently he is a tenured associate professor at the Electronics and Automation Engineering Department since 2009. His research interests are focused on Photovoltaic systems engineering, especially in the fields related to characterization of photovoltaic devices/systems and the necessary instrumentation for it

Jesús Montes Romero (M’89) received his B.S. in electronics engineering from University of Jaen, Spain, in 2012, and the M.S. in renewables energies. He is currently a Ph.D. student in the area of solar energy from University of Jaen, Spain. His research interest covers the developing of electronic systems, instrumentation, characterization and modelling of photovoltaic devices and systems.

PUBLICACIÓN V

Título	**"Software tool for the extrapolation to Standard Test Conditions (STC) from experimental curves of photovoltaic modules"**
Autores	Montes-Romero, J.; de la Casa, J.; Torres-Ramírez, M.; Firmán A.; Cáceres M.
Congreso	Technologies Applied to Electronics Teaching (TAEE)
Año	2016
DOI	10.1109/TAEE.2016.7528252

Software tool for the extrapolation to Standard Test Conditions (STC) from experimental curves of photovoltaic modules

J. Montes-Romero, M. Torres-Ramírez, J. de la Casa
IDEA Research Group, University of Jaen,
Campus Lagunillas, 23071 Jaen, Spain
J. Montes: jmontes@ujaen.es

A. Firman, M. Cáceres
GER – Grupo en Energías Renovables - FaCENA – UNNE,
Av. Libertad 5470 – 3400 Corrientes. Argentina

***Abstract*—A key aspect for the teaching of the photovoltaic technology is that the student perform experimental practices of measure the characteristic Current-Voltage (I-V) under natural sunlight of a photovoltaic cell, module or generator and, later, being able to extrapolate the extracted results into Standard Test Conditions (STC).**

This paper presents a software tool (*gotoSTC*) to facilitate the acquisition of this knowledge and support the learning process of our students.

***gotoSTC* allows processing experimental data from I-V curves and applies some of the accepted methods by the scientific community. The program has two functional options: on the first one, the characteristic parameters of one curve will be obtained from its I-V curve and STC extrapolation methods are applied to it; in the second option, a set of I-V curves of the same module are necessary to obtain the characteristic parameters and then applies the extrapolation methods. Graphical representations of the data are showed in order to present some of the existing relations between the parameters characterizing the device behavior.**

Keywords—Photovoltaic solar energy; software; LabVIEW; I-V curve; educational tool; extrapolaction to STC .

I. INTRODUCTION

Undoubtedly, the photovoltaic solar energy is part of the knowledge to be taught in any qualifications related to Renewable Energies, both in Secondary Education and the Bachelor and Master of our Universities. Creating educational environments that could be able to help the comprehension of specific aspects of technology should be part of the work developed by professors and university researchers; a transfer of knowledge that interrelate research work and teaching responsibilities.

In this work, a tool developed in LabVIEW© [1] which aims to support teaching/learning different methods of extrapolation to Standard Test Conditions (STC) is presented and, furthermore, helping in the understanding of basic concepts related to photovoltaic technology.

II. BACKGROUND

The PV module or photovoltaic generator is the main component of any photovoltaic system, either autonomous, grid-connected, or hybrid. This device is responsible for transforming the energy from the sun into electrical energy.

In fig. 1, the typical I-V curve of a photovoltaic element is shown. This characteristic I-V curve is composed by infinite pairs of current and voltage points. All of them are obtained varying the impedance connected to the module between zero to infinity. In the fig. 1 the most interesting points are also highlighted. The value of the parameters will depend on the module characteristics and the operating conditions to which has been acquired.

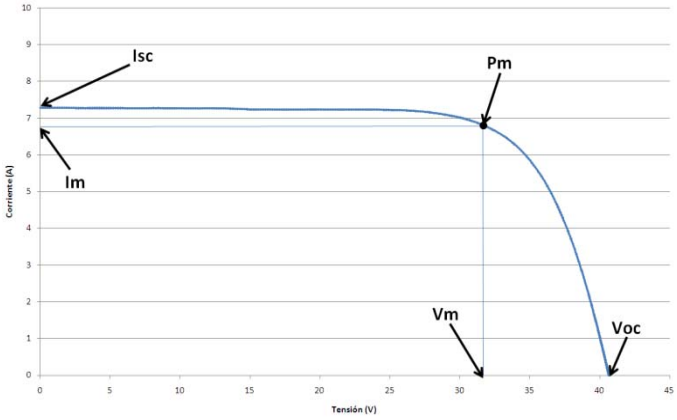

Fig 1. Characteristic I-V curve from a photovoltaic module and its main points of interest.

To characterize their products, manufacturers of PV modules will provide the value of the characteristic electrical parameters from which it is possible to estimate their basic behavior.

The main electrical technical data provided by manufacturers is shown in Table I. The value of these parameters is obtained when the module works in what is known as STC. These conditions, defined in standard IEC 60891, are shown in Table II.

978-1-5090-2264-9/16/$31.00 ©2016 IEEE

TABLE I. ELECTRICAL TECHNICAL CHARACTERISTICS OF PHOTOVOLTAIC MODULES PROVIDED BY MANUFACTURERS.

Pm	Module maximum power (W)
Vm	Module voltage at maximum power in STC (V)
Im	Module current at maximum power in STC (A)
Voc	Module open circuit voltage (V)
Isc	Module short circuit current (A)

TABLE II.STANDARD TEST CONDITIONS.

Normal irradiance (*G*)	1000W/m^2
Cell temperature (*Tc*)	25ºC
Solar spectrum	AM1.5

In addition, some temperature coefficients are provided in order to know the variation of the main characteristic points depending on the operating temperature of the module (Table III).

TABLE III. TEMPERATURE COEFFICIENTS.

α	Short circuit current temperature coefficient (%/ºC)
β	Open circuit voltage temperature coefficient (%/ºC)
γ	Maximum power temperature coefficient (%/ºC)
NOCT	Normal Operate Cell Temperature. Operating temperature when normal irradiance is 800 Wm^{-2} and ambient temperature is 20ºC.

The present paper is focused on the analysis of the curve I-V as an essential aspect for the understanding of the photovoltaic technology. From I-V curve can be obtained all parameters which allow the proper characterization of the module and verify that the data provided by the manufacturer correspond with reality. It is also a key experiment that allows obtaining reliable information on the actual power of a PV generator and hence detect problems, or to estimate the production of the generator.

There are two main procedures that allow us to obtain the characteristic curve of a photovoltaic module: Laboratory measurements using solar simulators [2]; and outdoor measures or under real sunlight, which allow us a characterization that will be referred as Real Sunlight Conditions (RSC). Both systems have advantages and disadvantages that should be considered in choosing the method to be used.

A solar simulator is a system that has a lamp power of high precision and capable of recreating the solar spectrum. Must be taken into account that using solar simulators are experiments within the laboratory, so standard test conditions can be recreated easily. Therefore, the IV curve obtained using this type of equipment is performed to the same operating conditions the manufacturers characterize their products. The main drawback of solar simulators is the high cost of the system and also this procedure, for obvious reasons, is not applicable in case of measuring photovoltaic systems installed outdoor. In fig. 2, one of these systems can be seen.

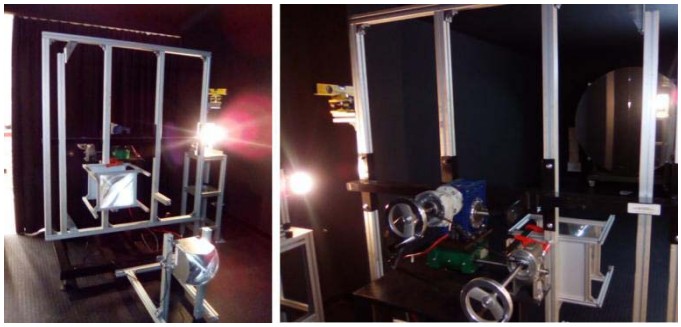

Fig 2. Solar simulator installed at the University of Jaen. On the left, front of the simulator is shown and on the right, the back to the simulator.

The RSC characterization is done by sun exposure PV module as seen in the example of fig.3, so no special equipment will be needed apart from the IV curve tracer [3][4][5] necessary for both methods. Obtain the curves in this way will be much less expensive, but it will be extremely difficult to find environmental conditions that allow the photovoltaic module work on STC, so it is necessary to use mathematical extrapolation methods to know electrical characteristics in STC from RSC experimental measures.

Fig 3. Solar tracker installed at the University of Jaen for the characterization of different PV modules in RSC.

In addition, together with the pairs of V-I values that shape the curve, it will also be necessary to obtain the value of the present meteorological variables when the I-V curve was obtained, which will influence the behavior of any photovoltaic generator. Fundamentally, and the level of precision at hand, the parameters needed will be incident irradiance and temperature. To achieve a higher level of precision, the cell temperature is measured instead of calculate it from ambient temperature.

The essential parameters to extract from the experimental characteristic I-V curve are: short circuit current (*Isc*), open circuit voltage (*Voc*) and maximum power (*Pm*). With these

basic parameters it is possible to use some extrapolation methods [6], with the help of some other auxiliary data that can be extracted from the I-V curve or are provided by the manufacturer (α, β, γ).

In addition to providing the characteristic parameters, the curve I-V provides through its shape, information for detecting anomalies in a PV module such as degradation, fractured cells, shading [7], mismatches [8] or hot spots. A defect or deformation of the expected curve means that the module has a fault and this can affect the proper operation and power of the PV [9] system [10] [11].

In conclusion, the most economical method for the characterization of PV modules is plotting curve I-V in RSC, so to normalize the information obtained through this procedure, it is necessary to study the different methods to extrapolate into STC.

III. Description of Extrapolation Methods to STC Implemented on GotoSTC.

There are published and accepted by the scientific community, a large number of procedures that attempt to answer the extrapolation to STC. These methods can be classified into two main groups:

- Algebraic procedures
- Numeric procedures

Both model the behavior of these semiconductor devices for input conditions (external parameters of meteorological type) depending on their intrinsic and / or technological characteristics. The second require much greater calculus capacity than the first one and there is a widespread idea that they are much more precise and accurate. In this case, we have decided to implement in *gotoSTC* both algebraic and numerical procedures.

Algebraic methods chosen for use in the application are: Araujo [12], constant Fill Factor and Osterwald [13]; while the numerical procedure used is the GER [14]. The first three methods perform calculations only for obtaining characteristic parameters of the PV module. The GER method, being a numerical method, make a reconstruction of the I-V curve with which it is possible to obtain all characteristic parameters that can provide a I-V curve and the electrical equivalent model.

The purpose is to use methods that, being simple, can achieve a good extrapolation results. Must be taken into account that there are more accurate methods of extrapolation to STC [15] [16], but due to its complexity has not thought it appropriate to use for educational activities.

The main proposal is to provide simple methods in order to allow students to perform extrapolation calculations manually during their studies without the need for excessively complex calculations, so *gotoSTC* tool can also be used to compare the results manually performed by the student with those obtained by the tool. This will help students and facilitate learning these extrapolation techniques which are necessary in work related to photovoltaic systems.

Furthermore, to simple algebraic methods, it was added to the tool a numeric procedure in order to be shown the main differences between algebraic procedures, where you can only obtain the characteristic parameters, and numeric procedures, where the whole I-V curve is simulated, giving the possibility to compare the complete I-V curve with the one obtained experimentally.

Three algebraic and one numeric procedures to extrapolate to STC have been chosen to be included in *gotoSTC* tool, so that each of them is briefly described below.

Araujo's method. Approach the values of cell voltage (V_M) and current (I_M) in the maximum power point from short circuit current (I_{SC}) and open circuit voltage (V_{OC}) using (1) and (2), with which you can obtain the maximum power (P_M) of the cell.

$$Isc = \frac{G}{G^*} \cdot I_{SC}^* \tag{1}$$

$$Voc = V_{OC}^* - \beta \cdot (T_C - 25) \tag{2}$$

$$V_M = V_{OC}\left[1 - \frac{b}{v_{oc}} \cdot \ln a - r_s \cdot (1 - a^{-b}\right] \tag{3}$$

$$I_M = I_{SC}(1 - a^{-b}) \tag{4}$$

$$r_s = 1 - \frac{FF^*}{FF_0} \tag{5}$$

$$a = v_{oc} + 1 - 2 \cdot v_{oc} \cdot r_s \tag{6}$$

$$b = \frac{a}{1+a} \tag{7}$$

$$v_{oc} = \frac{V_{OC}}{K \cdot T_c} \cdot e \tag{8}$$

$$FF_0 = \frac{v_{oc} - \ln(v_{oc} + 0.72)}{v_{oc} + 1} \tag{9}$$

where:
r_s = normalised cell series resistance;
FF^* = fill factor in STC;
u_{OC} = normalised open circuit cell voltage;
K = Boltzmann's constant = $1{,}38 \cdot 10^{-23}$ J·K^{-1};
e = $1{,}602 \cdot 10^{-19}$ C.

Constant Fill Factor's method (FFk). This method assumes the fill factor remains constant through all operating conditions. As in the Araujo's method, both cell short-circuit current and open-circuit voltage vary linearly with incident global irradiance and cell temperature, respectively, according

to (1) and (2). This way, using (10) can approximate the value of maximum power (P_M).

$$P_M = FF \cdot Voc \cdot Isc \quad (10)$$

Osterwald's method. This method accounts for being one of the simplest, and achieve a good estimation of maximum power (P_M).

$$P_M = P_M^* \cdot \frac{G}{G^*}[1 - \gamma \cdot (T_C - 25)] \quad (11)$$

where:
G = incident global irradiance (W·m–2);
G^* = incident global irradiance in STC (1000 W·m–2);
P_M = maximum power (W);
P^*_M = maximum power in STC (W);
T_C = cell temperature (ºC);
γ = maximum power temperature coefficient (ºC^{-1}).

GER's method. This method is based on a five parameters electrical model [17], where the simulation of the I-V curve will be held and the parameters to be determined can be extracted. Using the equations (1) and (2) to obtain the open circuit voltaje (V_{OC}) and the short circuit current (I_{SC}) in STC, the equation (12) is needed to calculate the thermal voltage (V_t) and the methodology described in [9] to find the series resistance (R_s) and the shunt resistance (R_{sh}). The value of current (I) can be obtained for each voltage (V) value using equation (13).

$$Vt = \frac{K \cdot Tc}{q} \quad (12)$$

$$I = Isc\left(1 - e^{\frac{V - Voc + I \cdot Rs}{m \cdot N \cdot Vt}}\right) - \frac{V + I \cdot Rs}{Rsh} \quad (13)$$

where:
Vt = thermal voltage;
Rs = series resistance;
Rsh = shunt resistance;
m = diode ideality factor;
N = number of series cell;
q = 1,602·10^{-19} C.

IV. Installation and use of *GOTOSTC*

The tool has been designed to process I-V curves of photovoltaic modules, so will require data files containing each of the I-V curves previously obtained experimentally. The format of the input files must be ".csv" but its configuration can adjust so that it is possible to use data files from multiple curve tracers, both commercial [5] as own development [4]. The minimum data for the proper functioning of the program that data files must contain are the following: the pairs of points of voltage and current that will shape the curve, the incident irradiance and ambient or module temperature to which they have been obtained this I-V curve. These data should be gathered in columns.

In the application is possible to configure the data extraction from experimental curves, so that it is possible to select in which column will be found each of the data groups from all the parameters. It is also possible to configure the separator between columns, being able to choose *";"* or tab. There is no file size limitation, allowing any number of rows and columns, as they have the above mentioned minimum parameters, because they will be necessary for the application of the methods described. Before start using the tool, it must be configured correctly to suit the curves that are to be used.

The tool is divided into two main parts: one where a single I-V curve is taken and the extrapolation methods discussed above are applied; and a second part where set of curves is taken to extrapolate them and the results are shown by a graph, in addition to providing the average of the characteristic parameters obtained in all I-V curves. Each of the parts of the program has a different purpose. The first part is designed in order to students can learn the methods of extrapolation to STC and observe their differences. In the second part, the main aim is to observe the existing relations between the obtained parameters in a graphic and easy way.

The figure 4 shows the part of extrapolation of a single curve. On the first place the file containing the experimental data of the I-V curve to be treated is chosen. Once selected, you can see on the left side of the application, the characteristic parameters in real sunlight conditions extracted from the I-V curve. Then, the extrapolation methods to STC in the application can be found.

For each of the methods few variables and results are observed. The variables are all parameters that are necessary for the implementation of the method, the minimum input data required by each method. Some of the variables cannot be modified due to they are extracted directly from the I-V curve used; therefore many of these parameters match with the values shown on the left side of the program. The reason to show again these variables is for the student to learn what parameters are necessary for the implementation of each of the methods.

It is also necessary to include some other parameters that can be modified, since it is not possible to obtain from I-V curve, so they should be provided by the student using the data sheet of the module manufacturer. These parameters are the open circuit voltage temperature coefficient (β), the maximum power temperature coefficient (γ), the number of series cell present in the module (Ns) and the Fill Factor expected in STC (FF). There is other parameter which does not appear in the data sheet: the diode ideality factor (m). This parameter is estimated from cell technology used in the module. These data can be modified; changing the results obtained, and may determine the influence of each on extrapolation methods.

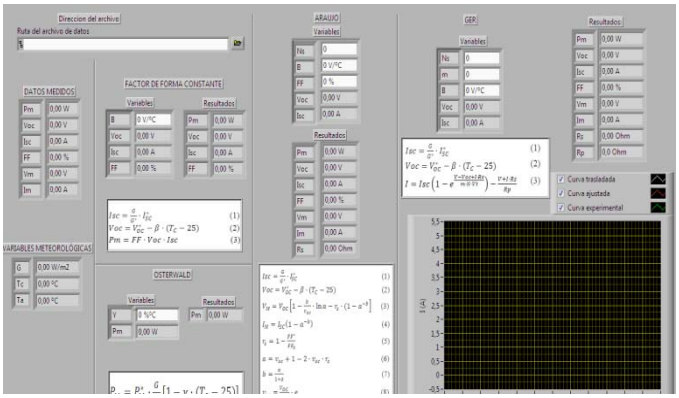

Fig 4. Part of the *gotoSTC* tool responsible for extrapolating a single experimental I-V curve.

Each method will include the expressions used for its implementation, in order to know how the result is obtained.

Furthermore, the GER method performs a numerical procedure that provides the reconstruction of I-V curve. The curves obtained are graphically displayed, being possible to observe the experimental curve obtained from the data file, the fitted curve from the method under the same environmental conditions to which the experimental curve was taken, and the curve extrapolated to STC also indicating its maximum power point. This way the student can appreciate the difference between a curve taken experimentally and a curve plotted from numerical methods.

The same methods mentioned above will be performed for part of extrapolation of multiple curves. After selecting the folder containing the desired files and activating button, it will start loading the files. The loading time of this process depends mainly on the size of the files containing the data. Once the charging of the curves ends, all de data are shown graphically. It is also possible to include data filters for irradiance, power and fill factor for these parameters taken into RSC. The purpose is to detect and eliminate wrong data. Mainly, you can find plotted curves with defects on the meteorological parameters measured, unwanted shading or any inconvenience that may change the expected result. The table of results shows the average of the STC values obtained by the methods performed.

In the graph, any data collected by the program can be represented, with the purpose to facilitate the understanding of the existing relations between the parameters that affect the behavior of PV modules. In this part of the program, can be also created a summary file that contains all the parameters obtained from the data files to use the results with other systems.

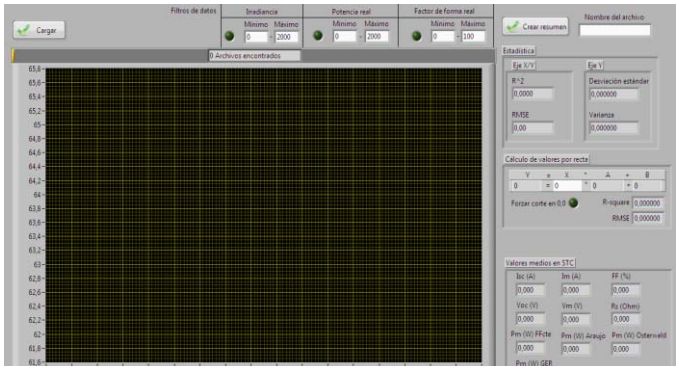

Fig 5. Part of the *gotoSTC* tool responsible for extrapolating multiple experimental I-V curves.

V. RESULTS AND DISCUSSION

The tool has been tested with I-V curves of different PV modules technology; both in the part of extrapolation for a single curve and using multiple curves. Have also been compared the data obtained by *gotoSTC* tool and those obtained by other tools in order to verify that the results were similar, ensuring the proper functioning of the system. The part of the tool to extrapolate a curve responds well to change variables during use, being a little more noticeable change of variables GER method due to the number of operations is far greater than the other methods used and may notice a slight waiting time to update its results.

In fig. 6 an example of use of the tool is presented. In this part, extrapolation to a single curve is performed, being able to observe the characteristics described above. For the following examples the module used is a Suntech STP160 polycrystalline technology mounted on solar tracker shown in fig.3.

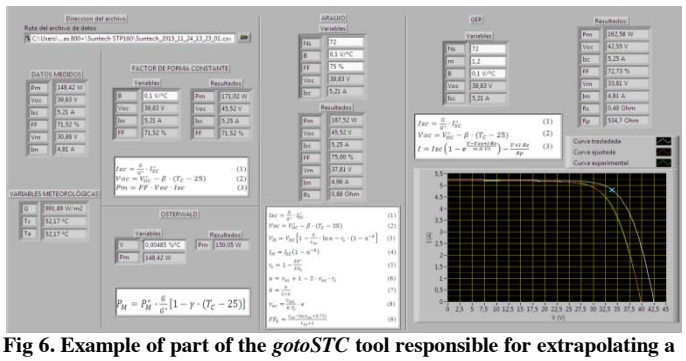

Fig 6. Example of part of the *gotoSTC* tool responsible for extrapolating a single experimental I-V curve.

Below, in fig. 7 Example of the part of the tool where multiple curves are analyzed is presented. In the exposed example is possible to appreciate the graph of relationship between the measured fill factor in RSC and cell temperature registered for each plotted I-V curve, being able to observe the relationship between both parameters, as well as using the linear fit adjustment for approximately calculate a value, as can be seen in the example of fig.7, the fill factor at 25ºC.

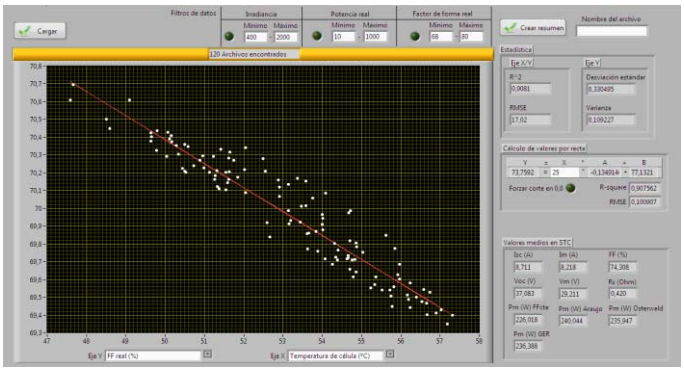

Fig 7. Example of the part of the *gotoSTC* tool responsible for extrapolating multiple experimental I-V curves.

VI. Conclusions

There has been a tool that can be used both for teaching purposes in any kind of education related to photovoltaic technology and research work, allowing quick and comprehensive analysis of a set of experimental curves.

It is characterized by its simplicity of operation. It is supported with theoretical material that allows students to settle knowledge of how the process of extrapolation to STC is done through several algebraic methods with very low computational complexity. Besides learning extrapolation methods, it could also help as graphic support in teaching explanations through the corresponding part of the program. With this, a large number of explanations of the existing relations between different characteristic parameters extracted directly from the I-V curve, meteorological variables and parameters extrapolated to STC.

The gotoSTC tool has started to be used in Bachelor and Master subjects directly related to PV technology during the current quarter. To evaluate whether the application has been successful helping the student, surveys will be carried to users about the application. The questions will be related to the ease of program usage, the assistance provided in the understanding of knowledge, possible improvements or defects which may be found, etc.

Acknowledgement

This communication, besides being considered by the authors as part of their work, and which is intended to demonstrate the importance of the binomial Research-Teaching should always coexist in a university professor, has been promoted, partly funded and is part of the work in the framework of two technology transfer projects:

- **Acciones de cooperación al desarrollo en el marco de la transferencia del conocimiento a universidades iberoamericanas. Caso de estudio: caracterización a sol real de módulos FV utilizando equipamiento de bajo coste**, funded by 'Plan Plurianual de I+D' from 'Centro de Estudios Avanzados en Energía y Medio Ambiente' of the University of Jaen.
- **EMERGIENDO CON EL SOL. Apoyo institucional al Centro de Energías Renovables de la Universidad Nacional de Ingeniería de Lima (Perú) en el campo de la generación de energía eléctrica empleando tecnología fotovoltaica,** funded by the program of 'Proyectos de Cooperación Internacional para el Desarrollo de la Agencia Andaluza de Cooperación Internacional'.

References

[1] National Instruments, http://www.ni.com/labview/ LabVIEW, National Instruments Website.

[2] International Electrotechnical Commission. Standard IEC 60904-9: Photovoltaic Devices. Part 9: Solar Simulator Performance Requirements. IEC Central Office: Geneva, Switzerland, 2007.

[3] Duran, E., Piliougine, M., Sidrach-De-Cardona, M., Galan, J., & Andujar, J. M. (2008). Different methods to obtain the I-V curve of PV modules: A review. Conference Record of the IEEE Photovoltaic Specialists Conference. http://doi.org/10.1109/PVSC.2008.4922578

[4] Neuenstein J., Podewils C (2009). "Los módulos y sus curvas." Photon. La revista de fotovoltaica, pp. 54-71.

[5] J.V. Muñoz, J. de la Casa, M. Fuentes, J. Aguilera, J.C. Bertolin. "NEW PORTABLE CAPACITIVE LOAD ABLE TO MEASURE PV MODULES, PV STRINGS AND LARGE PV GENERATORS". Procedings of 26th European Photovoltaic Solar Energy Conference 4276- 4280

[6] IEC 60891. "Photovoltaic Devices. Procedures for Temperature and Irradiance Corrections to Measure I-V Characteristics". 2nd edn, International Electrotec

[7] García, M., Maruri, J. M., Marroyo, L., Lorenzo, E. and Pérez, M. (2008), Partial shadowing, MPPT performance and inverter configurations: observations at tracking PV plants. Progress in Photovoltaics

[8] D. Picault, B. Raison, S. Bacha, J. de la Casa, J. Aguilera, Forecasting photovoltaic array power production subject to mismatch losses, Solar Energy, Volume 84, Issue 7, July 2010, Pages 1301-1309, ISSN 0038-092X,

[9] Sanchis, P., López, J., Ursúa, A., Gubía, E. and Marroyo, L. (2007), On the testing, characterization, and evaluation of PV inverters and dynamic MPPT performance under real varying operating conditions. Prog. Photovolt: Res. Appl., 15: 541–556. doi:10.1002/pip.763

[10] M.A. Munoz, M.C. Alonso-García, Nieves Vela, F. Chenlo, Early degradation of silicon PV modules and guaranty conditions, Solar Energy, Volume 85, Issue 9, September 2011, Pages 2264-2274, ISSN 0038-092X

[11] Ryan M. Smith, Dirk C. Jordan, and Sarah R. Kurtz, Outdoor PV Module Degradation of Current-Voltage Parameters, 2012 World Renewable Energy Forum

[12] Araujo, G., Sánchez, E., 1982. Analytical expressions for the determination of the maximum power point and the fill factor of a solar cell. Solar Cells 5, 377–386.

[13] Osterwald, C.R., 1986. Translation of device performance measurements to reference conditions. Solar Cells 18, 269–279.

[14] Firman, A., Toranzos, V., Busso, A., Cadena, C., & Vera, L. (2011). "Determinación del Punto de Trabajo de Sistemas Fotovoltaicos Conectados a Red: Método Simplificado de Traslación Punto a Punto a Condiciones Estándar de Medida". Avances en Energías Renovables y Medio Ambiente, 15, 1-8.

[15] CEI 60891, Procedures for temperature and irradiance corrections to measuremend I-V characteristics of crystalline silicon photovoltaic devices, First edition 04-1987, Ginebra, 1987.

[16] Ali M. Humada, Mojgan Hojabri, Saad Mekhilef, Hussein M. Hamada, Solar cell parameters extraction based on single and double-diode models: A review, Renewable and Sustainable Energy Reviews, Volume 56, April 2016, Pages 494-509, ISSN 1364-0321

[17] J.I. Rosell, M. Ibáñez, Modelling power output in photovoltaic modules for outdoor operating conditions, Energy Conversion and Management, Volume 47, Issues 15–16, September 2006, Pages 2424-2430, ISSN 0196-8904,

PUBLICACIÓN VI

Título	**"Analysing Concentrating Photovoltaics Technology Through the Use of Emerging Pattern Mining"**
Autores	García-Vico, A.M; Montes-Romero, J.; Aguilera, J; Carmona, J.; del Jesus, M.J.
Revista	Advances in Intelligent Systems and Computing
Congreso	International Joint Conference SOCO'16-CISIS'16-ICEUTE'16
Páginas, año	334-344, 2016
CiteScore Rank:	Computer Science: General Computer Science (156/195)
Categoría y posición	Engineering: Control and Systems Engineering (186/224)
Factor de impacto SJR	0.174
DOI	10.1007/978-3-319-47364-2_32

Analysing Concentrating Photovoltaics Technology Through the Use of Emerging Pattern Mining

A.M. García-Vico[1], J. Montes[2], J. Aguilera[2], C.J. Carmona[3(✉)], and M.J. del Jesus[1]

[1] Department of Computer Science, University of Jaén, 23071 Jaén, Spain
{agvico,mjjesus}@ujaen.es
[2] Department of Electronics and Automatization Engineering, University of Jaén, 23071 Jaén, Spain
aguilera@ujaen.es
[3] Department of Civil Engineering, University of Burgos, 09006 Burgos, Spain
cjcarmona@ubu.es

Abstract. The search of emerging patterns pursues the description of a problem through the obtaining of trends in the time, or characterisation of differences between classes or group of variables. This contribution presents an application to a real-world problem related to the photovoltaic technology through the algorithm EvAEP. Specifically, the algorithm is an evolutionary fuzzy system for emerging pattern mining applied to a problem of concentrating photovoltaic technology which is focused on the generation of electricity reducing the associated costs. Emerging patterns have discovered relevant information for the experts when the maximum power is reached for the cells of concentrating photovoltaic.

Keywords: Emerging pattern mining · Concentrating photovoltaics · Evolutionary fuzzy system · Supervised descriptive rule discovery

1 Introduction

In data mining process there are two inductions clearly differentiated, predictive and descriptive induction. However, the last years there has been a great interest in the community about supervised descriptive rule discovery [18]. Latter includes a group of techniques for describing a problem through supervised learning such as subgroup discovery [4,14] or emerging pattern mining (EPM) [9], amongst others.

This contribution presents the application of the EPM technique to a real-world problem. The main objective of this data mining technique is to search for patterns with the ability to find large differences between datasets or classes. This property has led to the use of EPM in predictive induction with good results but not in descriptive induction although they were defined for this purpose. Specifically, the EPM algorithm employed in this contribution is the EvAEP algorithm

M. Graña et al. (eds.), *International Joint Conference SOCO'16-CISIS'16-ICEUTE'16*, Advances in Intelligent Systems and Computing 527, DOI 10.1007/978-3-319-47364-2_32

which is an evolutionary fuzzy system (EFS) [13]. These systems are based on evolutionary algorithms [11] which offer advantages in knowledge extraction and in rule induction process. In addition, they use fuzzy logic [23] with the use of fuzzy sets with linguistic labels in order to represent the knowledge allowing to obtain representation of the information very close to the human reasoning [16].

The algorithm is applied to a Concentrating Photovoltaic (CPV) problem which is an alternative to the conventional Photovoltaic for the electric generation. CPV technology is based on using concentrated sunlight to produce electricity in a cheaper way by means of high efficiency multi-junction solar cells, specifically designed for this type of technology. The efficiency of this type of solar cells has experienced a fast evolution in the last decade and it has a very strong potential of increasing along next years. Despite of these expectations, several obstacles to develop CPV technology currently still remain, as the lack of CPV normalisation and standardisation, the lack of knowledge of the influence of the meteorological parameters on the performance of high efficiency multijunction solar cells. Therefore it is necessary to deepen in the study and knowledge of CPV technology. Results obtained in this contribution are very promising when maximum power is obtained by cells analysed.

The paper is organised as follows: Sect. 2 describes the background of the contribution with the presentation of EPM and CPV. Next, Sect. 3 shows the main properties and features of the algorithm EvAEP that is the first EFS for extracting EPs throughout the literature. Section 4 outlines the experimental framework, shows the results obtained, and an analysis about these results. Finally, some concluding remarks are outlined.

2 Background

2.1 Emerging Pattern Mining

The EPM was defined in 1999 [8] as itemsets whose support increase significantly from one dataset to another in order to discover trends in data. In this way, an itemset is considered as emerging when the growth rate (GR) is upper than one, i.e.:

$$GR(x) = \begin{cases} 0, & IF\ Supp_{D_1}(x) = Supp_{D_2}(x) = 0, \\ \infty, & IF\ Supp_{D_2}(x) = 0\ \wedge\ Supp_{D_1}(x) \neq 0, \\ \frac{Supp_{D_1}(x)}{Supp_{D_2}(x)}, & another\ case \end{cases} \quad (1)$$

where $Supp_{D_1}(x)$ is the support for the pattern x in the first dataset and $Supp_{D_2}(x)$ is the support with respect to the second dataset, i.e. $Supp_{D_1}(x) = \frac{count_{D_1}(x)}{|D_1|}$ and $Supp_{D_2}(x) = \frac{count_{D_2}(x)}{|D_2|}$. This concept could be generalised for one dataset with different classes, for example, $D_1 \equiv Class$ and $D_2 \equiv \overline{Class}$.

The most representative algorithm is DeEPs [19] which is based on the borders concept. A border is a pair of minimal and maximal patterns $< L, R >$ in order to represent all patterns within this border. As can be intuited the search

space could become huge considering a complex problem. Therefore, authors have used different heuristics and techniques in order to reduce the search space and obtaining better results.

To facilitate to the experts and the community the analysis of the knowledge extracted, this is represented through the use of rules (R) with the following representation:

$$R : Cond \rightarrow Class$$

where $Cond$ is commonly a conjunction of attribute-value pairs as definitions mention, and $Class$ is the analysed value for the class, i.e. the class with a high support in front of the remaining classes for the dataset.

2.2 CPV Technology

Photovoltaic technology has experienced a major boost because it is a method of generating electrical power by converting solar radiation into direct current electricity using solar panels composed of a number of solar cells containing a semiconductor material. A variant of this technology is the CPV which is based on using concentrated sunlight to produce electricity in a cheaper way by means of high efficiency multi-junction solar cells, specifically designed for this type of technology. The efficiency of this type of solar cells has experienced a fast evolution[1]. In addition, CPV technology needs to use solar trackers, allowing an important increment of the energy generated by the system with a lower cost. Despite of these expectations, several significant obstacles to the development of CPV technology currently still remain:

- The lack of CPV normalisation and standardisation.
- The complexity and variety of solar cells.
- The lack of knowledge of the influence of meteorological parameters on the performance of high efficiency multi-junction solar cells. In fact, in real projects the productivity of this type of technology has been below expectations.
- The lack of detailed experimental and operational data about real outdoor performance.
- The development of complex regression models for performance.

The most interesting parameter to analyse is the Maximum Module Power (P_m). For each kind of solar cell, the manufacturer measures the CPV module under certain atmospheric conditions (called Standard Test Conditions, STC) and provides the $P_{m,STC}$. Nevertheless, in a real operation these conditions are not satisfied and the performance of the CPV module can be very different from that indicated by the manufacturer. It is known that P_m is highly influenced by atmospheric conditions, but it is necessary to know what happens with the combination of real atmospheric conditions. This knowledge can be very useful for predicting energy production in a certain period of time.

[1] http://www.nrel.gov/ncpv/images/efficiency_chart.jpg.

The DNI is considered as the main atmospheric parameter which influences the outdoor electric performance of a CPV module. Using the DNI as the integration value along the whole wavelength range for a specific photovoltaic device is a common practice. Nevertheless, we can consider the DNI value for each wavelength value, obtaining the *solar spectrum distribution*. As has been widely demonstrated, the DNI, as well as its spectral distribution, have an important influence on the electric performance of multi-junction solar cells. It is well known that the multi-junction solar cells temperature affect to their electric performance. In this sense, the temperature has an almost negligible positive effect on the short circuit current delivered by the multi-junction solar cell, and a negative predominant effect on both the open circuit voltage and P_M [12,17]. The same behaviour is observed when analysing the impact of the temperature (T_A) on the electric performance of CPV modules equipped with multi-junction solar cells [21]. However, the own disposition of the multi-junction solar cells inside the CPV module makes it very difficult to measure their temperature. In this work, T_A is considered as influential factor, given a direct relation between cell temperature and T_A [1,2]. The consideration of the wind (W_S) as one of the influential factors whose contribution must be added to the study because it can perform a positive refrigerating effect on the electric performance of a CPV system, cooling the multi-junction solar cells which compose the module down, and obtaining therefore a better behaviour [7]. However, high W_S values can also exert a negative effect of misalignment on the tracker [20], displacing the multi-junction solar cells from their optimum arrangement in the solar beam direct trajectory. Finally, for this contribution have been considered the incident global irradiance (G) and the spectral irradiance distribution of G described through the average photon energy (APE) and the spectral machine radio (SMR). Both parameters intend to define the shape of the solar spectrum in an easy way. The use of one or the other depends of the monitorised parameter during the experimental campaign.

3 EvAEP: Evolutionary Algorithm for Extracting Emerging Patterns

This section describes the algorithm Evolutionary Algorithm for extracting Emerging Patterns (EvAEP) presented in [6]. This algorithm is able to extract emerging fuzzy patterns in order to describe a problem from supervised learning. The main objective of the EvAEP is the extraction of an undetermined number of rules to describe information with respect to an interest property for the experts. It is important to note that a target variable is able to have different values or classes, in this way the algorithm obtain patterns for all values of the target variable because it is executed once for each value.

The algorithm is an EFS [13] that is a well-known hybridisation between a fuzzy system [23] and a learning process based on evolutionary computation [10]. EvAEP employs an evolutionary algorithm with a codification "Chromosome = Rule" where only the antecedent part of the rule is represented, and

the antecedent is composed by a conjunction of pairs variable-value. Figure 1 represents the phenotype and genotype for a chromosome = rule in the EvAEP algorithm. As can be observed, the value 0 represents the absence of a variable in the representation of a rule.

$$\underbrace{\left|\begin{array}{c|c|c|c} x_1 & x_2 & x_3 & x_4 \\ 3 & \emptyset & 1 & \emptyset \end{array}\right|}_{Genotype} \Rightarrow \underbrace{\text{IF } (x_1 = 3) \text{ AND } (x_3 = 1) \text{ THEN } (x_{Obj} = ValorObjetivo)}_{Phenotype}$$

Fig. 1. Representation of a chromosome = rule for the EvAEP algorithm

On the other hand, if the variable has a continuous range, the algorithm employs a fuzzy representation with fuzzy sets composed by linguistic labels defined with uniform triangles forms.

The algorithm uses a mono-objective approach with an iterative rule learning (IRL) [22] which is executed once for each value of the target variable, i.e., for each class the best individuals are obtained in an iterative process. In this way, the algorithm iterates in order to obtain emerging patterns until a non-emerging pattern is obtained. Moreover, the algorithm stops if all instances for the class are covered for the patterns obtained previously or a pattern with null support is obtained.

The main operation scheme for the EvAEP algorithm is shown in Fig. 2.

The main elements of the algorithm are described in the following subsections.

BEGIN
Set of Emerging Patterns = ∅
repeat
  repeat
    Generate P(0)
    Evaluate P(0)
    repeat
      Include the best individual in P(nGen+1)
      Complete P(nGen+1): Cross and Mutation for individuals of P(nGen)
      Evaluate P(nGen+1)
      nGen ← nGen + 1
    until Number of evaluations is reached
    Obtain the best rule (R)
    Emerging Patterns ∪ R
    Marks examples covered by R
  until (GrowthRate(R) ≤ 1) OR (R has null support) OR (R not cover new examples)
until Class = ∅
return Emerging Patterns
END

Fig. 2. Operation scheme for EvAEP

3.1 Biased Initialisation

EvAEP generates an initial population (P_0) with a size determined through external parameter. The objective of this function is to create a part of the individuals with a maximum percentage of variables being part of the rule. Specifically, the algorithm creates a population with 50 % of the individuals generated in a random way completely, and the remaining individuals of the population must have at least one variable with a value and a maximum number of variables (80 %) with values.

This operator allows the obtaining of a first population with a wide generalisation in order to explore the major area in the search space. In the evolutionary process the main idea is to maximise precision of the rules.

3.2 Genetic Operators

The population of the next generation is generated through some genetic operators widely used throughout the literature. The algorithm employs an elitism size equal to one, in this way the best individual is saved directly in the population of the next generation. The best individual is measured through an aggregation function such as:

$$NSup(R) * 0.5 + Fitness(R) * 0.5 \tag{2}$$

where $NSup(R)$ is the number of examples covered for the rule R non-covered for the previous patterns obtained, divided by the number of remaining examples to cover for the class. The $Fitness$ is detailed in the following section. In case of tie, the individual with less number of variables is considered as the winner.

On the other hand, the algorithm employs the operator multi-cross point operator [15] and a biased mutation introduced in one algorithm of subgroup discovery [3].

3.3 Fitness Function

It is the key concept of the algorithm because the main objective is to search for emerging patterns with high values in confidence and precision, with the maximum generalisation possible, and finally, an interesting gain of accuracy for the community. The fitness employed by EvAEP is defined below:

$$Fitness(R) = \sqrt{TPr * TNr} \tag{3}$$

where a geometric average for an individual is used in order to maximise the precision in the class and non-class in a balance way. The first component (TPr) is known as *True Positive rate* or sensitivity and it measures the percentage of examples correctly classified for the class, and the second (TNr) is known as *True Negative rate* where the measurement of examples non-covered correctly is considered.

4 Experimental Study

The data were obtained from one model of CPV modules, whose main characteristics are solar cells type $Multijunction - GaInP/Ga(In)As/Ge$ with 25 solar cells and a concentration factor of 550. The measures were acquired at the rooftop of the Higher Polytechnical School of Jaén during the period between March 2013 and November 2013, forming a whole dataset composed of 8780 samples. The characteristics of data collected, recorded every 5 min, are shown in Table 1. In summary, this system is able to simultaneously measure P_m of the CPV modules and the outdoor atmospheric conditions that influence the performance of the module.

Table 1. Characteristics of data collected by the Automatic Test & Measurement System

Variable	Name	Range	Unit
DNI	Direct normal irradiance	[600, 1040]	W/m^2
T_A	Ambient temperature	[6, 44]	°C
W_S	Wind speed	[0, 25]	m/s
G	Incident global irradiance	[650, 1370]	W/m^2
APE	Spectral irradiance distribution of G, described through average photon energy	[1.72, 2.28]	
SMR	Spectral irradiance distribution of G, described through spectral machine radio	[0.65, 1.25]	

It is important to remark that the experimentation process is performed through a separation between training and test dataset. In this case, we use 80 % (training) of the whole dataset to calculate the EPs. Otherwise, 20 % (test) of the whole dataset was used to validate the descriptive capacity of the proposed model.

For the type of solar module under study (Fig. 3), P_m values under 64.5 W are not significant, and the samples of the dataset with these values have been removed. P_m values have been discretised in three different intervals according to the $P_{m,STC}$ provided by the manufacturer for this kind of module (150 W) and the expert criteria. These intervals are depicted in Table 2, where P_m *range* are the values of the intervals defined on P_m (in W) and % P_m *range* is the percentage with respect to the maximum power established by the manufacturer (150W). In addition, the percentage of instances for each values is shown.

The results obtained by the algorithm EvAEP have been summarised in Table 3 where the rule (R) and its quality measures GR, TPr and FPr are shown. As we have mentioned previously, the GR is the growth rate of the rule, TPr is the true positive rate and FPr is the false positive rate that measures the ratio between the examples covered incorrectly and the number of examples for the non-class.

Fig. 3. Solar tracker at High Technical School of the University of Jaen

Table 2. Intervals defined by experts for P_m variable

Interval	P_m range	% P_m range	% of instances
2	[64.5, 93]	(43 %, 62 %]	20 %
3	(93, 121.5]	(62 %, 81 %]	68 %
4	(121.5, 150]	(81 %, 100 %]	12 %

Table 3. Results obtained in *Concentrating Photovoltaic Module* dataset

Rule	GR	TPr	FPr
R_1: IF $DNI =$ Very Low THEN $P_m = 2$	5.30	0.524	0.098
R_2: IF $DNI =$ Low THEN $P_m = 2$	75.89	0.362	0.004
R_3: IF $G =$ Medium THEN $P_m = 3$	1.35	0.889	0.656
R_4: IF $APE =$ Low THEN $P_m = 3$	1.05	0.993	0.942
R_5: IF $DNI =$ Medium THEN $P_m = 3$	4.33	0.397	0.091
R_6: IF $DNI =$ High AND $APE =$ Low AND $T_A =$ Medium AND Ws = Medium THEN $P_m = 4$	3.87	0.037	0.009
R_7: IF $DNI =$ High AND $APE =$ Low THEN $P_m = 4$	9.92	0.134	0.013
R_8: IF $APE =$ Low AND $T_A =$ Low AND $W_S =$ Medium AND $SMR =$ High AND $G =$ High THEN $P_m = 4$	31.00	0.033	0.001
R_9: IF $APE =$ Low AND $T_A =$ Low AND $W_S =$ Low AND $SMR =$ High AND $G =$ High THEN $P_m = 4$	5.81	0.025	0.004
R_{10}: IF $APE =$ Low AND $T_A =$ Very Low AND $SMR =$ High THEN $P_m = 4$	21.31	0.046	0.002

As can be observed in the results obtained in this contribution could be performed different analysis conditioned to the power analysed:

- Low power: For this class are obtained the rules with the highest GR. In addition, the rules extracted have a good balance between TPr and FPr where the number of examples covered are in almost all cases of the class analysed.
- Medium power: In this class there is an emerging pattern that should be discarded, the rule 4 because is very general and the ratio between TPr and FPr is very similar and close to the 100 %, i.e. this rule covers all examples for the dataset both positive and negatives examples in the same ratio. On the other hand, rule 3 and 5 continue the tendency of the analysis where a major value for DNI is synonyms of major power.
- High power: For this class are obtained very specific rules but with good values in GR and relationships between TPr and FPr. As can be observed, all rules have a low value for APE which is a very interesting value, however it is important to note that this value is combined with a high value for DNI or SMR, rules 6, 7 or 8, 9, 10, respectively.

In general, a direct relationship between DNI and the P_m can be observed in the study. This assumption confirms the results obtained in a previous analysis performed through subgroup discovery [14] in the paper [5].

5 Conclusions

The CPV technology has been analysed from a new point of view in this contribution, the EPM data mining technique which is a descriptive induction based on supervised learning. The analysis has been performed through the EFS called EvAEP.

Results obtained in this study confirm the possible relationships between atmospheric variables and P_m suspected by CPV experts, as well as some new knowledge. The knowledge extracted on interval of $P_m = [43\,\%, 62\,\%]$ and $P_m = (62\,\%, 81\,\%]$ confirm the existing relations between DNI and P_m. However, there is a new interest obtained when the P_m is maximum because there is a relation in all rules, the values for APE which belongs to the linguistic label Low. In this way, there is an interesting further analysis with respect to the influence of this variable in the performance of the CPV module with maximum P_m and low values for APE.

Acknowledgment. This work was supported by the Spanish Science and Innovation Department under project ENE2009-08302, by the Department of Science and Innovation of the Regional Government of Andalucia under project P09-TEP-5045, and by Spanish Ministry of Economy and Competitiveness under project TIN2015-68454-R (FEDER Founds).

References

1. Almonacid, F., Pérez-Higueras, P., Fernández, E., Rodrigo, P.: Relation between the cell temperature of a hcpv module and atmospheric parameters. Sol. Energy Mater. Sol. Cells **105**, 322–327 (2012)
2. Antón, I., Martínez, M., Rubio, F., Núñez, R., Herrero, R., Domínguez, C., Victoria, M., Askins, S., Sala, G.: Power rating of CPV systems based on spectrally corrected DNI, vol. 1477, pp. 331–335 (2012)
3. Carmona, C.J., González, P., del Jesus, M.J., Herrera, F.: NMEEF-SD: non-dominated multi-objective evolutionary algorithm for extracting fuzzy rules in subgroup discovery. IEEE Trans. Fuzzy Syst. **18**(5), 958–970 (2010)
4. Carmona, C.J., González, P., del Jesus, M.J., Herrera, F.: Overview on evolutionary subgroup discovery: analysis of the suitability and potential of the search performed by evolutionary algorithms. WIREs Data Min. Knowl. Disc. **4**(2), 87–103 (2014)
5. Carmona, C.J., González, P., García-Domingo, B., del Jesus, M.J., Aguilera, J.: MEFES: an evolutionary proposal for the detection of exceptions in subgroup discovery. An application to Concentrating Photovoltaic Technology. Knowl. Based Syst. **54**, 73–85 (2013)
6. Carmona, C.J., Pulgar-Rubio, F.J., García-Vico, A.M., González, P., del Jesus, M.J.: Análisis descriptivo mediante aprendizaje supervisado basado en patrones emergentes. In: Proceedings of the VII Simposio Teoría y Aplicaciones de Minería de Datos, pp. 685–694 (2015)
7. Castro, M., Domínguez, C., Núez, R., Antón, I., Sala, G., A. K.: Detailed effects of wind on the field performance of a 50 kw CPV demonstration plant. In: AIP Conference Proceedings, vol. 1556, pp. 256–260 (2013)
8. Dong, G.Z., Li, J.Y.: Efficient mining of emerging patterns: discovering trends and differences. In: Proceedings of the 5th ACM SIGKDD International Conference on Knowledge Discovery and Data Mining, pp. 43–52. ACM Press (1999)
9. Dong, G.Z., Li, J.Y.: Mining border descriptions of emerging patterns from dataset pairs. Knowl. Inf. Syst. **8**(2), 178–202 (2005)
10. Eiben, A.E., Smith, J.E.: Introduction to Evolutionary Computation. Springer, Heidelberg (2003)
11. Eshelman, L.J., Schaffer, J.D.: Real-coded genetic algorithms and interval-schemata. In: Foundations of Genetic Algorithms 2, pp. 187–202. Kaufmann Publishers (1993)
12. Helmers, H., Schachtner, M., Bett, A.: Influence of temperature and irradiance on triple-junction solar subcells. Sol. Energy Mater. Sol. Cells **116**, 144–152 (2013)
13. Herrera, F.: Genetic fuzzy systems: taxomony, current research trends and prospects. Evol. Intel. **1**, 27–46 (2008)
14. Herrera, F., Carmona, C.J., González, P., del Jesus, M.J.: An overview on Subgroup Discovery: Foundations and Applications. Knowl. Inf. Syst. **29**(3), 495–525 (2011)
15. Holland, J.H.: Adaptation in Natural and Artificial Systems. University of Michigan Press, Ann Arbor (1975)
16. Hüllermeier, E.: Fuzzy methods in machine learning and data mining: status and prospects. Fuzzy Sets Syst. **156**(3), 387–406 (2005)
17. Kinsey, G., Hebert, P., Barbour, K., Krut, D., Cotal, H., Sherif, R.: Concentrator multijunction solar cell characteristics under variable intensity and temperature. Prog. Photovoltaics Res. Appl. **16**(6), 503–508 (2008)
18. Kralj-Novak, P., Lavrac, N., Webb, G.I.: Supervised descriptive rule discovery: a unifying survey of constrast set, emerging pateern and subgroup mining. J. Mach. Learn. Res. **10**, 377–403 (2009)

19. Li, J.Y., Dong, G.Z., Ramamohanarao, K., Wong, L.: DeEPs: a new instance-based lazy discovery and classification system. Mach. Learn. **54**(2), 99–124 (2004)
20. Lin, C.-K., Fang, J.-Y.: Analysis of structural deformation and concentrator misalignment in a roll-tilt solar tracker. In: AIP Conference Proceedings, vol. 1556, pp. 210–213 (2013)
21. Peharz, G., Ferrer Rodríguez, J., Siefer, G., Bett, A.: Investigations on the temperature dependence of CPV modules equipped with triple-junction solar cells. Prog. Photovoltaics Res. Appl. **19**(1), 54–60 (2011)
22. Venturini, G.: SIA: a supervised inductive algorithm with genetic search for learning attributes based concepts. In: Brazdil, P.B. (ed.) ECML 1993. LNCS, vol. 667, pp. 280–296. Springer, Heidelberg (1993). doi:10.1007/3-540-56602-3_142
23. Zadeh, L.A.: The concept of a linguistic variable and its applications toapproximate reasoning. Parts I, II, III. Inform. Sci. **8-9**, 199–249, 301–357, 43–80 (1975)

PUBLICACIÓN VII

Título	**"Contributions to the design and construction of characteristic curve tracers for photovoltaic devices"**
Autores	Fernández, E.F.; Firman, A.; Montes-Romero, J.; Cáceres, M.; Vera, L.H.; de la Casa, J.
Congreso	Technologies Applied to Electronics Teaching (TAEE)
Año	2018
DOI	10.1109/TAEE.2018.8476093

Contributions to the design and construction of characteristic curve tracers for photovoltaic devices

E.F. Fernández, J. Montes-Romero, J. de la Casa
IDEA Research Group, University of Jaén,
Campus Lagunillas, 23071 Jaén, Spain
E.F. Fernández: fenandez@ujaen.es

A. Firman, M. Cáceres, L.H. Vera
GER – Grupo en Energías Renovables - FaCENA – UNNE,
Av. Libertad 5470 – 3400 Corrientes. Argentina

***Abstract*— Tracing the characteristic *I-V* curve of any photovoltaic device is the essential experiment that allows us to obtain reliable information about its state and behavior. Therefore, it must be part of the practical content in any Bachelor's, Master's or PhD degree that teaches the students in the photovoltaic systems engineering field. This paper presents the progress-achievements of two research groups -from Argentina and Spain- in the design of electronic prototypes or ad-hoc systems that carried out this experiment and which have subsequently been integrated into teaching practices. In addition, this knowledge has been incorporated into the research area in which the groups are involved.**

Keywords*— *Photovoltaic systems engineering; electronic charges; Photovoltaic devices characterization, renewable energies teaching.

I. INTRODUCTION

Photovoltaic (PV) electrical generation has been a great success recently in the renewable energies field. As an example, during the period 2005-2015, an annual growth rate of 27 % of investment in PV technology was registered [1]. Besides, during 2016, 75 GWp has been installed in the world [2]. In late 2017, there was a surplus of 320 GWp of global installed power [3]. Currently, countries like China, Japan, USA and Germany are leading the amount of installed PV power, but there are reasons to think that this amount will continue growing around the world, especially in emerging countries due to the need of increasing their electric generation for their development.

Promoting and training qualified personal who lead this emerging market is considered of great importance. To achieve this goal, it is essential to include this topic in engineering studies [4].

There is a direct relationship between the electric and electronic engineering area, and the photovoltaic technology. As an example, the 1st generation of crystalline silicon PV cell is based on a PN junction. In addition, a big part of the equipment required to be used in PV systems (such as inverters, charge regulators, characterization devices, etc.) are widely studied in any degree related with electronic engineering.

To understand the PV technology, it is essential to know how the PV generator works. The experiment that provides more data about the behavior of any PV device is by tracing its *I-V* curve. The *I-V* curve is made up of pairs of points of current and voltage in which -depending on ambient conditions where the device was exposed during the experiment- a PV device can operate. From this set of points it is possible to obtain its main electrical parameters, as well as to determine any type of abnormalities, defects or malfunction states [5]–[8].

The research groups to which the authors belong have more than a decade of experience developing different architectures and design solutions directly related with that experiment. This equipment have been used in their research work and incorporated in their teaching tasks [9]–[12]. A review of the most outstanding achievements is presented next.

II. THEORETICAL FUNDAMENTS OF I-V CURVE TRACING

Figure 1 shows a typical *I-V* curve of a PV device. This characteristic curve is composed by current and voltage points obtained in working conditions when its output impedance varies from zero to infinite. Figure 1 also shows the points of main interest, generally given by manufacturers in their datasheets. Three principal locations can be distinguished: the short circuit current (*Isc*), the open circuit voltage (*Voc*) and the point of maximum power (*Pm*), this last one defined by the maximum voltage (*Vm*) and the maximum current (*Im*).

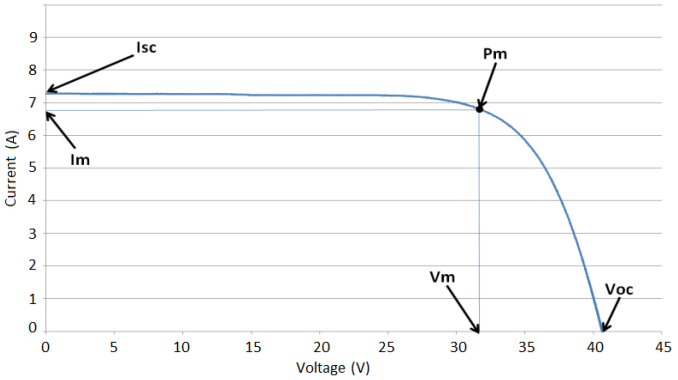

Figure 1. IV characteristic curve of a PV module and highlighted mains points.

Besides of these electrical values that can be obtained directly from the *I-V* curve, other important parameters can be obtained by adjusting these set of points by mathematical models [13], which adjust an equivalent electrical model of a cell, a module or of a PV generator. These parameters will be -in the case of the five parameters electrical model- the photogenerated current (*Iph*), the diode inverse saturation current (*Io*), the diode ideality factor (*m*), the series resistance (*Rs*) and the shunt resistance (*Rsh*) [14]–[17].

All electrical parameters obtained during the *I-V* curve tracing are depending on the PV device technology and the operations conditions. Evidently, the most influencial parameter

978-1-5386-0928-6/18/$31.00 ©2018 IEEE

is the plane incident irradiance. This parameter is almost directly proportional to the obtained current. In a second order of magnitude, the cell temperature that affects, like in any semiconductor, the voltage value.

The PV module manufacturers provide the basic electrical parameters values under specific ambient conditions known as Standard Test Conditions (STC), these are defined in the standard IEC 60891 [18] and these are: irradiance of 1000 W/m², cell temperature of 25°C and solar spectrum AM 1.5.

Finding natural conditions similar to those defined in the STC can be extremely complicated. For this reason, there are extrapolation methods to STC [19]–[21]. In this sense, there is a normalized procedure to perform a translation from an IV curve in the standard IEC 60904 [22]. These methods have been of interest in teaching articles intended for students of PV solar energy [23].

In order to achieve the characteristic *I-V* curve tracing, a common basic electronic laboratory equipment is necessary. Roughly, a curve *I-V* tracer is an electronic system able to produce an impedance variation between zero and infinite, thereby it makes a sweep in all the PV element range of work when it is polarized. Besides, for the reason exposed previously, the system must register quasi-simultaneously the ambient parameters at the moment of the test, mainly the irradiance and cell temperature. As its continuous measuring under the entire time test is not always possible, it can be determined at the beginning and at the end of the process only, and finally, check if the value have not changed significantly during the testing time to validate the experiment.

Although it is not one of the main objectives of this paper, for the irradiance measurement two main options can be found. One option is measuring by piranometers and the other is to measure by reference PV cells or reference PV modules [24]. If the reference PV device was constructed with the same materials as the device under test, and it is deployed coplanarly, this device will respond, angular and spectrally, in the same way as the device under test. It leads to neglecting spectral changes if these devices are calibrated under the reference spectrum AM 1.5.

In order to measure the cell temperature, it is indicated that its value is approximately the same when the measurement is done at the back of the PV module. The most used sensor to achieve this measurement is by a platinum resistance (PT100) coupled in the back of the PV module as is recommended in the IEC 61724-1 annex B [25]. Performing the measurement in four-wire configuration is also suggested to avoid voltage drop in the conductors and improve the accuracy.

As is obvious, the market offers equipment destined for IV curve tracing. This equipment presents the advantages of any commercial device: they have been tested and characterized by the manufacturer, but they often have a high price and it can be prohibitive for certain research groups or for dedicated teaching laboratories. Another inconvenience is that commercial products usually include exclusive sensors for irradiance and temperature measurement, which can be difficult to replace for other types if required. The algorithms of data treatment or translation to STC are closed and they cannot be accessed. In addition, they usually do not include detailed information about the measure uncertainties or the data treatment processes [26]–[28]. Summarizing, commercial equipment is usually created for professional use.

Any IV curve tracing system can be divided in a basic block diagram as is shown in Figure 2. In that figure, three main blocks can be distinguished: impedance variation block, measurement block and control block.

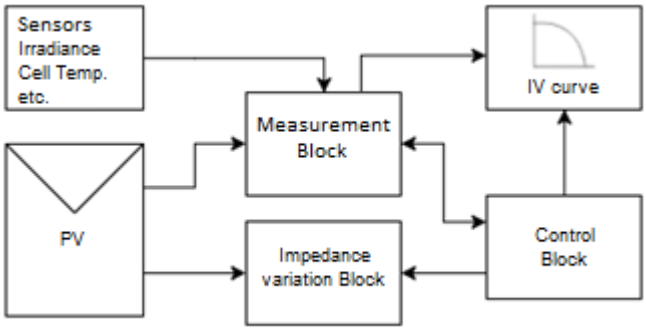

Figure 2. Basic block diagram of any *I-V*.

III. IMPEDANCE VARIATION BLOCK

The impedance variation block is responsible for performing the entire *I-V* curve sweep of PV module varying its polarization point. For this purpose, different types of procedures – summarized in [27] - can be distinguished. The type of procedure should be chosen and designed in function of the PV device electrical characteristics, and the available equipment and materials. The possible methods are: variable resistors, four quadrant power sources, DC/DC converters, active loads and capacitive loads.

The simplest method is using variable resistors. The impedance has to be modified manually, so the operation point can be chosen at each time. The main inconvenience of this method is the power dissipation. The resistor must dissipate all the energy generated by the PV device in each moment. This can be an interesting solution for teaching purposes if low power modules are used, and therefore, the heating problems of dissipation can be neglected. An automation of this method can be hard to carry out.

Another method is using commercial four quadrants power sources like, for example, those offered by Kepco [29]. This device can adjust the PV module operation point to a determined voltage in any of the four quadrants -being especially useful the first, but also the second and the fourth quadrant- and, performing like current sink, it absorbs the PV energy generated. The objective of polarizing from negative voltages to positive currents is to determine with accuracy Voc and Isc points when the axes crossing occurs. For example, for

Isc point, it can be difficult to obtain due to series resistances of other elements (wiring, switchers, contacts, shunts, etc). In this way the points can be perfectly determined. At first, this method can seem a simpler solution, however this type of power sources are devices of very high cost, with limited voltages and current ranges, and they have an important size that hinders their transport, relegating them to be used in laboratories. In this aspect, being able to adjust the PV device operation point is interesting for teaching purposes.

The combined experience of the research groups in that type of system is based in [30], where a four quadrant source to control the PV module operation point was used in an entire characterization system at the University of Málaga, as is shown in the Figure 3.

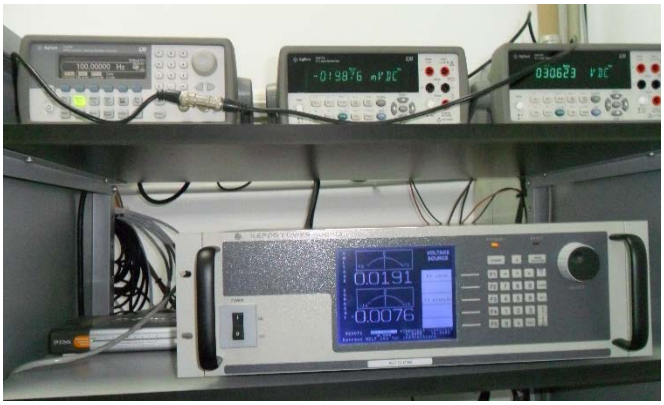

Figure 3. *I-V* curve tracer system based on a four-quadrant power source installed at the University of Málaga.

DC/DC converters are another possible solution to achieve *I-V* curve sweep. These converters have the possibility of changing its impedance depending on its duty cycle. This feature makes it appropriate to solve the sweep problem. A simplified schematic of a power stage of this type of converter is shown in the Figure 4. The main issue of that type of system is the management and dissipation of the energy generated by the PV device during the test. In order to be able to handle a greater amount of power, it is necessary to make series or parallel converters associations. This can be an advantage because it becomes a modular system. Nevertheless, special design strategies are required to avoid excessive ripple in the IV curve obtained.

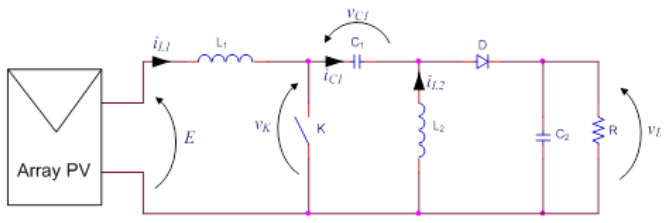

Figura 4. Simplified diagram of the power stage by DC/DC converters.

This type of load has been used for the research groups in bachelor thesis and it was published in [31]. In this system, four SEPIC (Single-ended primary-inductor converter) type converters were used, allowing *I-V* curve tracing up to *Voc* = 400 V and *Isc* = 10 A, achieving 400 W of dissipated direct power. One of the development systems can be seen in Figure 5.

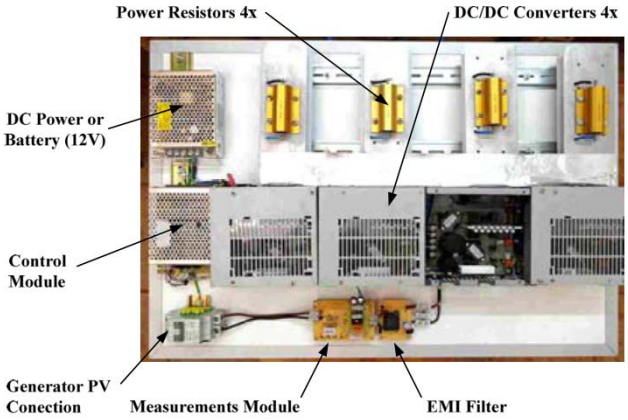

Figure 5. *I-V* curve tracer system based on DC/DC converters.

A relevant feature of the four quadrant power sources and the DC/DC converters is that the *I-V* curve sweep can be done in both directions. It is possible to trace from the point of *Isc* to *Voc* or backwards.

Performing the impedance variation through active type loads is also possible. Their operation is based on the work of transistors in active zone. To change its impedance, the working operation zone is changed from the saturation stage to short circuit stage, producing a variation in the PV module operation point from *Voc* to *Isc*. The transistors used must be able to dissipate the entire power generated during the *I-V* curve tracing, thus, the active load must have the necessary heat dissipation capacity. To solve this problem, parallel associations are done to increase that capacity. Even so, the maximum permitted junction temperature of these components cannot be exceeded. For that reason, it is advisable to use high sweep rates. One of the possible designs with an active load is shown in Figure 6.

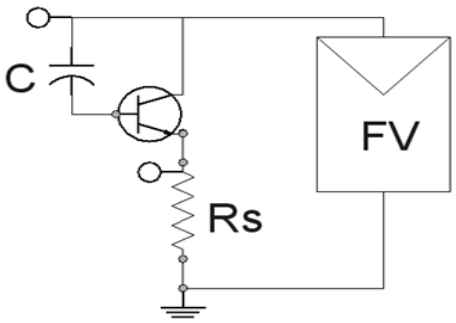

Figure 6. Simplified diagram of a power stage by active load with bipolar transistor.

As experience of the research groups, active loads based in bipolar transistors have been used to achieve the impedance

variation and the consequent power dissipation from the PV device [10]. A prototype of that system is shown in Figure 7.

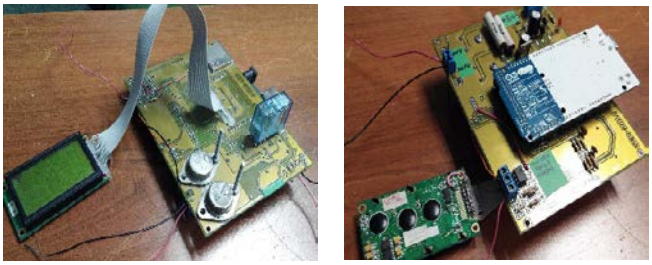

Figure 7. *I-V* curve tracer system based on active load by bipolar transistor installed at the Universidad Nacional del Nordeste.

Finally, the capacitive loads are another way to perform the *I-V* curve tracing. Its operation is based in a capacitive charge transient. For this, a completely discharged capacitor (or a bank of them) will start its charge process from zero impedance up to infinite when its charge is complete. During the charge process, the PV module varies its operation point completely. The voltage and current curves of this process can be seen in Figure 8.

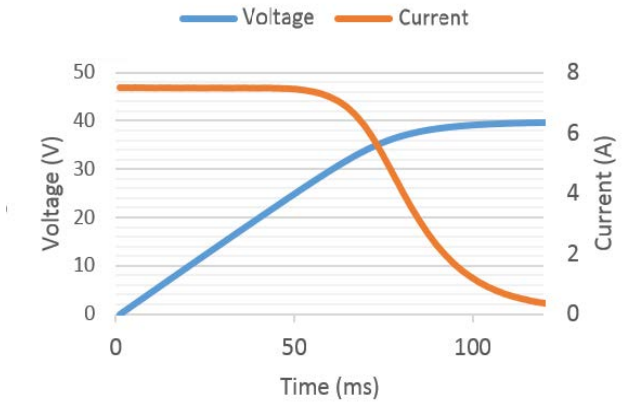

Figure 8. Voltage and current waveform in the capacitor charge process.

The main advantages of that type of load are the simplicity and there is no power dissipation during the tracing. The PV module generated energy is stored in the capacitor bank, which later will be discharged onto a power resistance in a completely controlled process. As a main disadvantage, this process does not permit the PV module polarization on a determined point. Besides, due to the waveform presented for the capacitor, the measures will be gradually more grouped as they approach to *Voc*, as Figure 8 shows.

The research groups have developed a wide experience in the design and implementation of systems using this method [9], [12], [32]. Due to the simplicity and the low cost of that type of charges, several models of I-V curve tracers based on this methodology have been made over the last few years, and it is the most common method at present in the research groups. Figure 9 shows a picture of one of the systems developed.

Figure 9. *I-V* curve tracer system based on a capacitive load and installed at the University of Jaén.

IV. Measurement Block

The measurement block will be responsible for acquiring-conditioning the voltage-intensity values simultaneously. In addition, this block will obtain the relevant environmental parameters present at the time of the experiment.

In Figure 10, a simplified connection diagram to perform the measurement of the voltage-current pairs is presented.

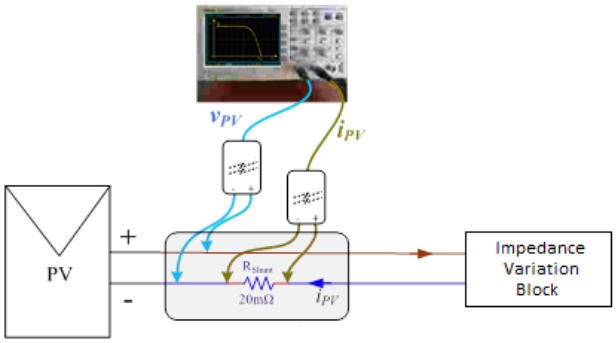

Figure 10. General schematic of the connections to perform the measurements of the PV device.

The measurement simultaneity of the voltage and current parameters is essential, so it is necessary to ensure that the measured pairs coincide with the same time base.

In most cases, the measurement of the current is done indirectly. For this purpose, the current measurement can be obtained by the voltage drop on a shunt resistor. Also, a Hall effect sensor can be used. This kind of sensor has the advantage of not requiring a physical connection with the circuit, but a drift in the measurement -which is complicated to quantify- has been reported. The voltage measurement –in most cases and

using commercial equipment- is done directly. Otherwise, a signal treatment must be done by a voltage divider circuit.

The simplest solution to perform the measurements is by the use of commercial oscilloscopes. A two-channel oscilloscope can perform the measurement of voltage and current of any PV module simultaneously. A better solution is using a four-channel instrument with isolated channels. This permits the measurement of the I-V pairs and the measurement of two basic ambient sensors.

The main advantages of using oscilloscopes to perform the measurements are the simplicity of its use, high sampling rate and the synchronization of the current and voltage measurements.

When using commercial multimeters, they must be able to allow synchronization through an external trigger, ensuring the measurements are performed simultaneously. Most of them can also perform resistance measurements, allowing the use of temperature resistive sensors directly.

The main advantage of these instruments is the high precision. As disadvantage –due to the need of two instruments- the rise in the final cost of the system, but the development of these instruments through software such as LabVIEW can be a very formative practice of any student.

Without dispose commercial equipment, electronic systems based, for example, on open-source hardware platforms can be used. The choice of the electronic components must satisfy the conditions exposed previously. The elaboration of an ad-hoc measurement system can be complex but it can be carried out by a specialized engineer.

As expected, not using commercial equipment will reduce substantially the budget of the system. The complexity of the design of a complete system and the difficulty of ensuring the measurement quality are the main obstacles of this kind of system.

For the measurement task, during the years of experience of the research groups, different kinds of oscilloscopes –two channel, four channel, isolated and common- has been used [31], [33]. In addition, a pair of commercial multimeters –one for voltage and another for current- has been used to measure the *I-V* curve [11], [12], [32]. Electronic measurement circuits have been also designed and developed, adapted to the specific needs of the PV systems.

V. CONTROL BLOCK

As stated in previous sections, once the impedance variation problem is solved with any kind of load, the measurements of current and voltage of the PV module can be taken together with the irradiance and temperature data. All the process is governed by the control block. This block can be a microcontroller device, a datalogger with digital inputs and outputs, a function generator, manual or automatic switches, etc. A control software, employed to sequence the process, manages all the components of the system, depending on the selected load.

In case of the four-quadrant power supplies, the control is performed directly, usually, through a PC. As is normal in commercial equipment, the control varies depending on the manufacturer. As a common characteristic, the control can be programed by software. Therefore, to perform the I-V sweep only a PC with the software is necessary.

The control of the DC/DC converters is carried out by pulse trains: square wave to activate the converters and triangular wave of voltage reference to vary the impedance of the converter. The simplest method to generate these signals is by the use of a signal generator. These instruments ensure the quality of the control signals. A more complex solution is to design the electronic circuit necessary to generate the signals. A possible schematic of this system is presented in Figure 11.

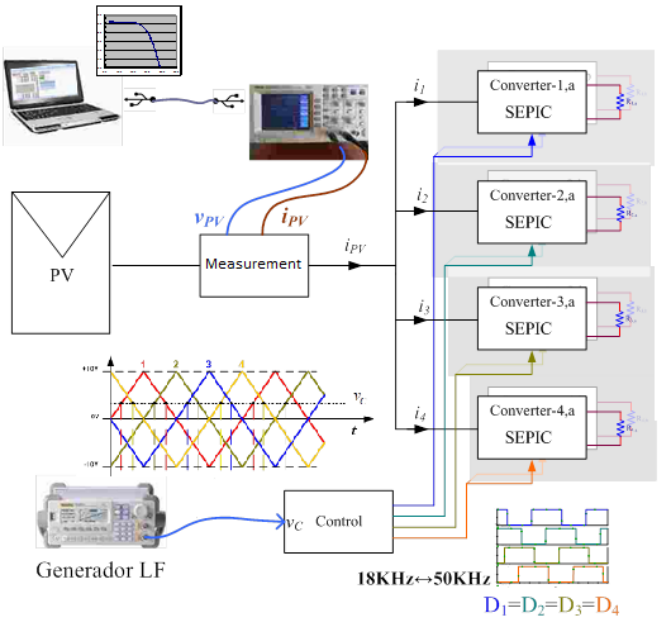

Figure 11. General schematic of a I-V tracing system by the use of DC/DC converters.

The control of active loads is different depending on the technology of the transistor. In the case of bipolar transistors, the control can be done by the current on the base of the transistor. As exposed in [10], the control is done automatically as function of the β parameter of the transistor through the charge of a control capacitor. The sweeping time of the *I-V* curve is governed by the equation (1). For transistors controlled by voltage on the gate (MOSFET and IGBT), the control can be done varying the voltage on an increasing or decreasing function such as sine wave, triangular wave, etc.

$$t = \frac{Voc^2 \cdot C \cdot \beta}{Pm} \quad (1)$$

Switches carry out the control of a capacitive load. The charge and discharge processes are highlighted. By closing the

charge switch SW1 (Figure 12), the process is started. It will stop when the capacitor is completely charged (capacitor voltage and Voc of the PV module are equal). Then, SW1 is opened and the discharge switch SW2 closed. The discharge process will start and the resistor will consume the stored energy in the capacitor. It must be taken into account that the switches must allow the voltage and current provided by the PV module. The dissipated power by these switches will be minimum, but they must allow the PV characteristics. In order to control the process, a wide variety of elements can be used as switches: any technology of transistors (BJT, MOSFET, IGBT), thyristors, solid state relays, electro mechanic relays, etc.

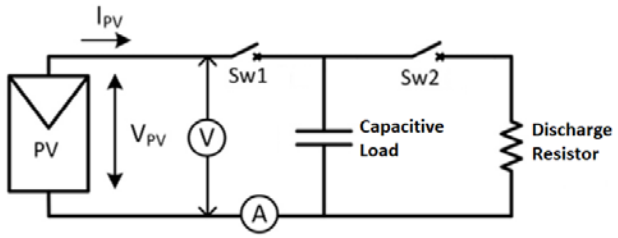

Figure 12. Simplified schematic of a power stage for a capacitive load.

The charging time of the capacitor can be estimated through the equation (2). It will be necessary to consider parameters of the PV generator such as *Voc* and *Pm*. It also depends on the capacity of the capacitor.

$$t = \frac{Voc^2 \cdot C}{Pm} \tag{2}$$

Among the control elements used by the research groups, Arduino boards, TIVA boards, NI-DAQ systems, dataloggers, parallel ports controlled by PC, manual switches, PIC microcontrollers, function generators, etc, can be highlighted.

Those systems can generate the necessary control signals to trace the *I-V* curve. As connection switches for capacitive loads, MOSFET and IGBT transistors, thyristors and solid state relays were used to develop those systems. As control software programming languages such as C, Visual Studio or LabVIEW, must be highlighted.

VI. Conclusions

This article presents descriptively the most relevant aspects of the design and construction of *I-V* curve tracers applied in photovoltaic technology.

Probably, the most important conclusion is the relative ease to incorporate this experiment in any subject related with PV technology with a basic electronic laboratory.

In addition, as is the case of the authors, those subjects are integrated in the electronic engineering or telecommunications degrees. In this case, the design, construction and programming of each block is highly formative for the students. It helps to consolidate and apply knowledge of main subjects in the area (Analog, Digital and Power electronics, Instrumentation, Data Acquisition Systems, etc). It is also considered an option as a bachelor or master thesis because of the integration of different knowledge related to the specialty and applied to a specific case.

Different methods to perform the *I-V* curve trace process have been presented. In order to guide the reader and simplify the process, three blocks have been highlighted: impedance variation, measurement and control.

Undoubtedly, the most important and complex part of the instruments employed to trace the *I-V* curve is the variable load that sweep the whole impedance range. All the different kinds of loads designed and developed by the research groups of the authors have been described and referred. Furthermore, the main parameters that must be considered in the design and implementation of this kind of system has been exposed. Also, references explaining in detail the developed systems have been included.

In this way, this article aims to support the teaching of photovoltaic solar energy through the implementation of *I-V* curve trace systems with teaching and researching purposes. This kind of equipment can be used for both undergraduate and graduate levels.

References

[1] Bloomberg New Energy Finance, “Global Trends in Clean Energy Investment,” 2017.

[2] SolarPower Europe, “Global market outlook for solar power 2017-2021,” 2017.

[3] Fraunhofer Institute for Solar Energy Systems, “Photovoltaics Report,” 2017.

[4] J. De Casa, M. Fuentes, J. V Muñoz, D. L. Talavera, G. Nofuentes, and J. Aguilera, “Herramientas para la docencia de créditos prácticos en asignaturas directamente relacionadas con la energía solar fotovoltaica .,” in *TAEE 2012*, 2012, pp. 168–173.

[5] M. García, J. M. Maruri, L. Marroyo, E. Lorenzo, and M. Pérez, “Partial Shadowing, MPPT Performance and Inverter Configurations: Observations at Tracking PV Plants,” *Prog. Photovolt Res. Appl.*, vol. 15, no. April, pp. 659–676, 2008.

[6] D. Picault, B. Raison, S. Bacha, J. de la Casa, and J. Aguilera, “Forecasting photovoltaic array power production subject to mismatch losses,” *Sol. Energy*, vol. 84, no. 7, pp. 1301–1309, 2010.

[7] M. Piliougine, C. Cañete, R. Moreno, J. Carretero, J. Hirose, S. Ogawa, and M. Sidrach-de-Cardona, “Comparative analysis of energy produced by photovoltaic modules with anti-soiling coated surface in arid climates,” *Appl. Energy*, vol. 112, pp. 626–634, 2013.

[8] A. Firman, V. Toranzos, A. Busso, L. Vera, and J. de la Casa, “Qualitative analysis of electrical mismatch losses in photovoltaic devices,” in *EUPVSEC*, 2013, pp. 3212–3215.

[9] C. Bello, V. Jimenez, V. Toranzos, A. Busso, L. H. Vera, and C. Cadena, “RELEVADOR PORTATIL DE CURVAS I-V DE PANELES FOTOVOLTAICOS COMO HERRAMIENTA DE DIAGNOSTICO IN SITU DE SISTEMAS DE GENERACION FOTOVOLTAICA,” *Av. en Energías Renov. y Medio Ambient.*, vol. 13, pp. 77–83, 2009.

[10] A. Firman, V. Toranzos, A. Busso, C. Cadena, and L. Vera, “Sistema híbrido para la caracterización eléctrica de arreglos fotovoltaicos,” *Av. en Energías Renov. y Medio Ambient.*, vol. 14, pp. 17–23, 2010.

[11] J. V. Muñoz, J. de la Casa, M. Fuentes, J. Aguilera, and J. C. Bertolín, “New portable capacitive load able to measure PV modules, PV strings and large PV generators,” in *26th European Photovoltaic Solar Energy Conference and Exhibition*, 2011, vol. 1, pp. 4276–4280.

[12] J. Montes-Romero, M. Piliougine, J. Muñoz, E. Fernández, and J. de la Casa, "Photovoltaic Device Performance Evaluation Using an Open-Hardware System and Standard Calibrated Laboratory Instruments," *Energies*, vol. 10, no. 11, p. 1869, 2017.

[13] A. M. Humada, M. Hojabri, S. Mekhilef, and H. M. Hamada, "Solar cell parameters extraction based on single and double-diode models: A review," *Renew. Sustain. Energy Rev.*, vol. 56, pp. 494–509, 2016.

[14] M. A. De Blas, J. L. Torres, E. Prieto, and A. García, "Selecting a suitable model for characterizing photovoltaic devices," *Renew. Energy*, vol. 25, no. 3, pp. 371–380, 2002.

[15] J. C. H. Phang, D. S. H. Chan, and J. R. Phillips, "Accurate analytical method for the extraction of solar cell model parameters," *Electron. Lett.*, vol. 20, no. 10, p. 406, 1984.

[16] E. F. Fernández, J. Montes-Romero, J. de la Casa, P. Rodrigo, and F. Almonacid, "Comparative study of methods for the extraction of concentrator photovoltaic module parameters," *Sol. Energy*, vol. 137, pp. 413–423, 2016.

[17] J. Montes-Romero, F. Almonacid, M. Theristis, J. de la Casa, G. E. Georghiou, and E. F. Fernández, "Comparative analysis of parameter extraction techniques for the electrical characterization of multi-junction CPV and m-Si technologies," *Sol. Energy*, vol. 160, no. December 2017, pp. 275–288, 2018.

[18] International Electrotechnical Commission, "IEC 60891, Photovoltaic Devices. Procedures for Temperature and Irradiance Corrections to Measure I-V Characteristics," Geneva, Switzerland, 2007.

[19] G. . Araujo and E. Sánchez, "Analytical expressions for the determination of the maximum power point and the fill factor of a solar cell," *Sol. Cells*, vol. 5, pp. 377–386, 1982.

[20] K. Emery and C. Osterwald, "Measurement of photovoltaic device current as a function of voltage, temperature, intensity and spectrum," *Sol. Cells*, vol. 21, no. 1–4, pp. 313–327, Jun. 1987.

[21] A. Firman, V. Toranzos, A. Busso, C. Cadena, and L. Vera, "Determinación del punto de trabajo de sistemas fotovoltaicos conectados a red: metodo simplificado de traslacion punto a punto a condiciones estandar de medida," *Av. en Energías Renov. y Medio Ambient.*, vol. 15, pp. 1–8, 2011.

[22] International Electrotechnical Commission, "IEC 60904-1, Photovoltaic Devices, Part 1: Measurement of Photovoltaic Current–Voltage Characteristics," Geneva, Switzerland, 2006.

[23] J. Montes-Romero, M. Torres-Ramírez, J. De La Casa, A. Firman, and M. Cáceres, "Software tool for the extrapolation to Standard Test Conditions (STC) from experimental curves of photovoltaic modules," in *Proceedings of 2016 Technologies Applied to Electronics Teaching, TAEE 2016*, 2016.

[24] A. Firman, L. Zini, R. Sanchez, and L. Vera, "Desarrollo y calibración de dispositivos fotovoltaicos para determinar el recurso solar utilizable por sfcr," *Av. en Energías Renov. y Medio Ambient.*, vol. 18, pp. 9–17, 2014.

[25] International Electrotechnical Commission, "IEC 61724-1: Photovoltaic system performance - Part 1: Monitoring," 2017.

[26] P. C. Neuenstein J., "Los módulos y sus curvas," *Photon. La Rev. fotovoltaica*, pp. 54–71, 2009.

[27] P. Hernday, "Field Applications for I-V Curve Tracers," *SolarPro*, no. August/September, pp. 76–106, 2011.

[28] Tritec, "Operating Instructions Tri-ka," 2010.

[29] Kepco Inc., "http://www.kepcopower.com/." .

[30] M. Piliougine, J. Carretero, L. Mora-Lõpez, and M. Sidrach-De-Cardona, "Experimental system for current-voltage curve measurement of photovoltaic modules under outdoor conditions," *Prog. Photovoltaics Res. Appl.*, vol. 19, no. 5, pp. 591–602, Aug. 2011.

[31] J. C. Bertolín, M. Fuentes, J. V. Muñoz, and J. de la Casa, "Applications of DC/DC converters for obtaining characteristic curves of PV generators," in *27th European Photovoltaic Solar Energy Conference*, 2012.

[32] J. V. Muñoz, M. Torres-Ramírez, B. García-Domingo, M. Fuentes, J. de la Casa, G. Nofuentes, and J. Aguilera, "Automatic monitoring system to assess the outdoor behaviour of photovoltaic modules," in *29th European Photovoltaic Solar Energy Conference and Exhibition*, 2014, pp. 2654–2657.

[33] G. Nofuentes, J. Aguilera, E. Álvarez, L. Hontoria, and J. de la Casa, "Estimación de la potencia máxima media en condiciones estándares de medida de un módulo fotovoltaico de silicio cristalino," in *X Simposio Peruano de Energía Solar*, 2003.

ANEXOS

ANEXO I

TÍTULO: "INFORME DE CALIBRACIÓN DE UN TRAZADOR DE CURVAS I-V DE MÓDULOS FOTOVOLTAICOS"

INSTITUCIÓN: CENTRO DE INVESTIGACIONES ENERGÉTICAS, MEDIOAMBIENTALES Y TECNOLÓGICAS (CIEMAT)

AUTOR: MIGUEL ALONSO ABELLA

ANEXO II

TÍTULO: "ROUND ROBIN TEST: ADQUISICIÓN DE CURVA I-V DE MODULO FOTOVOLTAICO (SI-POLY) CON PROTOTIPO DE INSTRUMENTO DESARROLLADO POR GER-UNNE-ARGENTINA, IDEA-UJA-ESPAÑA"

INSTITUCIÓN: LABORATORIO DE ENERGIA SOLAR UNIVERSIDADE FEDERAL DO RIO GRANDE DO SUL (LABSOL-UFRGS)

AUTORES: ARNO KRENSINGER Y CESAR WILHELM MASSEN PRIEB

Departamento de Energía
Unidad de Energía Solar Fotovoltaica

Universidad de JAÉN
Departamento de Ingeniería Electrónica y Automática
Edificio A-3 dependencia 434
Campus de las Lagunillas
23071 – Jaén (España)
Tel.: 953212804
Juan de la Casa Higueras delacasa@ujaen.es
Jesús Montes Romero jmontes@ujaen.es

INFORME DE CALIBRACIÓN DE UN TRAZADOR DE CURVAS I-V DE MÓDULOS FOTOVOLTAICOS

1. Objeto:

Calibrar el factor de forma y potencia máxima de la curva I-V un trazador de curvas I-V de módulos fotovoltaicos (FV).

2. Equipo a calibrar:

Trazador de curvas I-V de campos fotovoltaicos, sin modelo ni número de serie definidos. Es un prototipo.

3. Descripción del equipo y rangos de medida

El equipo es un trazador de curvas I-V de módulos fotovoltaicos, alimentado con conexión a la red eléctrica AC y con comunicación por puerto USB. Usa el método de medidas de 4 puntas y su funcionamiento se basa en la carga de un condensador por lo que el tiempo de trazado de la curva I-V depende de la intensidad y tensión del campo FV a medir. Como señales adicionales mide la irradiancia solar y la temperatura a través de sensores externos. La corriente se mide con un shunt externo de 10A/150 mV. La medida de la temperatura se realiza con una sonda externa pt-100.

Los rangos de los canales de entrada al trazador son

Rango de entrada de la señal de corriente: 0 a 160 mV.
Rango de entrada de la señal de tensión: 0 a 100 V.
Rango de entrada de la señal de irradiancia: 0 a 65 mV.
Rango de entrada de la señal de temperatura: 0 a 700 mV.

Rangos de medida:

Tensión	0 a 100 V
Intensidad	0 a 10 A
Temperatura	-10 a + 90 ºC
Irradiancia	0 a 1300 W/m^2

El trazador se controla desde un ordenador mediante un programa de medidas. Las constantes de calibración utilizadas en el programa de medidas son:

- Tensión. Cte 34.97, offset -2.4
- Corriente. Cte shunt 66.67, constante 24.76, offset 2.36
- Irradiancia. Cte calibración 28818, cte 60.01, offset -5.02
- Temperatura. Cte 5345.65 offset 8.43.

4. Patrones utilizados

Patrón de potencia Pm, intensidad Isc y tensión Voc en la medida de la curva I-V

Vatímetro Yokogawa WT3000, n/s 27E911394J.
El vatímetro tiene las siguientes precisiones básicas de medida:

En tensión DC	0.05% de la lectura + 0.05% del fondo de escala
En intensidad DC	0.05% de la lectura + 0.05% del fondo de escala
En potencia DC	0.05% de la lectura + 0.10% del fondo de escala

5. Procedimiento de calibración

Calibración por comparación directa entre los valores registrados en los datos de medida generados por el programa de control y medida y los valores registrados por el vatímetro, conectado en paralelo con el PVPM, al medir curvas I-V de un generador fotovoltaico del laboratorio en operación a sol real, con configuraciones serie-paralelo distintas para obtener los rangos de intensidad, tensión y potencia, según se indica en las tablas de resultados.

6. Resumen de Resultados

NOTA: Ver tablas y gráficos de calibración de la curva I-V (Isc, Voc, Im, Vm) y Pm en **Anexo 1**.

La desviación es la diferencia entre los valores del PVPM menos los valores de los patrones de referencia, expresada en porcentaje, en su caso, respecto del valor del patrón.

Calibración de la curva I-V y de la potencia Pm

Parámetro	Rango	Desviación (*)	Incertidumbre (*)
Isc	**1 a 10 A**	**- 0.10 %**	**± 0.02 A**
Voc	**20 a 80 V**	**- 0.4 %**	**± 0.2 V**
Pm	**20 a 250 W**	**+ 0.35 %**	**± 2 W**

(*) incluye las desviaciones e incertidumbres debidas a las variaciones instantáneas de la irradiancia solar ocurridas durante las medidas y errores en la obtención de parámetros de las curvas I-V.

Tabla 1. Calibración de la curva I-V y de la potencia Pm.

Realizado por:

Miguel Alonso Abella

Madrid, 8 de mayo de 2018

Avda. Complutense 40, 28040 Madrid. miguel.alonso@ciemat.es T 913466745

ANEXO 1

A continuación, se muestran las curvas I-V y las tablas de resultados de las medidas de las curvas I-V obtenidas con el trazador de curvas IV, a través de la interfase USB y el software de control y medidas y con el vatímetro WT3000 de Yokogawa, para distintas configuraciones serie-paralelo del generador fotovoltaico. Agrupando los datos de las curvas I-V medidas para las distintas potencias de salida del generador fotovoltaico se obtienen las tablas siguientes para los parámetros Isc, Voc, Pm, Im y Vm:

Parámetro	**Trazador IV**	**Referencia WT3000**	**Desviación (*)**	
			[A]	**[%]**
Isc [A]	0.94	0.95	-0.01	-1.06%
	1.04	1.04	0.00	-0.07%
	1.11	1.11	0.00	0.31%
	1.59	1.59	0.01	0.32%
	1.22	1.22	0.00	-0.07%
	1.72	1.7	0.02	1.16%
	1.83	1.84	-0.01	-0.55%
	1.87	1.88	-0.01	-0.53%
	4.54	4.53	0.01	0.29%
	1.96	1.96	0.00	0.17%
	6.78	6.84	-0.06	-0.89%
	6.86	6.97	-0.11	-1.66%
	8.06	8.04	0.02	0.20%
	8.21	8.22	-0.01	-0.11%
	8.84	8.85	0.00	-0.05%
	8.88	8.89	0.00	-0.02%
	8.76	8.77	0.00	-0.03%
	8.92	8.93	-0.01	-0.06%
	10.11	10.11	0.00	0.03%
	3.93	3.94	0.00	-0.03%
	5.25	5.25	0.00	-0.06%

(*) Incertidumbre menor a ± 0.5 %

Tabla 2. Valores de Isc medidos por el vatímetro WT3000 y el trazador IV.

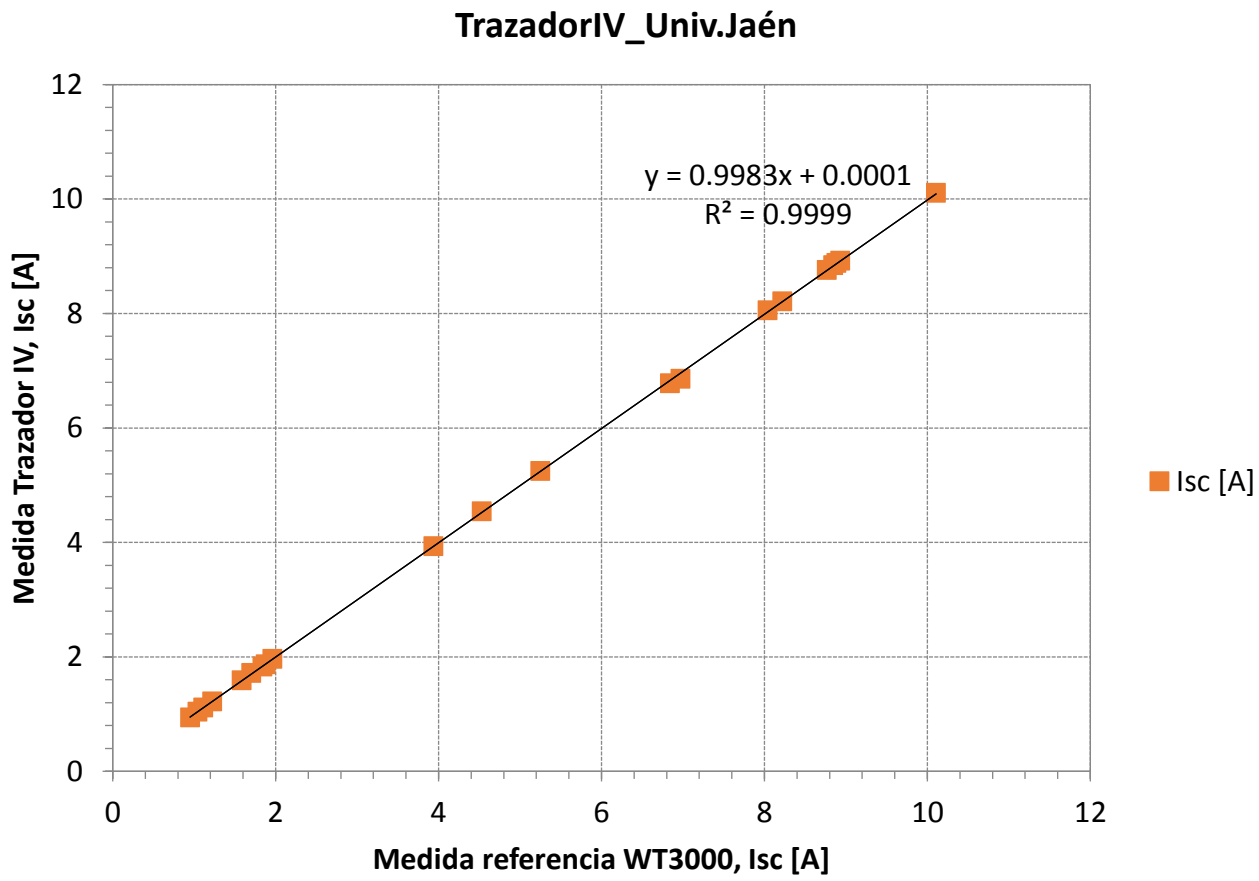

Figura 1. Valores de Isc medidos por el vatímetro WT3000 y por el trazador IV.

Parámetro	Trazador IV	Referencia WT3000	Desviación (*)	
			[V]	[%]
Voc [V]	26.46	26.48	-0.02	-0.08%
	26.26	26.43	-0.17	-0.64%
	26.15	26.28	-0.13	-0.50%
	26.04	26.08	-0.04	-0.15%
	26.13	26.24	-0.12	-0.45%
	25.80	25.97	-0.17	-0.66%
	58.77	58.77	0.00	0.00%
	58.61	58.64	-0.03	-0.05%
	38.79	38.97	-0.19	-0.48%
	38.81	38.96	-0.15	-0.39%
	38.59	38.70	-0.11	-0.28%
	38.74	38.80	-0.06	-0.17%
	38.88	38.96	-0.09	-0.22%
	38.53	38.75	-0.21	-0.55%
	39.40	39.50	-0.11	-0.28%
	38.77	39.03	-0.26	-0.67%
	38.99	39.15	-0.16	-0.41%
	38.45	38.67	-0.22	-0.57%
	39.04	39.29	-0.25	-0.63%
	76.94	77.29	-0.34	-0.45%
	75.85	75.95	-0.10	-0.14%

(*) Incertidumbre menor de ± 0.5 %

Tabla 3. Valores de Voc medidos por el vatímetro WT3000 y el trazador IV.

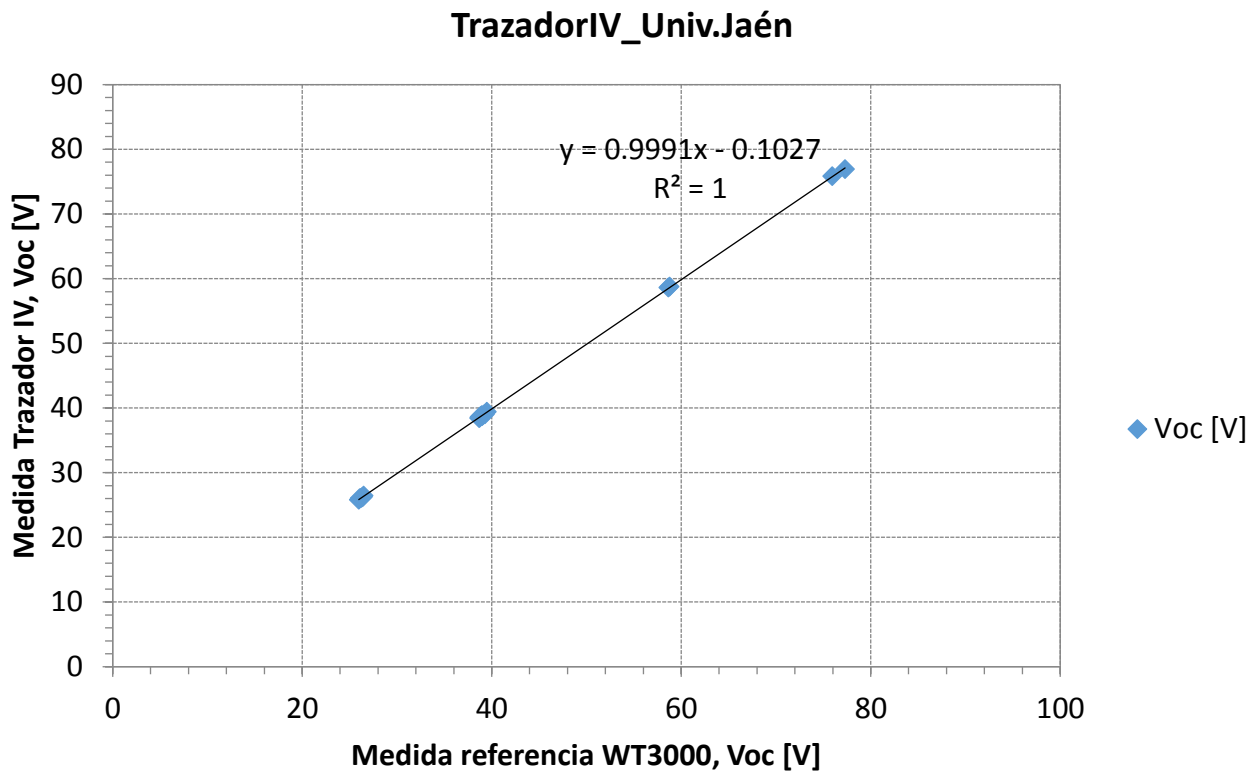

Figura 2. Valores de Voc medidos por el vatímetro WT3000 y por el trazador IV.

Parámetro	Trazador IV	Referencia WT3000	Desviación (*)	
			[W]	[%]
Pm [W]	17.1	17.0	0.1	0.80%
	19.1	18.9	0.2	1.21%
	20.1	20.0	0.1	0.51%
	28.1	27.8	0.3	1.05%
	22.2	21.9	0.3	1.20%
	29.6	29.5	0.1	0.35%
	71.7	71.1	0.6	0.83%
	73.3	73.1	0.2	0.26%
	113.9	113.3	0.6	0.49%
	51.3	50.9	0.4	0.77%
	164.7	163.6	1.1	0.67%
	169.0	167.6	1.4	0.83%
	189.1	189.4	-0.3	-0.15%
	190.4	191.5	-1.2	-0.61%
	209.7	208.9	0.7	0.35%
	206.4	205.7	0.6	0.31%
	205.3	204.9	0.4	0.19%
	204.5	203.6	0.9	0.43%
	229.3	228.5	0.8	0.34%
	199.9	200.0	-0.1	-0.05%
	258.6	259.0	-0.4	-0.17%

(*) Incertidumbre menor de ± 1 %

Tabla 4. Valores de Pm medidos por el vatímetro WT3000 y el trazador IV.

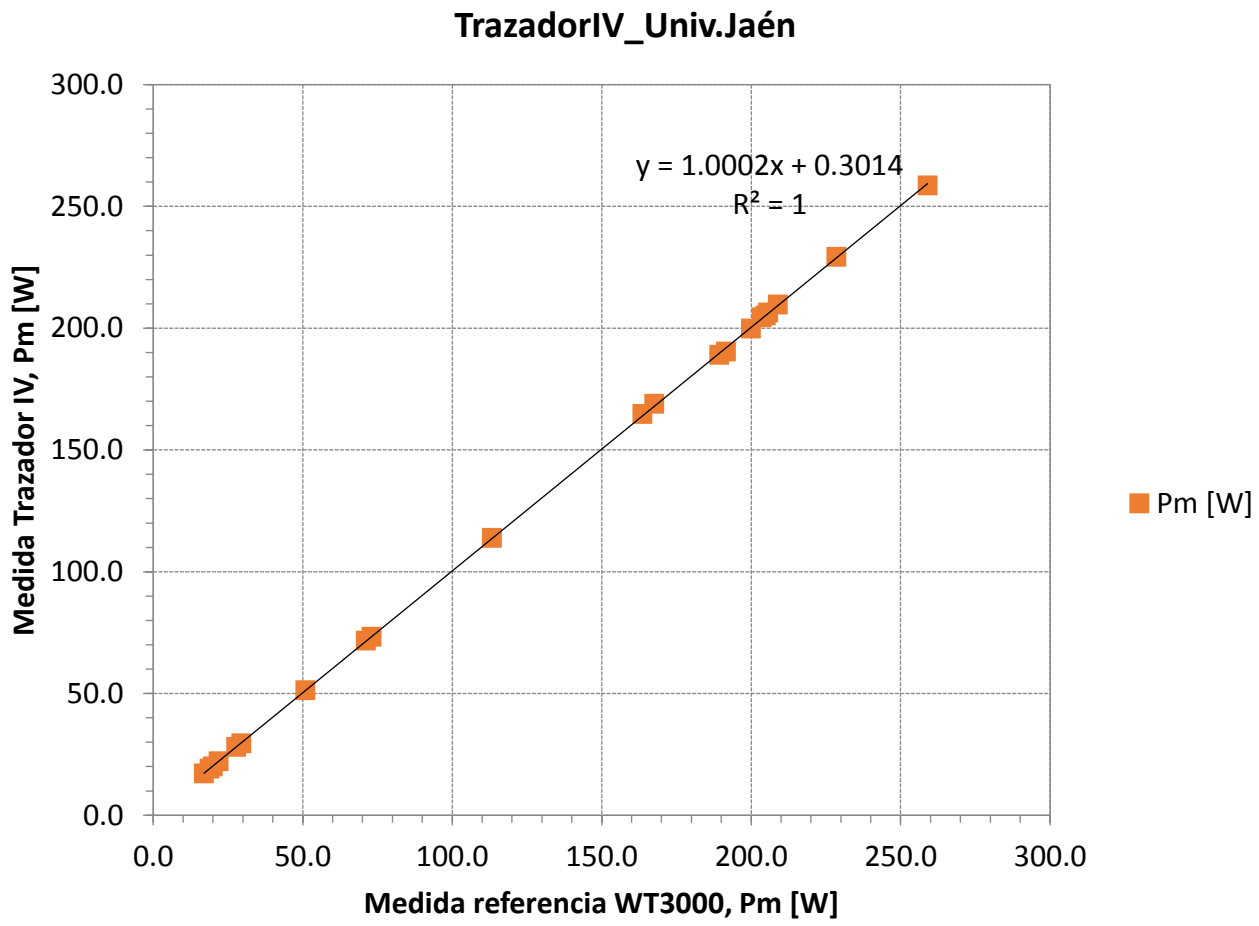

Figura 3. Valores de Pm medidos por el vatímetro WT3000 y por el trazador IV.

Parámetro	Trazador IV	Referencia WT3000	Desviación (*)	
			[A]	[%]
Im [A]	0.82	0.81	0.01	1.22%
	0.91	0.91	0.00	0.22%
	0.97	0.97	0.01	0.71%
	1.41	1.41	0.00	0.06%
	1.06	1.08	-0.01	-1.39%
	1.49	1.50	-0.01	-0.67%
	1.61	1.58	0.03	1.86%
	1.60	1.61	-0.01	-0.63%
	3.89	3.93	-0.04	-1.07%
	1.71	1.72	-0.01	-0.69%
	5.97	5.85	0.12	1.98%
	5.99	6.02	-0.03	-0.55%
	6.76	6.88	-0.12	-1.79%
	7.29	6.98	0.31	4.31%
	7.72	7.61	0.11	1.44%
	7.55	7.54	0.01	0.07%
	7.67	7.56	0.10	1.35%
	7.77	7.70	0.07	0.89%
	8.51	8.65	-0.14	-1.64%
	3.31	3.31	0.00	0.05%
	4.43	4.44	-0.02	-0.34%

(*)Incertidumbre menor de ± 1.0%

Tabla 5. Valores de Im medidos por el vatímetro WT3000 y por el trazador IV

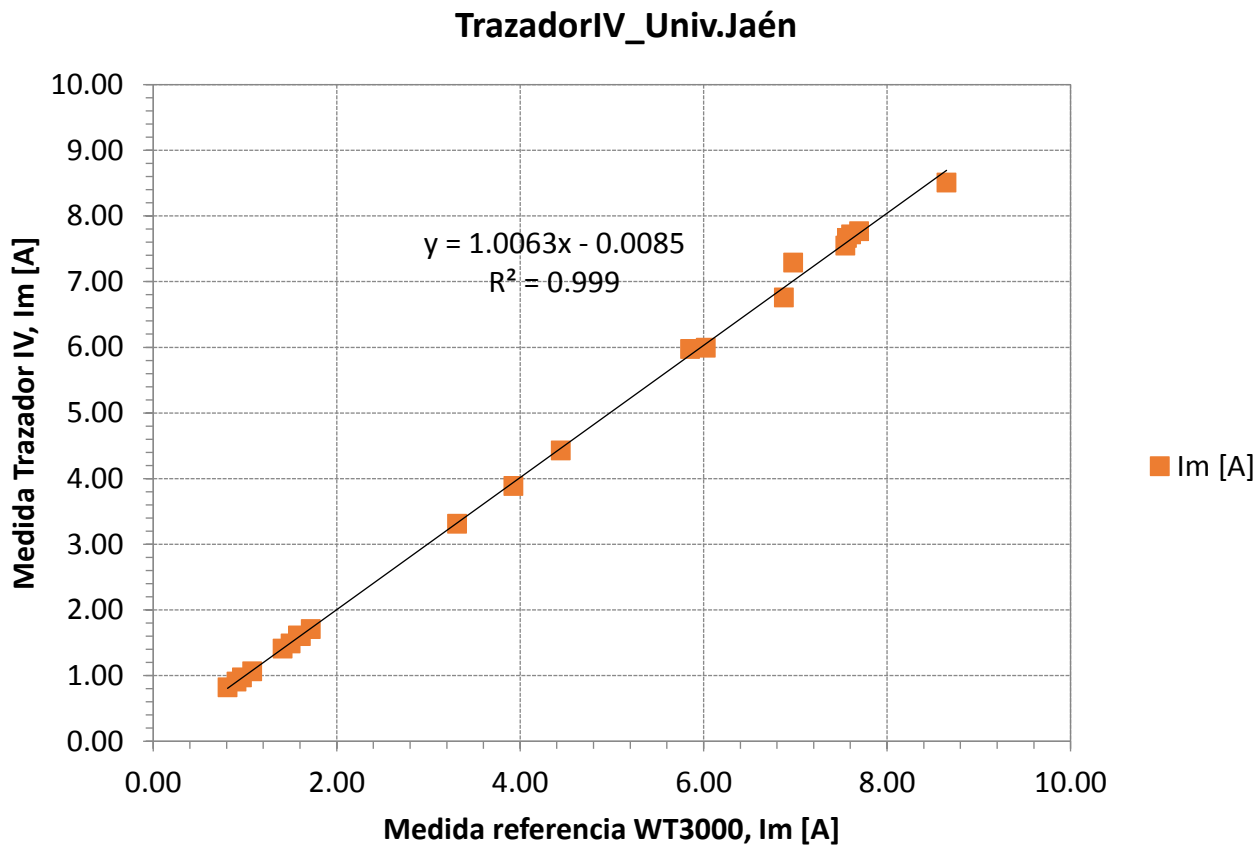

Figura 4. Valores de Im medidos por el vatímetro WT3000 y por el trazador IV.

Parámetro	Trazador IV	Referencia WT3000	Desviación (*)	
			[V]	[%]
Vm[V]	20.99	20.98	0.01	0.05%
	20.96	20.75	0.21	1.00%
	20.62	20.66	-0.04	-0.20%
	19.92	19.72	0.20	0.99%
	20.82	20.29	0.53	2.55%
	19.80	19.65	0.15	0.76%
	44.56	45.02	-0.46	-1.03%
	45.76	45.39	0.37	0.81%
	29.30	28.85	0.45	1.54%
	30.04	29.61	0.44	1.45%
	27.58	27.95	-0.37	-1.34%
	28.21	27.82	0.39	1.38%
	27.99	27.54	0.45	1.61%
	26.11	27.46	-1.34	-5.15%
	27.16	27.46	-0.30	-1.10%
	27.33	27.27	0.07	0.24%
	26.78	27.09	-0.32	-1.18%
	26.33	26.45	-0.12	-0.47%
	26.95	26.42	0.53	1.95%
	60.33	60.39	-0.06	-0.10%
	58.39	58.29	0.10	0.18%

(*)Incertidumbre menor de ± 1.5 %

Tabla 6. Valores de Vm medidos por el vatímetro WT3000 y por el trazador IV.

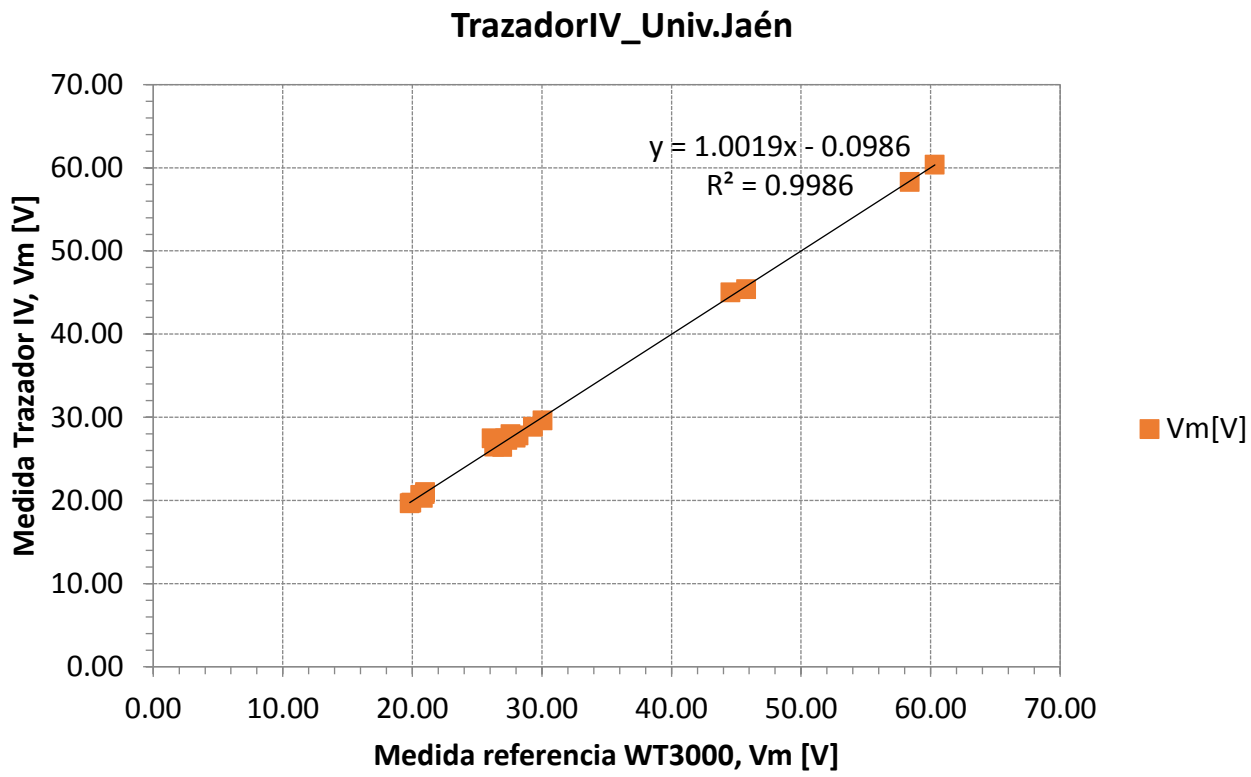

Figura 5. Valores de Vm medidos por el vatímetro WT3000 y por el trazador IV.

En las siguientes figuras se presentan a modo de ejemplo *algunas* de las curvas I-V medidas por el trazador de curvas IV y por el vatímetro.

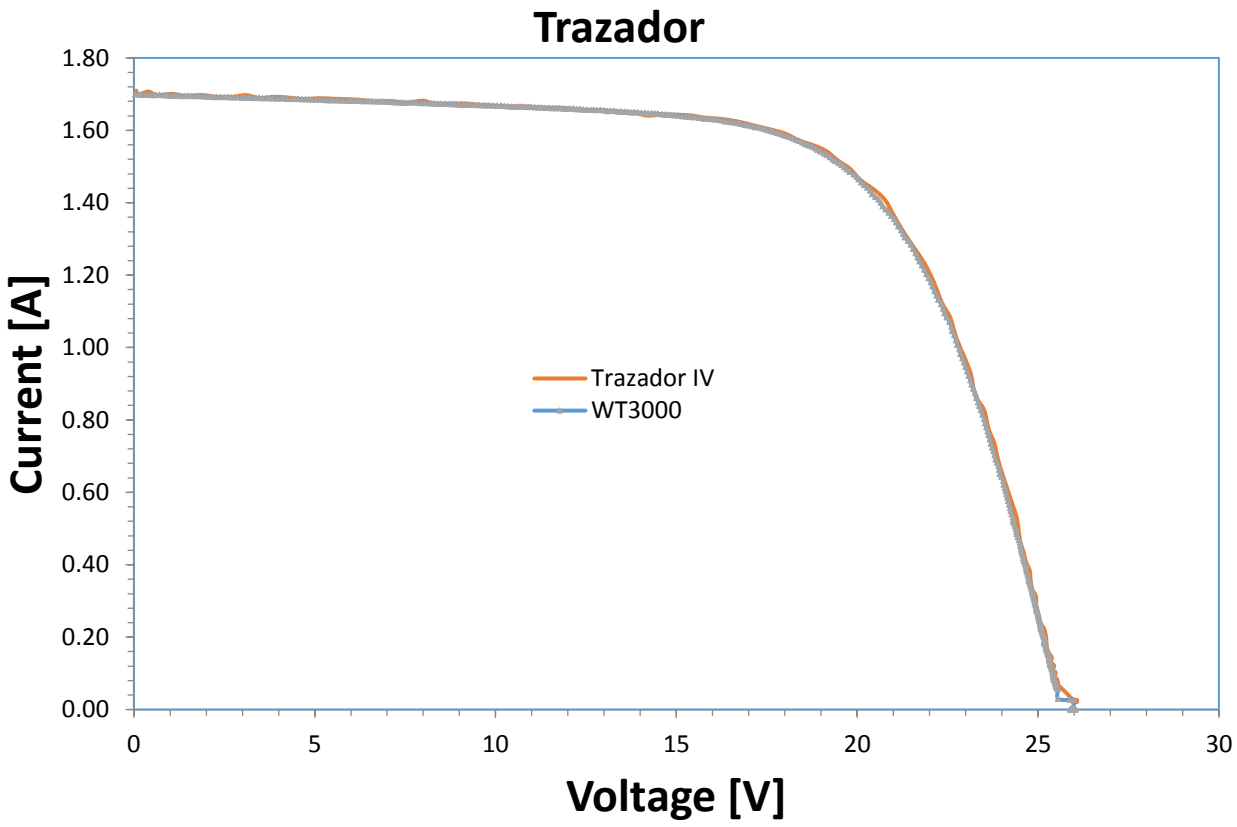

Figura 6. Curvas I-V medidas por el vatímetro WT3000 y por el trazador IV.

Parámetro	Trazador IV	Referencia WT3000	Desviación [%]
Isc [A]	1.72	1.70	1.50%
Voc [V]	25.80	25.97	-0.63%
Im [A]	1.49	1.50	-0.27%
Vm [V]	19.80	19.65	0.79%
Pm [W]	29.58	29.43	0.52%

Tabla 7. Parámetros de las curvas I-V medidas por el vatímetro WT3000 y por el trazador IV.

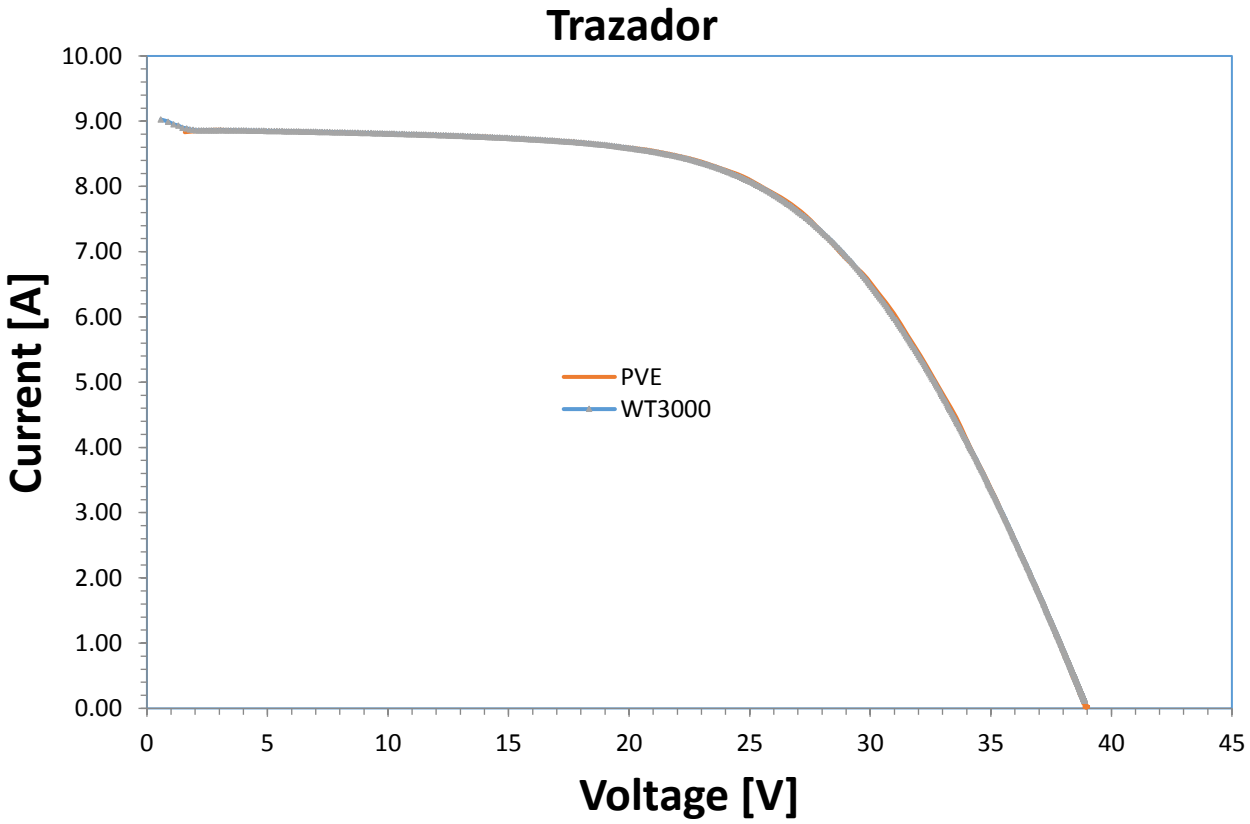

Figura 7. Curvas I-V medidas por el vatímetro WT3000 y por el trazador IV.

Parámetro	Trazador IV	Referencia WT3000	Desviación [%]
Isc [A]	8.88	8.89	-0.02%
Voc [V]	38.77	39.03	-0.67%
Im [A]	7.55	7.54	0.07%
Vm [V]	27.33	27.27	0.24%
Pm [W]	206.38	205.73	0.31%

Tabla 8. Parámetros de las curvas I-V medidas por el vatímetro WT3000 y por el trazador IV.

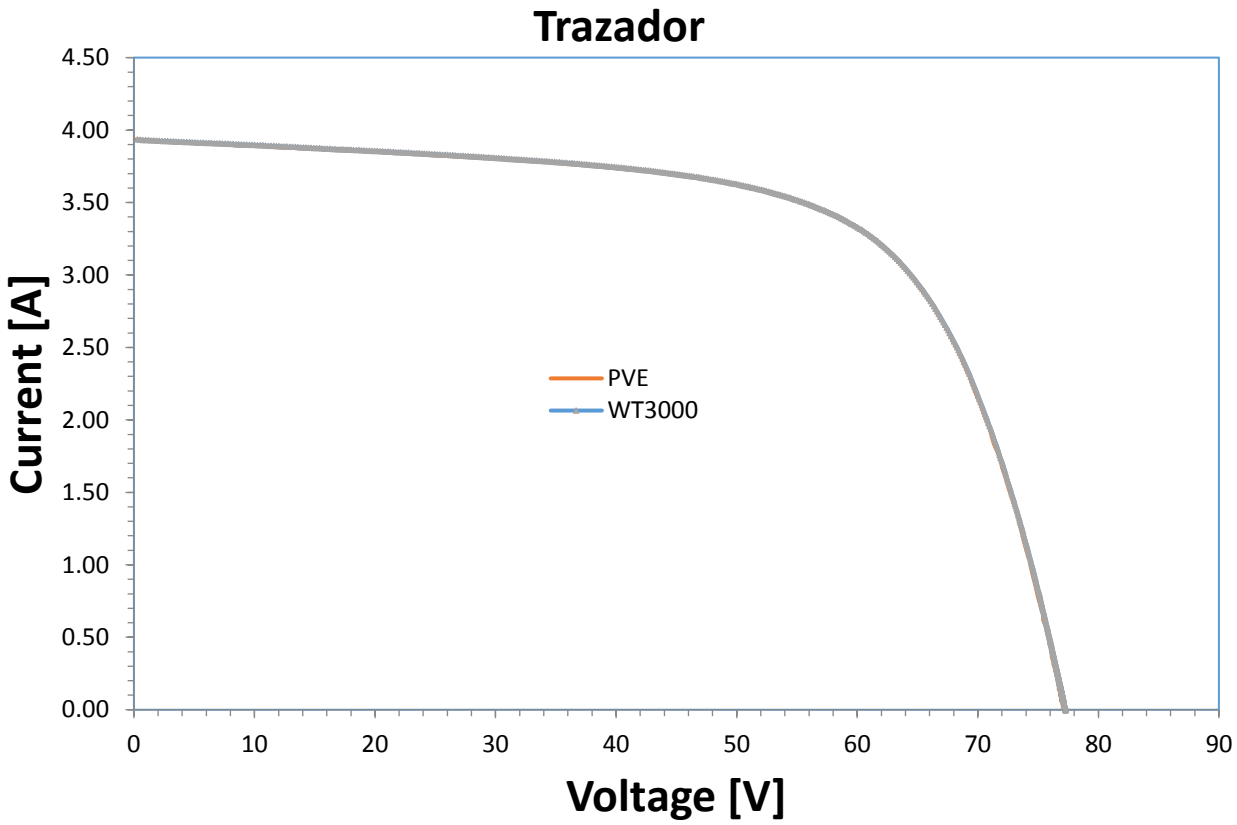

Figura 8. Curvas I-V medidas por el vatímetro WT3000 y por el trazador IV.

Parámetro	Trazador IV	Referencia WT3000	Desviación [%]
Isc [A]	3.93	3.94	-0.03%
Voc [V]	76.94	77.29	-0.45%
Im [A]	3.31	3.31	0.05%
Vm [V]	60.33	60.39	-0.10%
Pm [W]	199.87	199.97	-0.05%

Tabla 9. Parámetros de las curvas I-V medidas por el vatímetro WT3000 y por el trazador IV.

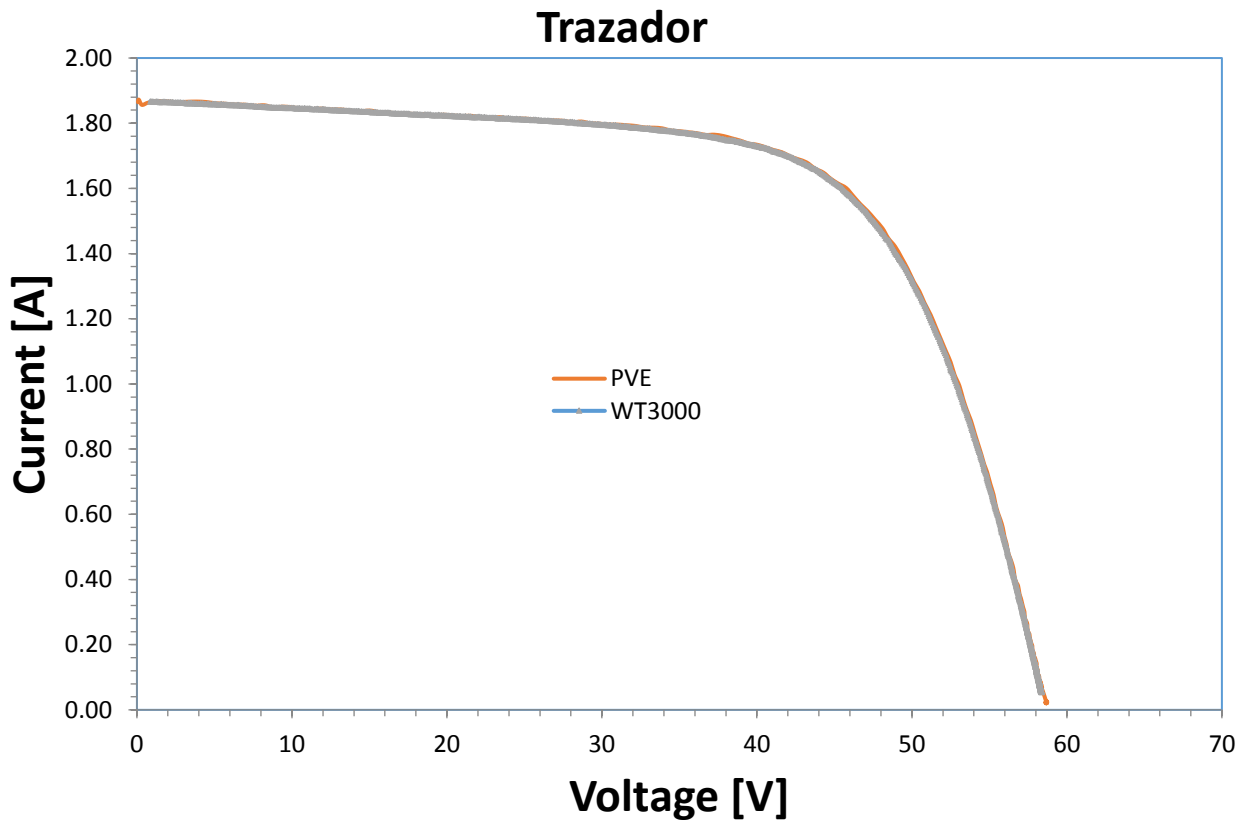

Figura 9. Curvas I-V medidas por el vatímetro WT3000 y por el trazador IV.

Parámetro	Trazador IV	Referencia WT3000	Desviación [%]
Isc [A]	1.87	1.88	-0.57%
Voc [V]	58.61	58.64	-0.06%
Im [A]	1.60	1.61	-0.29%
Vm [V]	45.76	45.39	0.82%
Pm [W]	73.27	72.88	0.53%

Tabla 10. Parámetros de las curvas I-V medidas por el vatímetro WT3000 y por el trazador IV.

LABORATORIO DE ENERGIA SOLAR

UNIVERSIDADE FEDERAL DO RIO GRANDE DO SUL

(LABSOL-UFRGS)

ROUND ROBIN TEST:

ADQUISICIÓN DE CURVA I-V DE MODULO FOTOVOLTAICO (Si-Poly) CON PROTOTIPO DE INSTRUMENTO DESARROLLADO POR GER-UNNE-ARGENTINA, IDEA-UJA-ESPAÑA

REPORTE DE RESULTADOS

AÑO 2017

1. INTRODUCCION

Se reportan resultados obtenidos durante ensayo de adquisición de curva corriente vs. tensión (I-V) para un módulo fotovoltaico de silicio policristalino expuesto a sol real. Se emplearon dos equipos de adquisición, uno desarrollado por dos entes en conjunto, el Grupo en Energías Renovables de la Universidad Nacional del Nordeste Argentina (GER-UNNE) y el Grupo IDEA de la Universidad de Jaén en España (IDEA-UJA) y un equipo de referencia perteneciente al Laboratorio de Energía Solar de la Universidad Federal de Río Grande do Sul (LABSOL - UFRGS).

El objetivo del ensayo es comparar el instrumento desarrollado para avalar su transferencia gratuita hacia la comunidad científico-educativa vinculada al área de la energía solar fotovoltaica.

2. MATERIALES

- Modulo FV ensayado:
  - Módulo SEG, SEGM675W

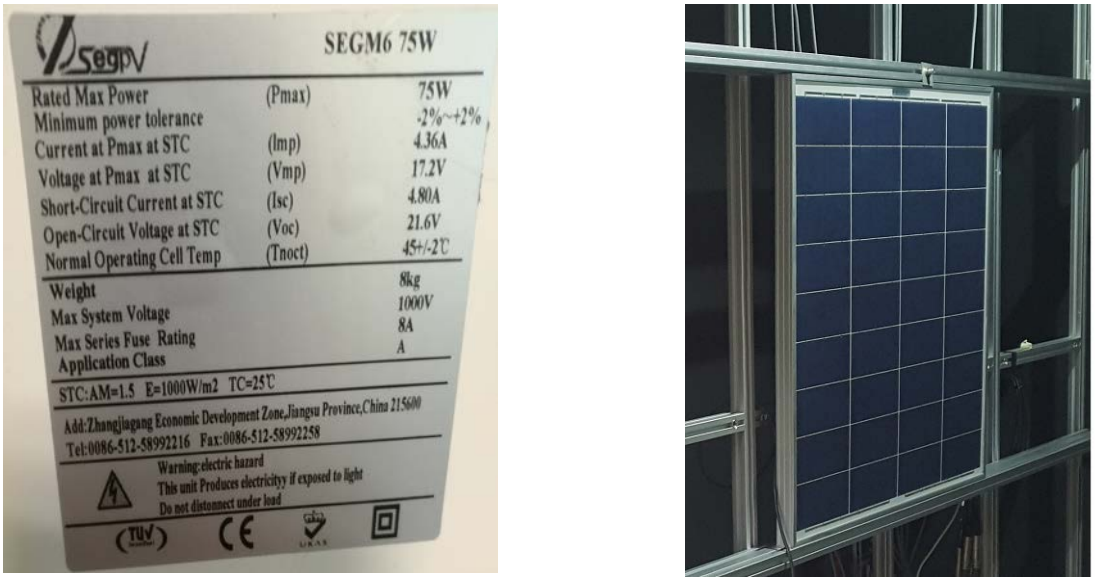

(a) (b)

Figura 1.- Fotografías del módulo bajo ensayo. a) Placa característica. b) Aspecto visual Posterior.

- Instrumento bajo ensayo:

Prototipo de instrumento trazador de curvas I-V basado en carga capacitiva, operado por PC, con software de control.

Características técnicas:

Channel	Measurement range	Transducer	Transducer operation range
PV module Current (*I*)	0 to 12 Amp	Shunt resistor class 0,5	0 to 15 A/150 mV
PV module Voltage (*V*)	-10 to 100 V	Atenuator 120 V/1,6 V	0 to 1,6 V
Irradiance (*G*)	0 to 1300 W/m2	Class 0,5 shunt connected Poly Si cell	0 to 3,5 A / 42 mV
Cell Temperature (*T*)	0 to 100 ºC	Open circuit Poly Si cell	0,5 V to 0,8 V
Cell Temperature (*T*)	0 to 100 ºC	PT100 Resistor	0,5 V to 0,7 V (with 5 mA constant current source)

- Instrumento de contraste:

Sistema de adquisición de curvas I-V para módulos fotovoltaicos expuestos a sol real propiedad del LABSOL (Figura 3). Compuesto por una fuente KEPCO BOP 100-10 MG y multímetros Agilent 3458A [1].

(b)

(b)

Figura 2.- Instrumental utilizado. a) Relevador de curvas I-V desarrollo GER-IDEA. b) Relevador de curvas I-V LABSOL.

3. METODOS

Se adquirieron curvas I-V del módulo SEGM675W expuesto a sol real con instrumento GER-IDEA y con instrumento LABSOL.

[1]-Gasparin F P, (2009), Desenvolvimento de un tracador de curvas características de módulos fotovoltaicos. Dissertação de Mestrado, PROMEC/UFRGS, Porto Alegre RS

- Condiciones de ensayo: Irradiancia (Sol real): 1099 W/m^2

  Temperatura de Módulo: 48 ºC

4. RESULTADOS

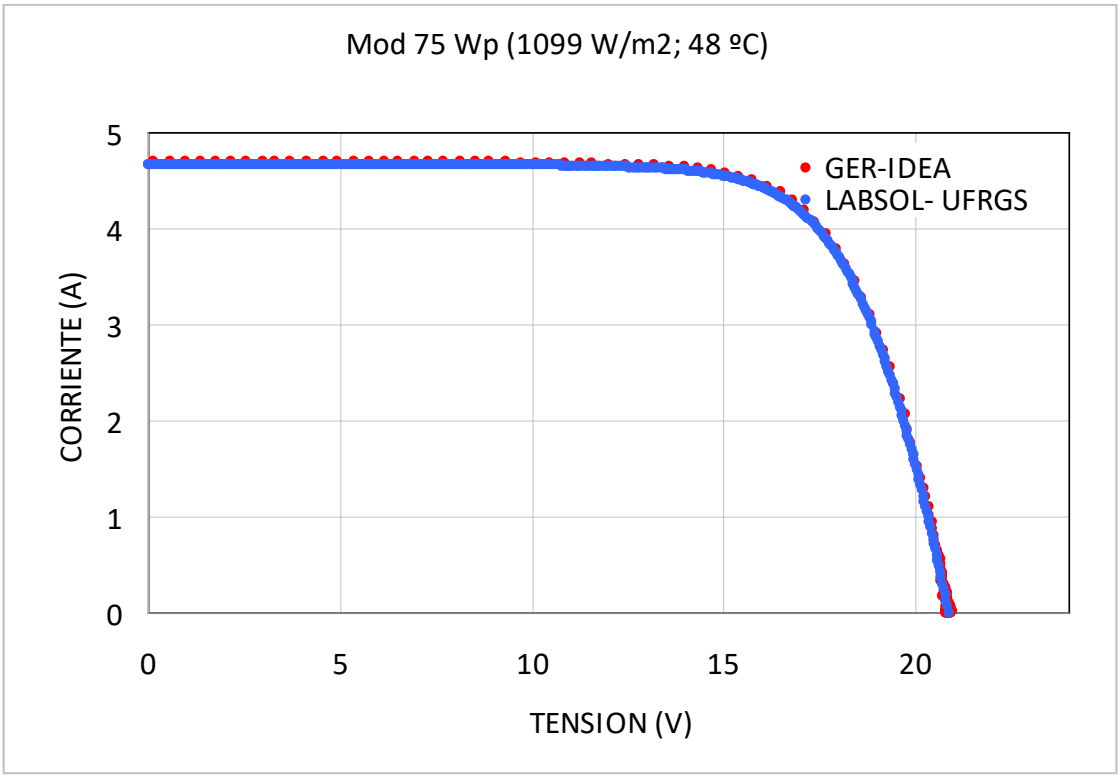

Figura 3.- Superposición gráfica de curvas I-V obtenidas para el módulo SEGM675W con ambos instrumentos.

PUNTOS CARACTERÍSTICOS

- Obtenidos por búsqueda directa entre datos adquiridos (valores mas próximos):

Mod 75 Wp	Relevador GER-IDEA	Relevador LABSOL
Isc (A)	4,70	4,67
Voc (V)	20,91	20,86
Ipm (A)	4,38	4,28
Vpm (V)	16,46	16,69
Ppm (W)	72,11	71,44

Tabla 1.- Parámetros característicos medidos con ambos instrumentos

Desvíos Porcentuales	
Parámetro	**Valor**
D Isc %	0,52
D Voc %	0,23
D Ipm %	2,35
D Vpm %	1,37
D Ppm %	0,94

Tabla 2.- Desvíos relativos porcentuales.

- Obtenidos por interpolación:

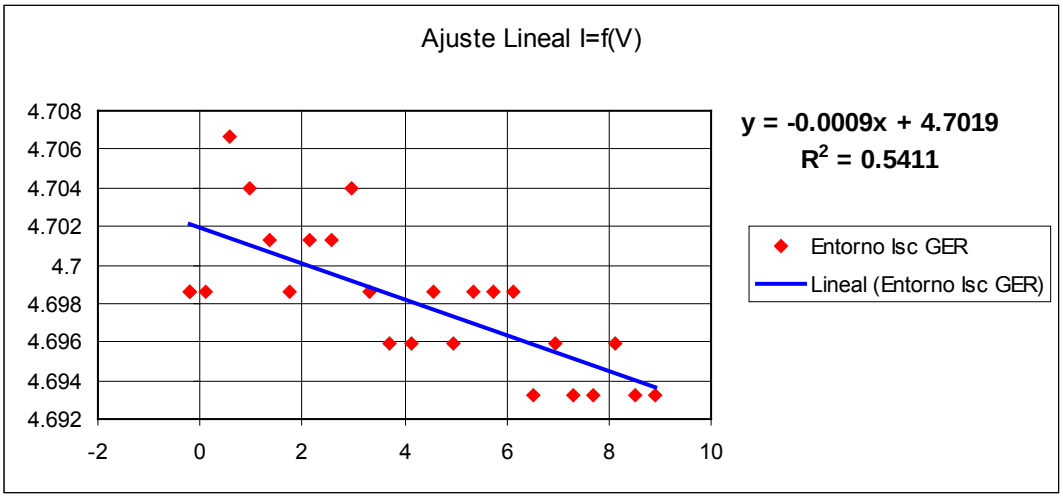

Figura 4.- Interpolación lineal para puntos en el entorno de Isc, datos adquiridos con instrumento GER-IDEA (valor obtenido: **Isc = 4,70 A**).

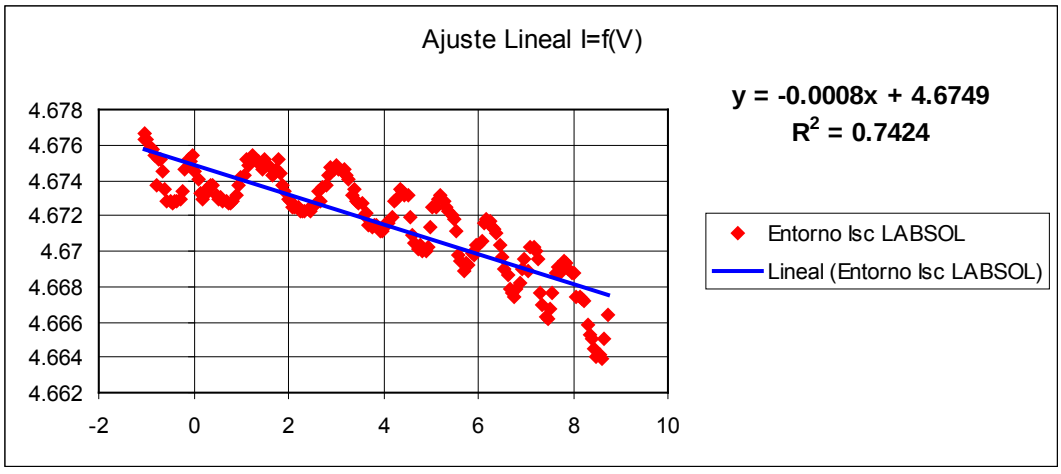

Figura 5.- Interpolación lineal para puntos en el entorno de Isc, datos adquiridos con instrumento LABSOL (valor obtenido: **Isc = 4,67 A**).

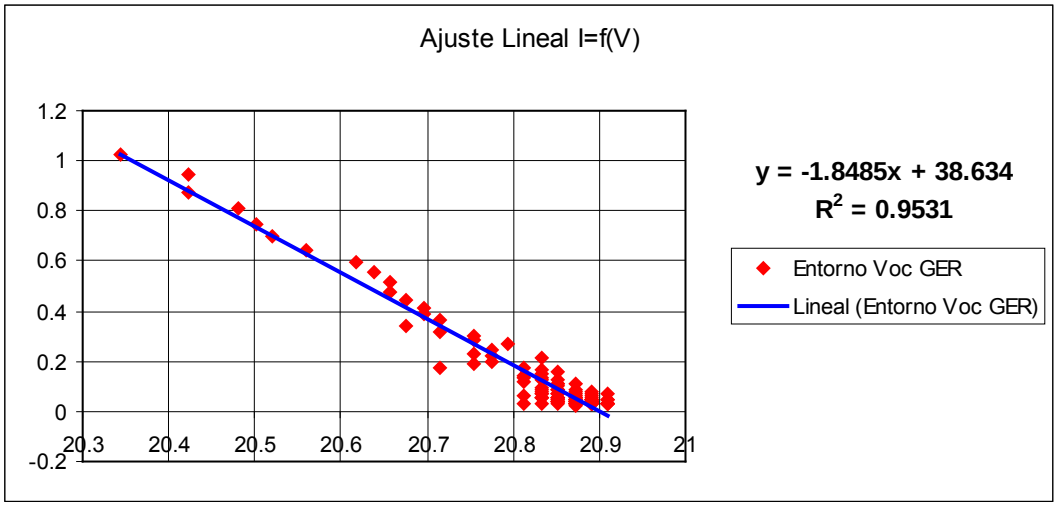

Figura 6.- Interpolación lineal para puntos en el entorno de Voc, datos adquiridos con instrumento GER-IDEA (valor obtenido: **Voc = 20,90 V**).

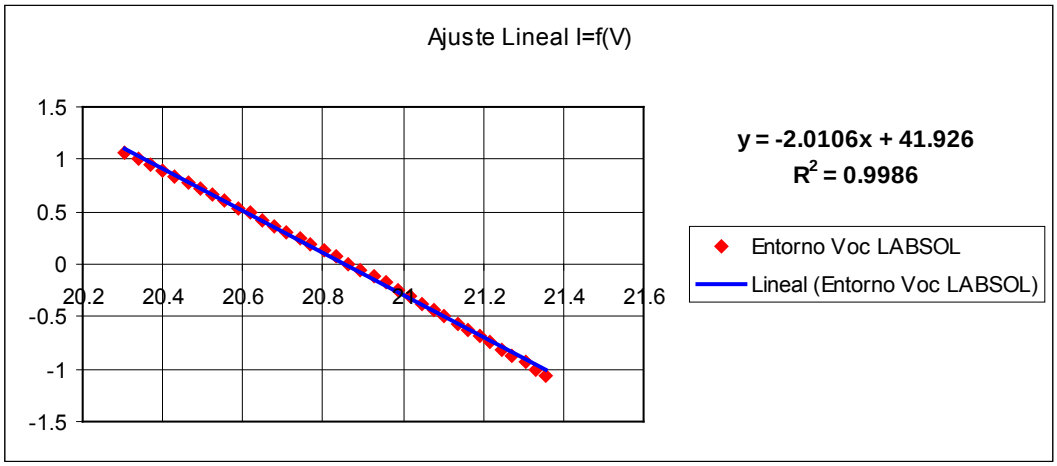

Figura 7.- Interpolación lineal para puntos en el entorno de Voc, datos adquiridos con instrumento LABSOL (valor obtenido: **Voc = 20,85 V**).

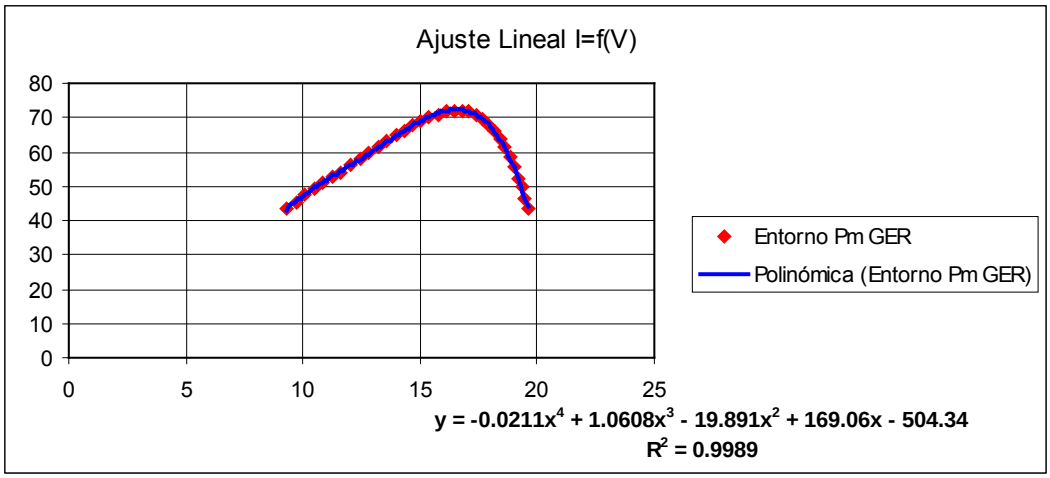

Figura 8.- Interpolación polinómica de orden 4 para puntos en el entorno de Ppm, datos adquiridos con instrumento GER-IDEA (valor obtenido: **Ppm = 71,14 W**).

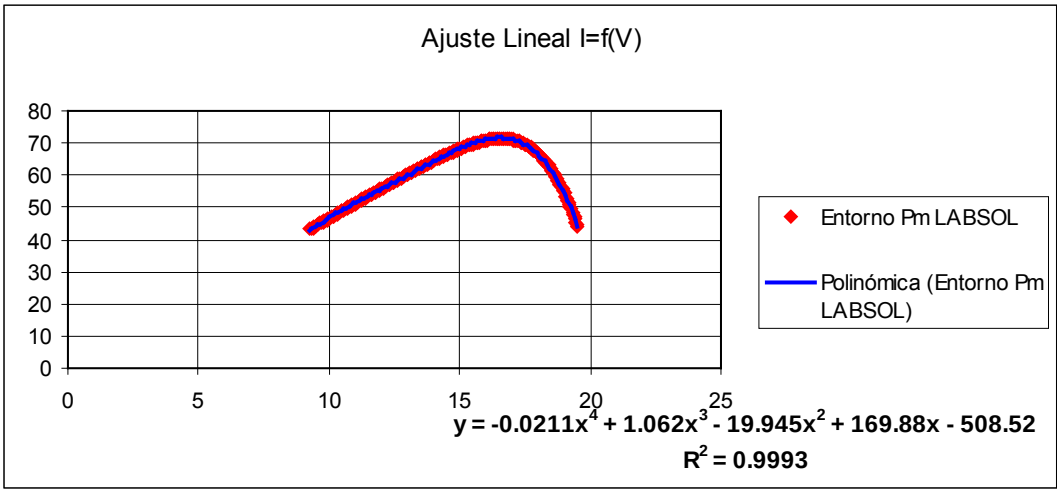

Figura 9.- Interpolación con ecuación polinómica de orden 4 para puntos en el entorno de Ppm, datos adquiridos con instrumento LABSOL (valor obtenido: **Ppm = 71,18 W**).

Desvíos Porcentuales	
Parámetro	**Valor**
D Isc %	0,58
D Voc %	0,23
D Ppm %	0,05

Tabla 3.- Desvíos relativos porcentuales.

Dr. Manuel Cáceres

Universidad Nacional del Nordeste

Dr. Arno Krensinger

Director LABSOL-UFRGS

Dr. Cesar Wilhelm Massen Prieb

Responsable técnico LABSOL UFRGS